

TECHNICAL UNIVERSITY OF MOLDOVA

JOURNAL OF ENGINEERING SCIENCE

Technical and applied scientific publication founded on 9 February 1995
Alternative title: Meridian ingineresc

2024 Vol. XXXI (3)

ISSN 2587-3474 eISSN 2587-3482

TECHNICAL UNIVERSITY OF MOLDOVA (PUBLISHING HOUSE)
"TEHNICA UTM" (PRINTING HOUSE)

According to the Decision of the NAQAER No. 19 from 06.12.2019, JES is classified as B+ journal

Main subjects areas of the Journal of Engineering Science:

A. Industrial Engineering

- Mechanical Engineering and Technologies
- Applied Engineering Sciences and Management
- Materials Science and New Technologies
- Electrical Engineering and Power Electronics
- Energy systems
- Light Industry, New Technologies and Design
- Industrial and Applied Mathematics
- Vehicle and Transport Engineering

B. Electronics and Computer Science

- Electronics and Communication
- Microelectronics and Nanotechnologies
- Biomedical Engineering
- Computers and Information Technology
- Automation

C. Architecture, Civil and Environmental Engineering

- Architecture, Urbanism and Cadaster
- Civil Engineering and Management
- Energy Efficiency and New Building Materials
- Environmental Engineering

D. Food Engineering

- Food Technologies and Food Processes
- Food Industry and Management
- Biotechnologies, Food Chemistry and Food Safety
- Equipment for Food Industries

The structure of the journal corresponds to the classification of scientific publications: *Engineering, Multidisciplinary.*

How to publish a paper:

- 1. Send the manuscript and information about the author to the **Editorial Board address**: jes@meridian.utm.md
- 2. Manuscripts are accepted only in English, by e-mail, in template file (www.jes.utm.md)
- 3. After a review, you will be notified of the editorial board's decision.
- 4. After the Journal has been published, we will send it to you immediately by mail.

Editor-in-Chief

Dr. hab. prof. univ. Viorel BOSTAN

Technical University of Moldova
viorel.bostan@adm.utm.md

Editorial Board

Abdelkrim Azzouz, Dr. Ing., Professor, Quebec University of Montreal, Canada

Adrian Gheorghe, PhD, Professor Old Dominion University, Norfolk, Virginia, 23529, USA

Adrian Graur, PhD, Professor University "Stefan cel Mare", Suceava, Romania

Cornel Ciupan, PhD, Professor Technical University of Cluj Napoca, Romania

Aurel-Mihail Țîțu, PhD & ScD, Dr. Habil., Professor, "Lucian Blaga" University of Sibiu, Romania Cristoph Ruland, PhD, Professor, University of SIEGEN, Germany

Dimitr P. Karaivanov, Dr.Sc., PhD, Professor University of Chemical Technology and Metallurgy, Sofia, Bulgaria

Dumitru Mnerie, PhD, Professor "Politehnica" University of Timișoara, Romania

Dumitru Olaru, PhD, Professor Technical University "Gh. Asachi", Iași, Romania

Florin Ionescu, PhD, Professor University Steinbes, Berlin, Germany

Frank Wang Professor of Future Computing, University of Kent, U.K.

Gabriel Neagu Profesor Institutul Național de Cercetare-Dezvoltare în Informatică București,

George S. Dulikravich, PhD, Florida International University, U.S.A.

Gheorghe Badea, Ph.Dr. in Engineering, Professor, Technical University of Civil Engineering Bucharest, Romania

Gheorghe Manolea, PhD, Professor University of Craiova, Romania

Grigore Marian, Dr.Sc., PhD, Professor Agrarian State University of Moldova, Chişinău, Republic of Moldova

Hai Jiang, Ph.D. Professor, Department of Computer Science, Arkansas State University, U.S.A.

Heinz Frank, PhD, Professor Reinhold Würth University, Germany

Hidenori Mimura, Professor, Research Institute of Electronics, Shizuoka University, Japan

Ion Bostan, Dr.hab., Acad. Academy of Science, Republic of Moldova

Ion Paraschivoiu, PhD, Professor Universite Technologique de Montreal, Canada

Ion Rusu, Dr. hab. Professor, Technical University of Moldova

Ion Tighineanu, Dr.hab., Acad. Academy of Science, Moldova

Ion Vişa, PhD, Professor University Transilvania of Braşov, Romania

Jorj Ciumac, Dr., Professor, Technical University of Moldova

Laurențiu Slătineanu, PhD, Professor Technical University "Gh. Asachi", Iași, Romania

Lee Chow, PhD, Professor, University of Central Florida, USA

Leonid Culiuc, Dr.hab., Acad. ASM, Institute of Applied Physic

Livia Nistor-Lopatenco, Ph.Dr. in Engineering, Associate Professor, Technical University of Moldova

Mardar Maryna, Doctor of Technical Science, Professor, Odessa National Academy of Food Technologies, Odessa, Ukraine

Mitrofan Ciobanu, academic MAS, Dr.Sc.,PhD, Professor Tiraspol State University, Chişinău, Republic of Moldova

Natalia Tislinschi, Dr., Ass. Professor, Technical University of Moldova

Oleg Lupan Dr.hab. Professor, Technical University of Moldova

Pavel Tatarov, Dr. hab., Professor, Technical University of Moldova

Pavel Topală, Dr.Sc., PhD, Professor, State University "Aleco Russo" from Bălți, Republic of Moldova

Peter Lorenz, PhD, Professor University of Applied Science Saar, Saarbrucken, Germania

Petru Cașcaval, PhD, Professor, "Gheorghe Asachi" Technical University of Iasi, Romania

Petru Stoicev, Dr.Sc., PhD, Professor, Technical University of Moldova, Chişinău, Republic of Moldova

Polidor Bratu, PhD, academic RATS, president ICECON S.A. București, Romania Radu Munteanu, PhD, Professor Technical University of Cluj Napoca, Romania Radu Sorin Văcăreanu, Dr. hab. Professor, Technical University of Civil Engineering Bucharest, Romania

Sergiu Zaporojan Dr., Professor, Technical University of Moldova
Spiridon Creţu, PhD, Professor Technical University "Gh. Asachi", Iaşi, Romania
Eden Mamut, PhD, Professor University "Ovidius" Constanţa, România
Stanislav Legutko, PhD, Professor Poznan University of Technology, Poland
Rafał Gołębski, Dr., Ass. Professor, Częstochowa University of Technology, Poland
Stefan Tvetanov, Dr., Professor, University of Food Technologies, Bulgaria
Ştefan-Gheorghe Pentiuc, Dr., Professor, University "Stefan cel Mare" of Suceava, Romania
Svetlana Albu, Dr. hab. Professor, Technical University of Moldova

Thomas Luhmann, Dr-Ing. habil. Dr. h.c. Professor, Jade University of Applied Sciences, Germany Tudor Ambros, Dr.Sc., PhD, Professor, Technical University of Moldova, Chişinău, Republic of Moldova

Valentin Arion, Dr.Sc., PhD, Professor, Technical University of Moldova, Chişinău, Republic of Moldova

Valentina Bulgaru, PhD, Assoc. professor, Technical University of Moldova, Chişinău, Republic of Moldova

Valeriu Dulgheru, Dr.Sc., PhD, Professor, Technical University of Moldova, Chişinău, Republic of Moldova

Vasile Tronciu Dr.hab. Professor, Technical University of Moldova

Victor Ababii, Dr. Professor, Technical University of Moldova

Victor Sontea Dr. Professor, Technical University of Moldova

Vilhelm Kappel, PhD, Institute of Research INCDIE ICPE-CA, Bucharest, Romania

Vladimir Zavialov, Dr. hab., Professor, National University of Food Technology, Ucraine

Vladislav Resitca, Dr., Ass. Professor, Technical University of Moldova

Yogendra Kumar Mishra, Dr. habil., Kiel University, Germany

Yuri Dekhtyar, Professor, Riga Technical University, Riga, Latvia

Responsible Editor Dr. hab. Rodica STURZA

Editorial Board address: jes@meridian.utm.md

Editorial Production:

Dr. hab. Aliona Ghendov-Moşanu Dr. Nicolae Trifan Dr. Țurcan Iuliu Dr. Svetlana Caterinciuc Dr. Rodica Cujba

CONTENT

A. Industrial Engineering		
Mihail Bîcioc	Technological assurance of mechanical processing of complex shaped parts based on machining centers with numerical control	8
Efim Arama, Valentina Pintea, Tatiana Shemyakova, Natalia Gasitoi	Growth of single crystals, photoelectric properties and the absorption edge of a new layered CuGa _{2.5} In _{2.5} S8 compound	18
Petru Todos, Ghenadie Tertea, Ilie Nuca	Harmonic analysis of magnetomotive force in the air gap of six- phase asynchronous machines	27
Maria Rotaru	Statistical simulation of reliability of networks with exponentially distributed unit lifetimes	44
Valentin Oleschuk	Flexible synchronous regulation of power electronic blocks of transformer-based photovoltaic stations	54
B. Electronics and Compute	r Science	
Ion Bolun	Performance required for common-use components of computer networks	63
Victor lapăscurtă, Dinu Țurcanu, Rodica Siminiuc	Integration of a data-driven software application and a multimodal large language model for enhanced nutritional guidance: a case study	<i>75</i>
C. Architecture, Civil and E	nvironmental Engineering	
Vladimir Polcanov, Alina Polcanova, Alexandru Cîrlan	Ensuring the long-term stability of deep cutting slopes formed by clay soils on Republic of Moldova roads	85
Aminu S. Dangamba, Toyese Oyegoke, Favour E. Ocheje, Mahmud A. Dikko, Mohammed S. Galadima	Evaluating the adsorption potential of sugarcane bagasse and lemongrass for Chromium (VI) removal in wastewater treatment	96
D. Food Engineering		
Natalia Vladei, Alexandra Arseni	Influence of potato and pea protein fining on the chromatic profile features of Rara Neagra wine	117
Svetlana Erşova, Olesea Saitan, Ruslan Tarna, Iurie Rumeus, Georgiana Gabriela Codină, Aliona Ghendov-Mosanu	Integration of spent grain into food products	130

Corina Tașca	Characteristics of biomass resulting from agro-industrial processes and possibilities of its evaluation in the context of the circular bioeconomy
Olga Smerea, Viorica Bulgaru	Anthocyanins – methods of extraction, stabilization and applications
Elena Sergheeva, Natalia Netreba	Oil crop pomace as a potential source of protein and dietary fiber.
	CUPRINS
A. Industrial Engineering	
Mihail Bîcioc	Asigurarea tehnologică a procesului de prelucrare mecanică a pieselor cu forme complexe pe centre de prelucrare cu comandă numerică
Efim Arama, Valentina Pintea, Tatiana Shemyakova, Natalia Gasitoi	Creșterea monocristalelor, proprietățile fotoelectrice și limitele de absorbție ale noului compusului stratificat CuGa _{2,5} In _{2,5} S ₈
Petru Todos, Ghenadie Tertea, Ilie Nuca	Analiza armonică a forței magnetomotoare în întrefierul mașinilor asincrone hexafazate
Maria Rotaru	Simularea statistică a fiabilității rețelelor cu durata de viață a unităților distribuite exponențial
Valentin Oleschuk	Reglare sincronă flexibilă a blocurilor electronice de putere a stațiilor fotovoltaice bazate pe transformator
B. Electronics and Compute	er Science
Ion Bolun	Performanța necesară a componentelor de uz comun ale rețelelor de calculatoare
Victor lapăscurtă, Dinu Țurcanu, Rodica Siminiuc	Integrarea unei aplicații software cu date și a unui model de limbaj mare multimodal pentru orientare nutrițională îmbunătită: un studiu de caz
C. Architecture, Civil and E	Environmental Engineering
Vladimir Polcanov, Alina Polcanova, Alexandru Cîrlan	Asigurarea stabilității de lungă durată a taluzurilor săpăturilor adânci formate din pământuri argiloase pe drumurile Republicii Moldova
Aminu S. Dangamba, Toyese Oyegoke, Favour E. Ocheje, Mahmud A. Dikko, Mohammed S. Galadima	Evaluarea potențialului de adorbiție al borhotului de trestie de zahăr și lemongrass pentru eliminarea Cromului (VI) în tratarea apelor uzate

D. Food Engineering		
Natalia Vladei, Alexandra Arseni	Influența tratării cu proteine de cartof și măzare asupra caracteristicilor profilului cromatic al vinului Rara Neagra	117
Svetlana Erşova, Olesea Saitan, Ruslan Tarna, Iurie Rumeus, Georgiana Gabriela Codină, Aliona Ghendov-Mosanu	Integrarea borhotului în sistemul de obținere a produselor alimentare	130
Corina Tașca	Caracteristica biomasei rezultate din procese agro-industriale și posibilității de valorificare în contextul bioeconomiei circulare	156
Olga Smerea, Viorica Bulgaru	Antocianine – metode de extracție, stabilizare și aplicații	179
Elena Sergheeva, Natalia Netreba	Şrot de oleaginoase ca sursa potențială de proteine și fibre alimentare	196

Vol. XXXI, no. 3 (2024), pp. 8 - 17 ISSN 2587-3474 eISSN 2587-3482

https://doi.org/10.52326/jes.utm.2024.31(3).01 UDC 621.914:004





TECHNOLOGICAL ASSURANCE OF MECHANICAL PROCESSING OF COMPLEX SHAPED PARTS BASED ON MACHINING CENTERS WITH NUMERICAL CONTROL

Mihail Bîcioc ', ORCID: 0009-0009-3319-6744

Technical University of Moldova, 168 Stefan cel Mare, Blvd., Chisinau, Republic of Moldova

*Corresponding author: Mihail Bîcioc, mihail.bicioc@doctorat.utm.md

Received: 08. 21. 2024 Accepted: 09. 25. 2024

Abstract. To achieve high precision in the machining of complex-shaped parts, the correct combination of technologies with the machining center is necessary, especially if it has only 3 axes, to obtain the best results. The present study focuses on technological assurance of the mechanical processing of complex-shaped parts on Computer Numerical Control (CNC) machining centers. The study proposes a methodology for optimizing the machining process by implementing appropriate technological measures, such as tool selection, cutting parameters, and cost-effective process planning. The proposed methodology aims to enhance the quality and productivity of the machining process while minimizing the production time and cost. The results of the study demonstrate the effectiveness of the proposed methodology in improving the machining performance and achieving the desired product quality.

Key words: CNC milling, technological assurance, complex surfaces, manufacturing efficiency, three-axis machines.

Rezumat: Pentru a obține o mare precizie în prelucrarea pieselor de formă complexă este necesară combinarea corectă a tehnologiilor cu centrul de prelucrare, mai ales dacă are doar 3 axe, pentru a obține cele mai bune rezultate. Prezentul studiu se concentrează pe asigurarea tehnologică a procesului de prelucrare mecanică a pieselor de formă complexă pe centrele de prelucrare cu comandă numerică. Studiul propune o metodologie de optimizare a procesului de prelucrare prin implementarea măsurilor tehnologice adecvate, cum ar fi selecția sculelor, parametrii de tăiere și planificarea procesului eficient din punct de vedere al costurilor. Metodologia propusă urmărește să sporească calitatea și productivitatea procesului de prelucrare, minimizând în același timp timpul și costul de producție. Rezultatele studiului demonstrează eficacitatea metodologiei propuse în îmbunătățirea performanței de prelucrare și atingerea calității dorite a produsului.

Cuvinte cheie: Frezare CNC, asigurare tehnologică, suprafețe complexe, eficiență în fabricație, mașini cu trei axe.

M. Bîcioc 9

1. Introduction

Today, Computer Numerical Control (CNC) machining centers have become essential in the modern mechanical processing industry. These machines are programmed to carry out complex operations with increased precision and efficiency, reducing the need for manual intervention and allowing for the production of superior quality products. To maximize performance and minimize errors in the mechanical processing process, it is important to ensure appropriate technology [1], choose and use durable tools [2,3], and ensure adequate High-Speed Machining (HSM) [4,5].

The profitability of the machining process is an important concern for any modern company. Additionally, the frequent change in quality conditions and the complexity of prismatic bodies make the machining process more difficult and costly. In the case of parts with complex shapes that require multiple technological operations, it is important to find solutions to ensure the required quality and precision. This may involve the use of more advanced machining technologies as well as the development of more efficient machining strategies. Furthermore, it is important to consider the costs and time required for each technological operation in order to achieve optimal profitability of the machining process.

The economic instability in recent years has made it difficult to acquire state-of-the-art equipment, especially for small companies. In this situation, 3-axis CNC machines remain a viable solution, offering many advantages in terms of serviceability and ease of use. However, if we focus on machining complex parts, 3-axis machines have disadvantages, such as ensuring precision, especially for the machining of complex parts, due to the limitation of movement.

There is an impressive volume of studies and research in the field, which have focused on various issues such as energy consumption [6], but a great emphasis has been placed on optimizing the actual execution stage, leading to the development of different methods and techniques of optimization [7,8]. In most cases, ensuring manufacturing processes is the priority criterion throughout the manufacturing chain, responding promptly from the product design stage, process planning, operation scheduling, tooling, and actual execution.

Therefore, the technological assurance of the machining process remains a problem that can still be studied and improved, especially in the context of our goal to maintain competitiveness and efficiency of the machining process on 3-axis machine tools in the future. Due to the movement limitations of 3-axis CNC machines, parts with complex surfaces require a different or rather particular approach due to areas that cannot be described by a simple equation or a standard geometric form. The combinations of curves, planes, sophisticated contours, and specific details represented by these surfaces create difficulties for the traditional method of realization and manufacturing. Therefore, there is an observed increase in the number of parts with complex shapes that become crucial in the aesthetic functionality and performance of mechanisms in various industries, creating new challenges for engineers.

Complex parts (Figure 1) have a wide range of applications in various industries and sectors, including the automotive, aviation, aerospace, medicine, and pharmacy industries. These parts are used as critical components such as engines, turbines, radiators, surgical instruments, separation devices, or prostheses, to provide superior performance and necessary solutions for users. As can be seen in modern industry, the use of complex-shaped parts is a key element.

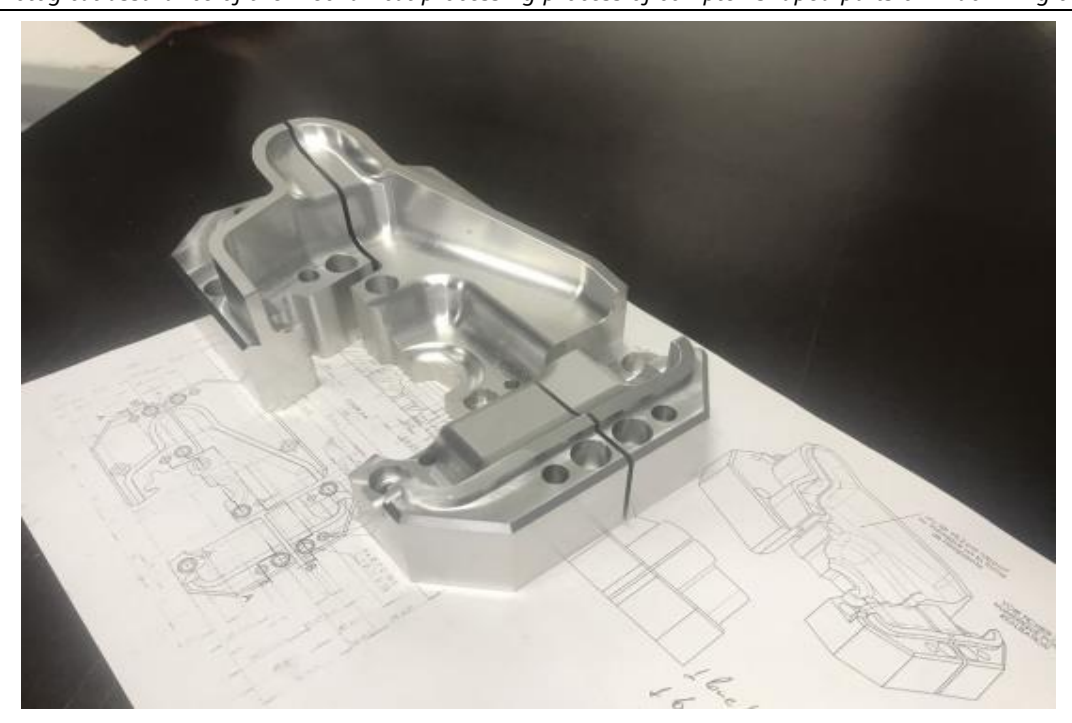


Figure 1. Assembly from different parts with complex shape [9].

In this context, ensuring the technological assurance of the machining process becomes crucial, and investment in advanced technological solutions such as appropriate software, strategies, or tools becomes the main element of success.

It is true that mechanical machining is an extremely important aspect in today's industry, and companies need to pay special attention to the machining processes to ensure efficient, precise, and high-quality production. In an increasingly competitive environment, the quality and efficiency of the machining process make the difference between success and failure. Therefore, it is important for companies to consider these aspects and invest in advanced technologies and adequate technological assurance to maintain their competitiveness.

Even though mechanical machining has made significant progress in recent decades, there are still challenges in achieving precise machining operations, strict tolerances, complex geometries, difficult-to-machine materials, or high productivity requirements, especially for owners of older machines such as 3-axis CNC machining centers, which face difficulties in performing certain operations. It is important to emphasize that technological assurance is not just an optional choice but an imperative necessity for companies in the machining industry.

As early as Wolfgang Kuehn. [10–13] pointed out that the digital factor, namely 3D simulation and visualization software, is the key to development, which can be introduced at various stages to improve product and process planning. Of course, since then, the software has evolved into an intelligent CAD/CAM system [14], responding to simple but automated CNC machine programming through the use of artificial intelligence and automatic learning. There is a myriad of products on the market that develop three-dimensional models and offer programming and toolpath visualization possibilities, or even the entire machine tool [9]. The most well-known ones are: SolidCam, NX, ArtCAM, Mastercam, Esprit, PowerMill, Fusion 360, each having specific features that make it difficult to choose the best software [15].

M. Bîcioc 11

2. Materials and Methods

A case study was conducted for the development of this article, describing an existing machining process on a complex component produced on a 3-axis machine. For the experimental part, a 3D model was developed, used in ultrasonic welding installations for plastic material. Figure 2 represents the machined model, consisting of a set of 3 components labeled as 1, 2, and 3, each having a number of complex zones labeled as A, B, and C.

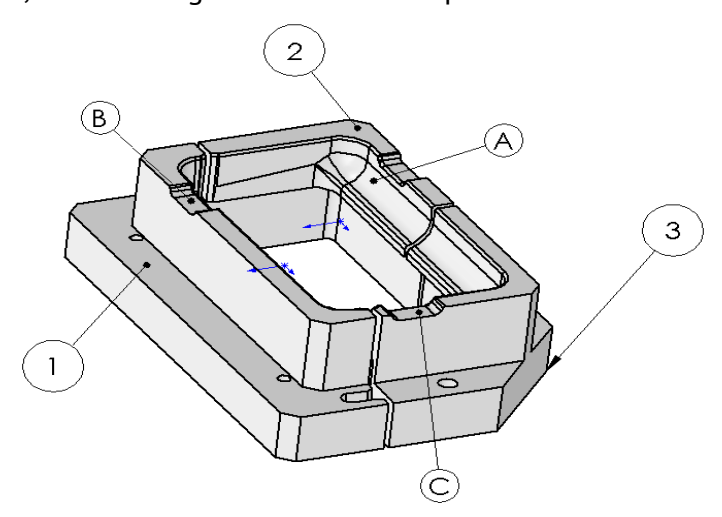


Figure 2. Analysis of the experimental model. The three components of the assembly are numbered by the number 1, 2 and 3, and by the letters A, B and C their complex areas are represented.

This model was created in Solidworks 2021 software. The process technology was developed for the 3-axis machining center AWEA AF 1000, utilizing a total of 14 tools for the execution of the work. The program for the technological process was created in Solidcam 2016 and processing time for each component is presented in Table 1.

Table 1

Track number	Number of Tools	Number of Installations	Total time, min
1	11	3	120
2	11	3	164
3	11	4	173

Processing time for each component

To improve this manufacturing process, it is necessary to first conduct an analysis following the steps mentioned above. After examining the program, it was identified that the most costly stages are the roughing and finishing of the complex surfaces, Figure 3.

This operation is carried out using an 8 mm ball nose tool with parameters described in table 2, using the HSS (High-Speed Steel) machining technique. The Paralel Cuts Constant Z technique is a constant machining technique that allows for obtaining a uniform and precise finish in a shorter time and with reduced effort.

This operation is carried out using an 8 mm ball nose tool with parameters described in table 2, using the HSS (High-Speed Steel) machining technique. The Paralel Cuts Constant Z technique is a constant machining technique that allows for obtaining a uniform and precise finish in a shorter time and with reduced effort.

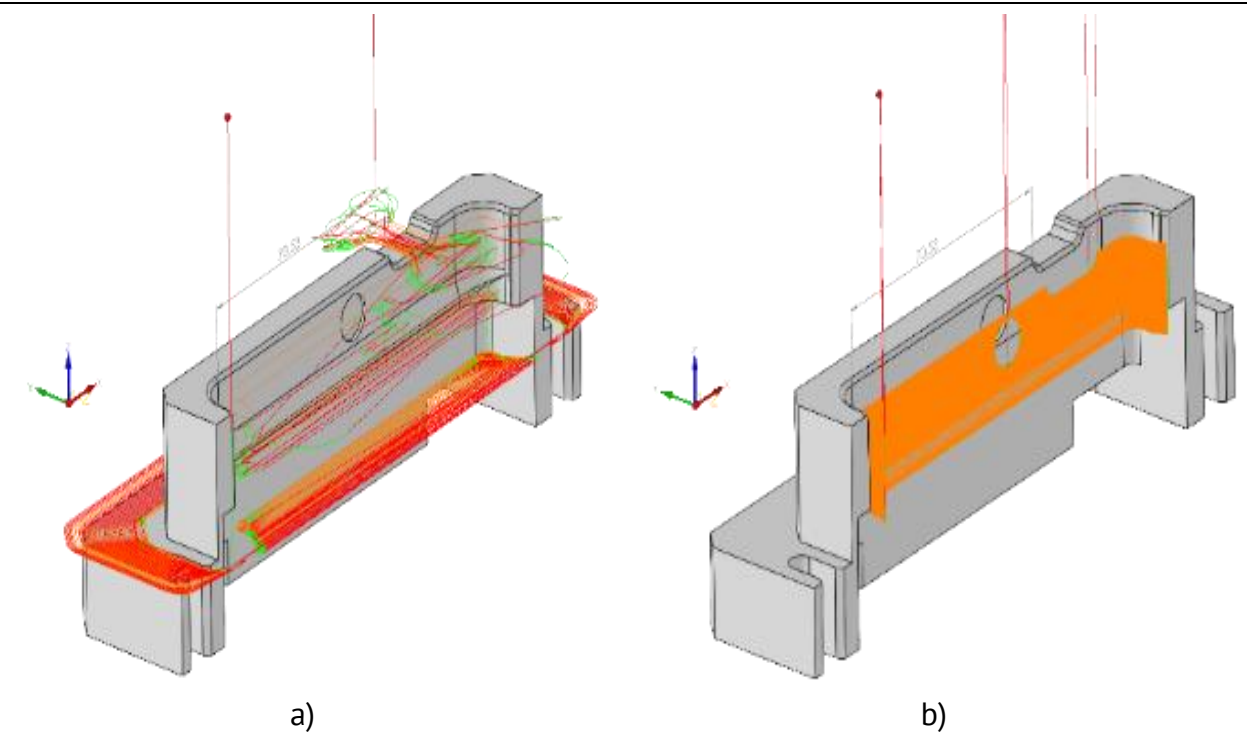


Figure 3. The area with the longest processing time. a) roughing operation; b) finishing operation.

Table 2

Tool parameters

Specification	Information
Diameter	4 mm
Shank	4 mm
Cutter length	15 mm
Rotation speed	6500 rpm
Cutting Depth	1/3 D
Cutting Width	1/2 D
Single Edge Feed	0.15 mm

Within the presented research framework, the discussion of surface roughness is focused on the universally recognized Rz.



Figure 4. Measurement of surface roughness using Form Talysurf 50 (Taylor Hobson Co Ltd).

M. Bîcioc 13

3. Solving the fixing problem

The examination of the second and third models showed that, in addition to the long processing times in the finishing and roughing operations, there is a problem with the fixation of the components, resulting in small linear errors and the occurrence of vibrations.

Following the analysis, it has been decided to use a 10 mm tool for the finishing operation. This decision was made due to the advantages offered by using a larger tool, such as easier access along the machined surface and a reduction in the total processing time.

In order to ensure better fixation of the part during the operation, a technological support has been developed. It is an essential component in the processing process, as it ensures stability and accuracy in positioning the part.

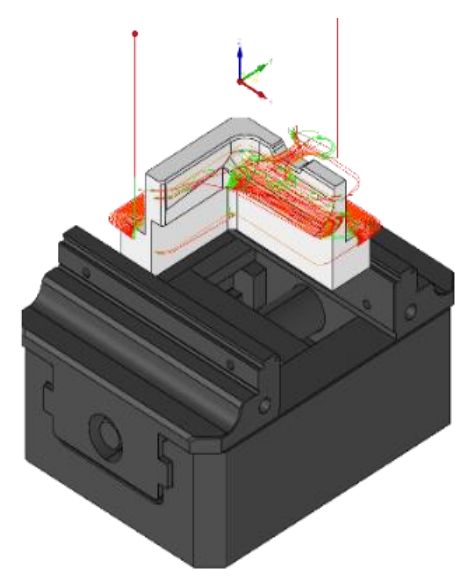


Figure 5. Fixing problems.

The technological support (Figure 5) is composed of the mirrored surfaces of the finished part, allowing for a solid and precise fixation of the part during the finishing operation. This support is designed to maintain the part in a stable position and provide easy access to the tool. Two technological holes were made to attach the support to the machine.

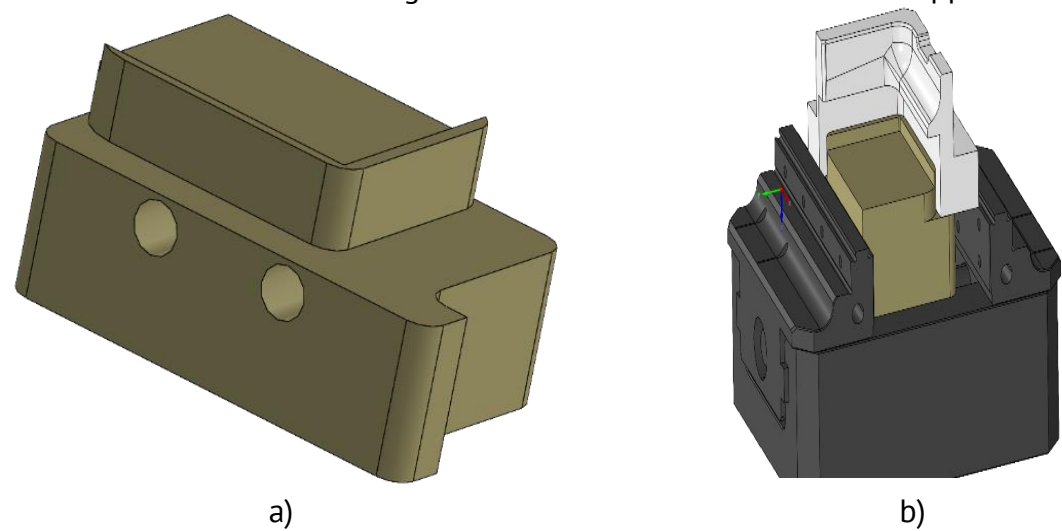


Figure 6. Technological support.

a) technological support; b) the assembly.

These holes are essential for proper mounting and fixation of the technological support onto the machine. By using these holes, the support is fixed in a secure and stable

position, capable of withstanding the general forces and vibrations during the finishing operation.

4. Results and Discussion

The values obtained from the data analysis for the two finishing options, the initial one and the optimized one, are presented in Table 3 for comparation.

Table 3 The times obtained between the initial method and the optimized one

	Finishing, min	Fixation, min
The initial example	0:14:27	0:02:45
The optimized example	0:11:28	0:03:15

The data presented shows that in terms of finishing time, the optimized option resulted in a reduction of approximately 3 minutes compared to the initial option. However, the time required for fixing the part on the support slightly increased for the optimized option. In terms of the quality of the obtained surfaces, the optimized option managed to produce more uniform surfaces without visible defects compared to the initial option. Figures 7 and 8 display the acquired results, with a slight variation in the Rz parameter, which is 1.26 in the first figure and 1.24 in the second. These results suggest that optimizing the finishing process led to an improvement in the quality of the processed surfaces, even though the fixing time slightly increased.

It is important to mention that these data are estimations and may vary depending on the machine and support specifications, as well as the quality and dimensions of the part. Therefore, we can recommend testing and adjusting the finishing process for each individual part to ensure maximum quality of the processed surfaces and optimization of processing time.

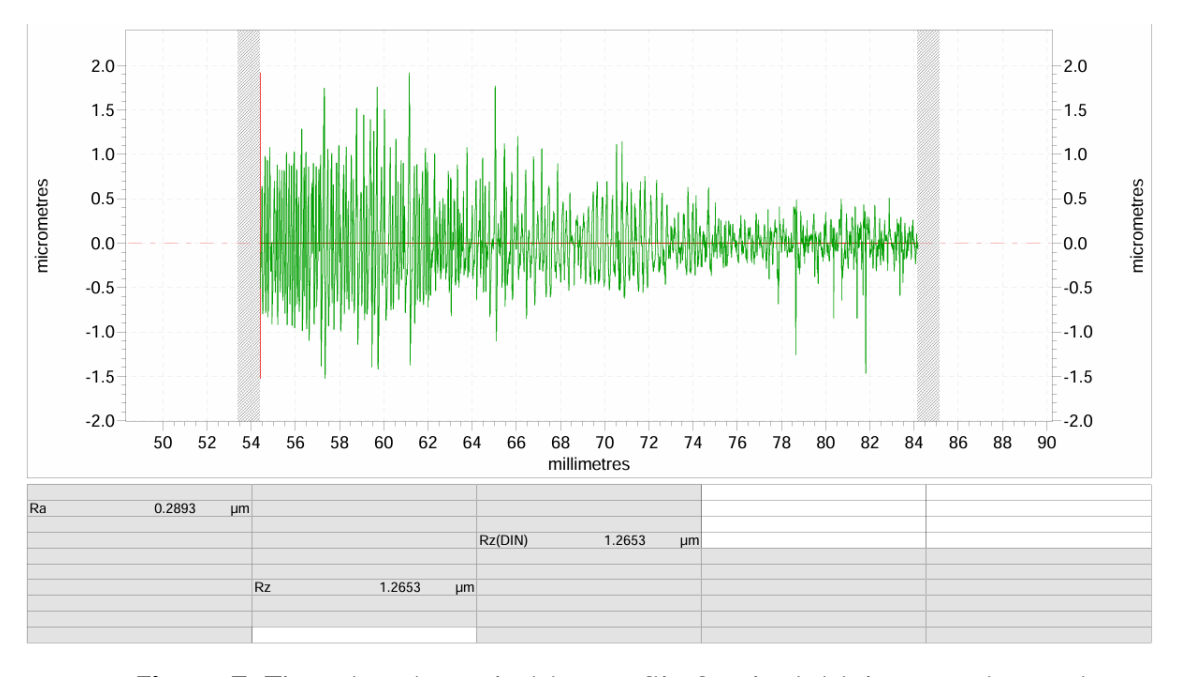


Figure 7. The micro-irregularities profile for the initial processing variant.

M. Bîcioc 15

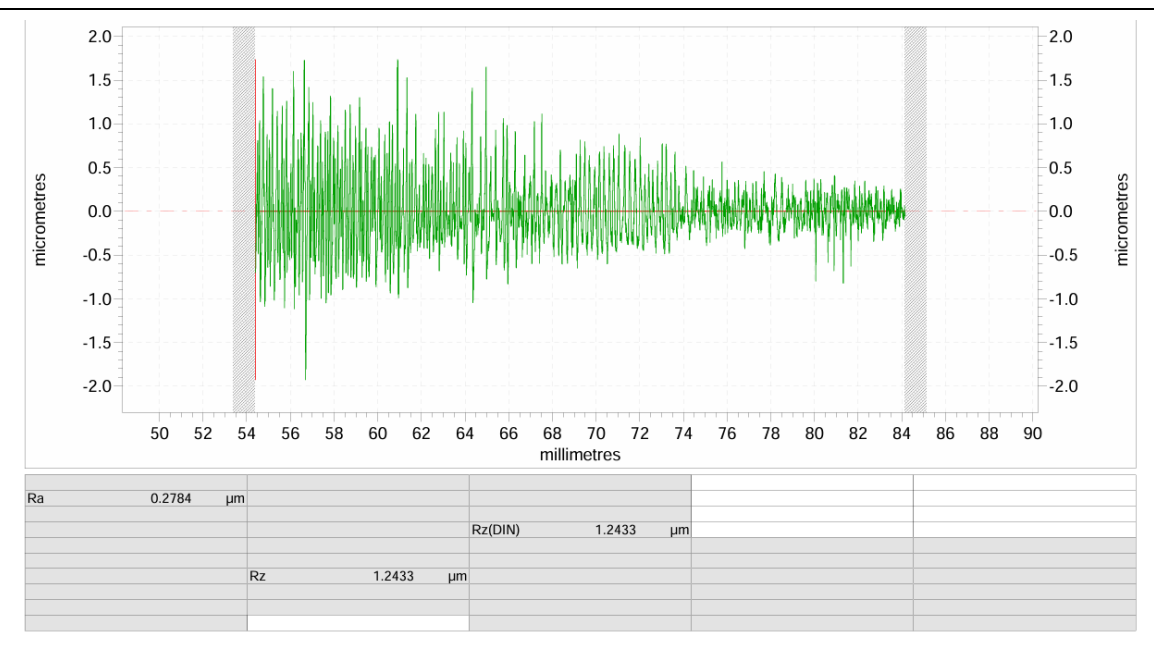


Figure 8. The micro-irregularities profile for the optimized processing variant.

The necessity of using special fixing supports for complex parts is not limited to this work alone, as exemplified in Wojnarowska's study [16]. For instance, in his research, he also proposed a support system for processing medical objects with complex geometry, such as cranial bone prostheses. He introduced a vacuum clamping system that proved the method's utility in producing complex components on a 3-axis milling machine, achieving good results in terms of surface roughness and precision. Additionally, a clamping support was put forth by Adli [17] to secure the pieces in place and consistently enhance the grip on thin parts during processing. In 2022, Ferchow [18] proposed integrated screw fixing supports, enabling the attainment of surface roughness results with a maximum Ra value of 1.42 μ m.

Ensuring precision and surface quality on 3-axis machines remains an ongoing area of research. To address these parameters, Eckert [19] presented a new clamping system based on a pneumatic chuck with three gripping jaws controlled by force to manage workpiece deformation. This was combined with a visual model recognition system to ensure high repeatability in positioning, achieving results with a repeatability of $\pm 0.1~\mu m$.

Consequently, it can be confidently stated that clamping systems are imperative for securing parts on 3-axis CNC machines, thereby enhancing surface precision and quality. Furthermore, these systems provide rigid and precise fixation, eliminating unwanted vibrations and movements during processing, thereby contributing to high-quality outcomes and increased productivity.

5. Conclusions

In conclusion, the analysis of the data obtained from the modifications made to the processing and fixing process of the parts showed that using a dedicated technical support during processing and optimizing the finishing process can lead to a reduction in processing time and an improvement in the quality of the obtained surfaces confirmed in the roughness analyses.

However, it is important to consider the costs and efforts involved in designing and manufacturing a dedicated technical support for each individual part in order to optimize the processing process and ensure maximum quality of the processed surfaces.

Furthermore, the optimization of the finishing process needs to be done on an individual basis for each part, taking into consideration the machine and support specifications, as well as the quality and dimensions of the part.

Therefore, these improvements can result in a significant enhancement of the processing processes and the production of higher quality parts.

Conflicts of Interest: The author declares no conflict of interest.

References

- 1. Toca, A.; Stroncea, A.; Stîngaci, I. Esenţa şi efectele compensării erorilor la prelucrarea mecanică. *Fiz. Tehn. Proc. Model. Exp.* 2012, 2, pp. 37–43.
- 2. Zhang, D. L.; Guo, J. L.; Zhou, T. R. CNC milling tool of choice to explore. *Adv. Mater. Res.* 2013, 706–708, pp. 1246–1249.
- 3. Yinsheng, W. Influence of CNC Tools on CNC Machining Technology. In: *IOP Conf. Ser.: Mater. Sci. Eng.*, Proceedings of the IOP Conference Series: Materials Science and Engineering, Montreal, Canada, 19 May 2019; IOP Publishing: Bristol, UK, 2019, 569(3), 032043.
- 4. Jacso, A.; Sikarwar, B. S.; Phanden, R. K.; Singh, R.; Ramkumar, J.; Sahu, G. R. Optimisation of tool path shape in trochoidal milling using B-spline curves. *Int. J. Adv. Manuf. Technol.* 2022, 121, pp. 3801–3816.
- 5. Wagih, M.; Maher, I.; El-Hofy, H.; Yan, J.; Hassan, M. A. Analysis and development of elliptical tool path in trochoidal milling. *CIRP J. Manuf. Sci. Technol.* 2023, 47, pp. 168–183.
- 6. Anderberg, S.; Beno, T.; Pejryd, L. Energy and cost efficiency in CNC machining from a process planning perspective. In: *Sustain. Manuf.: Shaping Global Value Creation*; 2012; pp. 393–398.
- 7. Moshat, S. Optimization of CNC end milling process parameters using PCA-based Taguchi method. *Int. J. Eng. Sci. Technol.* 2010, 2, pp. 95–102.
- 8. Ramli, K. D. N. R. Application of artificial intelligence methods of tool path optimization in CNC machines: A review. *Res. J. Appl. Sci. Eng. Technol.* 2014, 8, pp. 746–754.
- 9. Assembly from different parts with complex shape. Available online: https://isomeca-grup.com/works (accessed on 12 November 2023).
- 10. Kuhn, W. Digital Factory Simulation Enhancing the Product and Production Engineering Process. In: *Proc.* 2006 Winter Simul. Conf., Monterey, USA, 2006; pp. 1899–1906. doi: 10.1109/WSC.2006.322972.
- 11. Klancnik, S.; Brezocnik, M.; Balic, J. Intelligent CAD/CAM system for programming of CNC machine tools. *Int. J. Simul. Model.* 2016, 15, pp. 109–120.
- 12. Balic, J. Model of automated computer aided NC machine tools programming. *J. Achiev. Mater. Manuf. Eng.* 2006, 17, pp. 309–312.
- 13. Zhao, G.; Cheng, K.; Wang, W.; Liu, Y.; Dan, Z. A milling cutting tool selection method for machining features considering energy consumption in the STEP-NC framework. *Int. J. Adv. Manuf. Technol.* 2022, 120, pp. 3963–3981.
- 14. Wang, L. Remote real-time CNC machining for web-based manufacturing. *Robotics Comput. Integr. Manuf.* 2004, 20, pp. 563–571.
- 15. Matusova, M. Review of critical skills analysis in NC programming education. *Acta Tech. Napocensis Ser. Appl. Math. Mech. Eng.* 2024, 67, 1s.
- 16. Wojnarowska, W.; Kwolek, M.; Miechowicz, S. Selection of a workpiece clamping system for computer-aided subtractive manufacturing of geometrically complex medical models. *Open Eng.* 2021, 11, pp. 239–248.
- 17. Adli, M. A.; Ab Wahab, N.; Abd Razak, M. H.; Azizzi, M. R.; Bakar, M. H. A.; Sasahara, H.; et al. Micro-Influence of Vacuum Block Positions on Machinability of Acrylic Using Hybrid Vacuum Clamping System. *Int. J. Nanoelectron. Mater.* 2021, 14, pp. 145–158.
- 18. Ferchow, J.; Kälin, D.; Englberger, G.; Schlüssel, M.; Klahn, C.; Meboldt, M. Design and validation of integrated clamping interfaces for post-processing and robotic handling in additive manufacturing. *Int. J. Adv. Manuf. Technol.* 2022, pp. 1–27.
- 19. Ben-Hanan, U.; Eckert, U.; Mende, M.; Weiss, A.; Wertheim, R.; Azaria, U. Development of a Pneumatic Clamping System with Position and Force Control Machining. In: *Proceedings of the Global Conference on Sustainable Manufacturing*, Cham, Switzerland, 2022, pp. 184–192.

M. Bîcioc 17

Citation: Bîcioc, M. Technological assurance of the mechanical processing process of complex shaped parts on machining centers with numerical control. *Journal of Engineering Science* 2024, XXXI (3), pp. 8-17. https://doi.org/10.52326/jes.utm.2024.31(3).01.

Publisher's Note: JES stays neutral with regard to jurisdictional claims in published maps and institutional affiliations.



Copyright:© 2024 by the authors. Submitted for possible open access publication under the terms and conditions of the Creative Commons Attribution (CC BY) license (https://creativecommons.org/licenses/by/4.0/).

Submission of manuscripts:

jes@meridian.utm.md

https://doi.org/10.52326/jes.utm.2024.31(3).02 UDC 621.315.5:535





GROWTH OF SINGLE CRYSTALS, PHOTOELECTRIC PROPERTIES AND THE ABSORPTION EDGE OF A NEW LAYERED CuGa2.5In2.5S8 COMPOUND

Efim Arama ¹, ORCID: 0009-0005-8606-6266, Valentina Pintea ^{2*}, ORCID: 0000-0003-0137-4699, Tatiana Shemyakova ³, ORCID: 0000-0003-1668-0082, Natalia Gasitoi ⁴, ORCID: 0000-0002-5895-286X

¹"Nicolae Testemitanu" State University of Medicine and Pharmacy, Chisinau, Republic of Moldova

² Technical University of Moldova, Chisinau, Republic of Moldova

³ Institute of Applied Physics, Chisinau, Republic of Moldova

⁴Alecu Russo State University of Balti, Department of Mathematics and Informatics,

Balti, Republic of Moldova

* Corresponding author: Valentina Pintea: valentina.pintea@fiz.utm.md

Received: 09. 05. 2024 Accepted: 09. 30. 2024

Abstract. In this article, the conditions for obtaining monocrystals of $CuGa_{2.5}In_{2.5}S_8$, were investigated, their optical absorption edge, electrical and photoelectric properties. Using the criteria for the formation of new layered chalcogenides with octahedral and tetrahedral coordination of cations, it was hypothesized that due to the replacement of half of the In atoms in the $CuIn_5S_8$ spinel with Ga, which has a pronounced tendency to occupy the tetrahedral B sites in a denser packing of S atoms, a layered phase is formed. Melting of a stoichiometric mixture of Cu+2.5Ga+2.5In+8S led to the synthesis of a previously unknown single-phase product with a layered crystalline structure. Since copper, gallium, and indium sulfides are generally good photoconductors, it could be expected that the new compound would also exhibit high photosensitivity. The aim of this work was to investigate the conditions for obtaining of $CuGa_{2.5}In_{2.5}S_8$ single crystals, their optical absorption edge, electrical and photoelectric properties.

Keywords: ternary semiconductors, optical absorption, photoluminescence, photoconductivity, chalcogenides.

Rezumat. În acest articol, au fost investigate condițiile pentru obținerea monocrystalelor de CuGa_{2.5}In_{2.5}S₈, limita de absorbție optică și proprietățile lor electrice și fotoelectrice. Folosind criteriile pentru formarea noilor chalcogenide stratificate cu coordonare octaedrică și tetraedrică a cationilo, s-a admis că substituind jumătate dintre atomii de In din spinelul CuIn₅S₈ cu Ga, care prezentau o tendință pronunțată de a ocupa spațiile tetraedrice B într-o împachetare mai densă a atomilor de S, s-a format o fază stratificată. Fuziunea unui amestec stochiometric de Cu+2,5Ga+2,5In+8S a condus la sinteza unui produs monofazic necunoscut anterior, cu o structură cristalină stratificată. Având în vedere că sulfatul de cupru, galiu și indiu sunt, în general, buni fotoconductori, se putea aștepta că noul compus să prezinte, de asemenea, o sensibilitate fotoelectrică ridicată. Scopul acestei lucrări a fost de a investiga

condițiile de obținere a monocrystalelor de CuGa_{2,5}In_{2,5}S₈, limita de absorbție optică și proprietățile lor electrice și fotoelectrice.

Cuvinte cheie: compuși ternari semiconductori, absorbție optică, fotoluminescență, fotoconductivitate, calcogenizi.

1. Introduction

Semiconductor sulfide compounds of the class $A^{II}B_2^{III}C_4^{VI}$ (where A – Zn, Cd and B – In, Ga) are actively researched due to their unique physical properties – intense photoluminescence [1, 2] and high photosensitivity over a wide spectral range [2, 3]; they are high-resistance and stable under normal atmospheric conditions. In particular, the optical absorption, reflection, photovoltaic, and emission properties of ternary single crystals are described [2–4], which include various polytypic modifications [5, 6]. It has been demonstrated that CuGa_{2.5}In_{2.5}S₈ single crystals in the form of low-resistance thin films are a promising material for use in n-p type solar cells [7].

Criteria for the formation of new layered chalcogenides with octahedral and tetrahedral coordination of cations are presented in [8-10]. The groups of layered crystals according to their crystallochemical properties are also described in the generalization works [11-14]. Another classification of layered crystals can be based on the type of the element that serves as the source of anions. Substances containing chalcogens (*S*, *Se*, *Te*) as anions also form groups of chalcogenides and are classified as semiconductors.

Layered chalcogenide structures occupy a special place in the theory and applicability of solid-state materials. Various technological methods are used to obtain high-quality single crystals of these compounds, and different experimental and well-established theoretical methods are employed for structural studies. One of the most accessible technological methods known in the literature is a method of chemical transport reactions. This method is widely used for growing single crystals of various compounds from this family.

Monocrystals of $CuGa_{2.5}In_{2.5}S_8$ were obtained using chemical transport reactions in a closed system with iodine as a transportation agent. The advantage of this method is determined by the fact that chemical transport reactions occur at relatively low temperatures compared to other direct methods. The method of chemical transport reactions allows for the growth of single crystals with advanced parameters, of high quality, in the form of plates with an optically high-quality exterior surface. The perfection of the surface and the alignment of the main crystal faces enable the use of these crystals in devices, instruments, and for investigations of physical properties without the need for mechanical surface processing.

2. Experimental methodology

As a source of materials for crystal growth, the easily volatile components of chemical compounds can serve, which are subjected to thermal dissociation or appropriate recovery on the growth surface.

In this case, the crystallization processes occur in two successive stages: 1) the release (emission) of the substance as a result of the chemical decomposition reaction; 2) the incorporation of atoms into the crystalline lattice.

For the selection of substances, reversible heterogeneous reactions are used, the equilibrium constants of which, as usual, depend on temperature and the concentrations of all gaseous compounds. This means that even with some changes in conditions, the reversible

chemical process may occur, meaning that instead of crystallizing the substance, its dissolution may take place.

Since gaseous products are released during decomposition reactions, a steady and uniform process requires continuous removal, for which the use of flowing substances is appropriate.

The amount of crystallized substance emitted in a unit of time is determined by the yield of the decomposition reaction of the compound at a given temperature, the concentrations of the components involved in the reaction, and the flow rate of the gas mixture.

The method of transport reactions allows for the production of semiconductor compounds in the form of imperfect and very small crystals, the purity of which is unsatisfactory. Recrystallization of disaggregated compounds through melting or sublimation methods proves, for various reasons, to be ineffective or impossible. In these cases, interesting results can be achieved specifically by using the method of transfer reactions or gas transport reactions.

The essence of transfer reactions lies in the following: when the gaseous reagent A interacts with a solid, non-volatile substance that is to be processed at different temperatures and partial pressures, compounds of varying composition and concentrations of gaseous molecules, of the type ApXq, can be formed. This means the following reaction may occur:

$$X_{(TB)} + A_{(r)} \rightarrow A_p X_q + A_{p^I} X_{q^I} + A_{p^{II}} X_{q^{II}} + \dots,$$
 (1)

where: $X_{(TB)}$ - the solid and non-volatile substance, A_r - gaseous reagent, $A_p X_q$ - the formed chemical compound, $A_{p^I} X_{q^I}$, $A_{p^{II}} X_{q^{II}}$ - different compounds based on the composition and concentrations of gaseous molecules.

Under these conditions, an equilibrium state is established among the different compounds A_pX_q , characterized by fixed partial pressures of all gaseous compounds. If the temperature of the system is instantaneously changed, the equilibrium state will be disrupted, and the composition of the compounds in the mixture will change. With certain fluctuations in temperature (pressure range), the decomposition of one of the gaseous products may occur, resulting in the release of substance X.

Under these conditions, a state of equilibrium is established among the different compounds ApXq, characterized by stable partial pressures of all gaseous compounds. If the temperature of the system is instantaneously changed, the equilibrium state will be disrupted, and the composition of the compounds in the mixture will change. During certain temperature fluctuations (pressure ranges), the decomposition of one of the gaseous products may occur, resulting in the elimination of substance X.

Based on the experiment, we can highlight the following thermodynamic features of the growth conditions we used to obtain quality compounds and their application in studying the modifications of the energy spectrum characteristics of charge carriers in the investigated single crystals: in the process of crystal formation, the transport rate must not exceed their growth rate; for the homogeneous growth of crystals, it is necessary to maintain a uniform temperature distribution in the growth chamber. When transport occurs via diffusion, single crystals with perfect faces are grown; a well-thought-out selection of transport conditions allowed for the obtaining of crystals that correspond to the initial stoichiometry of the compound [13, 15].

The container consisted of quartz ampoules with an inner diameter of 15 mm and a length of 15 cm. In some experiments, the starting material was a mixture of high purity elemental components taken in stoichiometric ratios, while in other experiments a presynthesized compound $C_UGa_{2.5}In_{2.5}S_8$ was used. In both cases, under a temperature regime of 870 – 820 °C, plate-like monocrystals of deep red color with thicknesses ranging from 2 to 100 μ m and areas up to 80 mm² were grown. The crystals, similar to mica, could be easily cleaved. The advantage of this method lies in the fact that chemical transport reactions occur at relatively low temperatures compared to other direct methods. The chemical transport reaction method enables the growth of single crystals with advanced parameters and high quality, in the form of plates with optically high-quality surfaces. The perfection of the surface and the alignment of the main crystal faces allow these crystals to be used in devices, apparatus, and for investigations of physical properties without the need for mechanical surface processing [16-19].

X-ray studies revealed that the obtained compound crystallizes in a hexagonal lattice with parameters a = 3.82, c = 30.6 Å, and the \vec{c} axis is oriented perpendicular to the plates.

The crystal structure of most layered chalcogenides with octahedral and tetrahedral coordination of cations is described based on the closest hexagonal packing of anions, in which cations are arranged in layers within octahedral and tetrahedral voids [8, 9]. In this arrangement, a certain layer of voids remains completely free. The structural fragment (packet) between two layers of voids is connected to the adjacent packets by van der Waals forces. The obtained value of the c parameter for $CuGa_{2.5}In_{2.5}S_8$ indicates the presence of two five-layer packets (in terms of sulfur layers) in the unit cell. Rewriting the chemical formula of the compound as $Cu_{0.625}Ga_{1.5625}In_{1.5625}S_5$, it is evident that the average (per packet) cation position filling factor amounts to 93.75%, meaning this substance is a type of defective layered chalcogenides with octahedral and tetrahedral coordination and is likely a structural analogue of the known crystal modification GaInS with unit cell parameters a = 3.8134 μ c =30.656 Å belonging to the space group P6 [20, 21]. In the latter substance, cations occupy different layers in the packet with varying density, and the average filling factor is 83.33%. The close values of the unit cell parameters of the two comparable compounds suggest that in the obtained compound the "excess" cations are distributed among the free vacancies in the known structure leading to packet densification.

For the measurements, samples with coplanar indium electrodes and surface-barrier structures (SBS) $Pt-CuGa_{2.5}In_{2.5}S_8$ - In were prepared. In these structures, the semi-transparent platinum and dense indium contacts were deposited on opposite faces of the plates by thermal vacuum evaporation. The indium electrode served as an ohmic contact, while the platinum electrode functioned as a rectifying contact. To enhance the dark conductivity of the $CuGa_{2.5}In_{2.5}S_8$ crystals they were subjected to thermal treatment at temperatures of 600 – 650 °C for 10 - 15 min.

The dark specific resistance of specially undoped samples ranged from $3^{\cdot}10^{10}$ - $2^{\cdot}10^{12}$ and 10^{6} - 10^{10} Ohm·cm along and perpendicular to c-axis, respectively. Annealing of the crystals resulted in a reduction in resistivity p by up to 10 times. Measurement of the thermoelectric voltage sign for the low-resistance samples indicated that the crystals exhibit n-type conductivity.

The rectification ratio of the surface - barrier structures (SBS) at a voltage U = 3 V amounts to 10 - 100 and $10^3 - 10^4$ for structures made from high-resistivity and low-resistivity

crystals, respectively. The forward voltage corresponds to a positive potential on the platinum electrode. The SBS structures generate a photovoltage of 0.47 – 0.86 V under illumination.

Based on the experiment, we can highlight the following thermodynamic features of the growth conditions we used to obtain high-quality compounds and their application in studying the modification of the energy spectrum characteristics of charge carriers in the researched single crystals: in the process of crystal formation, the transport rate must not exceed their growth rate; for the homogeneous growth of crystals, it is necessary to maintain a uniform temperature distribution in the crystallization zone. When transport occurs through diffusion, single crystals with perfect faces are grown; thoughtful selection of transport conditions allowed for the attainment of crystals that correspond to the initial stoichiometry of the compound.

From the results obtained and the advantages of growth, the method of chemical transport reactions has proven to be the most technologically advanced for the studied materials [14].

3. Results and Discussion

The forward branch of the current - voltage characteristic (I - U curve) of the SBS structures with a low - resistivity base at voltages below 1 V is described by an exponential dependence j ~ $\exp(eV/\beta kT)$, where the ideality factor β ranges from 1.6 to 2.3. When the voltage increases, a transition to an ohmic dependence j~U occurs. Larger values of the ideality factor indicate a tunnel-recombination mechanism for current flow through the space charge region at the platinum - crystal interface. For some surface - barrier structures, a region with a smoothly varying ideality factor was observed Figure 1, curve 4. This fact can be attributed to a complex nature of the distribution of local centers with respect to energy; however, detailing the charge transport mechanism requires further experiments and is a separate task.

The forward branch of the I - U characteristics of the samples with a high-resistivity base is also superlinear. When the voltage increases, it generally becomes linear and then follows a power law dependence j~U, where π = 3.5 ÷ 5.6 (Figure 1, curves 1-3). This type of I – U characteristic indicates that at voltages U > 1V, the current flow is associated with charge transport through the SBS base and is determined by space charge limited currents with the presence of exponentially distributed traps in the crystal [21, 23]. The absence of a linear region in the I - U characteristics of some samples with a thickness less than 10 μ m is attributed to the fact that due to the low concentration of free electrons, the injection current exceeds the ohmic current even at low voltages.

The photocurrent spectra of SBS were studied in a photovoltaic mode using a load with a resistance of 10^7 Ohm, as well as with a direct bias of +4.5 V. The photoconductivity (PC) spectra were examined on coplanar $CuGa_{2.5}In_{2.5}S_8 - In$ samples. The red PC edge (Figure 2, curves 1 and 2) of the crystals is approximately 1.9 eV, whereas for the SBS photovoltaic effect it is approximately 2.0 eV. This discrepancy indicates that this semiconductor contains photosensitive centers in the forbidden zone, which contribute to the photoconductivity for hv<E_g. The photoconductivity maximum at 2.2 eV corresponds to the excitation of electrons from these localized states into the conduction band.

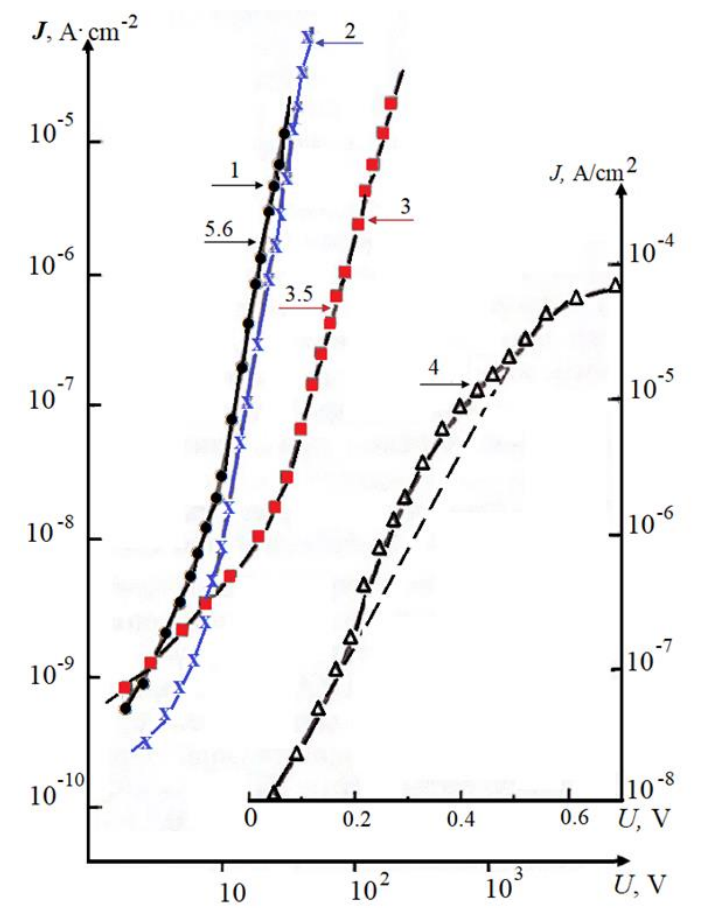


Figure 1. Forward-bias region of the current-voltage characteristics of the Pt - CuGa2.5In2.5S8 In structure at 300 K. Crystal thickness: (1) 5 μ m, (2) 7 μ m, (3) 27 μ m, and (4) 4 μ m.

Figure 2. Spectra of photoconductivity of CuGa2.5In2.5S8 single crystals (1) and the spectral distribution of the photoresponse of surface-barrier structures with a bias of + 4.5 V (2).

The photocurrent of SBS with a low-resistance base is proportional to the number of photons absorbed in the depleted region of the crystal, namely, it is related to the optical absorption coefficient. By extrapolating the steep region of the low-energy wing of the photocurrent spectrum for such samples (Figure 3, curve 4), we obtain a value for the band gap width of $CuGa_{2.5}In_{2.5}S_8$, which is approximately 2.23 eV.

This spectrum exhibits a maximum at 3.4 eV and a feature at 2.7 eV. On the high-nergy side of this feature the growth of photosensitivity with increasing photon energy (hv) becomes more gradual. This characteristic of the photocurrent spectrum and the significant distance of the maximum from the photoresponse onset are apparently related to the structural features of the allowed energy zones of $CuGa_{2,5}In_{2,5}S_8$ monocrystals.

The photoconductivity (PC) spectrum also exhibits a maximum at 3.4 eV and its slope changes around hv ≈ 2.7 eV. The possibility of observing features corresponding to interband electronic transitions in the spectral distribution of the PC is likely due to the low surface recombination rate, which allows the photocurrent to "track" changes in the optical absorption coefficient α . Indeed, layered crystals are characterized by low adsorption capability, and at the (0001) face of the crystal the outer layer consists of anions with a 2-charge, whose ion - covalent bonds are closed within the structural package, similarly to the

bulk of the crystal. On such a surface, the conditions for recombination of non-equilibrium electrons are, in the first approximation, the same as those in the bulk.

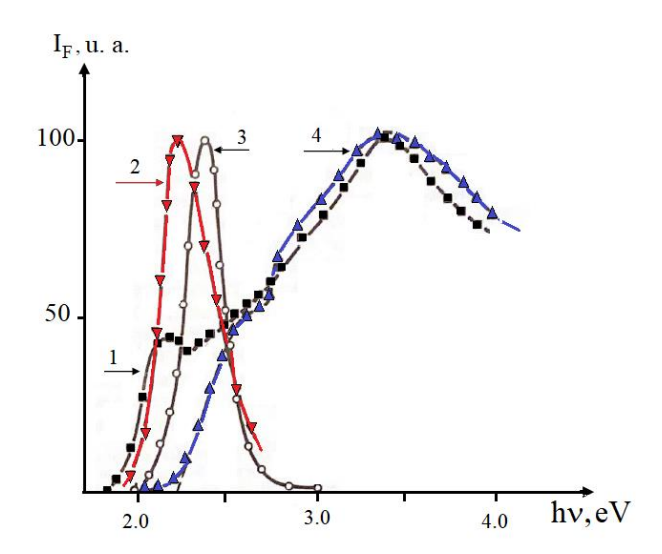


Figure 3. Optical absorption edge of CuGa2.5In2.5S8 single crystals at 300 K (1) and 70 K (2), and in a photovoltaic mode (3, 4) at 300 K, with thicknesses of 47 (1), 4 (2), 5 (3), and 4 μ m (4).

The photocurrent spectrum of SBS devices fabricated from specially undoped crystals features a band with a full width at half maximum of 0.15-0.25 eV (depending on the crystal thickness a, with values of $d = 20 \div 4$ µm, respectively.

Since the base resistance in these structures is much higher than that of the load, the condition for photocurrent generation is the light flux penetration into the bulk crystal and excitation of photocurrent in the base.

The photocurrent spectrum of the SBS with a positive bias (Figure 2, curve 2) corresponds to the crystal (base) photocurrent when light propagates along the charge transport direction. Since for $h\nu > E$ light is absorbed in the near-surface layer of the crystal, this results in a decrease in the base photocurrent and the photocurrent of SBS devices fabricated from specially undoped crystals.

The optical absorption edge of $CuGa_{2.5}In_{2.5}S_8$ single crystals in the 1.95–2.2 eV region is described by an exponential dependence $\alpha \sim \exp(hv/\Delta)$ where the parameter Δ is temperature independent and equals 43 meV (Figure 3). The presence of an exponential region in the absorption spectrum is characteristic for chalcopyrite type crystals (ZnS, CdS, and other compounds based on these elements). However, the latter have generally higher Δ values: such as 63 meV ($CdIn_2S_2Se_2$), 65 meV ($HgGaInS_4$), 44 meV ($HgGaInS_4$), 60 ÷ 77 meV ($CdGaInS_6$) [1, 2], and 98 meV ($ZnIn_2S_4$) [23]. This type of edge absorption, typical for various multicomponent compounds, is attributed to the presence of the density of state tails near the allowed energy bands caused by disorder in the cation sublattice [24].

4. Conclusions

The conditions for obtaining the new compound $CuGa_{2.5}In_{2.5}S_8$ were experimentally established using the method of chemical transport reactions, with iodine as the transport agent. This method allowed for the production of perfect single crystals with a high-quality

optical surface. The advantage of this method lies in the fact that chemical transport reactions occur at relatively low temperatures compared to other direct methods.

Single crystals of a new CuGa_{2,5}In_{2,5}S layered compound, with n-type conductivity and good photoconductive properties, were grown using chemical transport reactions with iodine. It was demonstrated that vacuum thermal treatment can significantly increase their dark conductivity within a wide range. Based on this material, surface - barrier structures were fabricated that exhibit a high rectification ratio and excellent photosensitivity.

The parameters of the hexagonal unit cell were determined, and the bandgap width was assessed. The presence of photosensitive centers in CuGa_{2.5}In_{2.5}S₈ crystals with a depth of approximately 1.9 eV was established. The absorption edge of this material features an extended exponential region with a characteristic parameter $\Delta = 43$ meV.

Conflicts of Interest: The authors declare no conflict of interest.

References

- 1. Zhitar, V.F.; Pavlenko, V.I.; Arama, E.D.; Shemyakova, T.D. Recombination properties of ZnIn₂S₄ single crystals. In: *Proceedings International Semicond. Conference CAS. Sinaia*, 2008, vol. 2, pp. 241-244.
- 2. Zhitary, V.F.; Pavlenko, V.I. Anisotropy of photoconductivity and luminescence of single crystals ZnIn₂S₄ and ZnIn₂S₄: Cu. In: *Inorganic materials*. 2010, 6 (4), pp. 402-405 [in Russian].
- 3. Georgobiani, A.N.; Radautsan, S.I.; Tiginianu, I.M. Wide-bandgap semiconductors: optical and photoelectric properties and application prospects. *FTP* 1985, 19 (2), pp.193-212 [in Russian].
- 4. Donika, F.G.; Zhitary, V.F.; Radautsan, S.I. *Semiconductors of the ZnS–In₂S₃ system*. Science, Chisinau, 1980, pp. 148-162 [in Russian].
- 5. Donika, F.G.; Radautsan, S.I.; Semiletov, S.A.; Donica, T.V.; Mustya, I.G. Crystal structure of the double-layer polytype ZnIn₂S₄ (II). *Crystallography* 1971, 17 (3), pp. 663-669 [in Russian].
- 6. Radautsan, S.I.; Donika, F.G.; Kyosse, G.A.; Mustya, G. Polytypism of ternary phases in the system Zn-In-S. *Phys. Stat. Sol.* 1970, 37 (2), pp. 123-131.
- 7. Vigil, O.; Calzadilla, O.; Seuret, D.; Vidal, J. $Znln_2S_4$ as a window in heterojunction solar cells. *Sol. Energ. Mater.* 1984, 10 (2), pp. 139-143.
- 8. Arama, E.D. *Optical Properties of Layered Multicomponent Sulfides*. Sirius, Chisinau, Republic of Moldova, 2004. 198 p. [in Romanian].
- 9. Moldovyan, N.A. Multinary layered chalcogenides with octahedral and tetrahedral coordination of cations. in: multinary chalcogenides $A^{II}B_2^{III}C_4^{VI}$. Science, Chisinau, Republic of Moldova, 1990. pp. 36-83 [in Russian].
- 10. Moldovyan, N.A. Crystallochemical conditions of formation of novel layered chalcogenides with mixed coordination of cations. *Inorg. Mat.* 1988, 4, pp. 1385-1387 [in Russian].
- 11. Goryunova, N. Complex Diamond-Like Materials. Sov. Radio, Moscow, USSR, 1968. pp. 268-272. [in Russian].
- 12. Donika, F.G.; Zhitar V.F.; Radautsan S.I. *Semiconductor Systems* $Z_{nS-In_2S_3}$. Science, Chisinau, Republic of Moldova, 1980, pp. 148-154.
- 13. Arama, E.; Georghita, E.; Pintea, V.; Jitari, V.; Şemiacov, T. Preparation of compounds $Zn_xIn_2S_{3+x}$ by the method of chemical transport reactions. *Engineering Meridian* 2008, 4, pp. 48-50 [in Romanian].
- 14. Arama, E. *Optical properties of layered multi-component sulfides*. Sirius, Chisinau, Republic of Moldova, 2004, pp.198-203 [in Romanian].
- 15. Pintea, V. Studying the peculiarities of the energy spectrum modification of charge carriers in the ternary semiconductors CdGa₂S₄ and ZnIn₂S₄ at high excitation levels. PhD Thesis. Chisinau, 2013, pp. 10-12 [in Romanian].
- 16. Vaipolin, A.A.; Nikolaev, Yu.A.; Rud, V.Yu.; Terukov, E.I.; Fernelius, N. Fabrication and properties of photosensitive structures of ZnIn₂S₄ single crystal. *Semiconductors* 2003, 37 (2), pp. 187-191.
- 17. You, S.H.; Hong, K.J.; Jeong, T.S.; Youn, C.J. Growth and electrical/optical properties of the photoconductive ZnAl₂Se₄ layers grown by hot wall epitaxy method. *J. Ceram. Process. Res.* 2014, 15 (1), pp. 4–8.
- 18. Surabala, M. *Structural, electronic and optical properties of chalcopyrite type semiconductors.* PhD Thesis. Department of Physics, Nat. Inst. of Technology, Rourkelamay, 2012, 181 p.
- 19. Amiraslanov, I.E.; Asadov, Yu.G.; Valiev, R.B.; Musaev, A.A.; Guseinov, G.G. Structure and intercalation of the two-packet polytype GalnS₃ (b, II). *Soviet physics. Crystallography* 1990, 35 (5), pp. 766-767.

- 20. Cheng, K.-W.; Huang, Ch.-M.; Yu, Ya-Ch.; Li, Ch.-T.; Shu, Ch.- Kai; Liu, Wang-Lin. Photoelectrochemical performance of Cu-doped ZnIn₂S₄ electrodes created using chemical bath deposition. *Solar Energy Materials & Solar Cells* 2011, 95(7), pp. 1940-1948.
- 21. Lampert, M.; Mark, P. Current injection in solids. Mir, Moscow, USSR, 1973. pp. 410-416 [in Russian].
- 22. Bozhko, V.V.; Novosad, A.V.; Davidyuk, G.E.; Kozer, V.R.; Parasyuk, O.V.; Neimantas, V.; Janonis, V.; Sakavicius, A.; Kazukauskas, V. Electrical and photoelectrical properties of Znln₂S₄ and CulnS₂ solid solutions. *Journal of Alloys and Compounds* 2013, (553), pp. 48−52.
- 23. Georgobiani, A.N.; Radautsan, S.I.; Tiginyanu, I.M. Wide-gap A^{II}B₂^{III}C₄^{VI} semiconductors: optical and photoelectrical properties and prospects. *Fiz. Techn. Polup.* 1985, 19, pp. 193-212.
- 24. Kashida, S.; Yanadori, Y.; Otaki, Y.; Seki, Y.; Panich, A.M. Electronic structure of ternary thallium chalcogenide compounds. *Phys. stat. solidi (a)* 2006, 203(11), pp. 2666-2669.

Citation: Arama, E.; Pîntea, V.; Shemyakova, T.; Gasitoi, N. Growth of single crystals, photoelectric properties and the absorption edge of a new layered CuGa_{2.5}In_{2.5}S₈ compound. *Journal of Engineering Science* 2024, XXXI (3), pp. 18-26. https://doi.org/10.52326/jes.utm.2024.31(3).02.

Publisher's Note: JES stays neutral with regard to jurisdictional claims in published maps and institutional affiliations.



Copyright:© 2024 by the authors. Submitted for possible open access publication under the terms and conditions of the Creative Commons Attribution (CC BY) license (https://creativecommons.org/licenses/by/4.0/).

Submission of manuscripts:

jes@meridian.utm.md

Topic

https://doi.org/10.52326/jes.utm.2024.31(3).03 UDC 621.313.33





HARMONIC ANALYSIS OF MAGNETOMOTIVE FORCE IN THE AIR GAP OF SIX-PHASE ASYNCHRONOUS MACHINES

Petru Todos, ORCID: 0000-0003-2368-3871, Ghenadie Tertea *, ORCID: 0000-0002-5410-8901, Ilie Nuca, ORCID: 0000-0001-7750-4846

Technical University of Moldova, 168 Stefan cel Mare, Blvd., Chisinau, Republic of Moldova Corresponding author: Ghenadie Tertea, ghenadie.tertea@bte.utm.md

Received: 07. 23. 2024 Accepted: 09. 15. 2024

Abstract. Asynchronous motors with six and more phases (usually n-three-phase) are increasingly accepted in electric drive systems of road transport, marine and even aeronautical transport. Multiphase machines are credited with multiple advantages such as: less torque ripple, better power distribution per phase, higher efficiency and fault tolerance capability compared to traditional three-phase machines. There are many publications, but few of them are dedicated to the in-depth study of the multiphase motor (m>3) and especially of the magnetic field in its air gap. The purpose of the present paper: the development of the mathematical model of the magnetomotive force in the air gap of the six-phase asynchronous machines, which determines the fundamental properties of the machine, the structure of the magnetic field and the torque developed, the efficiency, the error tolerance. The research is based on analytical studies and the results of suitable experimental measurements. The paper presents the mathematical model for the harmonic analysis of the magnetomotive force in the air gap of six-phase machines with possible variants of windings on the stator. Based on this study, it was demonstrated that only n-three-phase machines with asymmetrically arranged stator windings have the ability to attenuate higher harmonics with a major negative effect on the developed torque, the applicability and efficiency of traditional tools for reducing higher harmonics in the case of six-phase machines was confirmed. The results of measurements carried out on samples of six-phase machines confirm the findings and conclusions formulated in the paper.

Keywords: Induction machine, six-phase machine, air-gap magnetomotive force, harmonic analysis, asynchronous torques

Rezumat. Motoarele asincrone cu șase și mai multe faze (de regulă, n-trifazate) tot mai des sunt acceptate în cadrul sistemelor de acționare electrică a mijloacelor de transport rutier, naval și chiar aeronautic. Mașinilor multifazate li se atribuie multiple avantaje, cum ar fi: ondularea mai mică a cuplului, distribuția mai bună a puterii pe fază, eficiența mai mare și capacitatea de toleranță la erori în comparație cu mașinile trifazate tradiționale. Sunt multe publicații, dar puține din acestea sunt consacrate studiului aprofundat al motorului multifazat

(m>3) și în deosebi a câmpului magnetic în întrefierul acestuia. Scopul prezentei lucrări: elaborarea modelului matematic al forței magnetomotoare în întrefierul mașinilor asincrone hexafazate, care determină proprietățile fundamentale ale mașinii, structura câmpului magnetic și a cuplului dezvoltat, eficiența, toleranța la erori. Cercetarea se bazează pe studii analitice și pe rezultate ale măsurătorilor experimentale adecvate. În lucrare este prezentat modelul matematic pentru analiza armonică a forței magnetomotoare în întrefierul mașinilor hexafazate cu variante posibile de înfășurări pe stator. În baza acestui studiu, s-a demonstrat că doar mașinile n-trifazate cu înfășurări statorice dispuse asimetric dispun de capacitatea de atenuare a armonicilor superioare cu efect negativ major asupra cuplului dezvoltat, s-a confirmat aplicabilitatea și eficiența instrumentelor tradiționale de reducere a armonicilor superioare în cazul mașinilor hexafazate. Rezultatele măsurătorilor efectuate pe mostre de mașini hexafazate confirmă constatările și concluziile formulate în lucrare.

Cuvinte cheie: Mașina de inducție, mașina hexafazată, forța magnetomotoare în întrefier, analiza armonică, cupluri asincrone.

1. Introduction

Multiphase asynchronous motors (m>3) are becoming more and more popular for the electric drive of road, marine and even aeronautical vehicles due to their advantages such as less torque ripple, better power distribution per phase, efficiency higher and fault tolerance compared to three-phase ones [1-3]. An increased preference is observed in the application of n-three-phase machines which, in parallel with the simplicity of the construction and the simplicity of the manufacturing technologies, which do not differ from those applied to the production of conventional three-phase machines, add the operational advantages named above [4-7]. They are distinguished by the arrangement on the stator of 2, 3 or more identical three-phase sets of windings offset from each other at a predetermined angle (Figures 2b and 2c).

The study of the magnetic field in the air gap of electric motors has been an actual problem throughout the historical course of their development. In the gap, the electromagnetic and electromechanical transformations occur that determine the energy parameters but also the quality of the machine's operating characteristics [9-12]. Multiphase machines are no exception in this field either - especially n-three-phase ones. Results of the fundamental analytical research of the three-phase induction machine can be found in the works of R. Rihter [13], V. Radin [14], in the treatises of professors M. Covrig [10], A. Simion [15], I. Boldea [16], S. Deaconu [17], I. Kopilov [18], I. Boldea and Nasar S.A. [19]. And in recent publications the problem of the field and parasitic couples in the healthy regime and in the operation with errors in the power system is widely discussed [11, 12, 20].

In several works, the six-phase machines, which will be discussed in this paper, are attributed important advantages / performances regarding the reduction of the parasitic harmonics of the induction in the air gap, which ensures a better uniformity of the developed torque but also of reducing losses of energy in the machine compared to classic three-phase machines. However, it seems that none of these works specifies to which type of six-phase machines some or others of these advantages refer. The purpose of this paper is to determine the most suitable variants of winding topographies/architectures to achieve optimal levels of efficiency and reliability of electrical drive systems with n-three-phase induction machines.

Research objectives: a) performing a deep study of the harmonic structure of the magnetomotive force (MMF) in the air gap of the n-three-phase induction machine, b) defining the link between the harmonic structure, the type and parameters of the windings

used, c) tracing the methods of eliminating or reducing the negative effect of the higher harmonics of the MMF in six-phase machines (with various types of windings). The work is oriented towards an analytical study accompanied by arguments based on the results of the measurements performed on suitable experimental samples.

2. The magnetomotive force in the air gap of the induction machine with the multiphase stator winding

One of the main concerns in the design of electric machines is centered on the correct determination of the topology and constructive parameters of the windings, aiming to minimize the content of existing harmonics in the waveform of the magnetomotive force of the air gap.

The fundamental harmonic of the MMF results in a rotating magnetic flux and finally creates a mechanical torque that produces the useful work [10]. At the same time, the presence of higher spatial harmonics in the rotating wave of the MMF results in the formation of parasitic asynchronous torques, accompanied by power losses and the reduction of the energy efficiency of the machine. Another group of harmonics, of order multiple to 3, in the case of n-three-phase machines, forms pulsating waves accompanied by additional losses in the magnetic core, winding conductors and other metal parts [13-17]. In what follows, analytically, the spectrum of spatial harmonics of MMF in the gap of n-three-phase type machines will be determined. The final goal of the study being - highlighting the types of windings advantageous from the point of view of the spectrum of higher harmonics that produce parasitic asynchronous torques, with a significant negative impact on the machine's operating characteristics.

2.1 Magnetomotive force created by a single-phase winding

A single-phase winding (one coil), concentrated, with the number of turns w (Figure 1a) was examined. Each side of the coil occupies a slot of the ferromagnetic armatures, q=1, and the distance between the sides corresponds to a polar step $y=\tau$. The number of pairs of poles, formed by the magnetic field is p=1. If the current that runs through the coil is sinusoidal and is described with the relation (1):

$$i(t) = I_{m} \sin(\omega t), \tag{1}$$

where: I_m - is the amplitude of the current, $\omega=2\pi f$ - the pulsation, and f - represents the frequency of variation of the current intensity, then, the magnetomotive force along a polar step is represented by the relation (2):

$$F(X) = \begin{cases} +\frac{F_0}{2}, & \text{if } 0 < X < \pi \\ -\frac{F_0}{2}, & \text{if } 0 > X > -\pi \end{cases}$$
 (2)

where:

$$F_0 = I_m w k_w \sin(\omega t) = \sqrt{2} I w k_w \sin(\omega t) = 2F_m \sin(\omega t)$$
 (3)

 $X = \pi \cdot x/\tau$ - represents the distance along the curvature of the air gap, expressed in electrical degrees, x - represents the coordinate in metric expression, k_w - winding factor, I - the effective value of the current intensity, w- the number of turns of the winding.

For a given value of the current, for example, when $(\omega t = \pi/2 \text{ and } \sin(\omega t) = 1)$, the MMF distribution along the air gap is shown graphically with a step diagram as in figure 1a,

this curve being a symmetric periodic function, the Fourier expansion does not contain terms of even order and is represented by the relation:

$$F(x) = \frac{\sqrt{2}}{2} \text{ Iw } k_w \sin(\omega t) \left[a_1 \cos \frac{\pi x}{\tau} + a_3 \cos \left(3 \frac{\pi x}{\tau} \right) + \dots + a_{\nu} \cos \left(\nu \frac{\pi x}{\tau} \right) \right] \tag{4}$$

where a_1 , a_2 , ..., a_v are the Fourier coefficients, which are defined as follows:

$$a_{\nu} = \frac{1}{\pi} \int_{-\pi}^{+\pi} \cos(\nu X) dX = \frac{4}{\pi} \int_{0}^{\pi/2} \cos(\nu X) dX = \frac{4}{\pi \nu} \sin\left(\frac{\nu \pi}{2}\right)$$
 (5)

Inserting into (4) the coefficients a v, defined with relation (5), it results:

$$F(x) = \frac{2\sqrt{2}}{\pi} \text{ Iw sin}(\omega t) \sum_{1}^{n} \left[\frac{k_{w,\nu}}{\nu} \cos\left(\nu \frac{\pi x}{\tau}\right) \right]$$
 (6)

Thus, the MMF in the airs gap is represented by the fundamental harmonic (curve 1 in Figure 1b) and a lot of higher spatial harmonics (e.g. curves 3 and 5 in Figure 1b).

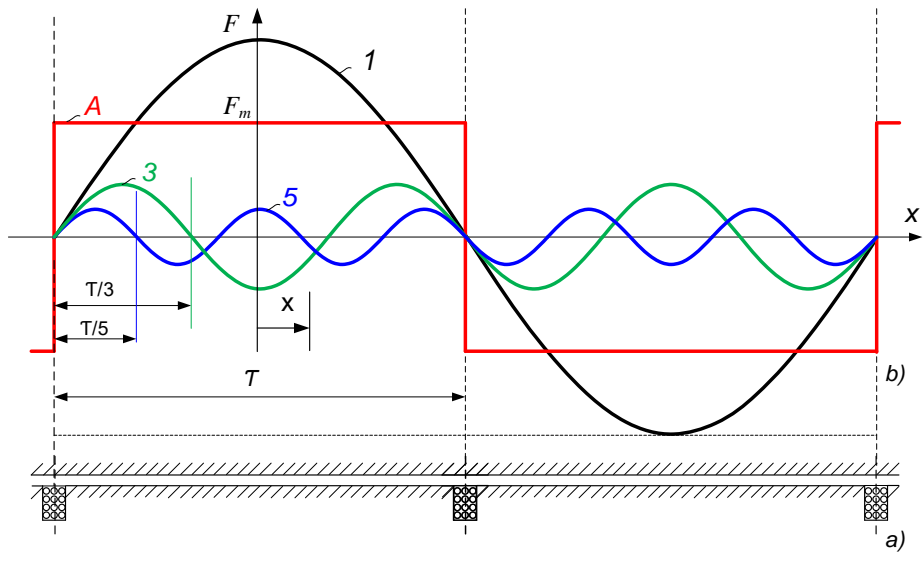


Figure 1. a) Air gap geometry (with the winding placed in the notches); b) MMF distribution along the air gap of an electric machine with a single-phase concentrated winding (curve A), and the component harmonics: fundamental (curve 1) and higher ones (curves 3 and 5).

From (6) it follows that a harmonic, with order number v, is described by the relation:

$$F_{\nu} = F_{m.\nu} \sin(\omega t) \cos\left(\nu \frac{\pi x}{\tau}\right) = \frac{2\sqrt{2}}{\nu \pi} I w k_{w.\nu} \sin(\omega t) \cos\left(\nu \frac{\pi x}{\tau}\right)$$
 (7)

The amplitude $F_{m.\nu}$ of the harmonic of order ν can be related to the amplitude of the fundamental $F_{m.1}$ and then:

$$F_{\nu} = \frac{F_{m.1}}{\nu} \frac{k_{w.v}}{k_{w.1}} \sin(\omega t) \cos\left(\nu \frac{\pi x}{\tau}\right) = F_{m.1} \frac{k'_{w.v}}{\nu} \sin(\omega t) \cos\left(\pi x \frac{v}{\tau}\right)$$
(8)

Here it was noted: $k_{w.1}$, $k_{w.v}$ – the winding factor, calculated for the fundamental and harmonic respectively v, $k'_{w.v}$ the winding factor for the harmonic v reported, $F_{m.1}=\frac{2\sqrt{2}}{\nu\,\pi}Iw$ - amplitude of the fundamental.

From relation (8) it is observed that the amplitude $F_{m.v}$ and the wavelength τ_v decrease proportionally to the order number v of the harmonic. A higher harmonic varies in time with the frequency f_1 but creates in the gap $(v \cdot p)$ pole pairs.

The magnetomotive force of a three-phase machine is defined by the MMF sum of three phase windings, described based on relations (6) and (8). But the MMF of 6-, 9- or 12-

phase machines (in general - of an n-three-phase machine) can be defined by the sum of the MMF of n sets of three-phase windings offset from each other in space at a prescribed angle θ . Figures 2a, 2b and 2c show the orientation diagrams of the axes of the phase windings of 3- and 6-phase induction machines. Of course, the phase shift λ of the phasors of the currents passing through the phases of the three-phase sets of windings will have the value equal to the gap θ , expressed in electrical degrees (Figures 2d, 2e and 2f). Figure 2 shows the generalized diagram for a machine with 2p=2.

Starting from these considerations, in the following the relations describing the upper harmonics (of order ν) of the MMF are defined for each phase separately, then of a three-phase set, later the variants practiced by six-phase composite windings are examined.

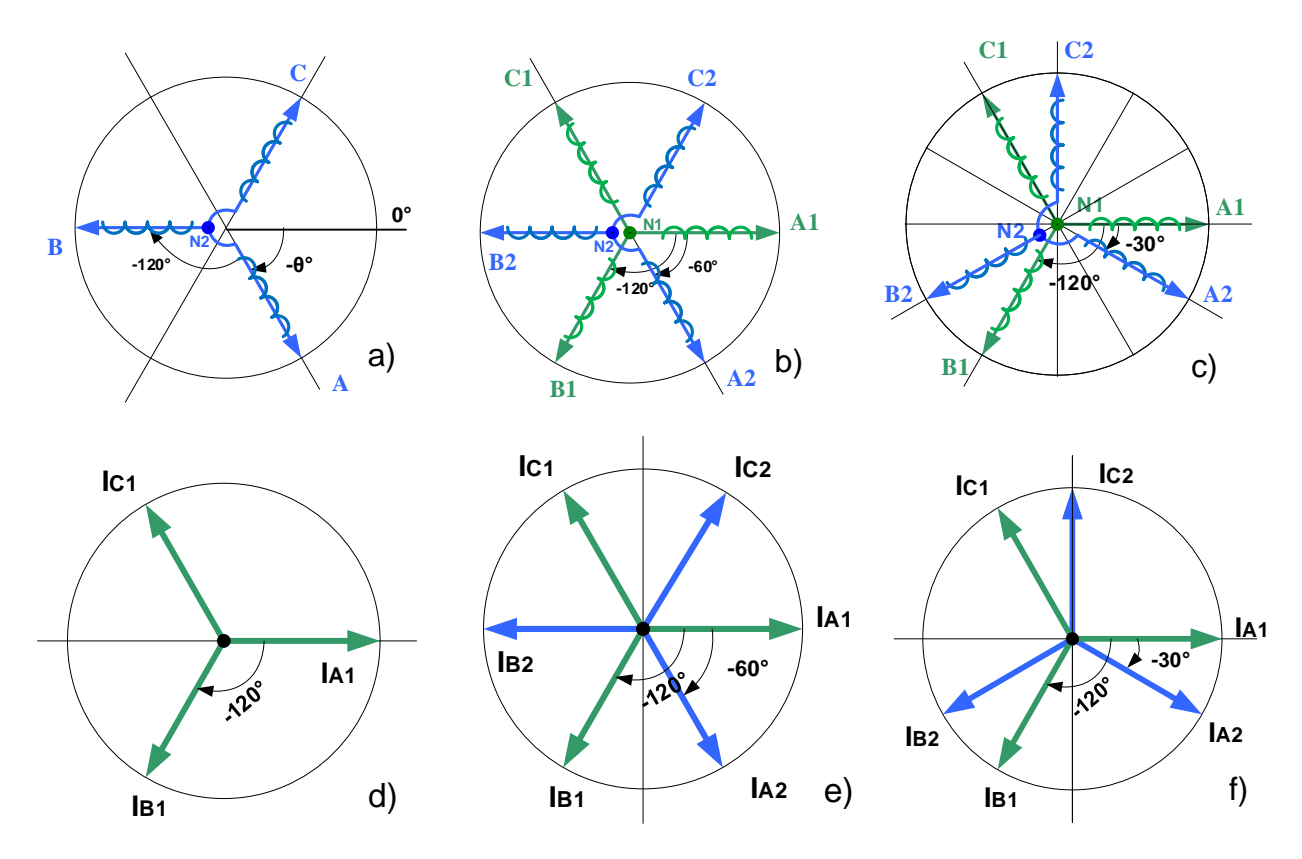


Figure 2. Stator winding type: a) three-phase; b) symmetrical hexaphase; c) asymmetrical hexaphase; d)-f) the phasors of the phase currents in the respective windings.

2.2 MMF in the air gap of the three-phase induction machine

In the case of a three-phase set of windings (Figure 2a), the phases being marked, for example, with A, B and C, are oriented under 120 electrical degrees to each other, and the three-phase set as a whole has a spatial offset of θ electrical degrees, in relation to the axis defined as reference (θ =0). Under these conditions, the relations for the ν - order harmonic of the phase MMF are presented as follows:

$$F_{A\nu} = F_{m1} \frac{k'_{w.v}}{v} \sin(\omega t - \theta) \cos\left(v \frac{\pi x}{\tau} - v\theta\right)$$
 (9)

$$F_{B\nu} = F_{m1} \frac{k'_{w.v}}{v} \sin(\omega t - \frac{2\pi}{3} - \theta) \cos\left(\nu \frac{\pi x}{\tau} - \nu \left(\frac{2\pi}{3} + \theta\right)\right)$$
 (10)

$$F_{C\nu} = F_{m1} \frac{k'_{w.v}}{v} \sin\left(\omega t - \frac{4\pi}{3} - \theta\right) \cos\left(\nu \frac{\pi x}{\tau} - \nu \left(\frac{4\pi}{3} + \theta\right)\right)$$
(11)

Under these conditions, the rotating components of the v-order harmonic of the MMF (F'_{Av} -direct and F''_{Av} -inverse) of the phase windings can be presented with relations (12)-(14):

$$F_{A\nu} = F'_{A\nu} + F''_{A\nu} = \frac{F_{m1}}{2} \frac{k'_{w.v}}{v} \left[\sin(\phi_{1\nu} + (\nu - 1) \theta) + \sin(\phi_{2\nu} - (\nu + 1) \theta) \right]$$
 (12)

$$F_{B\nu} = F'_{B\nu} + F''_{B\nu} = \frac{F_{m1}}{2} \frac{k'_{w.v}}{v} \left[\sin \left(\phi_1 + (\nu - 1) \left(\frac{2\pi}{3} + \theta \right) + \sin \left(\phi_2 - (\nu + 1) \left(\frac{2\pi}{3} - \theta \right) \right) \right]$$
 (13)

$$F_{C\nu} = F_{C\nu}' + F_{C\nu}'' = \frac{F_{m1}}{2} \frac{k_{w.v}'}{v} \left[\sin \left(\phi_1 + (\nu - 1) \left(\frac{4\pi}{3} + \theta \right) + \sin \left(\phi_2 - (\nu + 1) \left(\frac{4\pi}{3} - \theta \right) \right) \right] \quad (14)$$

where: $\phi_{1\nu}=\omega t-\nu\frac{\pi x}{\tau}$ - is the phase angle of the direct spin wave, and $\phi_{2\nu}=\omega t+\nu\frac{\pi x}{\tau}$ - is the phase angle of the inverse rotating wave of the harmonic ν .

Applying the decomposition $\sin(\alpha \pm \beta) = \sin\alpha \cdot \cos\beta \pm \cos\alpha \cdot \sin\beta$ and simplifying, based on relations (12-14), the following convenient relations are obtained for a tabular calculation of the components of the rotating wave of the MMF:

$$F'_{\nu} = \frac{F_{m1}}{2} \frac{k'_{w.v}}{v} [k_{1\nu} \sin(\varphi_{1\nu}) + k_{2\nu} \cos(\varphi_{1\nu})]$$
 (15)

$$F_{\nu}^{\prime\prime} = \frac{F_{m1}}{2} \frac{k_{w.v}^{\prime}}{v} [k_{3\nu} \sin(\phi_{2\nu}) - k_{4\nu} \cos(\phi_{2\nu})]$$
 (16)

where $k_{1\nu}$, $k_{2\nu}$, $k_{3\nu}$, $k_{4\nu}$ - called harmonic coefficients, are defined relations (17):

$$\begin{cases} k_{1\nu} = \cos\left((\nu - 1)\theta\right) + \cos\left((\nu - 1)\left(\frac{2\pi}{3} + \theta\right)\right) + \cos\left((\nu - 1)\left(\frac{4\pi}{3} + \theta\right)\right) \\ k_{2\nu} = \sin\left((\nu - 1)\theta\right) + \sin\left((\nu - 1)\left(\frac{2\pi}{3} + \theta\right)\right) + \sin\left((\nu - 1)\left(\frac{4\pi}{3} + \theta\right)\right) = 0 \\ k_{3\nu} = \cos\left((\nu + 1)\theta\right) + \cos\left((\nu + 1)\left(\frac{2\pi}{3} + \theta\right)\right) + \cos\left((\nu + 1)\left(\frac{4\pi}{3} + \theta\right)\right) \\ k_{4\nu} = \sin\left((\nu + 1)\theta\right) + \sin\left((\nu + 1)\left(\frac{2\pi}{3} + \theta\right)\right) + \sin\left((\nu + 1)\left(\frac{4\pi}{3} + \theta\right)\right) = 0 \end{cases}$$

$$(17)$$

Table 1 shows the results of the calculations performed for a three-phase winding in star connection for four scenarios of offset θ of phase A in relation to the reference axis.

Following the analysis of the results, included in this table, it is found:

- a) the harmonic coefficients in all the examined scenarios obtain the value 0 or ±m, where m is the number of phases of the winding, and the minus sign in front notifies a phase shift of 180 electrical degrees of the respective rotating wave;
- b) the even harmonic coefficients ($k_{2\nu}$, $k_{4\nu}$), for all examined values of the gap θ , have zero value, regardless of the harmonic order. Therefore, the spin waves (forward and reverse) in all the scenarios examined are sinusoidal (see relations (15) and (16));
- c) MMF waves of order $(2m \cdot k + 1)$ have the direction of direct rotation, and those of order $(2m \cdot k 1)$ rotate in the opposite direction (they are of opposite sequence). Here k 1 any integer.

Table 1

Calculated harmonic coefficients for a three-phase winding (m=3) with different values θ of the offset angle θ with respect to the reference axis

	The offset θ of the three-phase set of windings with respect to the reference axis (θ =0):															
ν	Scenario 1: $\theta = 0$ °				Scenario 2: $\theta = 30^{\circ}$				Scenario 3: $\theta = 60^{\circ}$				Scenario 4: θ=90°			
	k1.1	k2.1	k3.1	k4.1	k1.2	k2.2	k3.2	k4.2	k1.3	k2.3	k3.3	K4.3	k1.4	k2.4	k3.4	k4.4
1	3	0	0	0	3	0	0	0	3	0	0	0	3	0	0	0
3	0	0	0	0	0	0	0	0	0	0	0	0	0	0	0	0
5	0	0	3	0	0	0	-3	0	0	0	3	0	0	0	-3	0

	Continuation Table 2															Table 1
7	3	0	0	0	-3	0	0	0	3	0	0	0	-3	0	0	0
9	0	0	0	0	0	0	0	0	0	0	0	0	0	0	0	0
11	0	0	3	0	0	0	3	0	0	0	3	0	0	0	3	0
13	3	0	0	0	3	0	0	0	3	0	0	0	3	0	0	0
15	0	0	0	0	0	0	0	0	0	0	0	0	0	0	0	0
17	0	0	3	0	0	0	-3	0	0	0	3	0	0	0	-3	0
19	3	0	0	0	-3	0	0	0	3	0	0	0	-3	0	0	0
21	0	0	0	0	0	0	0	0	0	0	0	0	0	0	0	0
23	0	0	3	0	0	0	3	0	0	0	3	0	0	0	3	0
25	3	0	0	0	3	0	0	0	3	0	0	0	3	0	0	0

Note: v - harmonic number (order harmonic); k - harmonic coefficients.

2.3 MMF of the air gap of the six-phase induction machine

For a six-phase machine (Figures 2b and 2c) the harmonic coefficients are defined by summing the coefficients calculated for the three-phase sets that make up the machine winding. Table 2 shows the results of the calculations for four possible scenarios for the execution of the six-phase winding: a) symmetrical double-three-phase type with the gap between sets θ =0°, b) symmetrical type with θ =60°, c) and d) asymmetrical type with the gap between sets of 30 or 90 electrical degrees. Only the values of the synthetic coefficients K1 and K3 are presented in the table, given the fact that the coefficients K2 and K4 in all the examined scenarios have zero value.

Table 2

Calculated harmonic coefficients for 4 scenarios for making six-phase windings

m=6	Double 3-	phase	Symmetric	c, θ= 60°	Asymmetr	ic, θ=30°	Asymmetric, θ= 90°			
ν	K1= 2 k11	K3=2 k31	K1= k11+k13	K3= k31+k33	K1= k11+k12	K3= k31+k32	K1= k11+k14	K3= k31+k34		
1	6	0	6	0	6	0	6	0		
3	0	0	0	0	0	0	0	0		
5	0	6	0	6	0	0	0	0		
7	6	0	6	0	0	0	0	0		
9	0	0	0	0	0	0	0	0		
11	0	6	0	6	0	6	0	6		
13	6	0	6	0	6	0	6	0		
15	0	0	0	0	0	0	0	0		
17	0	6	0	6	0	0	0	0		
19	6	0	6	0	0	0	0	0		
21	0	0	0	0	0	0	0	0		
23	0	6	0	6	0	6	0	6		
25	6	0	6	0	6	0	6	0		

Note: v - harmonic number (order harmonic); k - harmonic coefficients; θ - phase shift.

This calculation algorithm can also be applied to other machines from the n-three-phase group: with 9, 12, 15, etc. phases. For example, the winding of the 12-phase machine can be synthesized from 4 three-phase sets offset by 30 electrical degrees. The calculation results demonstrate that the harmonic composition of the MMF will be similar to that of the asymmetrical six-phase machine.

Following the analysis of the obtained results (Table 2), the following practical conclusions can be drawn regarding the harmonic structure of the MMF and respectively of the magnetic field in the gap of an n-three-phase electric machine (it is about the spatial harmonics because the phase currents are considered sinusoidal):

- a) the magnetomotive force created in the gap by the phase windings of the multiphase induction machine contains only odd harmonics whose order is determined by the relation: $v=2k\pm1$, where k=0, 1, 2, 3, etc.;
- b) in the case of n- three-phase machines (with 3, 6, 9, 12 etc. phases), the third order harmonics in the phases of each three-phase set of windings have a gap of 0 between them, and do not form rotating magnetic fields, they only form pulsating fields. This phenomenon refers to all harmonic multiples of 3 (e.g. 3, 9, 15, 21, 27, 33...).
- c) increasing the number of three-phase sets within the multiphase stator winding leads to the annihilation / disappearance of higher harmonics only when they are arranged asymmetrically. For example, from the harmonic spectrum of the MMF of the asymmetric hexaphase machine, the harmonics are missing: 5, 7, 17, 19, 29, 31 ... (k m±1), where k=1, 3, 5 ...
- d) thus, it is found that in an asymmetric hexaphase machine the first of the higher harmonics of the MMF, which forms a rotating magnetic field, is the eleventh order. In the case of the machine with m=12, the first in this sense is the 23rd harmonic and has a relative amplitude value of at most 4.3%;
- e) the hexaphase machine with the double-three-phase winding or the symmetrical n-three-phase type behaves like a simple three-phase machine, In the MMF harmonic spectrum in these cases there are also waves of order 5 and 7, absent, moreover, in the case of asymmetrical hexaphase winding.

3. Decreasing the magnitude of higher harmonics

The negative influence of higher harmonics, especially those of order 5 and 7 in the case of double-three-phase or symmetrical six-phase machines, can be reduced by applying the classical methods used in the construction of three-phase asynchronous machines [13, 18, 19]:

- a) selection of the optimal number of sections q per pole and phase of the winding
- b) the shortening of the opening y of the winding sections in relation to the diametral polar pitch τ , c) inclination of the slots on the rotor or stator.

3.1 Application of distributed winding

From relations (10) and (11) we can see a directly proportional dependence of the amplitude of the MMF harmonics in relation to the winding factor $k_{w.v}$, which is the product of the factors: distribution $k_{q.v}$, and shortening $k_{sc.v}$: $k_{w.v} = k_{q.v} \cdot k_{sc.v}$

The relation (18), derived for the calculation of the distribution factor [10,14,15], includes only one parameter that can be manipulated - the number of slots per pole and phase q in which the sides of the phase winding sections are arranged:

$$k_{q,v} = \sin\left(q\frac{vp\pi}{z_1}\right) / \left(q\sin\left(\frac{vp\pi}{z_1}\right)\right) = \sin\left(v\frac{\pi}{2m}\right) / \left(q\sin\left(v\frac{\pi}{2mq}\right)\right)$$
 (18)

At the same time, it should be noted that increasing the number of phases m inevitably leads to a decrease in the possibilities of maneuvering with this parameter.

Table 3 shows the results of calculating the distribution factor for 6 types of windings for three-phase and six-phase machines, which differ by the number of phases m and the value of the parameter q. The scenario is considered: windings with diametral pitch, stator

slots without inclination. Based on these data, important conclusions can be drawn that must be taken into account when designing multiphase machines:

- a) in the case of windings with q=1, the distribution factor is unitary for the entire spectrum of harmonics;
- b) for symmetrical three-phase and six-phase machines, windings with at least 3 notches per pole and phase can be recommended, which ensure a significant reduction of the most influential harmonics: 5, 7, 11 and 13;
- c) in the case of hexaphase machines with asymmetrically arranged winding, a q=2 is sufficient to reduce harmonics 11 and 13. Harmonics 5, 7, 17, 19 are missing from the harmonic spectrum of the MMF, and those of order 23, 25 and above are insignificant as amplitude;
- d) when applying distributed windings (q>1) the fundamental harmonic of the MMF is slightly reduced (≤ 4.5%), which is easily compensated by a few extra turns in the phase winding.

Table 3
Change of the distribution factor according to the number of sections per phase and pole q and the order number of the harmonic v. For case: windings with diametral pitch, stator notches without inclination

	_		Harmonic order ∨:												
m	Ч	1	3	5	7	9	11	13	15	17	19	23	25		
3	1	1	1	1	1	1	1	1	1	1	1	1	1		
3	2	0.97	0.707	0.259	-0.259	-0.707	-0.966	-0.966	-0.707	-0.259	0.259	0.966	0.966		
3	3	0.96	0.667	0.218	-0.177	-0.333	-0.177	0.218	0.667	0.960	0.960	0.218	-0.177		
6	1	1	1	1	1	1	1	1	1	1	1	1	1		
6	2	0.99	0.924	0.793	0.609	0.383	0.131	-0.131	-0.382	-0.609	-0.793	-0.991	-0.991		
6	3	0.99	0.911	0.762	0.561	0.333	0.105	-0.096	-0.244	-0.323	-0.323	-0.095	0.105		

Note: m - the number of phases.

3.2 Applying the pitch shortening procedure

The procedure of shortening the coils (winding sections) of phase y in relation to the diametral opening ($y=\tau$) is applied to decrease the amplitude of only certain harmonics (one or two). In this case, it is handled with the y parameter of the winding but also with the winding mode (e.g. winding in two layers). The shortening factor is calculated with the relation [10,15]:

$$k_{sc} = \sin\left(v \,\beta_{sc} \frac{\pi}{2}\right),\tag{19}$$

where: $\beta_{sc} = y/\tau \,$ - is the relative value of the opening.

From (14) it follows that the harmonic with order number v can be canceled if y satisfies the equation:

$$y = 2k\tau/v, k \in N \tag{20}$$

If the solution is executable (y constitutes an integer number of notches), then the harmonic v does not appear in the expression of the induced electromotive voltages. For example, for a relative step of 4/5, the 5th harmonic is excluded, and for a relative step of 6/7, the 7th harmonic is excluded. As a rule, the shortening is done in such a way as to decrease two neighboring harmonics to the same extent. For example, when selecting the step $y/\tau=0.83$, the 5th but also the 7th harmonic is significantly reduced. In this context,

Figure 3 shows a parametric diagram of the relationship $k_{sc} = f(v, \beta_{sc})$, in which each curve refers to a spatial harmonic indicated in the menu.

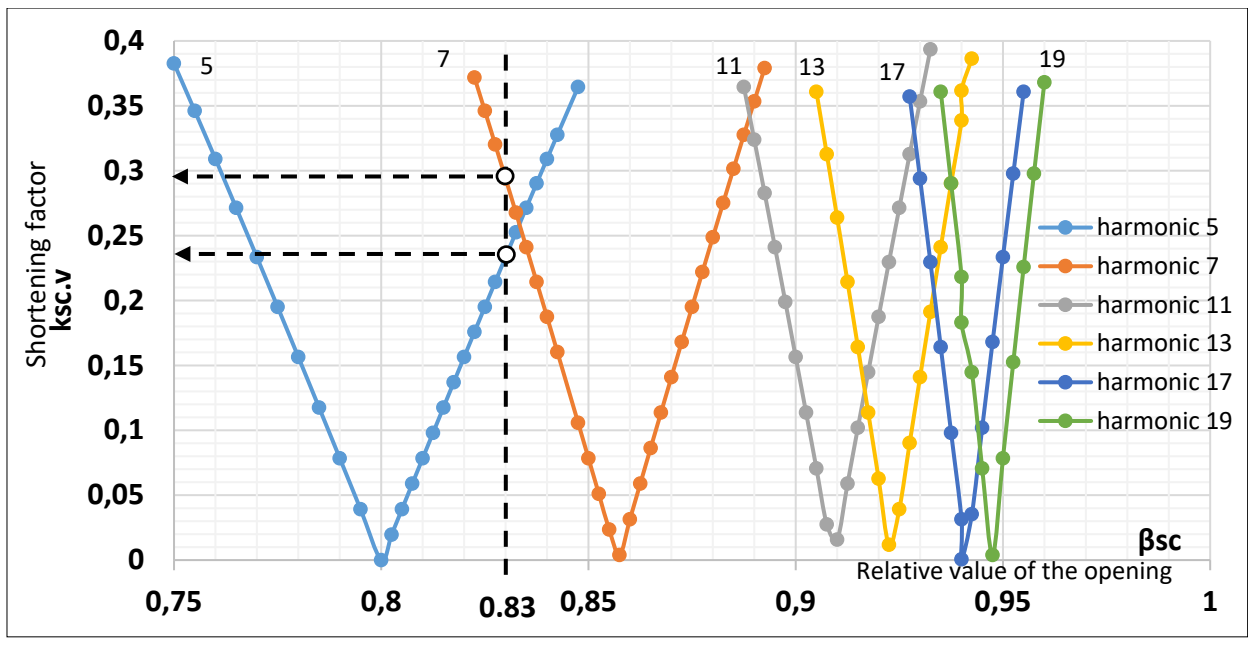


Figure 3. Shortening factor diagram.

3.3 Application of notch tilting procedure

At low and medium powers, the third method of reducing the amplitude of the higher harmonics of the MMF can be applied by tilting the rotor notches, if it is caged. The inclination factor expresses the degree of reduction of the MMF harmonic amplitude in relation to the inclination angle and is calculated with the relation [10,15]:

$$k_{in.v} = \frac{\sin vp\gamma}{vp\gamma} = \frac{\sin(b_r vp\pi/z_2)}{b_r vp\pi/z_2},$$
(21)

where: $2\gamma=\frac{b}{t_c}\frac{2\,\pi}{z_2}$ - the angle of inclination of the notches / the displacement between the ends of the notches, $t_c=2pR/z_2$ - pitch of notches, R- rotor radius, z_2 - the number of notches on the rotor, $b_r=b/t_c$ - the inclination expressed in steps of notches t_c .

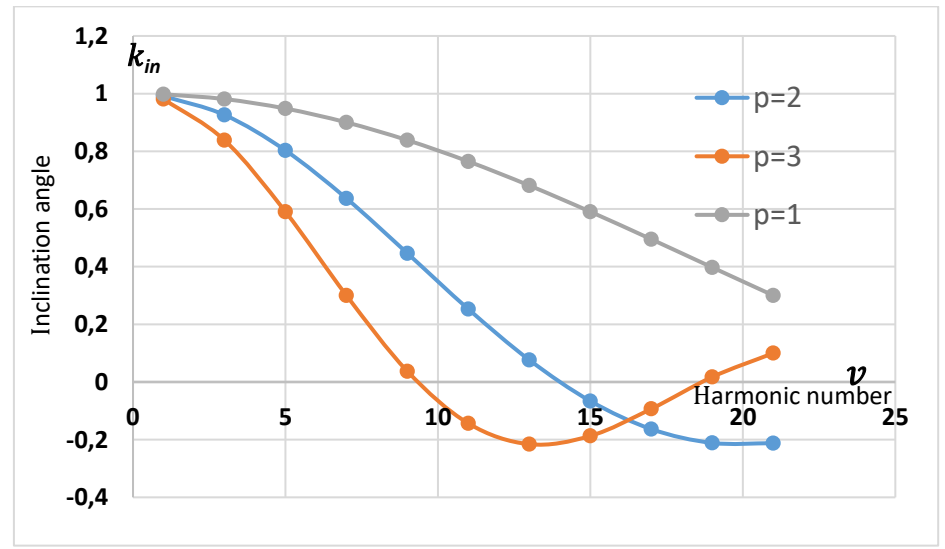


Figure 4. Chart of notch tilt factor $k_{in} = f(v)$, Note: p - the number of pole pairs.

The inclination is usually done with a step or half a step of rotor notch. The efficiency of the tilting procedure can be seen by analyzing the diagram in Figure 4, where the $k_{\rm in}=f(v)$, diagrams are presented, calculated for 3 variants of the number of pole pairs with $b_r=1$ and $z_2=28$.

It is observed that tilting the notches by one tooth pitch leads, for example, in the case of 6-pole machines to practically complete suppression of the upper harmonics, starting with the seventh.

For a rotor winding, the winding factor will be defined with the relation: $k_{wr.v} = k_{qr.v} \cdot k_{in.v}$.

At high powers the tilting procedure is not applied due to considerable additional losses caused by the appearance of transverse (leakage) currents between the rotor bars [13,14]. In these cases, the focus is on shortening the step of the stator winding, choosing the number and optimal ratio of the notches on the stator and rotor.

4. Validation of results

4.1 Argumentation of the measurement methodology and harmonic analysis of MMF, induction, magnetic flux and induced electromotive voltage

As noted above, the MMF and air-gap magnetic induction wave, determined by a stator winding, carried by a sinusoidal current, contains, in addition to the fundamental harmonic, a series of higher harmonics. From relation (8) it follows that the weight of each harmonic can be appreciated by the ratio $(k_{wa,v}/v)$ calculated for the winding, which determines the field (denoted for example by A). The winding factor $k_{wa,v}$ is calculated for the harmonic v. Each harmonic of the magnetic induction in the gap causes / induces in a certain winding (denoted, for example, with B), an electromotive voltage. The effective value or its magnitude is weighted by the calculated ratio $(k_{wb,v}/v)$. Here $k_{wb,v}$ is the winding factor calculated for winding B (in which the electromotive voltage is induced). Thus, the effective value or the amplitude of the electromotive voltage, induced in the winding B by the harmonic v of the magnetic field in the gap, created by the winding A, is weighted by the ratio $(k_{wa,v} \cdot k_{wb,v}/v^2)$.

In the case of the symmetrical six-phase machine the coils of the phase windings (one from each three-phase set) are arranged in the same slots. If a three-phase complete is powered, it will create a magnetic field in the gap, which induces in the second three-phase set electromotive voltages (EMV) identical to the self-induction electromotive voltages in the first set [6,20,21]. The harmonic structure of this voltage is also identical (with small deviations) to the harmonic structure of the air-gap induction and MMF. In this case $k_{wa.v} = k_{w.v}$, and the weight of EMV harmonics can be estimated with the ratio $(k_{w.v}^2/v^2)$.

Thus, the voltage induced in the secondary or self-induced in a stator phase can be defined with the relation:

$$e_{f}(\omega t) = E_{m.1} \sin \omega t \sum_{v} \left[\left(\frac{k'_{w.v}}{v} \right)^{2} \cos \left(v \frac{\pi x}{\tau} \right) \right]$$
 (22)

For an angle $\omega t = \pi/2$, x=0 at which all harmonics reach the value $\pm E_{m,v}$, it will be obtained:

$$E_{m.f} = E_{m1.f} \left[1 - \left(\frac{k'_{w.3}}{3}\right)^2 + \left(\frac{k'_{w.5}}{5}\right)^2 - \left(\frac{k'_{w.7}}{7}\right)^2 + \left(\frac{k'_{w.9}}{9}\right)^2 - \left(\frac{k'_{w.11}}{11}\right)^2 + \left(\frac{k'_{w.13}}{13}\right)^2 - \cdots \right] \quad (23)$$

In the case of asymmetric hexaphase machines, the axes of the three-phase sets are offset by 30° electrical, therefore the phase voltages in the secondary will have a reduced amplitude and a phase offset of (v \cdot 30°).

4.2 Program of the experimental study

Taking into account the above, the following program of the experimental study were defined:

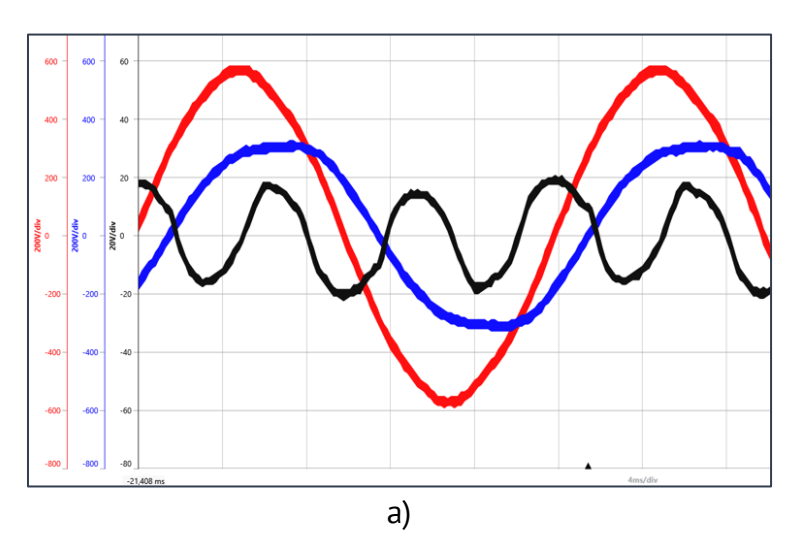
- 1. Taking the oscillograms of the line and phase voltages on a six-phase machine in induction mode with the aim of following the links between EMVs induced in the inductive (powered) and induced (secondary) phases of the six-phase machines in induction mode;
- 2. Taking the oscillograms of the line and phase voltages on the three-phase machines, their harmonic analysis to confirm the correctness of the calculation algorithm of the harmonic structure of the MMF in the gap of the induction machines with different number of poles and sections per pole and phase;
- 3. Taking the oscillograms of the phase voltages on the six-phase machines with symmetrically and asymmetrically arranged windings, the harmonic analysis of the phase voltages in order to determine the applicability of the developed calculation algorithm and the confirmation of the results of the analytical study on the harmonic structure of the MMF in the gap of n-three-phase machines;
- 4. Taking the oscillograms of the voltages between the nodes of the three-phase sets of the windings in relation to the neutral wire of the power supply in order to obtain experimental arguments regarding the value and orientation of the phasors of the MMF harmonics of multiple order to 3.

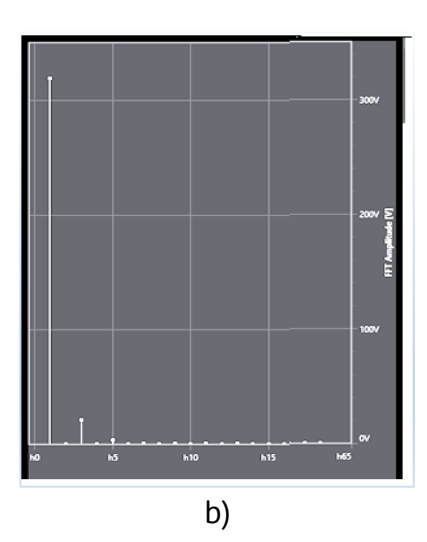
The experimental tests were carried out on 4 induction machines, made on identical constructive samples but with different stator windings: MA3F-1500 and MA3F-1000 – three-phase machines with 4 and 6 poles, respectively; MA6F-SIM and MA6F-ASIM – 6-pole hexaphase machines, with windings arranged symmetrically and asymmetrically, respectively. The windings of the examined machines are executed with diametral pitch, $y=\tau$. The machines' rotors are identical and each have 28 pitched notches.

The basic instrument used for measurements and harmonic analysis – oscilloscope type FLUKE 190-204 SCOPOMETER 4CH 200MHz 2.5GS/s.

4.3 Analysis of the results of the experimental study

Figures 5, 6 and 7 show examples of oscillograms, taken in the idling regime of the experimental samples described above.





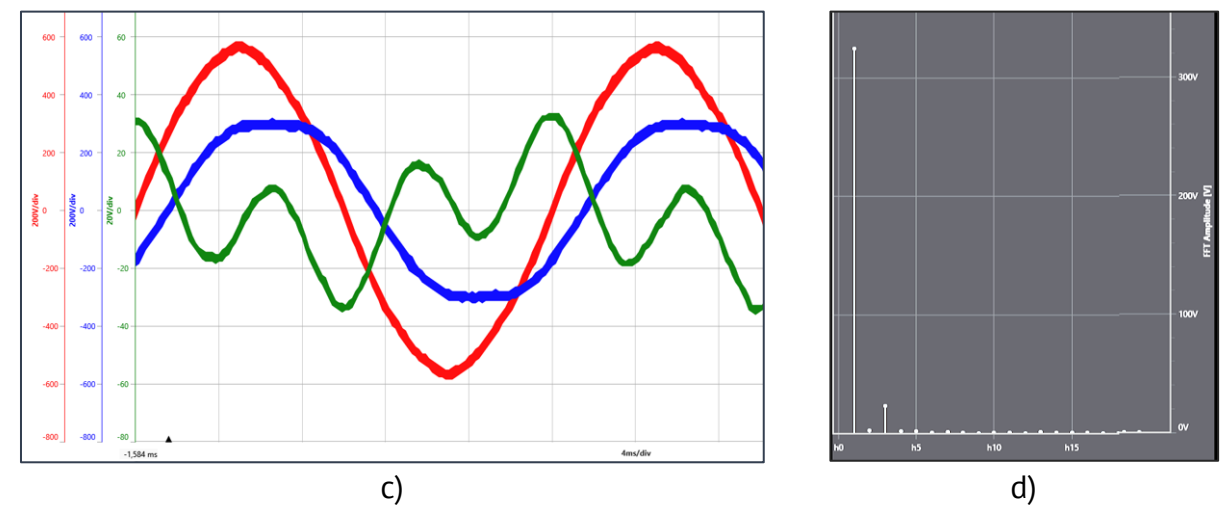


Figure 5. The MA6F-SIM six-phase machine in induction mode: a) and c) – voltage diagram for the primary and secondary set respectively: red - line voltage, blue - phase voltage, green - node voltage; b) and d) - the harmonic component of the phase voltages of the primary and secondary sets, respectively.

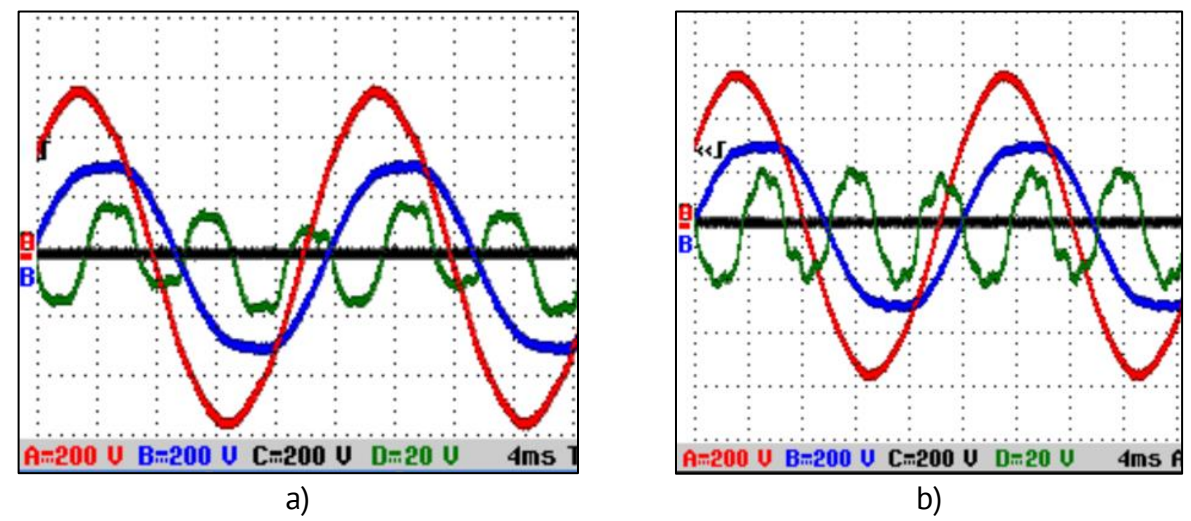
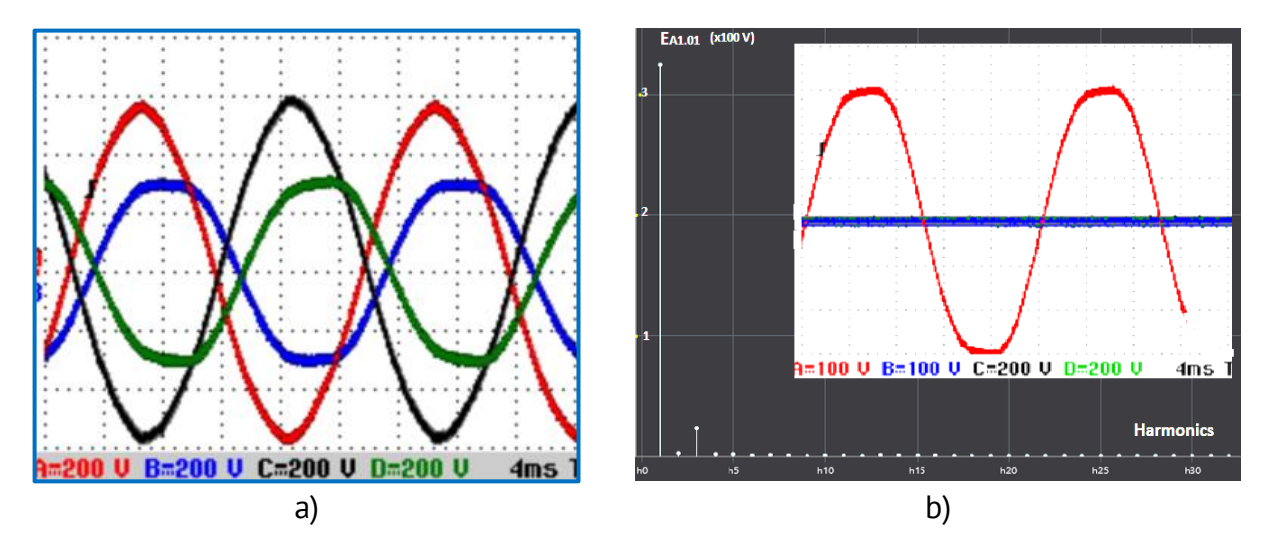


Figure 6. Voltage diagram: line (red), phase (blue) and node (green): a) machine MA3F-1000 rpm, b) machine MA3F-1500 rpm.



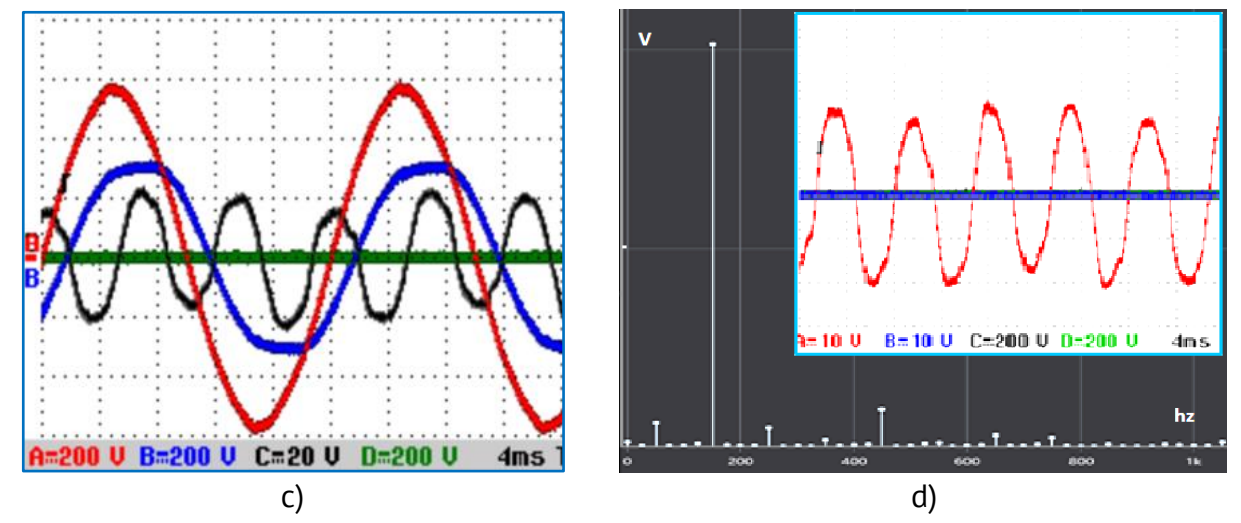


Figure 7. Voltage diagram and their harmonic structure. MA6F-SIM machine with 6-phase power supply, operating in idle mode: a) line and phase voltages: $E_{A1.C1}$ -red, $E_{A1.01}$ - blue, $E_{B2.C2}$ - gray , $E_{B2.02}$ - green; b) the harmonic structure of the phase voltage $E_{A1.01}$; c) voltage diagram of a three-phase set: $E_{A1.C1}$ - red, $E_{A1.01}$ - blue, $E_{01.02}$ - green, $E_{01.N}$ - gray; d) the harmonic structure of the voltage $E_{01.N}$

Table 4 shows the results of the harmonic analysis performed for each of the measured voltages, using the software provided with the FLUKE 190-204 oscilloscope. The table also includes the results of the calculations regarding the harmonic composition (TEM magnitude), based on the relations deduced above (18, 13, 14, 16).

Table 4
Harmonic structure of self-induction electromotive voltages in a phase winding

Order v	1	3	5	7	9	11	13	15
Example 1	MA3F: 2p=4, m=3, q=3, br=1, βsc=1, ksc=1							
$k_{w.v}^{\prime}$	1	0.694	0.227	-0.185	-0.347	-0.185	0.227	0.694
$E_{ m mf.v}$, calculating.	324	17.4	0.67	0.226	0.482	0.092	0.01	0.700
E _{mf.v} , measured	324	20.2	2.37	1.78	1.78	0	0	0
Example 2			MA3F: 2	p=6, m=3,	q=2, br=1	L, βsc=1		
$k_{w.v}'$	1	0.732	0.268	-0.268	-0.732	-1	-1	-0.732
E _{mf.v} , calculating	327.5	19.5	0.94	0.48	2.16	2.71	1.94	0.78
E _{mf.v} , measured	327.5	19.6	4.2	1.2	1	2	1.2	0.7
Example 3		MA6F-SIM: 2p=6, m=6, q=2, br=1, βsc=1						
$k_{w.v}'$	1	0.732	0.268	-0.268	-0.732	-1	-1	-0.732
$E_{\mathrm{mf.v}}$, calculating.	325	19.3	0.93	0.48	2.15	2.69	1.92	0.77
E _{mf.v} , measured	325	21	1.8	0.2	1.2	0.2	0.1	0.1
Example 4	MA6f-ASIM: 2p=6, m=6, q=1, br=1, βsc=1							
$k_{w.v}'$	0.9812	0.8385	0.5904	0.3	0.03	-0.144	-0.221	-0.187
$E_{ m mf.v}$, calculating.	319.3	25.91	0	0	0.004	0.057	0.096	0.052
E _{mf.v} , measured	319.3	21	2.0	0	0	0	0	0

Note: v - harmonic number (order harmonic); $E_{mf.v}$ - the self-induction electromotive voltages; p - the number of pole pairs; $k_{w.v}'$ - the winding factor calculated for the harmonic v; MA3F - three-phase machines with 4 and 6 poles, respectively; MA6F-SIM - 6-pole hexaphase machines, with windings arranged symmetrically; MA6F-ASIM - 6-pole hexaphase machines, with windings arranged asymmetrically.

Based on the results of the experimental tests and those obtained by calculation (table 4) it is found:

- The harmonic structure of the voltages induced in the phase windings of the sixphase machine in induction mode is identical to that of the voltages induced in the second complete three-phase. Thus, for the assessment of the harmonic structure of self-induction and induced voltages, the measurements performed on any of these three-phase sets connected in a star with isolated nodes in relation to the neutral wire of the power supply can be used.
- The line voltages do not contain higher harmonics, they keep the form of the line voltage imposed by the power supply.
- The signal captured as a potential difference between the node of a three-phase set and the neutral wire of the power supply comprises the entire spectrum of multiple harmonics at 3, present in the phase voltage of the winding.
- In the case of machines with symmetrically arranged windings with six-phase power supply, the potential difference between the nodes of the two three-phase sets is zero, which confirms the fact that the phasors of the respective harmonics in all 6 phases coincide. In the case of machines with asymmetrically arranged winding, the rated voltages ($E_{02.N2}$ and $E_{01.N1}$) have the same magnitude but are out of phase by 30°.
- The results of the measurements, carried out on experimental samples, largely correspond to the quantities determined by calculations (according to the methodology described in the paper) regarding the harmonic structure of the MMF, the magnetic field created by it in the air gap of the six-phase machines, and the voltages induced in the phase windings.

5. Conclusions

- 1. The mathematical model of the magnetomotive force in the air gap of the six-phase asynchronous machine with various variants of the stator winding structure was developed.
- 2. Results of the measurements carried out on experimental samples confirm, to a large extent, the accepted hypotheses and the relations proposed for the calculation of the harmonic structure of the magnetic field in the air gap of the six-phase asynchronous machines.
- 3. It has been shown that the harmonic structure of the MMF of six-phase induction machines improves substantially compared to three-phase if the winding is arranged asymmetrically. The 5th, 7th, 19th order harmonics are suppressed.
- 4. The symmetrical six-phase induction machine from the point of view of the harmonic structure of the MMF in the air gap is identical to a three-phase machine.
- 5. As effective tools for reducing the magnitude of the higher harmonics (parasites) of the MMF in the air gap of the six-phase machine, the following can serve: the use of distributed windings, the shortening of the winding step, the inclination of the rotor notches, but also the selection of the optimal number of notches on the stator and rotor

The results of the present paper will be used in further research devoted to the study of asynchronous torques created by higher spatial harmonics in the air gap and additional loss reduction technologies in six-phase motors in healthy and fault operating regimes.

Acknowledgments: The work was carried out within the UTM institutional sub-project number 020406 "Models, systems and technologies for energy efficiency, decarbonisation and digitization of energy, industry, construction and transport processes" (MoSiTed).

Contributions: The authors equally contributed to the conception, realization of the analytical and experimental study, writing and editing of this paper.

Conflicts of Interest: The authors declare no conflict of interest.

References

- 1. Dumitriu, C.; Popovici, L.; Popescu, M.; Tudor, E. Six-phase machine for driving electric vehicles. In: Symposium on Electric Motors SME'18. Bucharest, Romania, 2018. [in Romanian]
- 2. Niţucă, C.; Nucă, I.; Pleşca, A.T.; Chiriac, G.; Cazac, V; Burduniuc, M. Improving the cross-border public transportation using electric buses supplied with renewable energy. Tritonic, Bucharest, Romania, 2022, 220 p. ISBN 978-606-749-584-3.
- 3. Gwozdziewicz, M.; Kisielewski, P. Enclosure-less six-phase inductor motor. Elektrotechniczny Przegląd 2019, 6 (R. 95), pp. 141-144.
- 4. Sui, Y.; Zheng, P.; Wu, F.; Yu, B.; Wang, P.; Zhang, J. Research on a 20-Slot/22-Pole Five-Phase Fault-Tolerant PMSM Used for Four-Wheel-Drive Electric Vehicles. Energies 2014, 7, pp. 1265-1287.
- 5. Yepes, A.G.; Gonzalez Prieto, I.; Lopez, O.; Duran, M.J.; Doval-Gandoy, J. A Comprehensive Survey on Fault Tolerance in Multiphase AC Drives, Part 2: Phase and Switch Open-Circuit Faults. Machines 2022, 10(3), 221; https://doi.org/10.3390/machines10030221, 21 March 2022,78 p.
- Maeztu, M.Z.; Levi, E.; Jones, M. Regenerative Testing of Multiphase Machines with Multiple Three-phase Windings. In: 18th International Power Electronics and Motion Control Conference (PEMC), 26-30 August 2018, DOI:10.1109/epepemc.2018.8521904.
- 7. Cui, R.; Yu, S.; Li, S. Open-Switch Fault Detection Based on Open-Winding Five-Phase Fault-Tolerant Permanent-Magnet Motor Drives. *Machines* 2022, 10, 829.
- 8. Abdelwanis, M.I.; Rashad, E.M.; Taha, I.B.M.; Selim, F.F. Implementation and Control of Six-Phase Induction Motor Driven by a Three-Phase Supply. *Energies* 2021, 14, 7798.
- 9. Martins, F.S.; Alvarenga, B.P.; Paula, G.T. Electrical Machine Winding Performance Optimization by Multi-Objective Particle Swarm Algorithm. *Energies* 2024, 17, 2286.
- 10. Covrig, M. *Electrical machines. Magnetic fields, inductances, induced electromotive voltages.* ICPE Publishing House, Bucureşti, Romania, 1996, 1, 140 p. [in Romanian]
- Livadaru, L.; Bobu, A.; Munteanu A.; Vîrlan B.; Simion A. FEM-based Analysis on the Operation Three-Phase Induction Motor connected to Six-Phase Supply System. Part 1 - Operation under healty conditions. In: International Conference on Electromechanical and Power-Systems (SIELMEN), 2017, pp. 119-124, December 2017. DOI: 10.1109/SIELMEN.2017.8123310.
- 12. Livadaru, L.; Bobu A.; Munteanu A.; Vîrlan, B.; Simion A. FEM-based Analysis on the Operation Three-Phase Induction Motor connected to Six-Phase Supply System. Part 2 -Study on fault-tolerance capability conditions. In: *International Conference on Electromechanical and Power-Systems (SIELMEN)*, pp. 125-130, December 2017. DOI: 10.1109/SIELMEN.2017.8123311.
- 13. Richter, R. *Electric motors. Volume IV, Induction Machines*, Technical Ed., Bucharest, Romania, 1960, 447 p. [in Romanian].
- 14. Radin, V.I.; Bruschin, D.E.; Zaharovici, A.E. *Electricschie masini*. *Asincronnie masini*. Visshaia shcola, Moskva, Russia, 1988, 204 p. [in Russian].
- 15. Simion, A. Electrical machines. The Asynchronous Machine. PIM, Iasi, Romania, 2012, 3, 501 p. [in Romanian].
- 16. BOLDEA, I. *INDUCTION MACHINES HANDBOOK: TRANSIENTS, CONTROL PRINCIPLES, DESIGN AND TESTING.* 3RD ED. CRC PRESS, BOCA RATON, FLORIDA, SUA, 2023, 431 P.
- 17. Deaconu, S.I. Electrical machines. Politehnica, Timisoara, Romania, 2016, 449 p. [in Romanian].
- 18. Kopilov, I.P.; Klocov, B.K.; Morozkin V.P.; Tocarev, B.F. *Design of electric machines*. Iurait, Moscow, Russia, 2011. 767 p. [in Russian].
- 19. Boldea, I.; Nasar, S.A. The induction machines design handbook. 2nd ed. CRC Press, New York, SUA, 2010, 824 p.
- 20. Alemi-Rostamia, M.; Rezazadehb, G.; Tahamib, F.; Akbari-Resketic, H.R. Fault-Tolerant Capability Analysis of Six-Phase Induction Motor with Distributed, Concentrated and Pseudo Concentrated Windings. *International Journal of Science, Scientia Iranica* 2022, 31(10), pp. 775-789.
- 21. Todos, P.; Nuca, I.; Tertea, G.; Cazac, V. Identification of Parameters and Power Losses of Six-Phase Asynchronous Machines by Induction Regenerative Method. In: *10th International Conference on Modern Power Systems (MPS)*, 2023, Cluj-Napoca, Romania, pp. 1-6.

Citation: Todos, P.; Tertea, Gh.; Nuca, I. Harmonic analysis of magnetomotive force in the air gap of six-phase asynchronous machines. *Journal of Engineering Science* 2024, XXXI (3), pp. 27-43. https://doi.org/10.52326/jes.utm.2024.31(3).03.

Publisher's Note: JES stays neutral with regard to jurisdictional claims in published maps and institutional affiliations.



Copyright:© 2024 by the authors. Submitted for possible open access publication under the terms and conditions of the Creative Commons Attribution (CC BY) license (https://creativecommons.org/licenses/by/4.0/).

Submission of manuscripts:

jes@meridian.utm.md

Topic

https://doi.org/10.52326/jes.utm.2024.31(3).04 UDC 004.7





STATISTICAL SIMULATION OF RELIABILITY OF NETWORKS WITH EXPONENTIALLY DISTRIBUTED UNIT LIFETIMES

Maria Rotaru *, ORCID: 0000-0002-3198-0297

Technical University of Moldova, 168 Stefan cel Mare Blvd., Chisinau, Republic of Moldova
* Corresponding author: Maria Rotaru, maria.rotaru@isa.utm.md

Received: 08. 30. 2024 Accepted: 09. 26. 2024

Abstract. In this paper, there were deduced three new lifetime distributions of serial-parallel and parallel-serial networks, their distribution being approached by means of analytical and Monte-Carlo methods. The novelty of the distribution consists in the fact that the number of subnets is random, governed by the Poisson and Logarithmic distributions, the lifetimes of the units in each subnet being independent, identically, exponentially distributed random variables, the number of units in each subnet is the same constant integer number. It was shown that the most important theoretical characteristics of lifetime for such networks, as the mean value, the variance, the survival/reliability function, my be approximated, with desired accuracy, by the same corresponding characteristics, as the sample mean value, sample variance, empirical survival/reliability function simulated by Monte-Carlo methods. Results are illustrated tabularly and graphically for some concrete examples.

Keywords: mean value, variance, survival/reliability function, Monte-Carlo methods.

Abstract. În această lucrare au fost deduse trei noi distribuții de durată de viață a rețelelor de tip serial-paralel și paralel-serial, distribuția acestora fiind abordată prin metode analitice și metode Monte-Carlo. Noutatea distribuției constă în faptul că numărul de subrețele este aleatoriu, guvernat de distribuțiile Poisson și Logaritmică, duratele de viață ale unităților din fiecare subrețea fiind variabile aleatoare independente, identic, exponențial distribuite, numărul de unități din fiecare subrețea. este același număr întreg constant. S-a arătat că cele mai importante caracteristici teoretice ale duratei de viață pentru astfel de rețele, precum valoarea medie, varianța, funcția de supraviețuire/fiabilitate, pot fi aproximate, cu acuratețea dorită, prin caracteristicile corespunzătoare: valoarea medie a eșantionului, varianța eșantionului și funcția empirică de supraviețuire/fiabilitate, simulate prin metode Monte-Carlo. Rezultatele sunt ilustrate tabelar și grafic pentru unele exemple concrete.

Cuvinte cheie: valoare medie, varianță, funcție de supraviețuire/fiabilitate, metode Monte-Carlo.

1. Introduction

Serial-parallel and parallel-serial networks are usually found in many works [1-3] as a subsystem within complex networks, such as Wi-Fi, computers, and communication networks. The overall reliability of these larger networks depends on the reliability of these subnets [4]. Although these network types have been extensively studied, existing research

M. Rotaru 45

predominantly relies on static probabilistic models [5-6]. These models assume constant probabilities of network units remaining operational over time, with a fixed number of units [5] Architecturally, the structure of serial-parallel and parallel-serial networks is shown and described in the source [7].

However, the ever-changing nature of modern networks requires a more flexible approach. Networks are influenced by various factors, including environmental shifts, user behavior, and hardware wear and tear. All of these elements can affect the reliability of network components. As a result, there is an increasing demand for models that account for the dynamic nature of network reliability, considering fluctuations in operational probabilities and variations in the number of network units. In this context, research on serial-parallel and parallel-serial networks offers significant insights into the reliability of dynamic networks [8]. By examining how these simpler network architectures behave in changing environments, researchers can create more robust models for analyzing and predicting the reliability of complex networks. This empowers network engineers to design more resilient systems capable of withstanding the challenges posed by real-world conditions.

In this paper, we consider the dynamic mathematical models of serial-parallel (type A) networks and parallel-serial (type B) networks [9]. For the study we will take variants (type A or B) in which the network units have exponentially distributed lifetimes being independent, identically distributed random variables (*i.i.d.r.v.*) with the cumulative distribution function (*c.d.f.*) F(x) and the number of units in each subnet being the same and equal to N \geq 2.

Also, the number of subnets is a random variable M of PSD classes, independent of lifetimes of units.

2. Notions and auxiliary results

As the number of subnets is a variable of PSD classes [10], with Poisson or Logarithmic distribution, we will define according to the source [11] the Power Series Distribution.

Definition 1. We say that M is a Power Series Distributed random variable with power series function $A(\omega) = \sum_{m \geq 0} a_m \omega^m$ and power parameter of the distribution ω , shortly $M \in PSD$, if

$$P(M = m) = \frac{a_m \omega^m}{A(\omega)}, a_m \ge 0, m = 0, 1, 2, \dots \omega \in (0, \tau),$$

where the power series $\sum_{m\geq 0} a_m \omega^m$ is convergent with radius of convergence a positive number τ . As real networks invariably include at least one subnet, or each subnet contains at least one unit, the distribution of parameters must be 0-truncated. So, as a PSD, 0-truncated $Poisson(\omega)$ and $Log(\omega)$ distributions be represented as in [9] in this way.

Table 1
The representative elements of the PSD class for Poisson and Logarithmic truncated distributions

Distribution	a_m	ω	$A(\omega)$	τ
$Poisson^*(\omega)$,	$\left(\frac{1}{2} for m - 12\right)$	ω	$e^{\omega}-1$	+∞
$\omega > 0$	$\left\{\frac{1}{m!}, for \ m = 1, 2, \dots, \right.$			
	(0, $for m = 0$.			
$Log(\omega)$	$\left(\frac{1}{m} for m = 1.2\right)$	ω	$-\ln(1-\omega)$	1
$0 < \omega < 1$	$\begin{cases} \frac{1}{m}, for \ m = 1, 2, \dots, \end{cases}$			
	(0, $for m = 0$.			

Then, according to the paper [9] we have the following:

Proposition 1. The lifetime cumulative distribution functions (c.d.f.) for networks of type A and B, that we will call distributions of type Min(Max) - PSD and Max(Min) - PSD can be calculated respectively by the general formulas

$$F_{s-p}(x) = \left[1 - \frac{B\left(\omega\left(1 - (F(x))^{N}\right)\right)}{B(\omega)}\right] I_{[0,+\infty)}(x)$$
(1)

$$F_{p-s}(x) = \left[\frac{B\left(\omega\left(1 - \left(1 - F(x)\right)^{N}\right)\right)}{B(\omega)} \right] I_{[0,+\infty)}(x)$$
 (2)

where: F(x) is a c.d.f. of lifetime for each unit of subnet, N is the number of units in each of M subnets and $B(\omega)$ is a power series function of r.v. M.

We will denote the reliability function, also known as the survival function, of a network by R(x), where R(x) = 1 - F(x). Also, we denote by $R_{s-p}(x)$ the reliability of the serial-parallel network, and by $R_{p-s}(x)$ - the reliability of parallel-serial network. The reliability functions of the respective networks can be calculated by the formulas:

$$R_{s-p}(x) = \left[\frac{B\left(\omega\left(1-\left(F(x)\right)^{N}\right)\right)}{B(\omega)}\right] I_{[0,+\infty)}(x) + I_{(-\infty,0]}(x)$$
(3)

$$R_{p-s}(x) = \left[1 - \frac{B\left(\omega\left(1 - \left(1 - F(x)\right)^{N}\right)\right)}{B(\omega)}\right] I_{[0,+\infty)}(x) + I_{(-\infty,0]}(x)$$
(4)

3. Exponential *Min(Max)-Poisson and Max(Min)-Poisson* mixed distributions as a lifetime distributions

Thus, let consider that $F(x)=\left(1-e^{-\lambda x}\right)I_{[0,+\infty)}(x)$, x>0. If $M\sim Poisson^*(\omega)$, then $P(M=m)=\frac{\omega^m}{m!}/(e^\omega-1)$, $B(\omega)=(e^\omega-1)$. So, for (1), by knowing the formula of the function $B(\omega)$, we have that:

$$F_{s-p}(x) = \left[1 - \frac{e^{\omega\left(1 - \left(1 - e^{-\lambda x}\right)^{N}\right)} - 1}{e^{\omega} - 1}\right] I_{[0, +\infty)}(x)$$
(5)

Deriving **Error! Reference source not found.** with respect to x, we obtain that the probability density function (p.d.f.) $f_{s-p}(x)$ given by the following formula:

$$f_{s-p}(x) = \frac{N\omega\lambda(1 - e^{-\lambda x})^{N-1} e^{\omega\left(1 - \left(1 - e^{-\lambda x}\right)^{N}\right) - \lambda x}}{e^{\omega} - 1} I_{[0, +\infty)}(x)$$
(6)

In the same way we find that lifetime c.d.f. for networks of parallel-serial type:

$$F_{p-s}(x) = \left[\frac{e^{\omega(1-e^{-\lambda Nx})}-1}{e^{\omega-1}}\right]I_{[0,+\infty)}(x)$$
(7)

and its p.d.f. density function:

$$f_{p-s}(x) = \frac{N\omega\lambda e^{\omega(1-e^{-\lambda Nx})-\lambda Nx}}{e^{\omega-1}} I_{[0,+\infty)}(x)$$
 (8)

Due to the fact that lifetime of the Serial-Parallel distribution is a r.v.

$$U_{s-p} = min[max(X_{11,} X_{12,...} X_{1N}), max(X_{21,} X_{12,...} X_{N2}), ..., max(X_{M1,} X_{12,...} X_{MN})]$$

M. Rotaru 47

and lifetime of the Parallel-Serial distribution is a r.v.

 $V_{p-s} = max[min(X_{11}, X_{12},...X_{1N}), min(X_{21}, X_{12},...X_{N2}), ..., min(X_{M1}, X_{12},...X_{MN})],$

where: lifetimes of *i-th* unit in the *j-th* subnet X_{ij} are i.i.d.r.v, $X_{ij} \sim exp\{\lambda\}$, $\lambda > 0$, for i=1,2,...,N, N is the number of units in each subnet, and the number of all subnets is a r.v. $M \sim Poisson(\omega)$, $\omega > 0$ we say that their corresponding distributions are called, respectively, $Exponential\ Min(Max) - Poisson\ and\ Max(Min) - Poisson\ mixed\ distributions.$

Another important indicator is the hazard function [12], also known as failure rate function, that is denoted, for example in the case of Network of type A, by $h_{s-p}(x)$ and given by the formula $h_{s-p}(x) = f_{s-p}(x) \left(1 - F_{s-p}(x)\right)$. Applying the last formula to the cases we study, we get

$$h_{s-p}(x) = \frac{N\omega\lambda(1 - e^{-\lambda x})^{N-1} e^{\omega(1 - (1 - e^{-\lambda x})^{N}) - \lambda x}}{e^{\omega(1 - (1 - e^{-\lambda x})^{N}) - 1}}$$
(9)

and

$$h_{p-s}(x) = \frac{N\omega\lambda e^{\omega(1-e^{-\lambda Nx})-\lambda Nx}}{e^{\omega}(1-e^{1-e^{-\lambda Nx}})}$$
(10)

Remark 1. The lifetime distribution for parallel-serial networks will be excluded from our research because this distribution coincides with the distribution proposed and studied in the paper [13], as a lifetime distribution Exponential Max-Poisson mixed distribution.

Remark 2. Another distribution functions and pdf of the *r.v.* U_{s-p} and V_{p-s} for different combination are presented in the paper [3].

So, in the following, we will analyze from a statistical point of view, including through Monte Carlo validation, the serial-parallel type model, thus bringing a new lifetime distribution of serial- parallel networks. Thus, using general formula for lifetime p.d.f. (6) we will calculate, for our needs, the theoretical mean value and variance numerically, by means of System Mathematica 14.0, because our distribution depend, in fact, of 3 parameters: λ , ω and N. After we get the results, we will simulate in Mathematica these random variables using Monte-Carlo methods and check how well they approximate the theoretical mean value and the theoretical dispersion [14].

The Monte Carlo simulation algorithm in our case may be described as following:

- **Step 1**: Generate a sample of N values based on exponential distribution with parameter λ .
- Step 2: Take the maximum value of sample generated at the Step 1.
- **Step 3**: Generate the value of M using a zero-truncated Poisson distribution with parameter ω .
- **Step 4**: Generate a sample of M values by repeating M times the Steps 1-2.
- Step 5: Take the minimum value of the sample created at the Step 4.
- **Step 6**: Calculate, according to the Central Limit Theorem for independent and identically distributed random variables [15], the value $k = [(\sigma x_{1-\alpha/2}/\epsilon)^2] + 1$, where σ is the standard deviation of lifetime U_{s-p} , $x_{1-\alpha/2}$ is the $1-\alpha/2$ quantile for standard normal distribution N(0,1) and ϵ is the desired error of approximation for theoretical mean value $\mathbb{E}U_{s-p}$, taking $\alpha = 0.05$ and $\epsilon = 0.01$.
- **Step 7**: Generate a sample of k values by repeating steps 4-5 k times.
- **Step 8**: Calculate the mean value $\mathbb{E}\widehat{U_{s-p}}$ of the sample generated at the 7th step to approximate the theoretical mean value $\mathbb{E}U_{s-p}$.

Step 9: Calculate the variance $\mathbb{D}\widehat{U_{s-p}}$ of sample generated at the 7th step to approximate the value of $\mathbb{D}U_{s-p}$.

Table 2 Simulated vs theoretical values of mean and dispersion for Serial-Parallel model with $M \sim Poisson^*(\omega)$ i.e. $P(M=m) = \frac{1}{m} \frac{\omega^m}{m}$ m = 1.2 $\omega > 0$

	$M \sim Poisson(\omega), i.e. P(M = m) = \frac{1}{e^{\omega} - 1} \frac{1}{m!}, m = 1, 2,, \omega > 0$							
ω	λ	N	$\mathbb{E} oldsymbol{U}_{s-oldsymbol{p}}$	$\widehat{\mathbb{E} U_{s-p}}$	$\mathbb{D}U_{s-p}$	$\widehat{\mathbb{D}U_{s-p}}$		
0.5	1.25	3	1.348149323	1.338431878	0.888013261	0.872941761		
0.5	1.25	5	1.701888703	1.703793221	0.925795556	0.934127344		
0.5	1.25	8	2.04654821	2.044372993	0.946212854	0.942520703		
0.5	2.15	3	0.783777285	0.788386991	0.51509177	0.520160698		
0.5	2.15	5	0.98782637	0.985834986	0.536698953	0.535302996		
0.5	2.15	8	1.187243735	1.195373996	0.547304826	0.557221324		
0.5	3.65	3	0.46033396	0.460613746	0.302799361	0.302450773		
0.5	3.65	5	0.582155058	0.581128178	0.315834387	0.315438699		
0.5	3.65	8	0.700233886	0.699444238	0.324542748	0.320289999		
2	1.25	3	1.034266589	1.037160726	0.724065222	0.72071219		
2	1.25	5	1.368218002	1.369974019	0.760181813	0.761771466		
2	1.25	8	1.702108973	1.69811621	0.78666366	0.789075721		
2	2.15	3	0.601482708	0.600396316	0.419109425	0.415211898		
2	2.15	5	0.796446843	0.794904434	0.442090831	0.43995408		
2	2.15	8	0.991439749	0.989627481	0.460112171	0.460228158		
2	3.65	3	0.354989223	0.355135287	0.247767369	0.247998247		
2	3.65	5	0.468843135	0.46996092	0.26090492	0.262020569		
2	3.65	8	0.582949722	0.584418392	0.269372425	0.268073442		
10	1.25	3	0.459026258	0.459073661	0.234353946	0.234169648		
10	1.25	5	0.736948531	0.73813245	0.279303413	0.27924198		

Note: N – the number of units in each of M subnets; $\mathbb{E}U_{s-p}$ - the theoretical mean value; $\mathbb{E}\widehat{U_{s-p}}$ - the mean value calculated with Monte-Carlo simulated values; $\mathbb{D}U_{s-p}$ - the theoretical variance; $\mathbb{D}\widehat{U_{s-p}}$ - the variance calculated with Monte-Carlo simulated values.

In the Table 2 is shown how for lifetime p.d.f. (6) we calculated the theoretical mean value $\mathbb{E}U_{s-p}$ and variance $\mathbb{D}U_{s-p}$ numerically, using the Wolfram Mathematica 14.0 soft, depending on the values of the parameters λ , ω and N. After that, we simulated them in Wolfram Mathematica using Monte-Carlo methods described in the algorithm above, and obtained for the same parameters, that the empirical mean $\mathbb{E}\widehat{U_{s-p}}$ and empirical variance $\mathbb{D}\widehat{U_{s-p}}$ approximate the theoretical mean value and the theoretical dispersion very accurate, respecting the proposed admissible error ε =0.01. Also, we will follow the similarity in the graphic representation that follows.

It is easy to see how the number of simulations influences the resulting data by viewing the constructed empirical functions. For this we chose two values for the number of simulations k, the first case k=50, and the second case k=20735. The difference between the two cases is that for the second case the number k is calculated according to the Central Limit Theorem [15], as stipulated in the algorithm. In the Figure 2b, we notice that for the same parameters, when the number k was deduced according to the formula the empirical distribution function approximates the theoretical cumulative distribution very well, and for the larger number of iterations (simulated values) they tend to coincide.

M. Rotaru 49

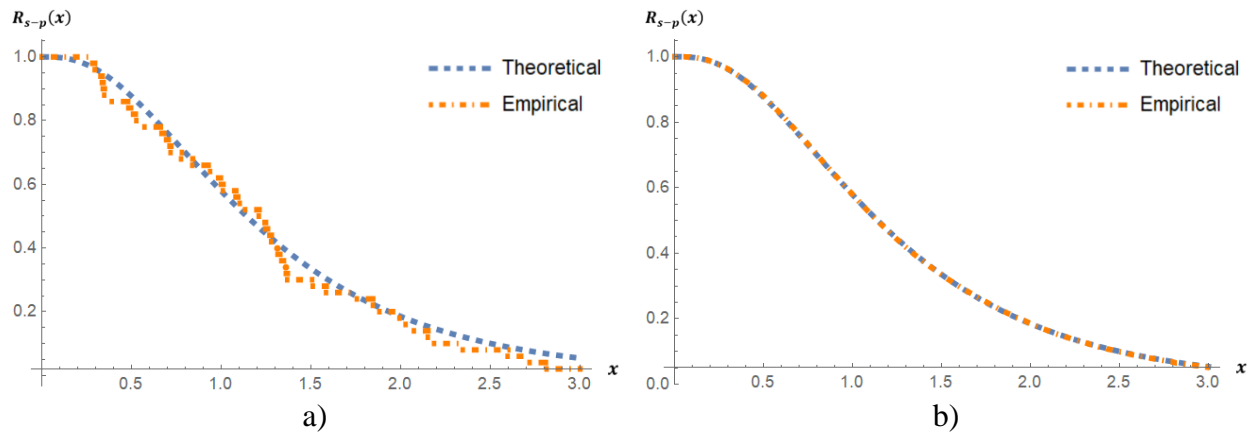


Figure 2. Survival function for $\omega = 0.5$, $\lambda = 1.25$, N = 3, $\varepsilon = 0.01$.

4. Exponential *Min(Max)-Logarithmic* and *Exponential Max(Min)- Logarithmic* mixed distributions as a lifetime distributions

With a similar approach as for the previous case, the study is extended with a new case where the value of M, the number of subnetworks, will be generated using the logarithmic distribution. With the appropriate substitutions, the following results $F(x) = (1-e^{-\lambda x})I_{[0,+\infty)}(x)$, x>0. If $M{\sim}Log(\omega)$, and $P(M=m)=\frac{-1}{\ln(1-\omega)}\cdot\frac{\omega^m}{m}$, $0<\omega<1$, $B(\omega)=-\ln(1-\omega)$ then, for **Error! Reference source not found.**) by knowing the formula of the function $B(\omega)$ and substituting it, we get that:

$$F_{s-p}(x) = \left[1 - \frac{\ln(\omega((1-e^{-\lambda x})^{N}-1)+1)}{\ln(1-\omega)}\right]I_{[0,+\infty)}(x)$$
 (11)

The first derivative of F(x) from **Error! Reference source not found.** yields the distribution density function f(x) and it is represented by the formula:

$$f_{s-p}(x) = \frac{N\lambda\omega(1 - e^{-x\lambda})^{N-1}}{\left(\omega\left(1 - \left(1 - e^{-x\lambda}\right)^{N}\right) - 1\right)\ln(1 - \omega)e^{x\lambda}}$$
(12)

In the same way, we calculate the lifetime distribution function F(x) for networks of parallel-serial type:

$$F_{p-s}(x) = \frac{\ln(1 + (-1 + (e^{-x\lambda})^N)\omega)}{\ln(1 - \omega)}$$
(13)

The distribution's density function can be represented as following:

$$f_{p-s}(x) = \frac{\lambda \omega N (e^{-x\lambda})^N}{\left(\left(1 - \left(e^{-x\lambda}\right)^N\right)\omega - 1\right)\ln(1 - \omega)}$$
(14)

Following a similar approach as in the initial case, we utilize the same formula to deduce the hazard function, also known as the failure rate function:

$$h_{s-p}(x) = -\frac{\lambda \omega N (1 - e^{-x\lambda})^{N-1}}{e^{x\lambda} \left(\omega (1 - e^{-x\lambda})^N - \omega + 1\right) \ln(\omega (1 - e^{-x\lambda})^N - \omega + 1)}$$
(15)

and

$$h_{p-s}(x) = -\frac{\lambda \omega N e^{-\lambda N x}}{(\omega e^{-\lambda N x} - \omega + 1)(\ln(1 - \omega) - \ln(\omega e^{-\lambda N x} - \omega + 1))}$$
(16)

In similar fashion, we analyze the next case. With respect to all the given constraints and by an analogous to the first part procedure, we will perform an analysis from a statistical point of view, including validation through Monte Carlo simulation, of the serial-parallel type

model and the parallel-serial type model. The main goal is to emphasize the two new lifetime distribution of serial- parallel and parallel-serial networks.

Table 3 Simulated vs theoretical values of mean and dispersion for serial-parallel model with $M_{\rm c} L_{\rm c} \sigma(\omega)$ i.e. $P(M=m) = \frac{1}{2} \frac{\omega^m}{m} = 1.2 \frac{1}{2} \frac{1}{2}$

0.15 1. 0.15 1. 0.15 2. 0.15 2. 0.15 3. 0.15 3. 0.15 3. 0.45 1. 0.45 1. 0.45 1. 0.45 1. 0.45 1.	.25	N 3	$\frac{d = m}{\mathbb{E} U_{s-p}}$	$\widehat{\mathbb{E}U}_{s-p}$	$\frac{,2,\ldots,0<\omega<}{\mathbb{D}U_{s-p}}$	$\widehat{\mathbb{D}U_{s-p}}$
0.15 1. 0.15 1. 0.15 2. 0.15 2. 0.15 3. 0.15 3. 0.15 3. 0.45 1. 0.45 1. 0.45 1. 0.45 1. 0.45 1.	.25	3				υP
0.15 1. 0.15 2. 0.15 2. 0.15 3. 0.15 3. 0.15 3. 0.45 1. 0.45 1. 0.45 1. 0.45 1. 0.45 1.			1.428972	1.420671	0.919236	0.916434
0.15 2. 0.15 2. 0.15 3. 0.15 3. 0.15 3. 0.45 1. 0.45 1. 0.45 1. 0.45 1. 0.45 1.	25	5	1.784603	1.790588	0.957371	0.962266
0.15 2. 0.15 2. 0.15 3. 0.15 3. 0.15 3. 0.45 1. 0.45 1. 0.45 1. 0.45 1.	. Z J	8	2.132027	2.136382	0.976682	0.978806
0.15 2. 0.15 3. 0.15 3. 0.15 3. 0.45 1. 0.45 1. 0.45 1. 0.45 1.	.15	3	0.829977	0.837779	0.534452	0.53958
0.15 3. 0.15 3. 0.15 3. 0.45 1. 0.45 1. 0.45 1. 0.45 1.	.15	5	1.03809	1.037251	0.555081	0.55459
0.15 3. 0.15 3. 0.45 1. 0.45 1. 0.45 1.	.15	8	1.238298	1.232948	0.567016	0.568323
0.15 3. 0.45 1. 0.45 1. 0.45 1.	.65	3	0.48913	0.488425	0.314865	0.311441
0.45 1. 0.45 1. 0.45 1.	.65	5	0.611045	0.604446	0.326281	0.319532
0.45 1. 0.45 1.	.65	8	0.729456	0.730239	0.333657	0.336813
0.45 1.	.25	3	1.324674	1.320241	0.882955	0.883411
	.25	5	1.676801	1.678226	0.919081	0.920216
0.45 2.	.25	8	2.022778	2.029045	0.942711	0.947784
	.15	3	0.771506	0.765819	0.514974	0.508486
0.45 2.	.15	5	0.975403	0.975921	0.534888	0.535843
0.45 2.	.15	8	1.1747	1.173953	0.549026	0.548143
0.45 3.	.65	3	0.454441	0.45114	0.303259	0.300944
0.45 3.	.65	5	0.574409	0.571679	0.315466	0.312011
0.45 3.	.65	8	0.691618	0.6897	0.322884	0.32016
0.95 1.	.25	3	0.893229	0.89389	0.741071	0.741699
0.95 1.	.25	5	1.212151	1.21096	0.796375	0.790388
0.95 1.	.25	8	1.534569	1.533734	0.8263	0.824371
0.95 2.	.15	3	0.520795	0.521037	0.431974	0.433642
0.95 2.	.15	5	0.704601	0.705342	0.459721	0.460441
0.95 2.	.15	8	0.894015	0.891345	0.482631	0.476985
0.95 3.	.65	3	0.30735	0.3059	0.25542	0.25435
0.95 3.	.65	5	0.415546	0.415356	0.272264	0.27161
0.95 3.			0.524733	0.525343	0.281704	0.281689

Note: N – the number of units in each of M subnets; $\mathbb{E} U_{s-p}$ - the theoretical mean value; $\mathbb{E} \widehat{U_{s-p}}$ - the mean value calculated with Monte-Carlo simulated values; $\mathbb{D} U_{s-p}$ - the theoretical variance; $\mathbb{D} \widehat{U_{s-p}}$ - the variance calculated with Monte-Carlo simulated values.

Table 3 presents the calculation of the theoretical mean and variance for the lifetime probability density function (p.d.f.) given in equation (6). We repeated the numerical calculations using Wolfram Mathematica 14.0, based on the parameters λ , ω , and N. Subsequently, we simulated these values using Monte Carlo methods as described in the preceding algorithm. The results confirm one more time that the empirical mean $\mathbb{E}\widehat{U_{s-p}}$ and empirical variance $\mathbb{D}\widehat{U_{s-p}}$ closely approximate the theoretical values, adhering to the proposed admissible error of ϵ =0.01. The following graphical representation further demonstrates this similarity.

M. Rotaru 51

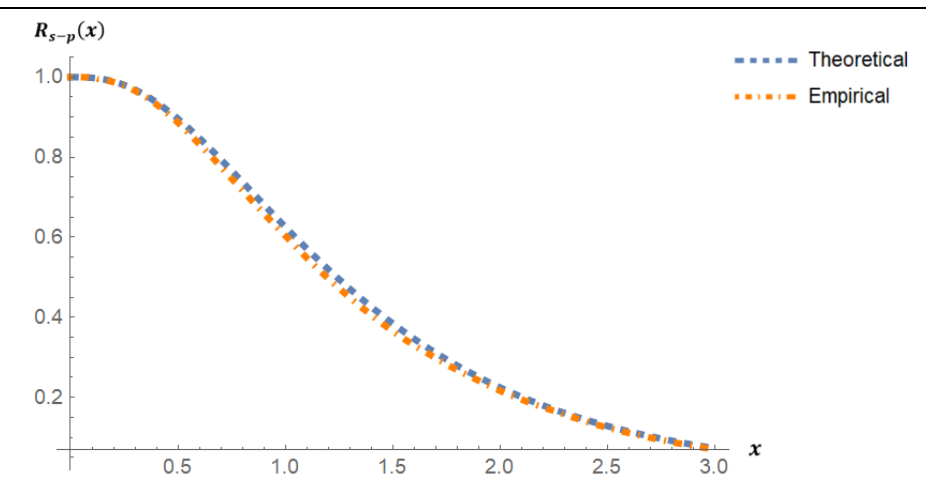


Figure 3. Survival function graph for $\omega = 0.5, \lambda = 1.15, N = 3, \varepsilon = 0.01$.

In the following table of values and graphical example, we observe how well the empirical functions approximates the theoretical values for parallel-serial networks with $M \sim Log(\omega)$.

Table 4 Simulated vs theoretical values of mean and dispersion for serial-parallel model with $M \sim Log(\omega)$, i.e., $P(M=m) = \frac{1}{\log N} \cdot \frac{\omega^m}{2}$, $m=1,2,\ldots,0<\omega<1$

	$-\ln(1-\omega)$ m, m						
ω	λ	N	$\mathbb{E} V_{p-s}$	$\widehat{\mathbb{E}V_{p-s}}$	$\mathbb{D} V_{p-s}$	$\widehat{\mathbb{D}V_{p-s}}$	
0.25	1.25	3	0.28581	0.28576	0.275492	0.277106	
0.25	1.25	5	0.171706	0.170882	0.165372	0.164594	
0.25	1.25	8	0.107111	0.107962	0.103412	0.102547	
0.5	2.15	3	0.183798	0.183041	0.169445	0.168233	
0.5	2.15	5	0.110467	0.111056	0.101673	0.101606	
0.5	2.15	8	0.069047	0.068979	0.063599	0.063494	
0.85	3.15	3	0.166029	0.166184	0.135527	0.135488	
0.85	3.15	5	0.0997884	0.100007	0.0813673	0.081666	
0.85	3.15	8	0.0623611	0.0623248	0.0508497	0.0506674	

Note: N – the number of units in each of M subnets; $\mathbb{E}V_{s-p}$ - the theoretical mean value; $\mathbb{E}\widehat{V_{s-p}}$ - the mean value calculated with Monte-Carlo simulated values; $\mathbb{D}V_{s-p}$ - the theoretical variance; $\mathbb{D}\widehat{V_{s-p}}$ - the variance calculated with Monte-Carlo simulated values.

For Table 4, we proceeded analogously to the steps for Tables 2 and 3, only we reduced the size of the displayed data set, but we note that the results are just as good, respecting the chosen error. So we continued to compute numerically in Wolfram Mathematica according to the parameters λ , ω , and N the calculation of the theoretical mean and variance, this time according to the lifetime probability density function (p.d.f.) given in equation (8) for parallel-serial model. As expected, the theoretical and empirical results tend to coincide. Even better, we see these results interpreted graphically below.

What we see in Figure 4 is that for k=34447 simulations, calculated according to the Central Limit Theorem [15], with the help of Wolfram Mathematica 14.0 software we obtained these estimates of the empirical and theoretical survival function. We notice that for sufficient number of simulations, these two functions tend to coincide.

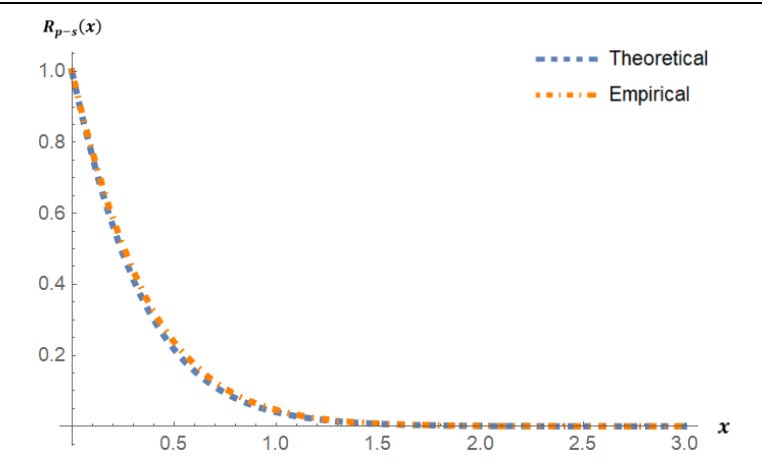


Figure 4. Survival function for $\omega = 0.5$, $\lambda = 1.25$, N = 3, $\varepsilon = 0.01$

5. Conclusion

The changing nature and evolution of networks encountered in engineering today lead to an increased demand for dynamic reliability analysis models. These models are complex and different in operation, requiring the models to be tailored to the problem, the network structure and how the subnets and units work. Starting from the goal of analyzing the reliability of networks with serial-parallel and parallel-serial architecture, we managed to derive 3 new lifetime distributions, distributions approached by analytical and empirical methods.

The studied dynamic networks have serial-parallel or parallel-serial architecture, each time the number of subnets being a random variable M of PSD classes, with Poisson or Logarithmic distribution. The number of units in each subnet is constant, greater than or equal to 2, the lifetimes of the units in each subnet being independent, identically, exponentially distributed random variables. In the aforementioned conditions, based on the general formulas for the calculation of the c.d.f., the calculation formulas for the cumulative distribution function, the reliability function and the hazard for these new three lifetime distributions were deduced.

Next, based on the deduced formulas, the theoretical mean value and the theoretical dispersion were calculated numerically, implementing the corresponding functions available in Wolfram Mathematica. Also, with the help of this software we simulated for the same parameters, random variables through the Monte-Carlo method and obtained the empirical mean and the empirical dispersion. We have presented the obtained data in tabular and graphical form, from where we can see that the theoretical and empirical values are very close, the difference between them does not exceed the admissible error shifted by us in the algorithm, and for a fairly large sample, these values tend to coincide. Thus, we validated the obtained theoretical results.

Acknowledgments. Institutional Project LIFETECH No. 020404, being implemented at the Technical University of Moldova.

Conflicts of Interest: The authors declare no conflict of interest.

References

- 1. Louzada, F.; Bereta, M.P.E.; Franco, M.A.P. On the Distribution of the Minimum or Maximum of a Random Number of i.i.d. Lifetime Random Variables. SCIRT 2012, pp. 350-353.
- 2. Adamidis, K.; Loukas, S. A lifetime distribution with decreasing failure rate. Statistics & Probability Letters. SCIRT 1998, 1(39), pp. 35-42.

M. Rotaru 53

3. Leahu, A.; Munteanu, B.GH.; Cataranciuc, S. On the lifetime as the maximum or minimum of the sample with power serial distributed size. Romai J 2013, 9(2), pp. 119-128.

- 4. Rausand, M.; Hoyland, A. System Reliability Theory Models, Statistical Methods, and Applications. Second Edition, Wiley-Interscience, New Jersey, USA, 2004, 644 p.
- 5. Terruggia, R. Reliability analysis of probabilistic networks. Doctoral thesis., University of Torino, Italy, 2010.
- 6. Kapur, K.C.; Lamberson, L.R. Reliability in engineering design. Wiley, India, 2009, 608 p.
- 7. Adrievschi-Bagrin, V.; Leahu, A. Reliability of serial-parallel networks vs reliability of parallel-serial networks with constant numbers of sub-networks and units. Journal of Engineering Science, 2022, 29(4), pp. 17-26.
- 8. Leahu, A.; Bagrin-Andrievschi, V.; Rotaru, M. Graphical methods as a complements of analytycal methods used in the research of dynamic models for networks reliability. In: Electronics, Communications and Computing (IC ECCO-2022): 12th intern. conf., 20-21 Oct. 2022, Chisinau, Republic of Moldova, 2022, pp. 168-171.
- 9. Leahu, A.; Andrievschi-Bagrin, V.; Ciorbă, D.; Fiodorov, I. Once again about the reliability of serial-parallel networks vs parallel-serial networks. In: Electronics, Communications and Computing: IC|ECCO-2021, Ed. 11, 21-22 octombrie 2021, Chisinau, Republic of Moldova, 2021, pp. 170-173.
- 10. Johnson, N.L.; Kemp, A.W.; Kotz, S. Univariate Discrete Distribution. Wiley-Interscience, New Jersey, USA, 2005, 688 p.
- 11. Leahu, A.; Andrievschi-Bagrin, V. Lifetime distributions and their approximation in realiability of serial/parallel networks. Analele Univ. Ovidius Constanța, 2020, 28(2), pp.161-172.
- 12. Lee, E.T.; Wenyu Wang, J. Statistical Methods for Survival Data Analysis. Wiley-Interscience, Oklahoma, SUA, 2003, 513 p.
- 13. Kuş, C. A new lifetime distribution. Computational Statistics & Data Analysis 2007, 51, pp. 4497 4509.
- 14. Krishnamoorthy, K. Handbook of Statistical Distributions with Applications. Chapman and Hall-CRC, University of Louisiana at Lafayette, USA, 2006, 376 p.
- 15. Leahu, A.; Pârțachi, I. Probabilități și Statistică Matematică. ASEM Chisinau, Republic of Moldova, 2022, 172 p.

Citation: Rotaru, M. Statistical simulation of reliability of networks with exponentially distributed unit lifetimes. *Journal of Engineering Science* 2024, XXXI (3), pp. 44-53. https://doi.org/10.52326/jes.utm.2024.31(3).04.

Publisher's Note: JES stays neutral with regard to jurisdictional claims in published maps and institutional affiliations.



Copyright:© 2024 by the authors. Submitted for possible open access publication under the terms and conditions of the Creative Commons Attribution (CC BY) license (https://creativecommons.org/licenses/by/4.0/).

Submission of manuscripts:

jes@meridian.utm.md

https://doi.org/10.52326/jes.utm.2024.31(3).05 UDC 621.311.243:621.314





eISSN 2587-3482

FLEXIBLE SYNCHRONOUS REGULATION OF POWER ELECTRONIC BLOCKS OF TRANSFORMER-BASED PHOTOVOLTAIC STATIONS

Valentin Oleschuk *, ORCID: 0000-0002-7413-4867

Institute of Power Engineering of Technical University of Moldova, 5 Academy Str., Chisinau, Republic of Moldova

* Corresponding author: Valentin Oleschuk, oleschukv@hotmail.com

Received: 08. 19. 2024 Accepted: 09. 24. 2024

Abstract. The paper presents the results of developing a scheme for synchronous pulse-width modulation (PWM) of signals in dual voltage source diode-clamped inverters (VSDCIs) used in grid-tied, transformer-based photovoltaic (PV) stations. This scheme is based on the continuous regulation of the switching frequency of the inverters relative to the magnitude of the DC voltages of the PV strings, ensuring equivalence of switching losses across each inverter. The proposed control and PWM techniques ensure the elimination of even-order harmonics and subharmonics in spectra of voltage at inverter-side windings of power transformer, helping to increase the operating efficiency of inverter-based PV stations. Simulation results showed a behavior of operation of dual-VSDCI-based PV installations with the proposed control strategy.

Keywords: control and modulation strategy, photovoltaic station, spectral analysis, switching frequency, voltage source diode-clamped inverter, voltage synchronization.

Abstract. Lucrarea prezintă rezultatele dezvoltării schemei de modulație sincronă a lățimii de impulsuri (PWM) a semnalelor duale invertoarelor de tensiune cu diode clampate (VSDCIs) ale stațiilor fotovoltaice (PV) bazate pe transformator obosit de rețea, bazată pe reglarea continuă a frecvenței de comutare a invertoarelor față de mărimea tensiunilor continue ale șirurilor fotovoltaice în condiția echivalenței pierderilor de comutare în fiecare invertor. Tehnicile de control și PWM propuse asigură eliminarea armonicilor de ordin egal și subarmonicilor în spectrele de tensiune la înfășurările de pe partea invertorului ale transformatorului de putere, ajutând la creșterea eficienței de funcționare a stațiilor fotovoltaice bazate pe invertori. Rezultatele simulării au arătat un comportament de funcționare a instalațiilor fotovoltaice bazate pe VSDCI dual cu strategia de control propusă.

Cuvinte cheie: strategie de control și modulație, stație fotovoltaică, analiză spectrală, frecvență de comutare, invertor de tensiune cu diodă clampate, sincronizare de tensiune.

1. Introduction

Photovoltaic stations are very popular installations in the area of renewable electrical energy [1-4], including large grid-tied photovoltaic power plants, integrated into the medium-voltage and high-voltage power supply systems [3].

V. Oleschuk 55

Voltage source inverters of various topologies are the main work-horses of photovoltaic (PV) systems, providing controlled conversion of dc voltage from PV strings into the required ac voltage for electrical energy consumers [5–11], including multilevel inverters [5,9], modular topologies of inverters [6], two-level inverters [7], three-level inverters [8], and multiphase inverters [10,11]. Also, powerful PV systems based on cascaded inverters should be mentioned [12-16], including standard cascaded inverters [12,13], and multilevel cascaded inverters [14–16].

Thus, the performance of PV stations depends on the pulsewidth modulation (PWM) strategies used to regulate the inverters. To ensure synchronization and symmetry of voltage waveforms of PV inverters at increased power levels, original schemes of synchronous modulation have been developed for control of inverters of some structures of PV systems [17-23], based on dual diode-clamped inverters [17,19,23], based on two standard three-phase inverters specifically connected to windings of the power transformer [18], and based on triple modulated inverters [20–22].

Accordingly, this paper provides the results of research of topology of PV installation based on two voltage source diode-clamped inverters (VSDCIs) adjusted by the modified control strategy based on flexible regulation of switching frequency (SwF) of VSDCIs in function of value of dc voltage of PV strings.

2. Structure and basic control and modulation schemes of VSDCI

Fig. 1,a shows topology of VSDCI. Fig. 1b presents the base voltage space vectors **V 1** ÷ **V 7** (marked by big arrows) of each VSDCI [17,23], and this control scheme assures elimination of common-mode voltage in PV systems on the base of VSDCI [17, 19, 20, 23]. Figs. 2 – 3 present switching state sequence and the base voltages of VSDCI adjusted by continuous (CPWM) and discontinuous (DPWM) synchronous PWM, Figures 2 and 3 [23].

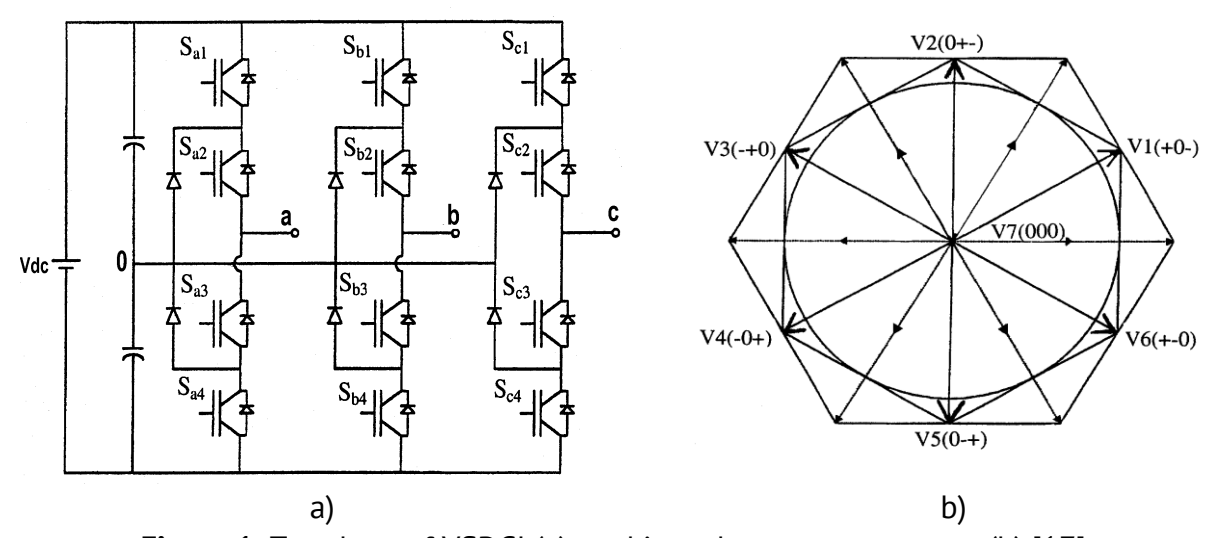


Figure 1. Topology of VSDCI (a), and its voltage space vectors (b) [17].

Basic set of control functions for determination of pulse patterns of VSDCIs for PV generation includes four formulas (1) – (4), where m is coefficient of PWM of VSDCI, and τ is duration of sub-interval which is in dependence of the SwF of VSDCI [17,23]. Figure 4 demonstrates switching sequence of VSDCI inside the 60° clock interval, and the corresponding pole V_{o} , V_{b} , and line V_{ob} voltages of VSDCI controlled by the scheme of CPWM [17].



Figure 2. Switching state sequence and the base voltages of VSDCI adjusted by the scheme of synchronous space-vector CPWM [23].

Figure 3. Switching state sequence and the base voltages of VSDCI adjusted by the sche-me of synchronous space-vector DPWM [23].

$$\beta_1 = 1.1m\tau \tag{1}$$

$$\beta_i = \beta_1 \cos[(j-1)\tau] \tag{2}$$

$$\gamma_i = \beta_{n-i+1} \{ 0.75 - 0.55 \tan[(n-j)\tau] \}$$
 (3)

$$\lambda_j = \tau - (\beta_j + \beta_{j+1})/2 \tag{4}$$

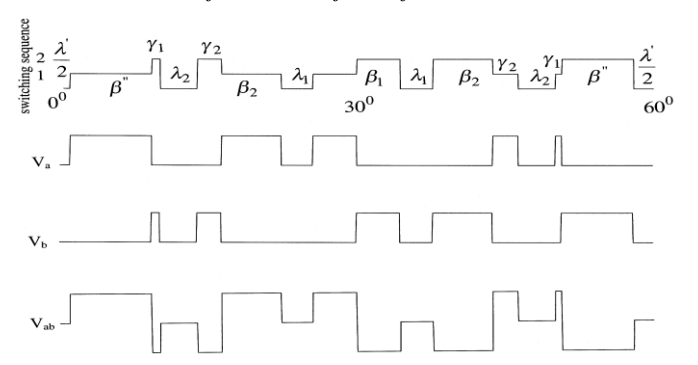


Figure 4. Contol pulses sequence and the base voltages of VSDCI regulated by algorithms of synchronous continuous PWM [17].

3. Grid-tied PV installation with dual VSDCIs

Figure 5 shows the structure of grid-tied PV system with two modulated VSDCIs supplied by dc voltages of two strings of PV panels [23]. The outputs of VSDCIs are tied with the inverter-side windings of the power transformer.

To provide rational operation of inverter-based PV systems, operating modulation index m of two VSDCIs should be controlled in accordance with formula connecting the highest value of dc-voltage $V_{dc-highest}$, minimum value of modulation index m_{min} , corresponding to this regime, and operating magnitude of dc voltage $V_{dc-lower}$:

$$m = (m_{min} V_{dc-highest})/V_{dc-lower}$$
 (5)

V. Oleschuk 57

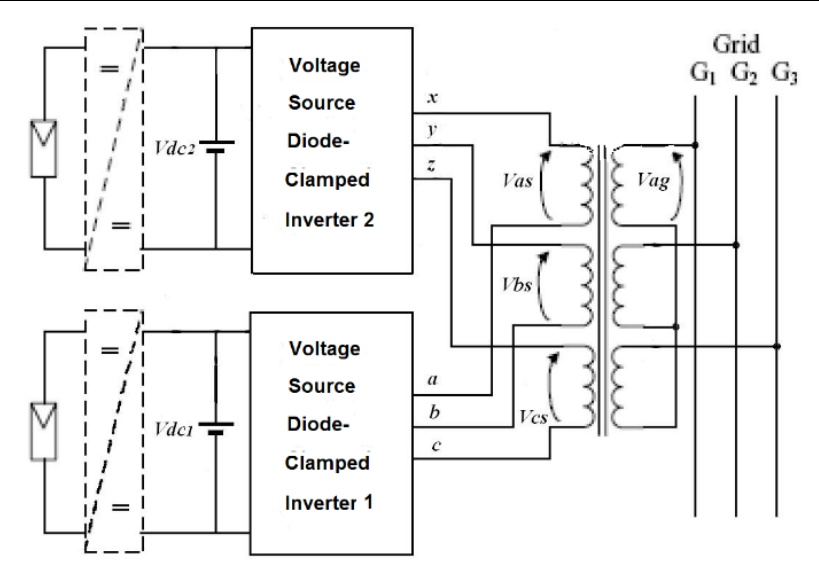
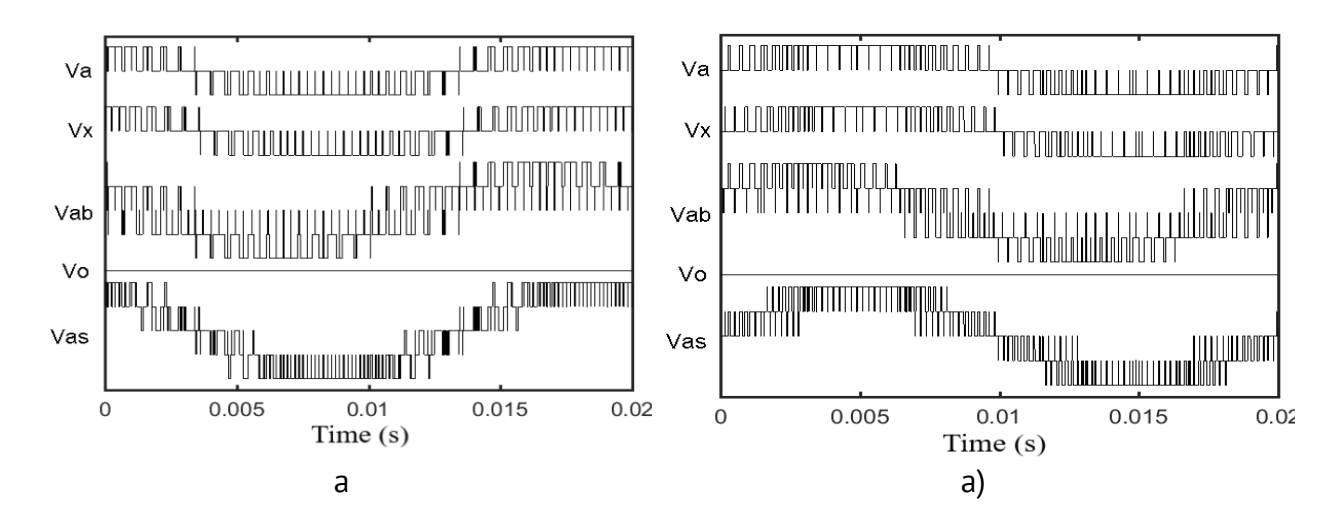


Figure 5. Structure of PV station with two modulated VSDCIs.

At the same time, to increase the operating efficiency of photovoltaic stations, it is advisable to smoothly regulate the SwF of each modulated VSDCI depending on the voltage magnitude of dc sources (provided that the switching losses of the two inverters are equal approximately). In particular, if PV station is supplied by the higher (highest) dc voltage $V_{dc-highest}$, the VSDCIs should be operated at lower SwF (at the rated SwF F_{s0} of VSDCIs), and if VSDCIs are supplied by the lower dc-voltage $V_{dc-lower}$, theirs SwF F_s can be increased correspondingly.

Figures 6 – 11 present the base voltages (pole voltages V_a , V_x , line voltage V_{ab} , common-mode voltage V_0 , and winding voltage V_{as} (with its spectrum) of PV station with two VSDCIs (Figure 5), regulated by algorithms of continuous (CPWM) and discontinuous (DPWM) synch-ronous PWM. The fundamental frequency of grid-tied PV station is $F = 50.0 \, Hz$. Diagrams in Figures 6 - 7 correspond to a case of relatively low dc voltage of PV panels, diagrams in Figures 8 – 9 correspond to a case of medium value of dc voltage of PV strings, and diagrams in Figures 10 – 11 correspond to a case of relatively high dc voltage. So, SwF of VSDCIs has been chosen for these cases in accordance with the mentioned above conditions of flexible regulation of system.



Vo

Vas

0

0.005

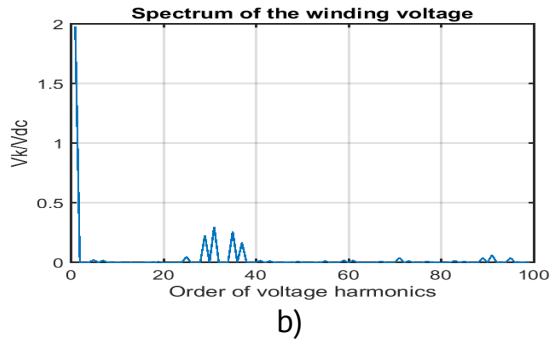
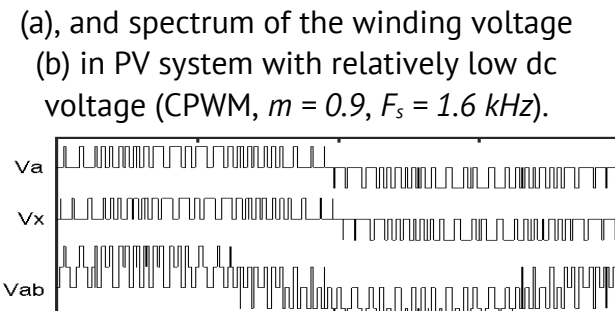
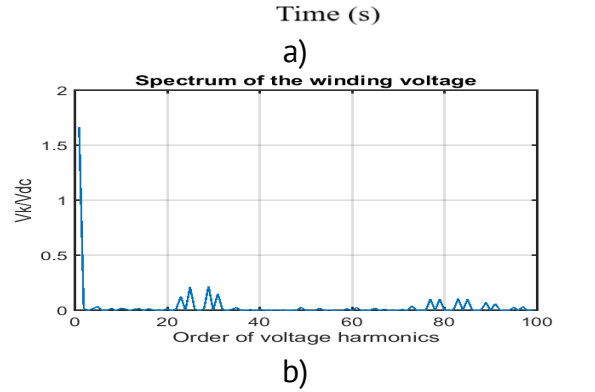


Figure 6. Waveforms of the base voltages (a), and spectrum of the winding voltage (b) in PV system with relatively low dc



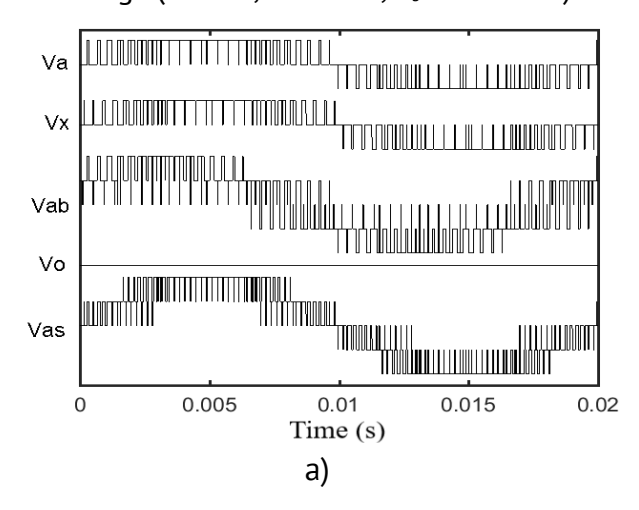


0.01

0.015

0.

Figure 8. Voltage waveforms (a), and spectrum of the winding voltage (b) in PV installation with medium dc voltage of PV strings (CPWM, m = 0.75, $F_s = 1.35$ kHz).



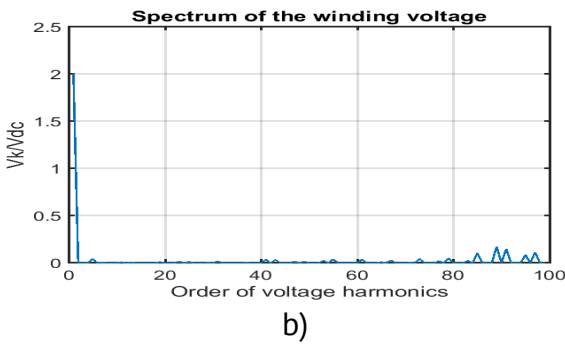
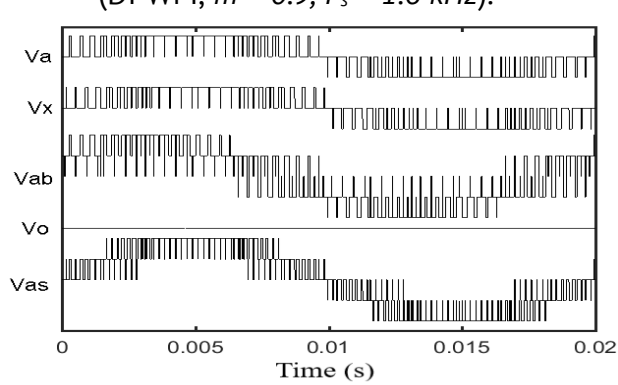


Figure 7. Waveforms of the base voltages (a), and spectrum of the winding voltage (b) in PV system with relatively low dc voltage (DPWM, m = 0.9, $F_s = 1.6$ kHz).



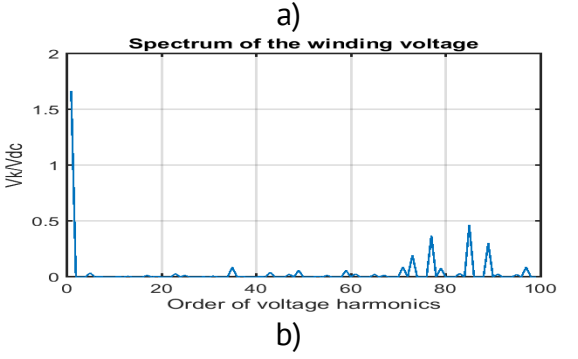
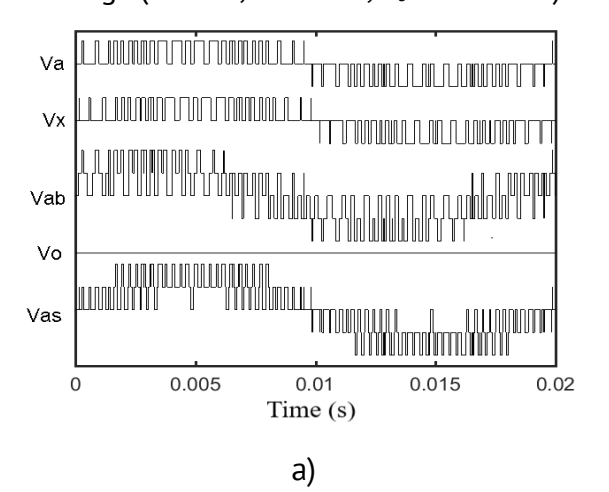
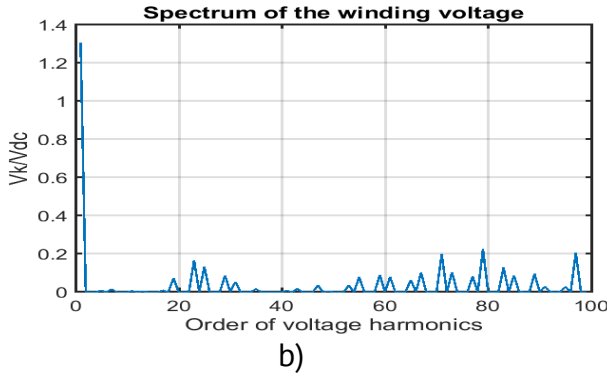


Figure 9. Voltage waveforms (a), and spectrum of the winding voltage (b) in PV installation with medium dc voltage of PV strings (DPWM, m = 0.75, $F_s = 1.35 \text{ kHz}$).



V. Oleschuk 59



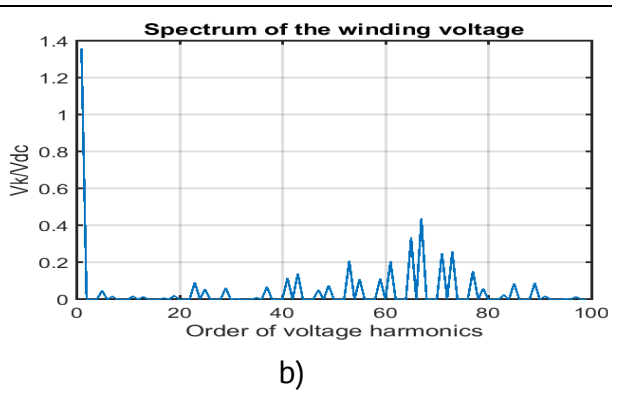


Figure 10. Waveforms of the base voltages (a), and spectrum of the winding voltage (b) in PV installation with relatively high dc voltage of PV strings (CPWM, m = 0.6, $F_s = 1.1 \text{ kHz}$).

Figure 11. Waveforms of the base voltages (a), and spectrum of the winding voltage (b) in PV installation with relatively high dc voltage of PV strings (DPWM, m = 0.6, $F_s = 1.1 \text{ kHz}$).

The presented in Figures 6 - 11 results of modeling and simulation of system with two VSDCIs show that the winding voltage V_{as} has quarter-wave symmetry, and in its spectrum there are no even harmonics and subharmonics in the analyzed regimes of regulation of gridtied PV installation.

Also, it is necessary to mention about specific two-stage control mode of operation of modulated VSDCIs in the zone of the highest modulation indices m of inverters (in the zone of overmodulation), if m > 0.907 [19]. Thus, boundary values of two indices of PWM of VSDCIs for standard two-stage regulation of inverters during overmodulation are equal to $m_{ov1} = 0.907$ and $m_{ov2} = 0.952$ ([19], $m_{\rm max} = 1$ in this case). In particular, basic PWM functions of VSDCIs for determination of duration of pulse control signals (1) – (4) include two special correcting indices of overmodulation $K_{ov1} = [1 - (m - m_{ov1})/(m_{ov2} - m_{ov1})]$ and $K_{ov2} = [1 - (m - m_{ov2})/(1 - m_{ov2})]$ [19].

Therefore, regimes of overmodulation of VSDCIs during flexible regulation of PV system correspond, in accordance with (5), to the case of relatively low dc voltage of PV panels of VSDCI-based photovoltaic station. As an example of operation of VSDCIs in the zone of overmodulation, Figures 12 - 13 show pole voltages V_a , V_x , line voltage V_{ab} , common-mode voltage V_0 , and winding voltage V_{as} (with its spectrum) of PV station with dual VSDCIs (Figure 5), regulated by algorithms of continuous (CPWM, Figure 12) and discontinuous (DPWM, Figure 13) synchronous PWM. Modulation index of VSDCIs is equal to m = 0.945, SwF of inverters is equal to $1.7 \, kHz$, and it corresponds to operation of inverters in the first part of the overmodulation zone. The fundamental frequency of grid-tied PV system is $F = 50 \, Hz$. The presented in Figures 12 - 13 diagrams prove the fact of quarter-wave symmetry of the base voltages in this control zone.

Figure 14 shows the results of calculating the Total Harmonic Distortion factor of the winding voltage V_{as} ($THD = (1/V_{as_1})(\sum\limits_{k=2}^{100}(V_{as_k}/k)^2)^{0.5}$) as a function of modulation index m of dual VSDCIs, calculated for three values of SwF of VSDCIs chosen in accordance with the mentioned above strategy of flexible control of the SwF of VSDCIs.

The data presented in Figure 14 show that for the presented topology of PV station regulation of dual VSDCIs by flexible algorithms of discontinuous synchronous PWM (DPWM) assure providing better value of THD factor at medium and higher coefficients of modulation

of two VSDCIs. In particular, for the analyzed cases, THD factor is better by the using of DPWM for control of VSDCIs, if m > 0.45 (case of relatively low dc voltage and relatively high SwF), if m > 0.5 (case of the medium magnitudes of dc voltage and medium SwF of VSDCIs), and if m > 0.55 (case of relatively high dc voltage and relatively low SwF).

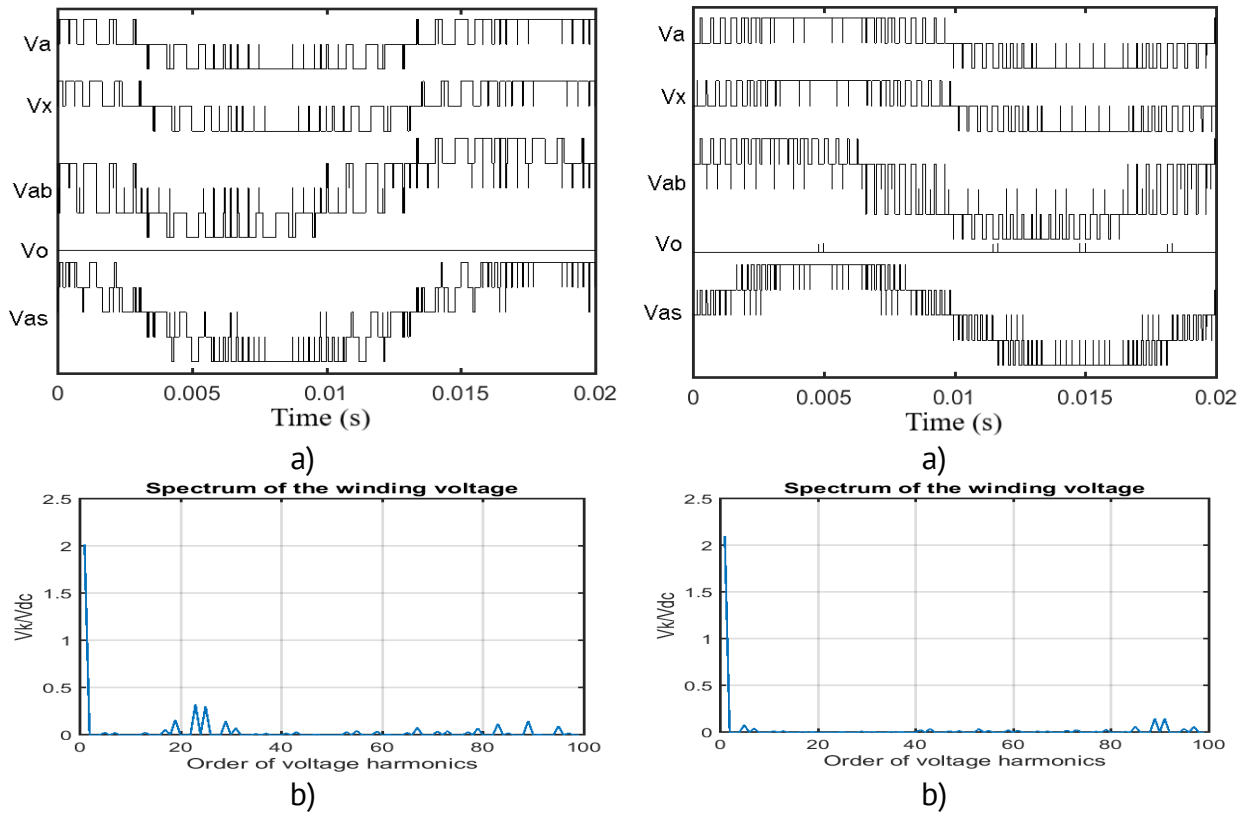


Figure 12. Waveforms of the base voltages (a), and spectrum of the winding voltage (b) in PV system with relatively low dc voltage and overmodulation control zone of VSDCIs (CPWM, m = 0.945, $F_s = 1.7$ kHz).

Figure 13. Waveforms of the base voltages (a), and spectrum of the winding voltage (b) in PV system with relatively low dc voltage and overmodulation control zone of VSDCIs (DPWM, m = 0.945, $F_s = 1.7$ kHz).

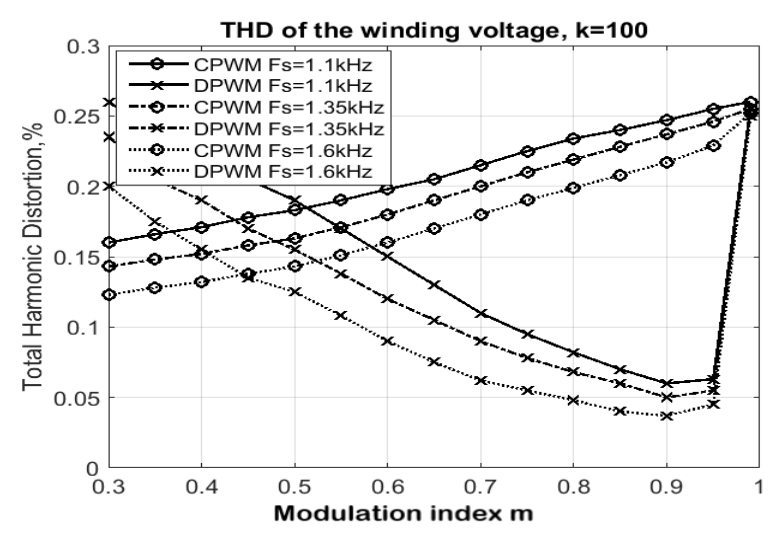


Figure 14. *THD* factor of the winding voltage of power transformer of grid-tied PV station as function of coefficient (index) of modulation *m* of dual VSDCIs for different values of its SwF.

V. Oleschuk 61

4. Conclusion

The developed strategy of control and synchronous PWM of two VSDCIs of grid-tied PV stations, based on continuous regulation of SwF of VSDCIs in function of current magnitude of dc voltage of PV strings under condition of equivalence of switching losses in each inverter, assures providing an improvement of harmonic composition of the winding voltage of the multi-winding power transformer, thereby helping to reduce losses and to increase the efficiency of operation of PV stations. Simulation results show, that discontinuous scheme of synchronous PWM, applied for regulation of dual VSDCIs, insures a better spectral composition of the winding voltage compared to the using of continuous scheme of synchronous pulsewidth modulation, if modulation index of VSDCIs for the corresponding control regimes has medium and upper medium values.

Conflicts of Interest: The authors declare no conflict of interest.

References

- 1. Kabir, E.; Kumar, P.; Kumar, S.; Adelodun, A.A.; Kim, K.H. Solar energy: potential and future prospects. *Renewable Sustainable Energy Reviews* 2018, 82, pp. 894–900.
- 2. Asmelash, E.; Prakash, G. Future of Solar Photovoltaic: Deployment, Investment, Technology, Grid Integration and Socio-Economic Aspects. Irena, Abu Dhabi, United Arab Emirates, 2019, 467 p.
- 3. Mansouri, N.; Lashab, A.; Sera, D.; Guerrero, G.M.; Cherif, A. Large photovoltaic power plants integration: A review of challenges and solutions. *Energies* 2019, 12, 3798.
- 4. <u>Maka</u>, A.O.M.; <u>Alabid</u>, J.M. Solar energy technology and its roles in sustainable development. *Clean Energy* 2022, 6(3), pp. 476-483.
- 5. Latran, M.B.; Teke, A. Investigation of multilevel multifunctional grid connected inverter topologies and control strategies used in photovoltaic systems. *Renewable and Sustainable Energy Reviews* 2015, 42, pp. 361-376.
- 6. Kumar, N.; Saha, T.K.; Dey, J. Modeling, control and analysis of cascaded inverter based grid-connected photovoltaic system. *International Journal of Electrical Power and Energy Systems* 2016, 78, pp. 165-174.
- 7. Jana, J.; Saha, H.; Bhattacharya, Das K. A review of inverter topologies for single-phase grid-connected photovoltaic systems. *Renewable Sustainable Energy Reviews* 2017, 72, pp. 1256–1270.
- 8. Jun-Seok Kim; Jung-Min Kwon; Bong-Hwan Kwon. High-efficiency two-stage three-level grid-connected photovoltaic inverter. *IEEE Trans. Ind. Electron.* 2018, 65(3), pp. 2368-2377.
- 9. Sinha, A.; Jana, K.S.; Das, M.K. An inclusive review on different multi-level inverter topologies, their modulation and control strategies for a grid connected photovoltaic system. *Solar Energy* 2018, 170, pp. 633-657.
- 10. Dogga, R.; Pathak, M.K. Recent trends in solar PV inverter topologies. Solar Energy 2019, 183, pp. 57–73.
- 11. Kolantla, D.; Mikkili, S.; Pendem, S.R.; Desai, A.A. Critical review on various inverter topologies for PV system architectures. *IET Renewable Power Generation* 2020, 14, pp. 3418–3438.
- 12. Grandi, G.; Rossi, C.; Ostojic, D.; Casadei, D. A new multilevel conversion structure for grid-connected PV applications. *IEEE Trans. Ind. Electron.* 2009, 56(11), pp. 4416–4426.
- 13. Oleschuk, V.; Griva, G. Simulation of processes in synchronized cascaded inverters for photovoltaic application. *International Review of Electrical Engineering* 2009, 4(5), pp. 975-982.
- 14. Latran, M.V.; Teke, A. Investigation of multilevel multifunctional grid connected inverter topologies and control strategies used in photovoltaic systems. *Renewable and Sustainable Energy Reviews* 2015, 42, pp. 361-376.
- 15. Wang, B.; Zhang, X.; Song, C.; Cao, R. Research on the filters for dual-inverter fed open-end winding transformer topology in photovoltaic grid-tied applications. *Energies* 2019, 12, 2338.
- 16. Sinha, A.; Jana, K.C.; Das, M.K. An inclusive review on different multi-level inverter topologies, their modulation and control strategies for a grid connected photovoltaic system. *Solar Energy* 2018, 170, pp. 633-657.
- 17. Oleschuk, V.; Tirsu, M.; Galbura, V.; Vasiliev, I. Transformer-based PV system with modified techniques of PWM of diode-clamped inverters. In: *Proc. of IEEE Int'l Conf. on Development and Application Systems* (DAS'2020), Suceava, Romania, 2020, pp. 106-111.

- 18. Oleschuk, V.; Ermuratskii, V. Two-inverter-based photovoltaic installation adjusted by the modified scheme of space-vector modulation. *Technical Electrodynamics* 2020, 5, pp. 26-30.
- 19. Oleschuk, V.; Vasiliev, I.; Griva, G.; Spertino, F. Schemes and techniques of synchronous modulation of PV inverters with high modulation indices: A survey. In: *Proc. of IEEE Int'l Symp. on Advanced Topics of Electrical Engineering* (ATEE'2021), Bucharest, Romania, 2021, 6 p.
- 20. Oleschuk, V. Algorithms of overmodulation regulation of neutral clamped inverters for photovoltaics. In: *Proc. of Int'l Conf. on Electronics, Communications and Computing of Moldova* (ECCO'2022), Chisinau, Republic of Moldova, 2022, pp. 84-89.
- **21.**Oleschuk, V. Grid-connected PV system employing three inverters regulated by synchronous scheme of PWM. *Technical Electrodynamics* 2022, 5, pp. 23-28.
- **22.**Oleschuk, V. Analysis and simulation of overmodulation modes of a three-inverter block of the photovoltaic installation. *Problems of the Regional Energetics* 2022, 3 (55), pp. 17–26.
- 23. Oleschuk, V.; Lupu, M. Photovoltaic stations with NPC inverters adjusted by specific control and PWM schemes and algorithms. In: *Proc. of IEEE Int'l Conf. on Electromechanical and Energy Systems* (SIELMEN'2023), Chisinau, Republic of Moldova, 2023, 6 p.

Citation: Oleschuk, V. Flexible synchronous regulation of power electronic blocks of transformer-based photovoltaic stations. *Journal of Engineering Science* 2024, XXXI (3), pp. 54-62. https://doi.org/10.52326/jes.utm.2024.31(3).05.

Publisher's Note: JES stays neutral with regard to jurisdictional claims in published maps and institutional affiliations.



Copyright:© 2024 by the authors. Submitted for possible open access publication under the terms and conditions of the Creative Commons Attribution (CC BY) license (https://creativecommons.org/licenses/by/4.0/).

Submission of manuscripts: jes@meridian.utm.md

https://doi.org/10.52326/jes.utm.2024.31(3).06 UDC 004.7





PERFORMANCE REQUIRED FOR COMMON-USE COMPONENTS OF COMPUTER NETWORKS

Ion Bolun*, ORCID: 0000-0003-1961-7310

Technical University of Moldova, 168 Stefan cel Mare Blvd., Chisinau, Republic of Moldova * Corresponding author: Ion Bolun, ion.bolun@isa.utm.md

Received: 09. 05. 2024 Accepted: 09. 28. 2024

Abstract. Sometimes, in practice, simple solutions of quick preliminary estimation of basic characteristics of a computer network are needed. In this aim, the backbone subnet and server set of wide area computer networks are examined. Based on Jackson's partitioning theorem and considering the linear dependence of the costs of channels, routers, and servers on their performance, a simplified analytical model for these components of the network is defined. Using this model, two optimization problems are formulated: minimizing the average response time to user requests of data processing and minimizing the summary cost of servers, channels and routers of the computer network. For both problems, analytical solutions regarding the necessary performances of channels, routers and servers are obtained. As expected, in the obtained analytical solutions, the equations for the optimization criteria of the two problems coincide, only their form being different. Calculations of performances according to these solutions are simple and can be done, for example, in MS Excel. Because the obtained in this way performances are positive real numbers, and the allowed performances of concerned entities are discrete ones, further adjustment of the solution in question, depending of the case, may be necessary. For such an adjustment, two algorithms are proposed. One of them solves the problem by reducing it to that of backpack. Another solves the problem based on the use of resource concentration rule.

Keywords: *algorithm, channel, cost, optimization, response time, router, server.*

Rezumat. Uneori, în practică, sunt necesare soluții simple de estimare rapidă preliminară a caracteristicilor de bază ale unei rețele de calculatoare. În acest scop, se examinează subrețeaua și setul de servere ale rețelelor de calculatoare de arie largă. Pe baza teoremei de partiționare a lui Jackson și luând în considerare dependența liniară a costurilor canalelor, ruterelor și serverelor de performanța acestora, este definit un model analitic simplificat al acestor componente ale rețelei. Folosind acest model, se formulează două probleme de optimizare: minimizarea duratei medii de răspuns la solicitările utilizatorilor de prelucrare a datelor și minimizarea costului sumar al serverelor, canalelor și ruterelor rețelei de calculatoare. Pentru ambele probleme sunt obținute soluții analitice privind performantele necesare ale canalelor, ruterelor si serverelor. Cum era de așteptat, în soluțiile analitice obținute, ecuațiile pentru criteriile de optimizare ale celor două probleme coincid, fiind

64 I. Bolun

diferită doar forma lor. Calculele performanțelor conform acestor soluții sunt simple și se pot face, de exemplu, în MS Excel. Deoarece performanțele astfel obținute sunt numere reale pozitive, iar performanțele admise ale entităților rețelei sunt discrete, poate fi necesară, în funcție de caz, o ajustare ulterioară a soluției în cauză. Pentru o astfel de ajustare, sunt propuși doi algoritmi. Unul dintre aceștia rezolvă problema reducând-o la cea a rucsacului. Celălalt rezolvă problema pe baza aplicării regulii de concentrare a resurselor.

Cuvinte cheie: algoritm, canal, cost, durată de răspuns, optimizare, ruter, server.

1. Introduction

The creation and development of computer networks involves considerable expenses. Minimizing these expenses is important. For this purpose many researches are carried out.

In a general form, the problem of computer networks synthesis consists in determining of their topology, of the number, deployment, productivity, operating regimes and functions of servers and communication nodes, the capacity of data transfer channels, the distribution of user requests between servers and the ways of data transfer and routing in the network, which would ensure the extreme of the accepted optimization criterion for the required quality of serving requests.

For large networks, the mathematical formalization and overall solution of the problem is very difficult. That is why various simplifications are usually resorted to, including the disaggregation of the general problem into several sub-problems.

In the field, models and algorithms are developed, several analytical solutions are obtained. It is especially the case to mention the Jackson partitioning theorem [1], the conservation law and the square root law of L. Kleinrock [2], the Gordon-Newell theorem [3], the algorithm of J. Buzen [4], the BCMP networks [5], the MVA method proposed by H. Reiser and S. Lavenberg and later developed by J. McKenna [6], the MVAC algorithm proposed by A. Conway, De Souza E Silva and S.S. Lavenberg [7], and the DAC algorithm developed by De Souza E Silva and S.S. Lavenberg [8]. Cloud processing has involved separate research with data centers [9, 10]. For example, the reliability of data centers is discussed in [11], and the placement of virtual machines for cloud data centers is explored in [12]. Also, researches in soft defined networks (SDN) is gaining momentum [13], including the choosing of the SDN operating system for cloud data centers [14].

However, the proposed methods and algorithms are, as a rule, relatively laborious, and sometimes in practice simple solutions are useful for quick preliminary estimation of basic characteristics of a network. The purpose of this paper is to propose simple ways of preliminary determination of approximate necessary performances of the common-use components of computer networks.

2. A Simplified Model of Computer Networks

From the multitude of computer network synthesis aspects, the model includes those related to estimating the necessary capacity of their servers, data transfer channels (hereafter channels) and routers. The model is an extension of the one proposed by L. Kleinrock for channels [2].

The process of computer network operation has a stochastic character. That is why their research uses, as a rule, the stochastic approach with the application of methods and

results of the theory of queues. For this purpose, computer networks are examined as networks of queues. Notes:

- rate β of the summary flow of requests to servers;
- rate γ of the summary flow of packets generated by user requests and the responses to them;
- the mean number g of packets per request, $g = \gamma/\beta$;
- the number of channels k_c , routers k_r and servers k_s ;
- packet rate through channel $i \lambda_{ci}$ and router $j \lambda_{rj}$;
- rate λ_{sl} of requests to server l;
- average size V_i of a packet transmitted through channel i;
- the average retention of a packet at channel i T_{ci} and at router j T_{rj} ;
- the average retention of a request at the server l T_{sl} and in the network T_{sl}
- summary cost C of channels, routers and servers.

Also, linear dependences are considered:

- of the channel *i* cost C_{ci} by its data transfer speed d_i [2]

$$C_{ci} = c_{ci}d_i, i = \overline{1, k_c}, \tag{1}$$

- of the ruter j cost C_{rj} by its packet processing rate μ_{rj}

$$C_{rj} = c_{rj}\mu_{rj}, j = \overline{1, k_r}, \tag{2}$$

- of the server l cost C_{sl} by its request processing rate μ_{sl}

$$C_{sl} = c_{sl}\mu_{sl}, l = \overline{1, k_s}, \tag{3}$$

where c_{ci} , c_{rj} and c_{sl} are coefficients of proportionality.

Moreover, it is considered that flows λ_{ci} ($i = \overline{1, k_c}$), λ_{rj} ($j = \overline{1, k_r}$) and λ_{sl} ($l = \overline{1, k_s}$) are elementary, and the times of packet transmission by channels, of packet processing by routers, and of request processing by servers are exponentially distributed.

It will be examined the steady-state operation of the network, which exists if the relationships occur:

$$\mu_{ci} > \lambda_{ci}, i = \overline{1, k_c}; \mu_{rj} > \lambda_{rj}, j = \overline{1, k_r}; \mu_{sl} > \lambda_{sl}, l = \overline{1, k_s},$$
(4)

where $\mu_{ci} = d_i/V_i$ is the packet transmission rate by channel i, $i = \overline{1, k_c}$.

Under the conditions and assumptions defined above, a computer network can be examined as an open exponential network of queues with a homogeneous flow of requests operating in steady state.

According to the Jackson partition theorem [1], any open exponential network of queues can be investigated as a set of isolated exponential queuing systems. Then the average time T_i of a request in the queuing system i of the network is determined [15] according to the relation $T_i = 1/(\mu_i - \lambda_i)$, where λ_i is the request flow rate, and μ_i – the request serving rate by station i. So, the relations take place:

$$T_{ci} = \frac{V_i}{d_i - \lambda_{ci} V_i}, i = \overline{1, k_c};$$
 (5)

$$T_{ri} = \frac{1}{\mu_{ri} - \lambda_{ri}}, i = \overline{1, k_r}; \tag{6}$$

66 I. Bolun

$$T_{si} = \frac{1}{\mu_{si} - \lambda_{si}}, i = \overline{1, k_s}. \tag{7}$$

Taking into account Eq. (1)-(3) and Eq. (5)-(7), is obtained:

$$T = \frac{1}{\gamma} \left(\sum_{i=1}^{k_c} \lambda_{ci} T_{ci} + \sum_{i=1}^{k_r} \lambda_{ri} T_{ri} \right) + \frac{1}{\beta} \sum_{i=1}^{k_s} \lambda_{si} T_{si} = \frac{1}{\gamma} \left(\sum_{i=1}^{k_c} \frac{\lambda_{ci} V_i}{d_i - \lambda_{ci} V_i} + \sum_{i=1}^{k_r} \frac{\lambda_{ri}}{\mu_{ri} - \lambda_{ri}} + g \sum_{i=1}^{k_s} \frac{\lambda_{si}}{\mu_{si} - \lambda_{si}} \right);$$
(8)

$$C = C_c + C_r + C_s = \sum_{i=1}^{k_c} c_{ci} d_i + \sum_{i=1}^{k_r} c_{ri} \mu_{ri} + \sum_{i=1}^{k_s} c_{si} \mu_{si}.$$
 (9)

The queuing network model is determined by Eq. (8) and Eq. (9) and conditions of InEq. (4). With this model, two problems of determining the performance required for common-use components of computer networks are usually of interest:

- minimizing the average time *T* in the network of the requests of data processing;
- minimizing the summary cost C of servers, channels and routers of the computer network. These are explored in Sections 3 and 4, respectively.

3. Minimizing the Average Response Time to User Requests

Problem 1. Let's, for the model {Eq. (8), Eq. (9)} and conditions of InEq. (4), the parameters are known: C; θ ; γ ; k_c ; k_r ; k_s ; λ_{ci} , V_i , c_{ci} , $i = \overline{1, k_c}$; λ_{ri} , c_{ri} , $i = \overline{1, k_r}$; λ_{si} , c_{si} , $i = \overline{1, k_s}$, where C is the maximum allowed total cost of servers, channels and routers of the network. It is required to determine the necessary performances d_i , $i = \overline{1, k_c}$ of channels, those μ_{si} , $i = \overline{1, k_s}$ of routers and those μ_{si} , $i = \overline{1, k_s}$ of network servers that would minimize the average response time T to data processing requests at the total cost C of servers, channels and routers which would not exceed the given value C, i.e.:

$$T = \frac{1}{\gamma} \left(\sum_{i=1}^{k_c} \frac{\lambda_{ci} V_i}{d_i - \lambda_{ci} V_i} + \sum_{i=1}^{k_r} \frac{\lambda_{ri}}{\mu_{ri} - \lambda_{ri}} + g \sum_{i=1}^{k_s} \frac{\lambda_{si}}{\mu_{si} - \lambda_{si}} \right) \rightarrow \min$$
 (10)

upon compliance with the restriction

$$C = \sum_{i=1}^{k_c} c_{ci} d_{ci} + \sum_{i=1}^{k_r} c_{ri} \mu_{ri} + \sum_{i=1}^{k_s} c_{si} \mu_{si} \le C^*$$
(11)

in conditions of InEq. (4).

Solving. From the essence of the problem, it is obvious that the solution of the problem corresponds to the limit value in Eq. (11), that is, C = C. Then the problem {Eq. (10), Eq. (11)} can be solved using the method of Lagrange multipliers. The respective Lagrangian L is

$$L = \frac{1}{\gamma} \left(\sum_{i=1}^{k_c} \frac{\lambda_{ci} V_i}{d_i - \lambda_{ci} V_i} + \sum_{i=1}^{k_r} \frac{\lambda_{ri}}{\mu_{ri} - \lambda_{ri}} + g \sum_{i=1}^{k_s} \frac{\lambda_{si}}{\mu_{si} - \lambda_{si}} \right) + \chi \left(\sum_{i=1}^{k_c} c_{ci} d_i + \sum_{i=1}^{k_r} c_{ri} \mu_{ri} + \sum_{i=1}^{k_s} c_{si} \mu_{si} - C^* \right),$$
 (12)

the conditioned optimization problem {Eq. (10), Eq. (11)} reducing to an unconditioned optimization problem – minimizing L. Here χ is the Lagrange multiplier.

The Lagrangian L contains $k_c + k_r + k_s + 1$ unknowns: χ ; d_i , $i = \overline{1, k_c}$, μ_{ri} , $i = \overline{1, k_r}$ and μ_{si} , $i = \overline{1, k_s}$. To minimize L, the partial derivatives of L with respect to the unknowns are determined; they are equalized to 0, resulting a system of $k_c + k_r + k_s + 1$ equations. By solving

this system, the analytical expressions for the performances d_i , $i = \overline{1, k_c}$, μ_{ri} , $i = \overline{1, k_r}$ and μ_{si} , $i = \overline{1, k_s}$ can be obtained. One has:

$$\begin{cases}
\frac{\partial L}{\partial d_{ci}} = \frac{1}{\gamma} \cdot \frac{-\lambda_{ci} V_i}{\left(d_i - \lambda_{ci} V_i\right)^2} + \chi c_{ci} = 0, \ i = \overline{1, k_c} \\
\frac{\partial L}{\partial \mu_{ri}} = \frac{1}{\gamma} \cdot \frac{-\lambda_{ri}}{\left(\mu_{ri} - \lambda_{ri}\right)^2} + \chi c_{ri} = 0, \ i = \overline{1, k_r} \\
\frac{\partial L}{\partial \mu_{si}} = \frac{g}{\gamma} \cdot \frac{-\lambda_{si}}{\left(\mu_{si} - \lambda_{si}\right)^2} + \chi c_{ri} = 0, \ i = \overline{1, k_r} \\
\frac{\partial L}{\partial \chi} = \sum_{i=1}^{k_c} c_{ci} d_i + \sum_{i=1}^{k_r} c_{ri} \mu_{ri} + \sum_{i=1}^{k_s} c_{si} \mu_{si} - C^* = 0.
\end{cases} \tag{13}$$

From the equations of the first line of Eq. (13), are obtained $(d_i - \lambda_{ci} V_i)^2 = \frac{\lambda_{ci} V_i}{\gamma \chi c_{ci}}, \ i = \overline{1, k_c}, \ \text{from where}$

$$d_i = \lambda_{ci} V_i \pm \sqrt{\frac{\lambda_{ci} V_i}{\gamma \chi c_{ci}}}, \ i = \overline{1, k_c}.$$
 (14)

For steady-state operation (see InEq. (4)), only the "+" sign should be considered in Eq. (14). Thus,

$$d_{i} = \lambda_{ci} V_{i} + \sqrt{\frac{\lambda_{ci} V_{i}}{\gamma \chi c_{ci}}}, \quad i = \overline{1, k_{c}}.$$

$$(15)$$

Similarly, from the equations of the second line of Eq. (13), taking into account InEq. (4), it is obtained

$$\mu_{ri} = \lambda_{ri} + \sqrt{\frac{\lambda_{ri}}{\gamma \chi c_{ri}}}, \quad i = \overline{1, k_r}.$$
 (16)

Respectively, from the equations of the third line of Eq. (13), taking into account the conditions of InEq. (4), one has

$$\mu_{si} = \lambda_{si} + \sqrt{\frac{\lambda_{si}}{\gamma \chi c_{si}}}, \ i = \overline{1, k_s}. \tag{17}$$

Substituting d_i ($i = \overline{1, k_c}$), μ_{ri} ($i = \overline{1, k_r}$) and μ_{si} ($i = \overline{1, k_s}$) from the last line of Eq. (13) with expressions of Eq. (15), Eq. (16) and Eq. (17), respectively, it is obtained

$$\frac{1}{\sqrt{\gamma \chi}} = \frac{C^* - \sum_{i=1}^{k_c} c_{ci} \lambda_{ci} V_i - \sum_{i=1}^{k_r} c_{ri} \lambda_{ri} - \sum_{i=1}^{k_s} c_{si} \lambda_{si}}{\sum_{i=1}^{k_c} \sqrt{c_{ci} \lambda_{ci} V_i} + \sum_{i=1}^{k_r} \sqrt{c_{ri} \lambda_{ri}} + \sum_{i=1}^{k_s} \sqrt{g c_{si} \lambda_{si}}}.$$
(18)

68 I. Bolun

Substituting in Eq. (14)-(16) $1/\sqrt{\chi}$ by the expression of Eq. (16), are obtained:

$$d_{ci} = \lambda_{ci} V_i + H \sqrt{\lambda_{ci} V_i / c_{ci}}, \quad i = \overline{1, k_c}, \tag{19}$$

$$\mu_{ri} = \lambda_{ri} + H\sqrt{\lambda_{ri}/c_{ri}}, \quad i = \overline{1, k_r}, \tag{20}$$

$$\mu_{si} = \lambda_{si} + H\sqrt{g\lambda_{si}/c_{si}}, \ i = \overline{1,k_s}, \tag{21}$$

where

$$H = \frac{C^* - \sum_{i=1}^{k_c} c_{ci} \lambda_{ci} V_i - \sum_{i=1}^{k_r} c_{ri} \lambda_{ri} - \sum_{i=1}^{k_s} c_{si} \lambda_{si}}{\sum_{i=1}^{k_c} \sqrt{c_{ci} \lambda_{ci} V_i} + \sum_{i=1}^{k_r} \sqrt{c_{ri} \lambda_{ri}} + \sum_{i=1}^{k_s} \sqrt{g c_{si} \lambda_{si}}}.$$

Substituting expressions of Eq. (19), Eq. (20) and Eq. (21) for d_{ci} ($i = \overline{1, k_c}$), μ_{ri} ($i = \overline{1, k_r}$) and μ_{si} ($i = \overline{1, k_s}$) in Eq. (10), the expression for the optimal value \mathcal{T} of \mathcal{T} is obtained

$$T^* = \frac{\left(\sum_{i=1}^{k_c} \sqrt{c_{ci} \lambda_{ci} V_i} + \sum_{i=1}^{k_r} \sqrt{c_{ri} \lambda_{ri}} + \sum_{i=1}^{k_s} \sqrt{g c_{si} \lambda_{si}}\right)^2}{\gamma \left(C^* - \sum_{i=1}^{k_c} c_{ci} \lambda_{ci} V_i - \sum_{i=1}^{k_r} c_{ri} \lambda_{ri} - \sum_{i=1}^{k_s} c_{si} \lambda_{si}\right)}.$$
 (22)

The analytical solution of the problem is constituted by Eq. (19)-(22). ■

It should be noted that the value of the time T can also be determined according to Eq. (10), that is, the relations {Eq. (10), Eq. (19)-(21)} can also be used as a solution. The expected values of quantities T, d_i ($i = \overline{1, k_c}$), μ_{ri} ($i = \overline{1, k_r}$) and μ_{si} ($i = \overline{1, k_s}$) can be calculated relatively easily, including in MS Excel.

Remark 1. Of course, the values of quantities d_i ($i = \overline{1, k_c}$), μ_{ri} ($i = \overline{1, k_r}$) and μ_{si} ($i = \overline{1, k_s}$), obtained according to Eq. (19)-(21), are positive real numbers, and the allowed performances of channels, routers and servers that could be used in the network are discrete ones, belonging to a finite set. Therefore, further adjustment of the solution in question, depending of the case, may be necessary.

It is useful to present the Eq. (22) in the form

$$T^* = \frac{A}{\gamma(C^* - B)},\tag{23}$$

where

$$A = \left(\sum_{i=1}^{k_c} \sqrt{c_{ci} \lambda_{ci} V_i} + \sum_{i=1}^{k_r} \sqrt{c_{ri} \lambda_{ri}} + \sum_{i=1}^{k_s} \sqrt{g c_{si} \lambda_{si}}\right)^2$$
(24)

and

$$B = \sum_{i=1}^{k_c} c_{ci} \lambda_{ci} V_i + \sum_{i=1}^{k_r} c_{ri} \lambda_{ri} + \sum_{i=1}^{k_s} c_{si} \lambda_{si}.$$
 (25)

From Eq. (24) and Eq. (25), it can be seen that if conditions of InEq. (4) are not taken into account, then the expressions for determining the values of the quantities A and B do not depend on the capacities of channels, routers and servers. Also, the value of the average response time T to data processing requests is inversely proportional to the maximum allowed summary cost C^* of channels, routers and servers. So, the smaller the value of the difference $\Delta C = C^* - C^*$ will be, the smaller the value of the difference $\Delta T = T^* - T$ will be, where C^* and T^* are the values of quantities C and T at allowed values of performances of channels, routers and servers of the network. From here, the essence of the problem of the necessary adjustment of the solution of Problem 1 mentioned in Remark 1 it follows.

Problem 2 – adjusting the solution of Problem 1. Let the initial data of Problem 1 and also the increasing strings of performances of common-use components that can be used in the network are known: D_{ci} , $i = \overline{1, n_c}$ of the given data transfer speeds of channels; D_{ri} , $i = \overline{1, n_r}$ of packet processing rates by routers and D_{si} , $i = \overline{1, n_s}$ of request processing rates by servers. It is required to adjust the solution of problem {Eq. (10), Eq. (11)} obtained according to Eq. (19)-(21) so that, at allowed values of performances of common-use entities (channels, routers and servers) of the network and respecting the conditions of InEq. (4), to minimize the value $\Delta C = C - C^*$.

Solving the problem by reducing it to that of backpack. Obviously, the adjusted solution (performances allowed for common-use components) should be as close as possible to the original one. Therefore, it is unlikely to be appropriate to increase the performance of a component by more than the next value in the range of allowed performances.

This aspect is the basis of **Algorithm 1** for the heuristic solution of Problem 2:

- 1. Initial data: C, T; D_{ci} , $i = \overline{1, n_c}$; D_{ri} , $i = \overline{1, n_r}$; D_{si} , $i = \overline{1, n_s}$; c_{ci} , λ_{ci} , V_i , d_i , $i = \overline{1, k_c}$; c_{ri} , λ_{ri} , μ_{ri} , $i = \overline{1, k_r}$; c_{si} , λ_{si} , μ_{si} , $i = \overline{1, k_s}$.
- 2. $h := \max\{D_{ci}, i = \overline{1, n_c}; D_{ri}, i = \overline{1, n_r}; D_{si}, i = \overline{1, n_s}\} + 1.$
- 3. $D_{c,n_c+1} \coloneqq h$; $D_{r,n_r+1} \coloneqq h$; $D_{s,n_s+1} \coloneqq h$.
- 4. Taking into account conditions of InEq. (4), are determined:

$$\begin{split} u_{ci} &:= z | \min_{z=1,n_{c+1}} \{D_{cz} \geq \lambda_{ci}\}, i = \overline{1, k_c}; \\ u_{ri} &:= z | \min_{z=1,n_r+1} \{D_{rz} \geq \lambda_{ri}\}, i = \overline{1, k_r}; \\ u_{si} &:= z | \min_{z=\overline{1,n_{s+1}}} \{D_{sz} \geq \lambda_{si}\}, i = \overline{1, k_s}. \end{split}$$

- $5. \ \ u_c := \max_{i=1,k_c} \{u_{ci}\}, i = \overline{1,k_c}; u_r := \max_{i=1,k_r} \{u_{ri}\}, i = \overline{1,k_r}; u_s := \max_{i=1,k_s} \{u_{si}\}, i = \overline{1,k_s};$
- 6. If $u_c = n_c + 1$ or $u_r = n_r + 1$ or $u_s = n_s + 1$, then the problem has no solutions, because the conditions of InEq (4) of network steady-state operation are not met.
- 7. The performances allowed for common-use components are determined according to the solution of Problem 1:

$$\begin{split} \check{d}_i &:= D_{cz} | \big\{ D_{cz} \leq d_i < D_{c,z+1} \big\}, z_{ci} \coloneqq z, i = \overline{1, k_c}; \\ \check{\mu}_{ri} &:= D_{rz} | \big\{ D_{rz} \leq d_i < D_{r,z+1} \big\}, z_{ri} \coloneqq z, i = \overline{1, k_r}; \\ \check{\mu}_{si} &:= D_{sz} | \big\{ D_{sz} \leq d_i < D_{s,z+1} \big\}, z_{si} \coloneqq z, i = \overline{1, k_s}. \end{split}$$

8. The minimum reasonable performances for common-use entities are determined:

$$\bar{d}_i$$
: = max{ $D_{cu_{ci}}$; \check{d}_i }, $i = \overline{1, k_c}$;

70 I. Bolun

$$\bar{\mu}_{ri} := \max\{D_{ru_{ri}}; \check{\mu}_{ri}\}, i = \overline{1, k_r};$$
$$\bar{\mu}_{si} := \max\{D_{su_{si}}; \check{\mu}_{si}\}, i = \overline{1, k_s}.$$

9. The summary costs \overline{C} are determined at the minimum reasonable performances for common-use entities:

$$\overline{C} = \sum_{i=1}^{k_c} c_{ci} \overline{d}_{ci} + \sum_{i=1}^{k_r} c_{ri} \overline{\mu}_{ri} + \sum_{i=1}^{k_s} c_{si} \overline{\mu}_{si}.$$

10. The reserve $\Delta \bar{C}$ of available financial resources is determined:

$$\Delta \bar{C} := C^* - \bar{C}$$
.

- 11. For each of common-use component *i* of the network, the additional cost is determined when replacing its current performance with the next one from the allowed series of performances:
 - a) if $\bar{d}_i \leq d_i$, then $\Delta C_{ci} \coloneqq c_{ci}(D_{c,z_{ci}+1} D_{cz_{ci}})$, otherwise $\Delta C_{ci} \coloneqq 0$, $i = \overline{1, k_c}$;
 - b) if $\bar{\mu}_{ri} \leq \mu_{ri}$, then $\Delta C_{ri} \coloneqq c_{ri}(D_{r,z_{ri}+1} D_{rz_{ri}})$, otherwise $\Delta C_{ri} \coloneqq 0$, $i = \overline{1, k_r}$;
 - c) if $\bar{\mu}_{si} \leq \mu_{si}$, then $\Delta C_{si} \coloneqq c_{si}(D_{s,z_{si}+1} D_{sz_{si}})$, otherwise $\Delta C_{si} \coloneqq 0$, $i = \overline{1, k_s}$.
- 12. An algorithm for solving the backpack problem is applied: among sizes ΔC_{ci} $(i = \overline{1, k_c})$, ΔC_{ri} $(i = \overline{1, k_r})$ and ΔC_{si} $(i = \overline{1, k_s})$ to select the ones which would minimize $\Delta C = C' C^*$.

Solving the problem using the resource concentration rule. Obviously, if $C^* \neq C$, then the time T must be calculated according to Eq. (10) and not to Eq. (22) or, equivalently, to Eq. (23). Therefore, in such cases, taking into account the opportunity to concentrate the resources [2], when increasing the performance it is appropriate to base on the rule: component i is preferable to component j, if $\Delta C_i/\Delta T(i) < \Delta C_j/\Delta T(j)$, where $\Delta T(i)$ is the decrease in time T caused by the increase ΔC_i in the cost of component j. Following this rule is all the more successful the higher the values of the quantities n_c , n_r and n_s . Another solves the problem based on the resource concentration rule

This rule is the basis of Algorithm 2 for the heuristic solution of Problem 2:

- 1-11. Steps 1-11 coincide with Steps 1-11 of Algorithm 1.
- 12. $g_{ci} = \Delta C_{ci}/\Delta T(c,i), i = \overline{1, k_c}; g_{ri} = \Delta C_{ri}/\Delta T(r,i), i = \overline{1, k_r}; g_{si} = \Delta C_{ci}/\Delta T(s,i), i = \overline{1, k_s}.$
- 13. Arrangement of quantities g_{ci} , $i = \overline{1, k_c}$; g_{ri} , $i = \overline{1, k_r}$ and g_{si} , $i = \overline{1, k_s}$ in ascending order forming two arrays: a_i , b_i , $i = \overline{1, k_c + k_r + k_s}$ where a_i specifies the type (c, r or s), and b_i the order number of the capacity of the common-use network component in the respective performances' string $(\overline{1, k_c}, \overline{1, k_r} \text{ or } \overline{1, k_s})$.
- 14. Increase to the next performance in the performances' series in ascending order of b_i up to $b_i | \min\{\Delta C_i \ge 0\}$. The adjusted solution is obtained,

4. Minimizing the Total Cost of Network Components

Problem 3. Let, for the model {Eq. (8), Eq. (9)} and conditions of InEq. (4), the parameters are known: \mathcal{T} ; \mathcal{B} ; \mathcal{Y} , k_c ; k_r ; k_s ; λ_{ci} , V_i , c_{ci} , $i = \overline{1, k_c}$; λ_{ri} , c_{ri} , $i = \overline{1, k_r}$; λ_{si} , c_{si} , $i = \overline{1, k_s}$, where \mathcal{T} is the maximum allowed average response time to data processing requests. It is required to determine the necessary capacities d_i , $i = \overline{1, k_c}$ of channels, those μ_{ri} , $i = \overline{1, k_r}$ of routers and those μ_{si} , $i = \overline{1, k_s}$ of network servers that would ensure a minimum summary cost \mathcal{C} of channels, routers and servers of the network at the average response time \mathcal{T} to data processing requests in the network that would not exceed the given value \mathcal{T} , i.e.:

$$C = \sum_{i=1}^{k_c} c_{ci} d_{ci} + \sum_{i=1}^{k_r} c_{ri} \mu_{ri} + \sum_{i=1}^{k_s} c_{si} \mu_{si} \to \min$$
 (26)

upon compliance with the restriction

$$T = \frac{1}{\gamma} \left(\sum_{i=1}^{k_c} \frac{\lambda_{ci} V_i}{d_{ci} - \lambda_{ci} V_i} + \sum_{i=1}^{k_r} \frac{\lambda_{ri}}{\mu_{ri} - \lambda_{ri}} + g \sum_{i=1}^{k_s} \frac{\lambda_{si}}{\mu_{si} - \lambda_{si}} \right) \le T^*$$
(27)

in conditions of InEq. (4). ■

Solving. From the essence of the problem, it is obvious that the solution corresponds to the limit value in Eq. (27), that is, T = T. Then the problem {Eq. (26), Eq. (27)} can be solved using the method of Lagrange multipliers. The respective Lagrangian L is

$$L = \sum_{i=1}^{k_c} c_{ci} d_i + \sum_{i=1}^{k_r} c_{ri} \mu_{ri} + \sum_{i=1}^{k_s} c_{si} \mu_{si} + \chi \left(\frac{1}{\gamma} \left(\sum_{i=1}^{k_c} \frac{\lambda_{ci} V_i}{d_i - \lambda_{ci} V_i} + \sum_{i=1}^{k_r} \frac{\lambda_{ri}}{\mu_{ri} - \lambda_{ri}} + g \sum_{i=1}^{k_s} \frac{\lambda_{si}}{\mu_{si} - \lambda_{si}} \right) - T^* \right). \tag{28}$$

The Lagrangian L contains $k_c + k_r + k_s + 1$ unknowns: χ ; d_i , $i = \overline{1, k_c}$; μ_{ri} , $i = \overline{1, k_r}$ and μ_{si} , $i = \overline{1, k_s}$. The partial derivatives of L with respect to unknowns equalized to 0 are:

$$\begin{cases}
\frac{\partial L}{\partial d_{ci}} = c_{ci} + \frac{\chi}{\gamma} \cdot \frac{-\lambda_{ci}V_i}{\left(d_i - \lambda_{ci}V_i\right)^2} = 0, \quad i = \overline{1, k_c} \\
\frac{\partial L}{\partial \mu_{ri}} = c_{ri} + \frac{\chi}{\gamma} \cdot \frac{-\lambda_{ri}}{\left(\mu_{ri} - \lambda_{ri}\right)^2} = 0, \quad i = \overline{1, k_r} \\
\frac{\partial L}{\partial \mu_{si}} = c_{ri} + \frac{g\chi}{\gamma} \cdot \frac{-\lambda_{si}}{\left(\mu_{si} - \lambda_{si}\right)^2} = 0, \quad i = \overline{1, k_r} \\
\frac{\partial L}{\partial \mu_{si}} = \frac{1}{\gamma} \left(\sum_{i=1}^{k_c} \frac{\lambda_{ci}V_i}{d_i - \lambda_{ci}V_i} + \sum_{i=1}^{k_r} \frac{\lambda_{ri}}{\mu_{ri} - \lambda_{ri}} + g \sum_{i=1}^{k_s} \frac{\lambda_{si}}{\mu_{si} - \lambda_{si}} \right) - T^* = 0.
\end{cases}$$

Similarly to the determination of expressions of Eq. (15)-(17), from the first three lines of Eq. (29) and taking into account the observance of conditions of InEq. (4) of operation in the steady state, it is obtained:

$$d_{i} = \lambda_{ci}V_{i} + \sqrt{\frac{\chi\lambda_{ci}V_{i}}{\gamma c_{ci}}}, \ i = \overline{1, k_{c}};$$
(30)

$$\mu_{ri} = \lambda_{ri} + \sqrt{\frac{\chi \lambda_{ri}}{\chi c_{ri}}}, \ i = \overline{1, k_r}; \tag{31}$$

$$\mu_{si} = \lambda_{si} + \sqrt{\frac{g\chi\lambda_{si}}{\gamma c_{ri}}}, \ i = \overline{1, k_r}.$$
 (32)

Substituting d_i , $i = \overline{1, k_c}$; μ_{ri} , $i = \overline{1, k_r}$ and μ_{si} , $i = \overline{1, k_s}$, from the last line of Eq. (29) with expressions of Eq. (30)-(32), respectively, as a result of some simple transformations, one obtains

72 I. Bolun

$$\sqrt{\chi} = \frac{\sum_{i=1}^{k_c} \sqrt{c_{ci} \lambda_{ci} V_i} + \sum_{i=1}^{k_r} \sqrt{c_{ri} \lambda_{ri}} + \sum_{i=1}^{k_s} \sqrt{g c_{si} \lambda_{si}}}{T^* \sqrt{\gamma}}.$$
(33)

Substituting in Eq. (30)-(32) $1/\sqrt{\chi}$ by the expression of Eq. (33), one has:

$$d_{i} = \lambda_{ci} V_{i} + \frac{G\sqrt{c_{ci}\lambda_{ci}V_{i}}}{T^{*}\gamma c_{ci}}, i = \overline{1, k_{c}},$$
(34)

$$\mu_{ri} = \lambda_{ri} + \frac{G\sqrt{c_{ri}\lambda_{ri}}}{T^*\gamma c_{ri}}, i = \overline{1, k_r},$$
(35)

$$\mu_{si} = \lambda_{si} + \frac{G\sqrt{gc_{si}\lambda_{si}}}{T^* \chi_{c_{si}}}, i = \overline{1, k_s},$$
(36)

where

$$G = \sum_{i=1}^{k_c} c_{ci} \lambda_{ci} V_i + \sum_{i=1}^{k_r} c_{ri} \lambda_{ri} + \sum_{i=1}^{k_s} c_{si} \lambda_{si}.$$

Substituting expressions of Eq. (34), Eq. (35) and Eq. (36) for d_i , $(i = \overline{1, k_c})$, μ_{ri} $(i = \overline{1, k_r})$ and μ_{si} $(i = \overline{1, k_s})$ in Eq. (26), the expression for the optimal value C of quantity C, one has

$$C^* = \sum_{i=1}^{k_c} c_{ci} \lambda_{ci} V_i + \sum_{i=1}^{k_r} c_{ri} \lambda_{ri} + \sum_{i=1}^{k_s} g c_{si} \lambda_{si} + \frac{1}{\gamma T^*} \left(\sum_{i=1}^{k_c} \sqrt{c_{ci} \lambda_{ci} V_i} + \sum_{j=1}^{k_r} \sqrt{c_{rj} \lambda_{rj}} + \sum_{i=1}^{k_s} \sqrt{g c_{si} \lambda_{si}} \right)^2.$$
(37)

The analytical solution of the problem is constituted by Eq. (34)-(37). It should be noted that the value of cost C can also be determined according to Eq. (26), i.e. the relations {Eq. (26), Eq. (34)-(36)} can also be used as a solution. The expected values of the quantities C, d_i ($i = \overline{1, k_c}$), μ_{ri} ($i = \overline{1, k_r}$) and μ_{si} ($i = \overline{1, k_s}$) can be calculated relatively easily, including in MS Excel.

Remark 2. Of course, the values of quantities d_i , $i = \overline{1, k_c}$; μ_{ri} , $i = \overline{1, k_r}$ and μ_{si} , $i = \overline{1, k_s}$ obtained according to Eq. (34)-(36), are positive real numbers, and the performances for channels, routers and servers that could be used in the network are discrete ones, belonging to a finite set. Therefore, an additional adjustment of the solution may be necessary.

Eq. (33) can be presented in the form

$$C^* = \frac{A}{\gamma T^*} + B. \tag{38}$$

Comparing Eq. (23) and Eq. (38), it can be seen that they coincide, differing only in their form. Thus, the relationships between the quantities \mathcal{T} and \mathcal{C} for Problems 1 and 3 are the same.

From Eq. (24) and Eq. (25), it can be seen that if conditions of InEq. (4) are not taken into account, then the expressions for determining the values of quantities A and B do not depend on the capacities of channels, routers and servers. Also, the value of the summary cost C of core components of the network is inversely proportional to the average response

time T to data processing requests. So the smaller the value of difference $\Delta T = T^* - T$ will be, the smaller the value of the difference $\Delta C = C - C^*$, where C^* and T^* are the values of quantities C and T at allowed values of capacities of core components of the network. From here, the essence of the problem of necessary adjustment of the solution of Problem 3 mentioned in Remark 2.

Problem 4 - adjusting the solution of Problem 3. Let the initial data of Problem 3 and also the increasing strings of capacities of components that can be used in the network are known: D_{ci} , $i = \overline{1, n_c}$ of data transfer rates of channels, D_{ri} , $i = \overline{1, n_r}$ of packet processing rates by routers and D_{si} , $i = \overline{1, n_s}$ of request processing rates by servers. It is required to adjust the solution of problem {Eq. (22), Eq. (23)} obtained according to Eq. (30)-(32) so that, at allowed values of capacities of core entities of the network and respecting the conditions of InEq. (4), to minimize the value $\Delta T = T^* - T^*$.

Solving. The adjustment of the solution of Problem 3, so that the allowed capacities of channels, routers and servers are used, is performed in a similar way to that described in Algorithms 1 and 2 of the adjustment of the solution of Problem 1, but reversing the roles of T and C.

5. Conclusions

Because of considerable expenses with the creation and development of computer networks, it is important their minimization. Moreover, sometimes it is useful the quick preliminary estimation of basic characteristics of the network. In this aim, taking into account the Jackson's partitioning theorem [1] and considering the linear dependence of the costs of channels, routers, and servers on their performance, a simplified analytical model of the backbone subnet and server set of wide area computer networks is defined. Based on this model, two optimization problems are formulated: minimizing the average response time to user requests of data processing and minimizing the summary cost of servers, channels and routers of the computer network. For these problems, simple analytical solutions regarding the necessary performances of channels, routers and servers are obtained. In the analytical solutions, the equations for the optimization criteria of the two problems differ only in their form. Knowing the initial data, the performances of common-use components of computer networks can be calculated, for example, in MS Excel.

Obtained in this way performances are positive real numbers. Usually they do not coincide with the allowed performances of channels, routers and servers, which take values from a series of discrete numbers. This is why, if necessary, the problem of adjusting the obtained values of performances of analytical solutions to the allowed discrete performances of the common-use network components, is formulated. To solve it, two algorithms are proposed: by reducing the initial problem to that of backpack and by using the resource concentration rule. The first of them is exact, but relatively complex, and the second one is simple, but not exact.

Conflicts of Interest: The author declares no conflict of interest.

References

- 1. Jackson, J.R. Networks of waiting lines. *Operations Research* 1957, 5, pp. 518-521.
- 2. Kleinrock, L. Queuing systems, vol II: Computer applications. Willey, New York, SUA, 1976, 576 p.
- 3. Gordon, WJ.; Newell, G.F. Closed queuing systems with exponential servers. *Operations Research* 1967, 15, pp. 254-265.

74 I. Bolun

4. Buzen, J.P. Computational Algorithms for Closed queuing networks with exponential servers. *Communications of the ACM* 1973, 16 (9), pp. 527-531.

- 5. Baskett, F.; Chandy, K.M.; Muntz, R.R.; Palacios, F.G. Open, closed and mixed networks of queues with different classes of customers. *Journal of the ACM* 1975, 22 (2), pp. 248–260.
- 6. McKenna, J.; Mitra, D. Asymptotic expansions for closed markovian networks with state-dependent service rates. *Journal of the ACM* 1986, 33 (3), pp. 568 592.
- 7. Conway, A.E.; De Souza E Silva, E.; Lavenberg, S.S. Mean value analysis by chain of product-form queuing networks. *IEEE transactions on computers* 1989, 38 (3), pp. 432 442.
- 8. De Souza E Silva, E.; Lavenberg S.S. Calculating joint queue-length distributions in product-form queuing networks. *Journal of the ACM* 1989, 36 (1), pp. 194-207.
- 9. Qing, Y. Data center network architecture design for cloud computing. *Converter*, 2021, 1, pp. 23–29.
- 10. Baby Nirmala, M. Cloud based big data analytics: WAN optimization techniques and solutions. *Adapt. Learn. Optim.* 2015, 19, pp. 237–254.
- 11. Wu, H.; Wu, B.; Wang, Z. Research on the overall reliability of data centers. In: *Proceedings of the 2023 4th International Conference on Big Data Economy and Information Management*, May 29, 2024, pp. 802-807.
- 12. Sahena, D.; Gupta, I; Kumar, J.; Singh, A.K.; Wen, X. A Secure and Multiobjective Virtual Machine Placement Framework for Cloud Data Center. *IEEE Systems Journal* 2021, 1, pp. 1-12.
- 13. Sadiku, I.B.; Ajayi, W.; Sakpere, W.; John-Dewole, T.; Badru, R.A. Effect of traditional and software-defined networking on performance of computer network. *Sci. J. Inform.* 2022, 9 (2), pp. 111–122.
- 14. Zaher, M.; Molnár, S. A Comparative and Analytical Study for Choosing the Best Suited SDN Network Operating System for Cloud Data Center. *Annals of Emerging Technologies in Computing*, 2022, 6 (1), pp. 43-59.
- 15. Robertazzi, T.G. *Computer networks and systems: queuing theory and performance evaluation.* Springer-Verlag, New York, SUA, 1994, 368 p.

Citation: Bolun, I. Performance Required for Common-use Components of Computer Networks. *Journal of Engineering Science* 2024, XXXI (3), pp. 63-74. https://doi.org/10.52326/jes.utm.2024.31(3).06.

Publisher's Note: JES stays neutral with regard to jurisdictional claims in published maps and institutional affiliations.



Copyright:© 2024 by the authors. Submitted for possible open access publication under the terms and conditions of the Creative Commons Attribution (CC BY) license (https://creativecommons.org/licenses/by/4.0/).

Submission of manuscripts:

jes@meridian.utm.md

https://doi.org/10.52326/jes.utm.2024.31(3).07 UDC 004.42:613.2





INTEGRATION OF A DATA-DRIVEN SOFTWARE APPLICATION AND A MULTIMODAL LARGE LANGUAGE MODEL FOR ENHANCED NUTRITIONAL GUIDANCE: A CASE STUDY

Victor Iapăscurtă ^{1,2*}, ORCID: 0000-0002-4540-7045, Dinu Țurcanu ¹, ORCID: 0000-0001-5540-4246, Rodica Siminiuc ¹, ORCID: 0000-0003-4257-1840

¹ Technical University of Moldova, 168 Ștefan cel Mare Blvd., Chisinau, Republic of Moldova ² N. Testemitanu University of Medicine and Pharmacy, 165 Ștefan cel Mare Blvd, Chisinau, Republic of Moldova * Corresponding author: Victor lapăscurtă, victor.iapascurta@doctorat.utm.md

> Received: 07, 18, 2024 Accepted: 08, 19, 2024

Abstract. In the realm of health and wellness, the integration of data-driven technology and artificial intelligence (AI) has opened up new possibilities for personalized and data-driven approaches. HN-Assistant, a software application designed to analyze an individual's nutritional state and provide tailored recommendations, offers a powerful tool for promoting healthy eating habits. The HN-Assistant can also analyze how good a food product is at covering the estimated nutrient requirements. However, when combined with the capabilities of advanced AI assistants based on LLMs, the potential for comprehensive and insightful nutritional guidance is taken to new heights. This paper describes an attempt at integrating the proprietary software application HN-Assistant with GPT-40 to empower final users to make better nutritional decisions. The application was built in R programming language using the Shiny package, and the interaction between HN-Assistant and GPT-40 is based on an API in Python.

Keywords: software application; data-driven analytics; nutrition; artificial intelligence; large language model.

Rezumat. În domeniul sănătății și al bunăstării, integrarea tehnologiei bazate pe date și a inteligenței artificiale (AI) a deschis noi posibilități pentru abordări personalizate și bazate pe date. HN-Assistant, o aplicație software concepută pentru a analiza starea nutrițională a unui individ și pentru a oferi recomandări personalizate, reprezintă un instrument puternic pentru promovarea obiceiurilor alimentare sănătoase. HN-Assistant poate analiza, de asemenea, cât de bun este un produs alimentar pentru a acoperi cerințele estimate de nutrienți. Cu toate acestea, atunci când sunt combinate cu capacitățile asistenților AI avansati bazați pe LLM, potențialul de îndrumare nutrițională cuprinzătoare și perspicace este dus la noi culmi. Această lucrare descrie o încercare de integrare a aplicației software proprietare HN-Assistant cu GPT-40 pentru a permite utilizatorilor finali să ia decizii nutriționale mai

bune. Aplicația a fost construită în limbajul de programare R folosind pachetul Shiny, iar interacțiunea dintre HN-Assistant și GPT-40 se bazează pe un API în Python.

Cuvinte cheie: aplicație software; analiză bazată pe date; nutriție; inteligență artificială; model de limbaj mare.

1. Introduction

In today's fast-paced world, it can be challenging to make informed decisions. Fortunately, technological advancements have led to the development of software applications that aid users in making more knowledgeable decisions, especially when combined with the capabilities of large language models (LLMs). One of the areas which can benefit from such a combination is healthy nutrition.

With many food choices available today, determining which options genuinely benefit our health can be challenging. International organizations like the European Food Safety Authority (EFSA) [1], the Food and Drug Administration (FDA) [2], the World Health Organization (WHO) [3], and others play a vital role in providing recommendations for healthy nutrition. These organizations use their expertise and global reach to develop evidence-based guidelines that inform policies, regulations, and public health initiatives. By promoting safe and nutritious food choices, these recommendations contribute to the well-being of populations worldwide and help address global health challenges. Individuals, policymakers, and food industry stakeholders must rely on and implement these recommendations to foster healthier eating habits and improve public health on a global scale.

The web-based software application Healthy Nutrition Assistant (HN-Assistant) [4,5] was the first step towards helping users make more informed decisions about their nutrition. It excels in calculating essential parameters such as Body Mass Index (BMI) [6,7], Basal Metabolic Rate (BMR) [8-10], and Total Daily Energy Expenditure (TDEE) [11,12]. It also provides detailed recommendations for daily macronutrients, vitamins, and mineral requirements based on an individual's unique profile.

By generating visual representations of the nutrient distribution through radar charts, the HN-Assistant offers a clear and concise overview of the nutritional adequacy of a given food product or dietary plan.

The application was built using concepts primarily based on EFSA recommendations.

The integration of data-driven software applications like HN-Assistant with multimodal language models such as GPT-40 represents the next step in the advancement of personalized nutrition. HN-Assistant provides detailed nutritional evaluations based on user data, while GPT-40 can interpret and expand on these evaluations through natural language processing and multimodal capabilities.

This paper presents the mentioned software application and elaborates on its integration with an LLM, GPT-4o. The obtained synergy seems to offer a more comprehensive approach to nutritional guidance.

2. Materials and Methods

The HN-Assistant data-driven software application was built using the Shiny(R) package [13]. This package provides various tools and functionalities for creating an interactive and visually appealing nutrition application. With Shiny, developers can easily incorporate data visualization techniques, such as charts, graphs, and interactive dashboards,

to present nutritional information more engagingly and understandably. These visualizations can help users comprehend complex nutritional data and make more informed food choices.

Furthermore, Shiny applications can be easily deployed across various platforms, including desktops, smartphones, and tablets, making them accessible to a broader audience. This flexibility ensures that users can access the application whenever and wherever they need it, whether grocery shopping, dining out, or cooking at home. The application's convenience and portability further encourage users to engage with it regularly and consistently make healthier choices.

The LLM model used in this research is a generative pre-trained transformer (i.e., GPT-4o) [14], and the interaction between HN-Assistant and GPT-4o is based on an application programming interface (API) in Python [15].

3. Integrating the software application with an LLM

3.1. Multimodal language models: a versatile tool

Multimodal language models like GPT-40 can process and generate text, images, and other data types, making them versatile tools for interpretation and communication. These models can analyze complex datasets, translate technical information into user-friendly language, and provide context-aware recommendations. Their ability to engage in interactive dialogue enhances user experience by offering personalized and adaptive advice.

3.2. Synergistic integration

Integrating HN-Assistant with GPT-40 allows for a more dynamic and interactive nutritional counseling experience. The data-driven insights from HN-Assistant can be seamlessly translated into actionable advice through GPT-40's language capabilities. For instance, when HN-Assistant outputs nutritional deficiencies, GPT-40 can suggest specific foods or dietary adjustments to address these gaps, tailoring the advice to individual preferences and cultural contexts.

The integration provides a holistic user experience by combining precise data analysis with intuitive communication. Users receive not only raw data but also comprehensible guidance that considers their lifestyle and goals. This interactive approach can increase user engagement and adherence to nutritional recommendations.

The integrated system can adapt recommendations in real time through continuous learning and feedback mechanisms. As users input new data or preferences, the system can refine its advice, ensuring that nutritional guidance remains relevant and practical. This adaptability is crucial in addressing the dynamic nature of individual dietary needs.

3.3. Challenges and considerations

Despite the potential benefits, integrating HN-Assistant with a multimodal LLM poses challenges. Ensuring data privacy and security is paramount, as sensitive health information is involved. Additionally, the system must be designed to avoid biases and inaccuracies that could arise from algorithmic processing. Continuous updates and validation against current nutritional science are necessary to maintain the credibility and reliability of the guidance provided.

4. Results

4.1. The use of the HN-Assistant application alone

The created software application prompts the user to input general information such as age, gender, weight, height, and level of physical activity (Figure 1).

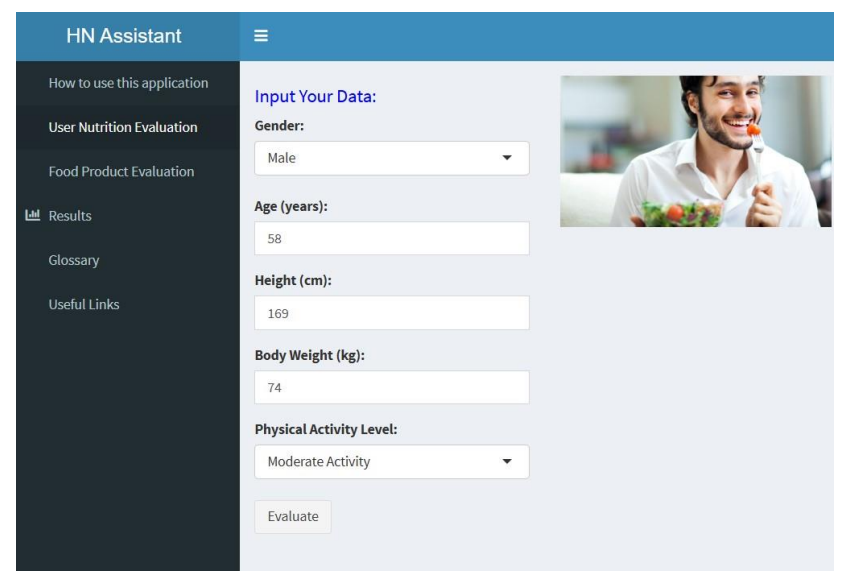


Figure 1. The interface for the input of the user data.

The application is also able to evaluate a food product of interest by inputting data available on the food product label (Figure 2).

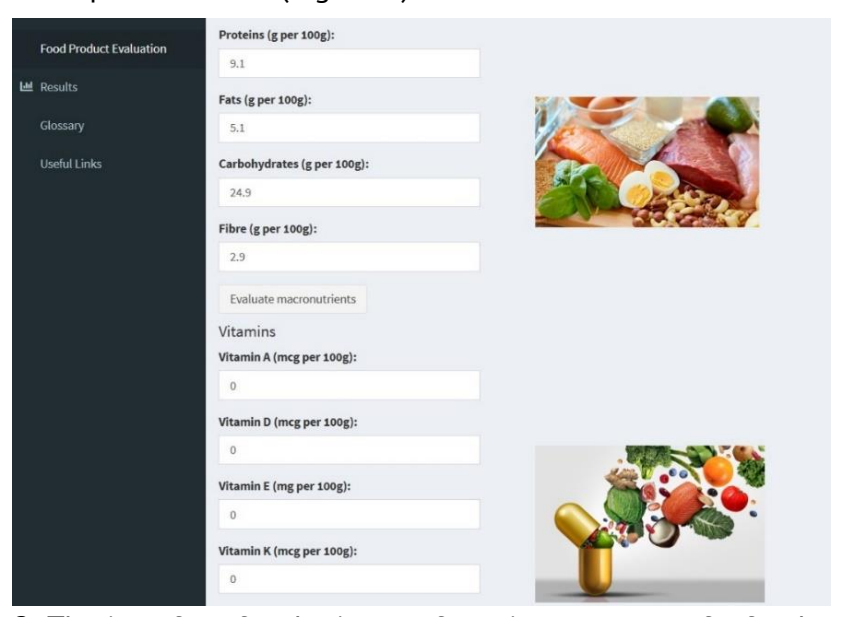


Figure 2. The interface for the input of nutrient content of a food product.

Based on this information, the application estimates several basic parameters concerning the user's nutritional state (e.g., BMI, BMR, and TDEE). It classifies the nutritional status of the user (e.g., normal or over/underweight, obesity, or malnutrition). Based on input information, it will also calculate daily nutrient requirements (e.g., macronutrients, vitamins, and minerals). The results of the analysis and estimations can be visualized by pressing the 'Results' icon on the left vertical panel of the application (Figures 1 and 2).

Table 1 presents the results provided by HN-Assistant for a 58-year-old male, 1.69 cm tall, weighing 74 kg, and showing moderate physical activity.

Table 1

Estimation results for a 58-year-old individual

Main Nutritional State Parameters

Your Body Mass Index is 25.9. Nutritional State - Overweight.

Your Basal Metabolic Rate equals 1648 kcal.

Based on Your Physical Activity Your Total Daily Energy Expenditure represents 2637 kcal.

Nutrient Requirements

	_			
Requirement				
61.40				
87.90				
29.30				
263.70				
10.00				
	61.40 87.90 29.30 263.70			

32.00

Your Daily Vitamin Requirements

Fibre (g)

Vitamin	Requirement	
Vitamin A (μg)	700.00	
Vitamin D (μg)	15.00	
Vitamin E (mg)	12.00	
Vitamin K (μg)	70.00	
Thiamin (B ₁) (mg)	1.10	
Riboflavin (B ₂) (mg)	17.67	
Niacin (B ₃) (mg)	17.67	
Pyridoxine (B ₆) (mg)	18.77	
Folate (B ₉) (µg)	330.00	
Cobolamin (B ₁₂) (μg)	3.40	
Vitamin C (mg)	110.00	
Varia Daile Minaral Danimananta		

Your Daily Mineral Requirements

Mineral	Requirement
Potassium (mg)	3500.00
Calcium (mg)	950.00
Iron (mg)	11.00
Zinc (mg)	16.00

Then, the input of information concerning a food product of interest is followed. This information is available on the product label and is quantified for 100 g/mL. The application will estimate the coverage rate of certain nutrients by 100 g of product, comparing it with the requirements values calculated in the previous step. The results can be visualized in the 'Results' section as radial diagrams for three groups of nutrients: macronutrients, vitamins, and minerals. Figures 3 to 5 depict these results for a food product consisting of 100 g of tofu and 100 g of banana.

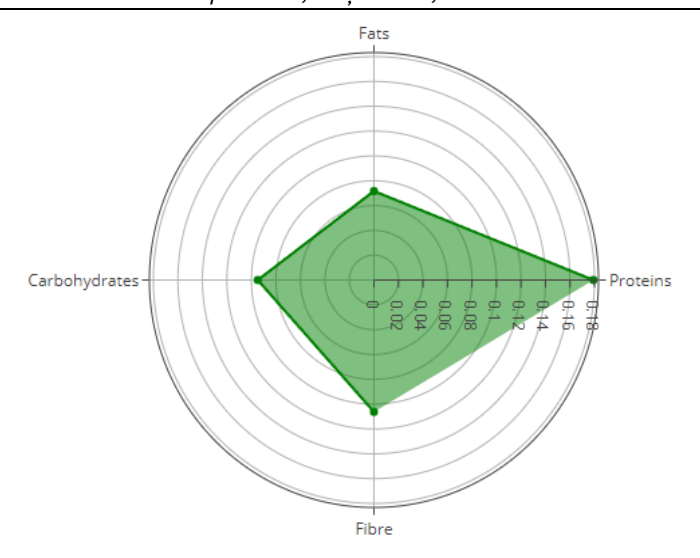


Figure 3. Macronutrient coverage by the product.

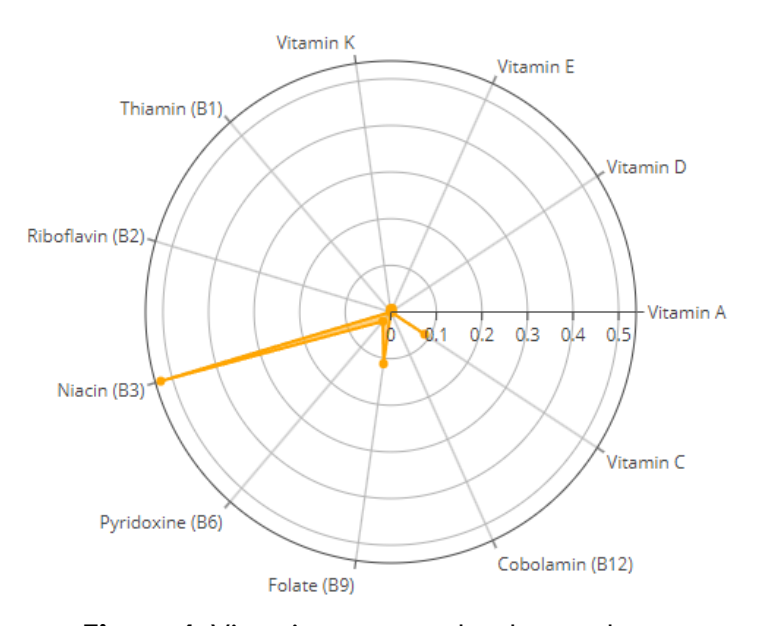


Figure 4. Vitamin coverage by the product.

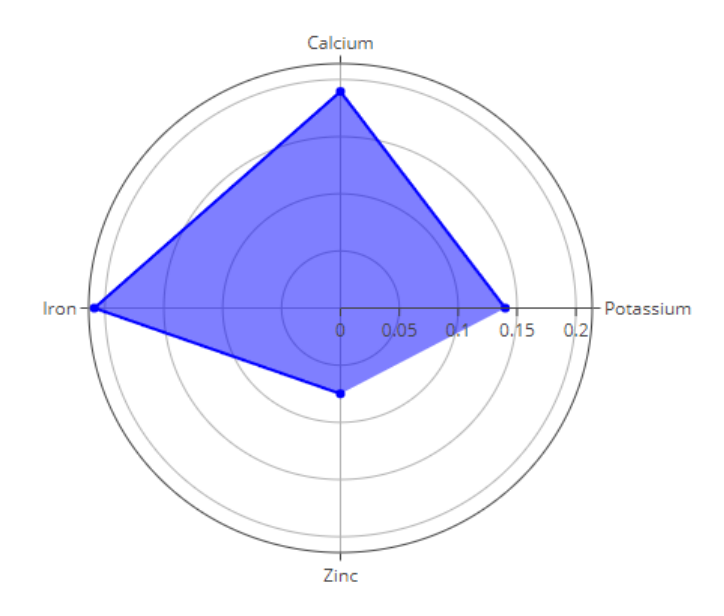


Figure 5. Mineral coverage by the product.

4.2. Results of coupling HN-Assistant and GPT-40

While HN-Assistant's quantitative analysis and data visualization capabilities are impressive, AI assistants like GPT-40 bring complementary skills to the table. These language models, trained on vast amounts of data, possess a wealth of knowledge spanning various domains, including nutrition, health, and wellness. They can provide in-depth explanations, contextual information, and evidence-based insights that enhance the understanding and practical application of the numerical data provided by HN-Assistant. A Python API is used to interact with GPT-40.

Figure 6 presents the prompt passed to the LLM.

I will provide you the evaluation results using a proprietary software application for a male 58 years old, 1.69 cm tall, weighing 74 kg, with a moderate level of physical activity. You should comment the results and provide nutrition recommendations. The application also provides conclusions concerning how much a certain product covers certain nutrition requirements. I will provide the results of the evaluation of a food product with the main components, tofu and banana, 100 g each. The results are three radial diagrams. Comment about how good this product is for the person evaluated. Provide a conclusion up to 100 words long. The diagrams are as follows: {the diagrams}.

Figure 6. The prompt passed to the LLM.

Figures 7 and 8 illustrate the output generated by GPT-40 when information from the HN-Assistant is provided.

The evaluation indicates a BMI of 25.9, classifying as overweight. To manage weight, consider a balanced diet with a slight calorie deficit. Focus on whole foods, lean proteins, and plenty of vegetables to meet your macronutrient needs. Limit added sugars to 10g/day. Ensure adequate intake of fiber (32g) and essential vitamins and minerals, particularly Vitamin D (15mcg), Vitamin C (110mg), and calcium (950mg). Regular physical activity is beneficial, so maintain or increase your current level. Hydration and portion control are also key. Consulting a nutritionist for personalized advice could be advantageous.

Figure 7. The GPT-4o output concerning nutrition recommendations for the evaluated individual (by HN-Assistant).

The tofu and banana combination provides a balanced profile of macronutrients, with moderate protein and carbohydrate content. However, it falls short in covering vitamin needs, particularly Vitamin D, B12, and C. Mineral coverage is limited, especially in zinc and iron. This product can be a part of a balanced diet but should be complemented with other foods rich in essential vitamins and minerals to meet daily requirements. Including leafy greens, nuts, and fortified foods can help achieve a more comprehensive nutritional intake.

Figure 8. The GPT-4o output concerning the conclusion about the analyzed food product (by HN-Assistant).

As can be noticed from the prompt (Figure 6), the LLM was limited to providing short outputs (i.e., up to 100 words). This was done for brevity. When necessary, this limit can be modified.

4. Discussion

Integrating HN-Assistant with multimodal language models like GPT-40 heralds a transformative era in personalized nutrition. This synergy merges precision in data-driven analysis with the adaptability and engagement of advanced language processing, offering a comprehensive approach to dietary management that can significantly enhance individual health outcomes.

By combining analytical capabilities with interpretative power, users receive not just raw data but also personalized, actionable insights. This integration allows for a nuanced understanding of nutritional needs, considering individual factors such as lifestyle, preferences, and health goals. For instance, when HN-Assistant identifies a deficiency in a particular nutrient, GPT-4o can suggest foods or meal plans tailored to the user's dietary habits and cultural context, leading to more effective dietary changes and improved adherence.

The interactive nature of GPT-40 enhances user engagement by providing explanations, answering questions, and adapting recommendations in real-time. This dialogue-based approach demystifies complex nutritional concepts, making them more accessible and less intimidating for users. As a result, individuals are more likely to understand and follow the guidance provided, leading to better health outcomes. Moreover, the system's ability to adapt to user feedback and changing circumstances ensures that the advice remains relevant and effective over time.

One standout feature is the capacity for real-time adaptation. As users input new data, the system can instantly adjust its recommendations, ensuring ongoing support that aligns with current needs and goals. Such adaptability is crucial in addressing the fluid nature of human health and lifestyle changes.

Despite its potential, the integration is not without challenges. Ensuring privacy and security of user data is critical, especially given the sensitivity of health-related information. Robust measures must protect against data breaches and unauthorized access. The system must also minimize biases and inaccuracies, which could lead to inappropriate recommendations. Continuous validation against current nutritional science is necessary to maintain credibility and reliability.

An additional way to improve the results of the integration would be adding a retrieval augmented generation (RAG) module. This supposes the creation of a vector database containing relevant information concerning nutritional aspects (e.g., based on information from credible sources like [1-3]) and supplementing the query passed to the LLM with the information from this database using semantic similarity [16-18].

As technology evolves, integrating data-driven applications with multimodal models will likely become more sophisticated [19-21]. Future iterations could incorporate additional data sources, such as biometric sensors or genetic information, to provide even more personalized and precise nutritional guidance. Expanding the system's capabilities to include mental health and wellness support could offer a holistic approach to health management.

5. Conclusions

The integration of HN-Assistant with multimodal language models like GPT-40 represents a significant advancement in personalized nutrition. By combining precise data analysis with adaptive, user-friendly communication, this approach has the potential to revolutionize dietary management, promote healthier lifestyles, and improve individual wellbeing. As we continue to refine and expand these technologies, their impact on public health and individual empowerment will grow, contributing to a healthier, more informed society.

Conflicts of Interest: The authors declare no conflict of interest.

References

- 1. European Food Safety Authority. Available online: https://www.efsa.europa.eu/en (accessed on 16.11.2024).
- 2. U.S. Food and Drug Administration. Available online: https://www.fda.gov/ (accessed on 16.11.2024)
- 3. World Health Organization/Nutrition. Available online: https://www.who.int/health-topics/nutrition#tab=tab_1 (accessed on 16.11.2024)
- 4. HN-Assistant. Available online: https://viapascurta.shinyapps.io/HN_Assistant/ (accessed on 16.11.2024)
- 5. Siminiuc, R. Exploratory analysis of nutritional security in the Republic of Moldova, doctor habilitatus thesis in engineering sciences, Technical University of Moldova, Chisinau, Republic of Moldova, 27.06.2024
- 6. Blackburn, H.; Jacobs, D. Jr. Commentary: Origins and evolution of body mass index (BMI): continuing saga. *Int. J. Epidemiol.* 2014, 43(3), pp. 665-669.
- 7. Global BMI Mortality Collaboration; Di Angelantonio, E.; Bhupathiraju, Sh.N.; Wormser, D.; Gao, P.; Kaptoge, S.; Berrington de Gonzalez, A.; Cairns, B.J.; Huxley, R.; Jackson, Ch.L. et al. Body-mass index and all-cause mortality: individual-participant-data meta-analysis of 239 prospective studies in four continents. *Lancet* 2016, 388, pp. 776-786.
- 8. Heymsfield, S.B.; Smith, B.; Dahle, J.; Kennedy, S.; Fearnbach, N.; Thomas, D.M.; Bosy-Westphal, A.; Müller, M.J. Resting Energy Expenditure: From Cellular to Whole-Body Level, a Mechanistic Historical Perspective. *Obesity* 2021, 29(3), pp. 500-511.
- 9. Ballesteros, FJ.; Martinez, VJ.; Luque, B.; Lacasa, L.; Valor, E.; Moya, A. On the thermodynamic origin of metabolic scaling. *Sci. Rep.* 2018, 8(1), p.1448.
- 10. Pavlidou, E; Papadopoulou, S.K.; Seroglou K.; Giaginis, C. Revised Harris-Benedict Equation: New Human Resting Metabolic Rate Equation. *Metabolites* 2023, 13(2), p. 189.
- 11. Müller, M.J.; Enderle, J.; Bosy-Westphal, A. Changes in Energy Expenditure with Weight Gain and Weight Loss in Humans. *Curr. Obes. Rep.* 2016, 5(4), pp.413-423.
- 12. Wiklund, P. The role of physical activity and exercise in obesity and weight management: Time for critical appraisal. *J. Sport Health Sci.* 2016, 5(2), pp. 151-154.
- 13. Web Application Framework for R shiny-package. Available online: https://shiny.posit.co/r/reference/shiny/1.4.0/shiny-package.html (accessed on 16.11.2024)
- 14. OpenAI; Achiam, J.; Adler, S.; Agarwal, S.; Ahmad, L.; Akkaya, I.; Aleman, F.L.; Almeida, D.; Altenschmidt, J.; Altman, S. et al. GPT-4 Technical Report," OpenAI. GPT-40. arXiv:2303.08774v6, 2024.
- 15. Van Rossum, G.; Drake, F.L. Python 3 Reference Manual. Scotts Valley, CreateSpace, CA, 2009, 242p. ISBN:978-1-4414-1269-0.
- 16. Lewis, P.; Perez, E.; Piktus, A.; Petroni, F.; Karpukhin, V.; Goyal, N.; Küttler, H.; Lewis, M.; Yih, W-t.; Rocktäschel, T.; Riedel, S.; Kiela, D. Retrieval-augmented generation for knowledge-intensive NLP tasks. *Advances in Neural Information Processing Systems* 2020, 33, pp. 9459–9474.
- 17. Gaoa, Y.; Xiongb, Y.; Gao, X.; Jia, K.; Pan, J.; Bi, Y.; Dai, Y.; Sun, J.; Wang, M.; Wang, H. Retrieval-Augmented Generation for Large Language Models: A Survey. 2024 arXiv:2312.10997v5.
- 18. lapăscurtă, V.; Kronin, S.; Fiodorov, I. Retrieval-augmented generation using domain-specific text: a pilot study. *Journal of Engineering Science* 2024, 31 (2), pp. 48-59.
- 19. Turcanu, D.; Siminiuc, R. Software for nutritional assessment of individuals with gluten eating disorders. *Journal of Engineering Science* 2023, 30(3), pp. 164-172.
- 20. Zhi, D.; Calhoun, V.D. Data-driven multimodal fusion: approaches and applications in psychiatric research. *Psychoradiology* 2023, 3, pp. 1–19.
- 21. Brenner, M.; Hess, F.; Koppe, G.; Durstewitz, D. Integrating Multimodal Data for Joint Generative Modeling of Complex Dynamics. arXiv:2212.07892v2, 2024.

Acknowledgements. This work was supported by the National Agency for Research and Development (NARD) under the grant number 23.70105.5107.05 for the project Exploratory analysis of food security in the Republic of Moldova based on metrics of sustainable and nutritional quality (SNuQ) of food products, implemented at the Technical University of Moldova. We also acknowledge the support of the Technical University of Moldova through grant number 020405 for the project Optimizing food processing technologies in the context of the circular bioeconomy and climate change. We express our gratitude to all contributors and institutions involved in the successful execution of these research initiatives.

Citation: Iapăscurtă, V.; Țurcanu, D.; Siminiuc, R. Integration of a data-driven software application and a multimodal LLM for enhanced nutritional guidance: a case study. *Journal of Engineering Science* 2024, XXXI (3), pp. 75-84. https://doi.org/10.52326/jes.utm.2024.31(3).07.

Publisher's Note: JES stays neutral with regard to jurisdictional claims in published maps and institutional affiliations.



Copyright:© 2024 by the authors. Submitted for possible open access publication under the terms and conditions of the Creative Commons Attribution (CC BY) license (https://creativecommons.org/licenses/by/4.0/).

Submission of manuscripts:

jes@meridian.utm.md

Fascicle

Topic

Architecture, Civil and Environmental Engineering Civil Engineering and Management

ISSN 2587-3474 eISSN 2587-3482

Vol. XXXI, no. 3 (2024), pp. 85 - 95

https://doi.org/10.52326/jes.utm.2024.31(3).08 UDC 551.435:625.7(478)





ENSURING THE LONG-TERM STABILITY OF DEEP CUTTING SLOPES FORMED BY CLAY SOILS ON REPUBLIC OF MOLDOVA ROADS

Vladimir Polcanov, ORCID: 0000-0001-8389-2128, Alina Polcanova, ORCID: 0000-0001-5826-8278, Alexandru Cîrlan *, ORCID: 0000-0003-4009-2790

Technical University of Moldova, 168 Stefan cel Mare, Blvd., Chisinau, Republic of Moldova * Corresponding author: Alexandru Cîrlan, alexandru.cirlan@cms.utm.md

> Received: 08. 20. 2024 Accepted: 09. 25. 2024

Abstract. The article presents research results on identifying the causes of landslide deformations along the M21 road, Brest-Chişinău-Poltava in the Republic of Moldova, using Maslov's physico-technical theory of creep, along with proposals for their stabilization. It highlights the geomorphological and geological characteristics contributing to landslide formation, focusing on the rheological properties of clayey soils. The studies included stability calculations based on laboratory investigations aimed at determining strength and rheological properties. Results demonstrated the dependence between soil moisture and structural cohesion, influencing landslide resistance and creep deformations. Proposed values for residual strength characteristics of clayey soils ensure long-term stability of deep excavation slopes without creep deformations, as well as values allowing economically feasible excavations with partial reduction of structural cohesion without compromising slope stability during operation.

Keywords: loss of stability, rheology, soil strength, physico-technical theory, creep.

Rezumat. În articol sunt prezentate rezultatele cercetările pentru identificarea cauzelor deformărilor de alunecare de-a lungul drumului M21 Brest-Chișinău-Poltava din Republica Moldova, folosind teoria fizico-tehnică de fluaj propusă de Maslov. N.N., precum și propuneri de stabilizare a acestora. S-au evidențiat caracteristicile geomorfologice și geologice care contribuie la formarea alunecărilor, cu accent pe proprietățile reologice ale pământurilor argiloase. Studiile au inclus calcule de stabilitate folosind rezultatele investigațiilor de laborator care aveau ca scop determinarea proprietăților de rezistență și celor reologie. Rezultatele au demonstrat dependența între umiditatea pământului și coeziunea structurală, influențând rezistența la alunecare și dezvoltarea deformărilor de fluaj. Au fost propuse valorile caracteristicilor de rezistență reziduală a pământurilor argiloase care ar asigura stabilitatea de lungă durată a taluzurilor săpăturilor adânci, fără a prezenta deformații de fluaj, precum și valorile acestora care ar permite realizarea economica a săpăturilor, cu reducerea parțială a coeziunii structurale, însă fără a afecta stabilitatea taluzurilor pe durata de exploatare.

Cuvinte cheie: pierderea stabilității, reologie, rezistența pământului, teoria fizico-tehnică, fluaj.

1. Introduction

In the practice of construction and operation of roads from Republic of Moldova there are many problems due to numerous incidents of landslide processes (Figures 1 and 2).



Figure 1. Landslide processes along the M21 road, Brest-Chisinau-Poltava *Foto: Polcanov Vladimir, May 2015.*



Figure 2. Deformation of the left slope of the deep excavation at PC1441+00 of the M21 road, Brest-Chisinau-Poltava

Foto: Cirlan Alexandru, April 2017.

The geomorphological features of the territory determine the execution of deep excavations for the roads design. Undercutting often leads to the development of landslides, which can develop even on the slopes with inclination 5-6°.

In Republic of Moldova were recorded more than 16 thousand landslides. Most of them occupy the middle and upper side of slopes and develop in sand-clay rocks of middle-Sarmatian age (N_1S_2). Typically, landslides are generated on ancient and old landslide displacements, therefore, development of today landslides has inherited character.

Analysis of nature and manifestation conditions of landslide processes on the territory of Republic of Moldova revealed the role of rheological processes in the breaking the stability of natural slopes. At the same time, research has shown that the slopes stability of the road excavations was not studied enough [1].

The need to obtain reliable theories regarding the behavior of earth masses to solve complex engineering problems was postulated as early as Karl von Terzaghi's 1925 publication [2].

In the 1930s, the necessity to address practical problems, particularly the failure of some French dams and the commencement of construction works for the support structures of the hydroelectric power plant on the Svir River in Russia, situated on a thick layer of clays, prompted further research in this direction.

At the end of the 1930s, began the study of rheological processes of soils to determine the types and nature of soil deformations. These deformations were classified into: initially conditioned instantaneous deformations (reversible and irreversible); stable creep (attenuated) and progressive creep, as presented in various studies [3, 4].

Henkel D. J. [5] and Šuklje L. [6, 7] obtained the long-term strength curve, similar to those presented by other researchers, comparing the soil strength at the moment of slope failure with that before failure. They found that over 50-55 years, the soil strength decreased by 2.5-3 times.

Peterson R. provided clear examples of slope failures occurring 1/2-4 years after construction due to a reduction in their strength by up to 50%, as a result of the gradual decrease in soil strength over time [8].

The study of the rheological properties of soils is closely linked to the concept of "soil strength." Dr. B. Tiedemann first presented results on determining residual strength of intact clay structures [9]. Similar tests were conducted by Dr. M.J. Hvorslev in 1937 on two clays consolidated from suspension [10]. In 1952, J. MacNeil Turnbull provided practical guidance for the approximate determination of residual strength in some compacted soils [11].

Skempton A.W. [12, pp. 79-80], while studying the stability of slopes and embankments formed from overconsolidated English clays, addressed the issue of peak and residual strength, as slope stability directly depends on these characteristics. According to Skempton A.W.'s findings, the value of residual cohesion is very small or approximately zero. In other words, during the transition from peak to residual strength, the structural cohesion is completely depleted, and the internal friction angle decreases by 1-2°, and in some cases even by 10°. This statement by Skempton A.W. was contested by several renowned scholars, notably Maslov N.N., who demonstrated that structural cohesion in soils cannot be completely excluded, a point later agreed upon by Skempton A.W. in subsequent works.

Of particular interest is Maslov N.N.'s theory of soil strength, which posits that soil strength depends on the internal friction angle φ_w determined by the state of compaction-moisture and the total cohesion divided into structural cohesion C_c , which does not depend on the soil's compaction-moisture state, and viscous (hydrocolloidal) cohesion Σ_w , characteristic for each compaction-moisture state [4, 13].

In the study of landslide soil strength by scholars from the Goldstein M.N. school, based on the stable effect of loading regimes on strength, the concept of "long-term strength limit" was analyzed as the minimum possible value of strength for infinitely slow deformations during the formation and development of landslides. The reduction in shear

strength is explained by increased clay moisture in the shear zone and the realignment of clay particles parallel to the shear direction [14-16].

Marinescu C. mentioned in his work that shear strength is a complex function resulting from the combination of two functions expressing interdependent processes: the physicochemical characteristics of the soil and the manner in which it is loaded over time [17, pp. 95-96].

Christensen R.W. links clay deformation processes to a combination of recoverable deformations resulting from the bending and rotation of individual particles, and non-recoverable deformations resulting from the relative movement between adjacent particles at their contact points [18].

Considering that strength is largely determined by the duration of loading, some scholars, such as Cristescu S.L., Ştefănică M., Marin M. [19], presenting classical aspects of rheology, emphasize the real-world applicability of these concepts.

In addition to applied static loads, practical and theoretical interest also focuses on dynamic loads such as earthquakes, vibrations, etc. Research by Hu H., Yu D., Gu H. [20] in this direction has enabled the determination of rheological characteristics and the development of a rheological model that considers objective factors such as climate, weather, geological conditions, terrain features, etc.

The present work is focused on identifying the causes of landslide deformation along the M21 road Brest-Chisinau-Poltava in connection with its upcoming reconstruction and the need for such design solutions that will ensure its long-term safe operation.

2. Materials and Methods

For preventing the landslides in the future was identified the following main objectives of research:

- · were studied the causes of landslide deformation in deep excavations,
- were received the design values for rheological properties of clay soils involved in landslide movement,
- were proved the economically viable and reliable profiles for slope excavations.

Soil analysis was mainly carried out on samples of the natural structure selected in the target areas destroyed by landslides. Some of the samples were tested after prolonged moisturizing in a sand bath. Indicators of physical properties of soils were determined by standard methods.

To obtain the values of strength characteristics, the direct shear tests were carried out by "fast shear" method.

The rheological characteristics: "creep threshold" and "coefficient of viscosity" were obtained by "constant deformation rate" method proposed by prof. Maslov N.N. [13]. The long-term strength parameters were set in accordance with the views of prof. Goldstein M.N. and his disciples: Turovskaya A.Y., Chernenko N.B., Timofeeva T.A [21, 22].

3. The results of the research

The peculiarities of geomorphological conditions of M21 road Brest-Chisinau-Poltava within the territory of the Republic of Moldova, which borders Ukraine, requires designing a significant number of road embankments, with height from 3-6 up to 15-20 meters and with deep excavations from 6 to 24 meters.

In areas where red-brown silty clay (aldl $Q_{\text{III-IV}}$) are a part of geological structure, these soil layers are involved in active deformation. As a result, for these areas are characteristic

steep, close vertical, walls of breakdowns with height 12 and more meters. Below, in the clay rocks (N_1S_1) strains are characterized by plastic flow.

Based on the results of field work, existing cross-sections were built and compared with design cross-sections to identify the causes of slope deformations (Figure 3).

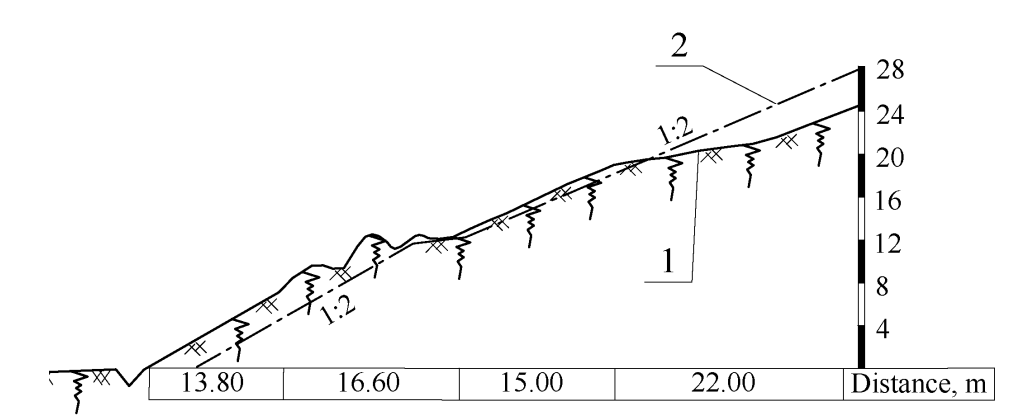


Figure 3. Schematic cross-section of left slope excavation: 1 – existing cross-section; 2 – design cross-section.

An analysis of the available material revealed the deformation confined to the watered clay sequence. Their main reason is the considerable steepness of slopes that the design was administered without regard to characteristics of clay rocks, causing the possibility of creep deformation and strength reduction of clay soil in time under the influence of long-acting shear stresses, as well as processes of weathering and additional moisture during rainfalls or other precipitations.

In order to study rheological parameters, soil sampling and laboratory tests were performed to determine: soil strength, creep threshold, and coefficient of viscosity.

The research results for strength of clays revealed natural moisture content in the range of solid consistency is primarily manifested discreteness factor that reflects the structural and textural characteristics of soil and degree of impairment of structural connections through natural zones of weakening defining the nature of deformation of hard clays, and the overlapping impact on the strength of strata of density, moisture content and consistency.

This is true not only for the majority of the studied landslides Neogene-Quaternary clay rocks in Moldova, but for Neogene clays of Odessa and Caucasus, which are forming landslide slopes. Factor of consistence, reflecting the role of hydrocolloidal cohesion in the overall cohesion and coefficient of viscosity, begins to manifest itself in transition from solid samples in to a semi-solid and semi-plastic state, and it's more determining for the character of deformation in plastic clays.

An approximate relationship $\tau = f(I_L)$ has been used for the samples, tested by the method of "prepared surface of shift", which simulates the loss of structural cohesion. Using the method of density-moisture by prof. Maslov N.N., dependence of internal friction angle and hydrocolloidal cohesion on the consistency was obtained (Figure 4).

The performed studies of the strength properties allowed at this stage to disclose the excavation with recommended design strength characteristics [23]:

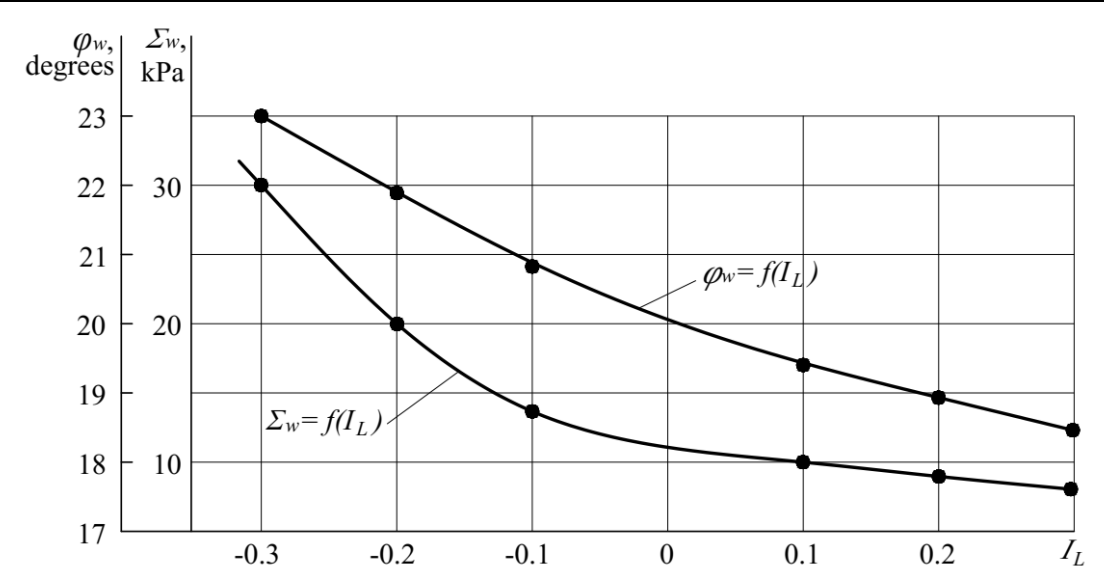


Figure 4. Graphs of the dependence of hydrocolloidal cohesion (Σ_w) and the angle of internal friction (φ_w) on consistency (I_L)

- excluding the time factor and the presence of weak areas, with possible failure of cohesion due to the additional moisturizing: for the depth $h \le 15\text{m} \varphi = 16^\circ$; C = 44kPa; for $h > 15\text{m} \varphi = 16^\circ$; $C = \Sigma_w + 0.5 \cdot C_c = 85\text{kPa}$;
- including the time factor: for the depth $h \le 15$ m, $\varphi = 16^\circ$; $\Sigma_w = 20$ kPa; for h > 15m values of residual strength $\varphi = 10^\circ$; $\Sigma_w = 9$ kPa;

In order to study the possibility of transition of the clay soils, which are forming the slopes of the excavations, in the state of creep, were determined by "creep threshold" values. According to Maslov N.N. [4, 13], its theoretical expression is defined by Eq. (1):

$$\tau_{\lim} = p_n \cdot \mathsf{tg}\,\varphi_w + C_c \tag{1}$$

The process of creep in all cases will proceed under the influence of the remaining part of the shear stress $\Delta \tau$, defined by Eq. (2):

$$\Delta \tau = \tau - \tau_{\text{lim}} = \tau - (p_n \cdot \lg \varphi_w + C_c)$$
 (2)

in the above expressions:

 Σ_w – hydrocolloidal cohesion, kPa;

 C_c – structural cohesion, kPa;

 φ_w – true angle of internal friction, degree;

 p_n – normal stress, kPa.

In most cases applied to the Neogene clays in Moldova, the local environment deprives us from the possibility of direct use of theoretical expression of determining the values of the "creep threshold" for natural soil structure. In these conditions, it is associated with exceptional heterogeneity of the rock.

It should be noted that despite the presence of considerable research in "creep threshold" this issue couldn't be considered fully resolved to this day. It attributes this fact, in particular, to an undisclosed feature of the nature of hard structural cohesion (C_c).

Rigid structural cohesion connections may have ionic nature; defined by cementation, crystallization, etc. In all cases, they are irreversible. However, studies carried out by Acad. Kazarnovskii V.D. show that hydrocolloidal nature of cohesion (Σ_w) in clay soils of hard and

semi-solid consistence, which we encounter in the study of rocks that form the slopes of Moldova, may also condition the nature of the irreversible fragile shear strain. Thus, it is possible to determine to greater or lesser degree, the value of "creep threshold", like the rigid connection of the structural cohesion (C_c). This question is still not studied enough. However, in terms of rheological analysis, it has a primary importance.

In these circumstances, there is no way to fully trust the theoretical schemes and necessity to establish calculated values of "creep threshold" for the selected species of soil experimentally. Experiments were carried out on a "constant speed" by the method of Sotnikov S.N., improved by Polcanov V.N. It was performed more than 50 experiments lasting from 1 to 40 days at a speed $v=a\cdot10^{-8}...a\cdot10^{-10}$ m/s. The samples were tested at natural moisture content, and after, were moisturized in boxes with wet sand. This allowed determination of the "creep threshold" in the range from solid to semi-plastic consistence and plotting graphs of it dependency on the consistency (Figure 5).

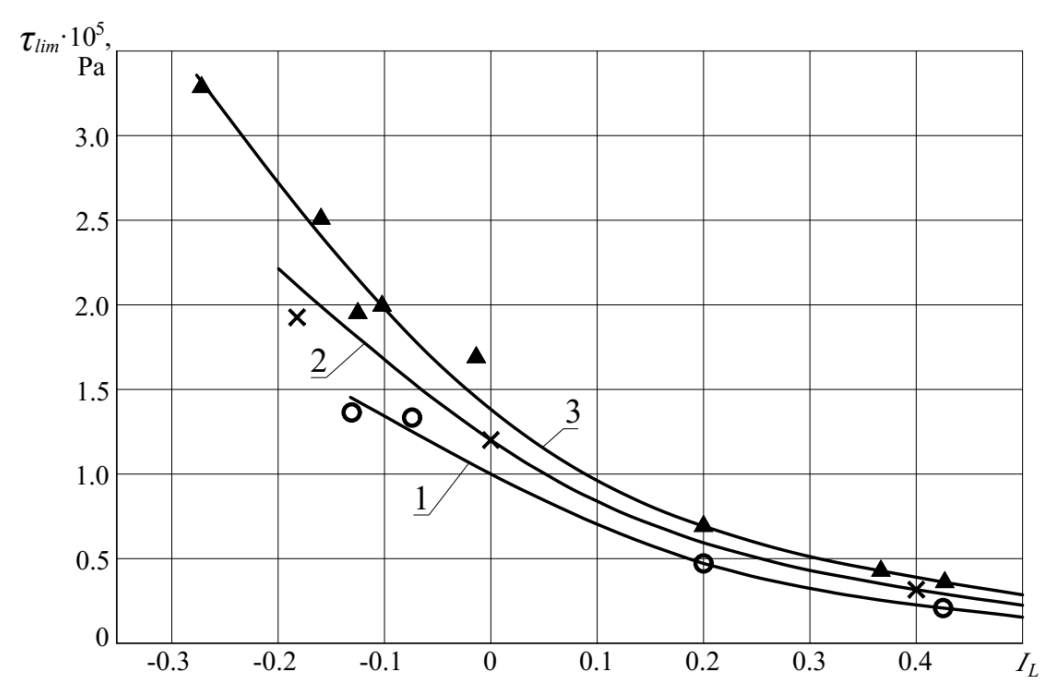


Figure 5. The graphs of dependence between "creep threshold" (τ_{lim}) of Neogene clays from cover layer and consistency (I_L), for different values of vertical loading, by tests with $v=5.8\cdot 10^{-10} \text{m/s}$:

1 – for vertical loading $p=1\times10^5$ Pa; 2 – for $p=2\times10^5$ Pa; 3 – for $p=3\times10^5$ Pa.

Following the processing of the experimental data were obtained the expressions characterizing "creep threshold" (τ_{lim}) for clays from different zones of the landslide massif. These expressions are presented in Eq. (3):

$$\begin{split} &\tau_{\text{lim,1}} = 0.16p_n + 40kPa \text{ - for cover layer;} \\ &\tau_{\text{lim,2}} = 0.25p_n + 75kPa \text{ - for the bedrock layer;} \\ &\tau_{\text{lim,3}} = 0.09p_n + 9kPa \text{ - for the landslide displacement zone.} \end{split}$$

These equations have been used during the rheological analysis. The possibility of development of creep deformation in the fundamental and cover stratum, as well as in the weakened area of their contact.

For the forecast of speed of creep deformation in slope excavation was used the dependence between viscosity and consistency. This allowed to establish the speed of the displacement of the cover array applied to the calculated index of liquidity (I_L).

Given the exceptional importance of the calculations for estimating the rate of creep surveyed landslides, similar calculations were performed for different values of the coefficient of viscosity (η) and degree of preservation primary structure of the soil (Figures 6-7).

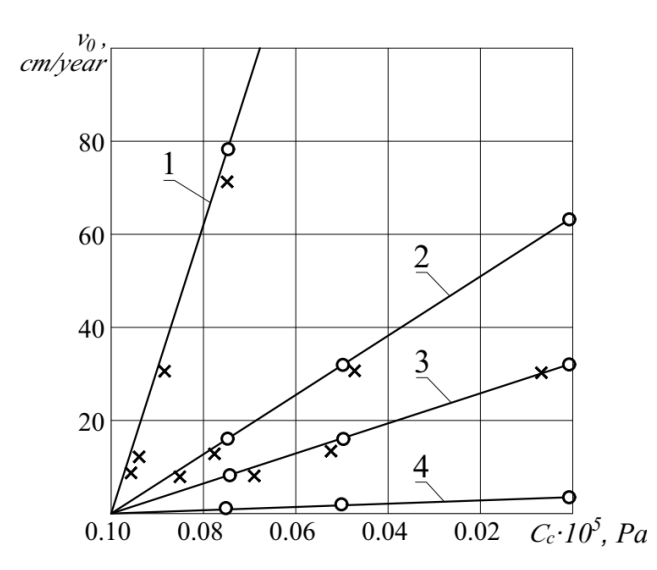


Figure 6. The graphs of dependence between speed of creep deformation (v_0) and structural cohesion (C_0) for different values of coefficient of viscosity (η):

- 1 for $\eta = 10^{11} \text{ Pa·s}$;
- 2 for $n=5.10^{11} Pa.s$;
- 3 for $\eta = 10^{12} \text{ Pa·s}$;
- 4 for $\eta = 10^{13} \, \text{Pa} \cdot \text{s}$.

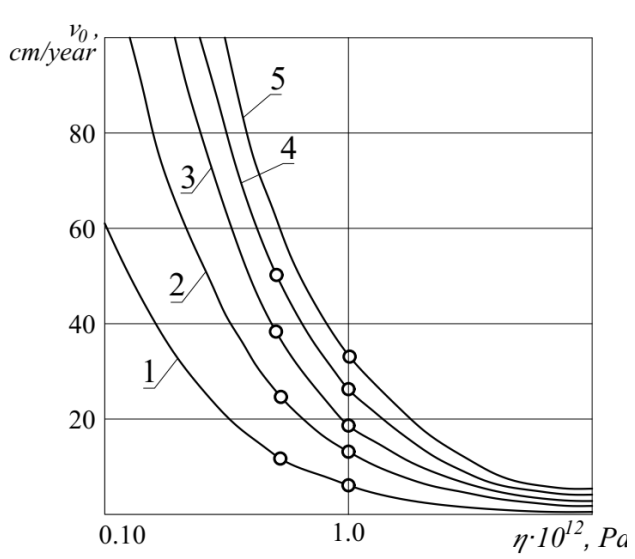


Figure 7. The graphs of dependence between speed of creep deformation (v_0) and coefficient of viscosity (η) at different values of structural cohesion (C_c) :

- 1 for $C_c = 0.08 \cdot 10^5 \, \text{Pa}$;
- 2 for $C_c = 0.06 \cdot 10^5 \, \text{Pa}$;
- 3 for $C_c = 0.04 \cdot 10^5 \text{ Pa}$;
- 4 for $C_c=0.02\cdot10^5$ Pa;
- 5 for $C_c=0$ Pa.

It was found that in a soil with hard structural cohesion (C_c) defined by value approximatively equal to C_c =10kPa, speed of landslide displacement is practically zero. Essential value has the viscosity of the soil: if C_c =8 kPa, and η =10¹¹ Pa·s, v_o =60cm/year; at the same values of C_c and η =10¹³ Pa·s, v_o =0.

Comparison of theoretical speeds creep deformation and actual field data for the dynamics of the landslide deformations on the surveyed sites has given satisfactory results.

In other words, the calculations and field studies were indicate the possibility of landslide movement with intensity of the order of several centimeters per year, followed by acceleration in time as a result of constant manifestation of creep.

As noted above, development of active deformation of slopes excavations is due to fall of watered strength in clay soils as a result of creep processes under the influence of tangential stresses caused by excessive steepness of slopes. In connection with the areas for future reconstruction on the results of exploration and of the research proposed by typification of the excavations by their geological structure. At the same time, based on the

available materials and complexity of engineering-geological conditions, the following type's solutions were offered:

- 1. excavations, disclosed in homogeneous soils;
- 2. excavations, disclosed in sand-clay soils;
- 3. excavations, disclosed in difficult conditions, macroscopically homogeneous, sometimes watered, sand-clay soils.

For excavations with the known geological structure were constructed profiles of equal slope stability (with safety factor K=1.2), taking into account the rheological characteristics of clay soils, obtained during the executed researches (Figure 8).

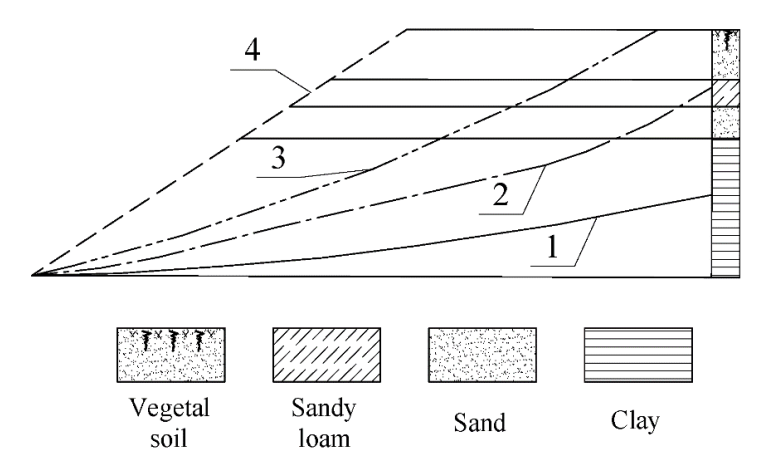


Figure 8. The cross-sections of excavation on P14375-14379, designed taking into account the rheological properties of soils:

- 1 for C_c =9kPa, ϕ =5° (respectively S=0.09p_n+9kPa);
- 2 for C_c =40kPa, ϕ =9° (respectively S=0.16p_n+40kPa);
- 3 for C_c =65kPa, ϕ =12° (respectively S=0.21p_n+65kPa);
- 4 for slope ratio 1:1.5.

As it is known, the real stability reserve is determined by the validity of the selected characteristics. Because of this, the main difficulty is to assess the accumulation time critical deformation, which in turn depends on the adopted "parameters" long-term strength ("creep threshold", "residual strength" and others.) The latter does not have a clear definition and require concretization and the accumulation of research results.

4. Conclusions and recommendations

- 1. Studies were show clay rocks in the bedrock have high values of rheological parameters. As a consequence, the development of the creep deformation in the strata at the depth of the bed-rock clays without visible surfaces of weakening were excluded.
- 2. The emergence of local surface displacements accrues at the cover stratum, which do not affect the overall stability of the slope.
- 3. Development of creep deformation by the weakened zones was confirmed by landslide manifestations, which took place on the slopes of excavations.
- 4. Essential influence on the speed of displacement was rendered by the coefficient of viscosity of soil (η). When η =8·10¹¹Pa·s, and the value of structural cohesion C_c =8kPa, the displacement speed can reach values v=60cm/year. With the same value of the structural cohesion and the coefficient of viscosity η =5·10¹³Pa·s the rate of displacement is reduced to zero.

- 5. Excavations, whose cross sections were designed based on the average statistical strength values (S=0.29p+65kPa) were found to be unstable. The deformations of their slopes were traced after 10 years on all the studied areas of the road.
- 6. The study of the rheological properties of the soil ensures the right choice of design parameters for design strength profiles slopes of deep excavations and allows to prove the need of protection measures to prevent the possibility of creep deformation.
- 7. Disclosure excavations by residual strength (S=0.09p+9kPa) eliminates the possibility of further development of deformation, it is uneconomical and impractical.
- 8. Long-term slope stability is provided by the disclosure of excavations in view of the rheological properties of soils. In these cases, the equilibrium condition is reached, assuming the partial destruction of the structural cohesion (S=0.16p+40kPa).
- 9. Disclosure of excavations on these parameters strength is economically feasible and ensures the safety of traffic and the service life of linear structures.
- 10. In some particular areas, the disclosure of excavations considering rheological characteristics of soils will require considerable land allotment. Therefore, in such areas to ensure long-term stability is recommended to provide lightweight retaining structures designed for active pressure under limiting conditions in combination with an appropriate drainage system.

Conflicts of Interest: The authors declare no conflict of interest.

References

- 1. Polcanov, V.N. The role of rheological processes in the development of landslides on the territory of Moldova. Tehnica UTM, Chisinau, Republic of Moldova, 2013, 176 p. [in Russian].
- 2. Terzaghi, K. Erdbaumechanik auf Bodenphysikalischer Grundlage. Franz Deuticke, Leipzig-Vienna, 1925, 399 p.
- 3. Vyalov, S.S. Rheological foundations of soil mechanics. Vysshaja shkola, Moscow, 1978, 448 p. [in Russian]
- 4. Maslov, N. N. Soil Mechanics in construction practice (landslides and their control). Stroyizdat, Moscow, 1977, 320 p. [in Russian].
- 5. Henkel, D.J. Investigation of two long-term failures in London clay slopes at Wood Green and Northolt. In: Proceedings of the 4th International Conference on Soil Mechanics and Foundation Engineering, London, UK, 12-24 August 1957, pp. 315-320.
- 6. Suklje, L. Common factors controlling the consolidation and the failure of soils. In: Proceedings of the Geotechnical Conference, Shear Strength Properties of Natural Soils and Rocks, Oslo, Norway, 1967; Norwegian Geotechnical Institute, Oslo, Norway, 1968, pp. 153-158.
- 7. Suklje, L. Rheological problems of soil mechanics. Stroyizdat, Moscow, 1973. 485 p. [in Russian].
- 8. Peterson, R. Discussion. In: Proceedings of the 3rd International Conference on Soil Mechanics and Foundation Engineering, Zurich, Switzerland, 16th-27th August 1953, 211 p. [in German].
- 9. Tiedemann, B. Über die Scherfestigkeit bindiger Böden. Bautechnik 1937, 15, 1937, pp. 400–403.
- 10. Hvorslev, M.J. Über die Festigkeitseigenschaften gestörter bindiger Böden. In: Ingeniörvidenskabelige Skrifter, Series A, Copenhagen, Danmark, 1937, 159 p.
- 11. Turnbull, J. McN. Shearing resistance of soils. In: Proceedings of the 1st Australia-New Zealand Conference on Soil Mechanics and Foundation Engineering, Melbourne, Australia, June 1952; University of Melbourne, 1952, pp. 48-81.
- 12. Skempton, A.W. Long-term Stability of Clay Slopes. In: IV Rankine Lecture, Geotechnique, 1964, 14, pp. 75-102.
- 13. Maslov, N.N. Physical and technical theory of creep of clay soils in construction practice. Stroyizdat, Moscow, 1984, 176 p. [in Russian].
- 14. Goldstein, M.N.; Ter-Stepanyan, G.I. Long-term strength of clays and deep creep of slopes. In: Materials for the IV International Congress on Soil Mechanics and Foundation Engineering, Moscow, USSR, 1957, pp. 43-52 [in Russian].
- 15. Goldstein, M.N.; Babitskaya, S.S. Methodology for determining the long-term strength of soils. Osnovania, fundamenty i mekhanika gruntov, 1959, 4, pp. 11-14. [in Russian].

- 16. Goldstein, M.N.; Babitskaya, S.S. Calculation of slope stability taking into account creeping shear. Voprosy geotehniki 1964, 7, pp. 85-95 [in Russian].
- 17. Marinescu, C. Ensuring the stability of embankments and slopes. Modern concepts and solutions. Tehnică, Bucuresti, Romania, 1988, vol. 1, 355 p. [in Romanian].
- 18. Christensen, R.W.; Kim, J.S. Rheological model studies in clay. Clays and Clay Minerals 1969, 17 (2), pp. 83-93.
- 19. Cristescu, S.L.; Ştefănică, M.; Marin, M. Rheology of soils. Politehnica, Timișoara, Romania, 2015, 546 p. [in Romanian].
- 20. Hu, H. Rheological model and rheological equation of sullage soft soil under dynamic loading. Rock Soil Mech. 2007, 28(2), pp. 237-240.
- 21. Goldstein, M.N.; Turovskaya, A.I.; Chernenko, N.B. On the long-term strength of the clay soil in the strata of landslide slopes. Osnovania, fundamenty i mekhanika gruntov, 1978, 5, pp. 16-19. [in Russian].
- 22. Timofeyeva, T.A.; Polcanov, V.N. On the long-term stability of natural and cutting slopes in Moldova. In: Proceedings of the seventh International Symposium on Landslides, Trondheim, Norway, 17-21 June 1996, pp. 1387-1390.
- 23. Cîrlan, A. Investigation of the rheological properties of soils for the assessment the base stress-strain state. Ph. D. Thesis, Technical University of Moldova, Chisinau, 2019 [in Romanian].

Citation: Polcanov, V.; Polcanova, A.; Cîrlan, A. Ensuring the long-term stability of deep cutting slopes formed by clay soils on Republic of Moldova roads. *Journal of Engineering Science* 2024, XXXI (3), pp. 85-95. https://doi.org/10.52326/jes.utm.2024.31(3).08.

Publisher's Note: JES stays neutral with regard to jurisdictional claims in published maps and institutional affiliations.



Copyright:© 2024 by the authors. Submitted for possible open access publication under the terms and conditions of the Creative Commons Attribution (CC BY) license (https://creativecommons.org/licenses/by/4.0/).

Submission of manuscripts:

jes@meridian.utm.md

https://doi.org/10.52326/jes.utm.2024.31(3).09 UDC 66.021.2.081.3:546.766:628





EVALUATING THE ADSORPTION POTENTIAL OF SUGARCANE BAGASSE AND LEMONGRASS FOR CHROMIUM (VI) REMOVAL IN WASTEWATER TREATMENT

Aminu S. Dangamba ^{1,2}, ORCID: 0009-0001-7709-1524, Toyese Oyegoke ^{1,2*}, ORCID: 0000-0002-2026-6864, Favour E. Ocheje^{1,2}, ORCID: 0009-0004-5831-857X, Mahmud A. Dikko ¹, ORCID: 0009-0007-0827-5032, Mohammed S. Galadima ¹, ORCID: 0009-0000-1144-9549

¹ Chemical Engineering Department, Ahmadu Bello University Zaria, Nigeria.

² Green Science Promoters' Forum of Pencil Team, Ahmadu Bello University Zaria, Nigeria.

* Corresponding author: Toyese Oyegoke, *OyegokeToyese@qmail.com*

Received: 08. 15. 2024 Accepted: 09. 24. 2024

Abstract. The increasing levels of chromium (VI) ions in textile wastewater pose significant environmental challenges, necessitating effective treatment methods. This study evaluates the biosorption potential of sugarcane bagasse (SCB) and lemongrass (LM), both individually and in blend form, for the removal of chromium (VI) ions. Batch adsorption experiments were conducted to assess the impact of contact time and adsorbent dosage on removal efficiency. BET analysis revealed that the blend had the highest surface area (1047.885 m²/g), enhancing its adsorption capacity, while FTIR spectroscopy identified key functional groups such as hydroxyl and carbonyl that facilitate metal binding. Results indicated that the blend exhibited superior adsorption capacity, with kinetic studies showing that the adsorption process followed a Pseudo-second order model, suggesting chemisorption as the dominant mechanism. Isotherm analyses indicated that the Langmuir model best-described adsorption on SCB, while the Freundlich model was more suitable for LM and the blend. This research recommends the practical application of SCB and LM in wastewater treatment and encourages further investigation into their potential for removing other heavy metals, highlighting a sustainable approach to environmental remediation.

Keywords: Chromium, Biosorption, Sugarcane, Bagasse, Lemongrass, Wastewater, Adsorption.

Rezumat. Nivelurile crescânde de ioni de crom (VI) în apele uzate din industria textilă reprezintă provocări semnificative de mediu, necesitând metode eficiente de tratare. Acest studiu evaluează potențialul de biosorbție al borhotului de trestie de zahăr (SCB) și lemongrass (LM), atât individual, cât și sub formă de amestec, pentru îndepărtarea ionilor de crom (VI). A fost efectuată adsorbția în loturi pentru a evalua impactul timpului de contact și al dozei de adsorbant asupra eficienței de îndepărtare. Analiza BET a arătat că amestecul a avut cea mai mare suprafață (1047,885 m²/g), sporind capacitatea sa de adsorbție, în timp ce spectroscopia FTIR a identificat grupuri funcționale cheie, cum ar fi hidroxil și carbonil, care facilitează legarea metalelor. Rezultatele au indicat că amestecul a prezentat o capacitate de

adsorbție superioară, studiile cinetice arătând că procesul de adsorbție a urmat un model de ordinul pseudo-doi, sugerând chimisorbția ca mecanism dominant. Analiza izotermelor a indicat că modelul Langmuir a descris cel mai bine adsorbția pe SCB, în timp ce modelul Freundlich a fost mai potrivit pentru LM și amestec. Această cercetare recomandă aplicarea practică a SCB și LM în tratarea apelor uzate și încurajează investigarea ulterioară a potențialului lor de îndepărtare a altor metale grele, evidențiind o abordare durabilă a remedierii mediului.

Cuvinte cheie: crom, biosorbție, trestie de zahăr, borhot, lemongrass, ape uzate, adsorbție.

1. Introduction

Water pollution has become one of the most critical environmental challenges, largely due to the discharge of toxic and hazardous chemicals from industrial activities [1]. As industrial development accelerates, substantial amounts of wastewater and domestic sewage containing metal ions are released into water bodies worldwide, significantly contributing to water pollution [2]. Metals released from industries such as tanning, sewage treatment, refining, pharmaceuticals, and textiles accumulate in soil ecosystems, adversely affecting the diversity, density, and physiological functioning of soil microbes [3]. Among numerous heavy metal pollutants, cadmium (Cd), lead (Pb), mercury (Hg), arsenic (As), and chromium (Cr) have been identified as top priorities due to their high toxicity and significant implications for public health [4]. Notably, chromium exists primarily in two forms: trivalent Cr (III) and hexavalent Cr (VI). The relationship between these forms is significantly influenced by environmental pH and oxidative characteristics. Public concern centers particularly on Cr (VI) ions, which is 100 times more hazardous than Cr (III) ions and poses serious health risks due to its carcinogenic, mutagenic, and teratogenic properties. The U.S. Environmental Protection Agency (EPA) has established a limit of 0.05 mg/L for Cr (VI) in drinking water, while the maximum allowable concentration in industrial wastewater is set at 0.1 mg/L [5].

To protect environmental and public health, it is essential to eliminate heavy metals, commonly used in various industries, from water and wastewater through effective treatment techniques. Several control technologies have been developed to treat metal-contaminated water, including chemical precipitation, ion exchange, membrane filtration, coagulation-flocculation, and solvent extraction. However, these methods face challenges such as high operational costs, significant energy requirements, low efficiency, and the generation of large quantities of toxic sludge [6]. Consequently, there is an urgent need for more viable and sustainable approaches to remove heavy metals from wastewater.

Among these methods, biosorption has gained attention as a promising alternative due to its advantages, including the regeneration of biosorbents, potential for metal recovery, minimization of toxic sludge, high removal efficiency, and low operational costs. Biosorption is a physiochemical process that occurs naturally in certain biomass, allowing these materials to passively concentrate and bind pollutants onto their cellular structures. While the application of biomass in environmental cleanup has been established for some time, researchers and engineers aim to harness this phenomenon as an economical solution for removing toxic heavy metals from industrial wastewater [7]. Recent studies have investigated various biomass-based adsorbents, including cyanobacterial biomass [8], *Streptomyces rimosus* [9], peanut husk [10], eucalyptus bark [11], sugarcane bagasse (SCB), and orange peel composites [12], as well as *Eucalyptus tereticornis* composites [13] for effectively removing heavy metals from wastewater.

Sugarcane, SCB (*Saccharum officinarum*) is a lignocellulosic tropical plant extensively cultivated in regions such as Brazil, India, China, Mexico, and South Africa, making it a vital component of the global sugar industry [14]. Following sugar extraction through chewing or refining, large quantities of bagasse are produced, which is often incinerated for energy generation. Sugarcane bagasse consists of approximately 46% cellulose, 24.5% hemicellulose, and 19.95% lignin [15]. The biosorbents derived from SCB contain various functional groups, including –COOH, -OH, -NH2, -OCH3, and –SH, facilitating the attraction and binding of pollutants through chelation, complexation, coordination, and hydrogen bonding [16].

Lemongrass (LM), scientifically known as *Cymbopogon citratus*, is a perennial grass that can grow up to 1.5 meters tall, with multiple stiff stems arising from rhizomatous rootstock. Commonly used in local cuisine and in the manufacture of soap and candles due to its citrus scent, lemongrass belongs to the Cymbopogon section of the *Andropogoneae* in the family *Poaceae*. It contains various compounds, including terpenes, flavonoids, and alkaloids, depending on its habitat. The oil extracted from lemongrass has been utilized to treat various ailments, including coughs, colds, rheumatism, digestive issues, bladder problems, and as a mouthwash for toothaches and sore gums [17]. Additionally, lemongrass (LM) serves as a biosorbent due to its functional groups, such as carbonyl, carboxyl, and hydroxyl, which facilitate the removal of hazardous pollutants [18].

Given their unique chemical compositions and availability, SCB and LM were selected as representative biosorbents for this study. To the best of the author's knowledge, no data have been published on the removal of Cr (VI) ions using SCB and LM individually or in combination. The primary aim of this study is to evaluate the performance of SCB, LM, and their blend in removing Cr (VI) ions from textile wastewater. The effects of contact time and adsorbent dosage on adsorption capacity will be determined using batch systems, and the optimal conditions for Cr (VI) ions removal will be assessed through Response Surface Methodology (Central Composite Design) utilizing Design Expert version 13. The biosorption data will be analyzed and reported using various equilibrium isotherm and kinetic models.

2. Materials and methods

2.1. Materials and Chemicals

In this study, all materials and chemicals were of commercial and analytical grade purity, purchased from BDH Chemicals Ltd. (Poole, England), and were used without further purification. Aquatron A4000 distilled water was utilized for standardization and preparation of all samples to mitigate potential interference from other ions and impurities. The equipment employed included a magnetic stirrer, beakers, filter paper, and sample bottles.

2.2. Collection of Wastewater

This research focused on two natural and renewable lignocellulosic fibers. Sugarcane bagasse was collected from a sugarcane juice vendor on the Ahmadu Bello University campus in Zaria, while lemongrass was harvested in Funtua Town, Katsina State, Nigeria. Both biomasses were identified at the Herbarium section of the Biological Science Department at Ahmadu Bello University, Zaria, Kaduna, Nigeria. The sugarcane bagasse (SCB) and lemongrass (LM) were meticulously washed with tap water followed by distilled water to eliminate adhering dirt and other particulate matter. The cleaned biomasses were dried at room temperature and then in an oven at 65°C until a consistent weight was achieved. The

dried biomass was finely crushed into a powder and sieved to a particle size of \leq 1.44 mm. The fine powder was immersed in 0.1 M NaOH for 24 hours to remove impurities, increase the surface area of the biosorbent, and activate more functional groups. After 24 hours, the biosorbents were thoroughly rinsed with distilled water until a neutral pH was obtained. The NaOH-treated biomass was further dried in an oven at 45°C for 6 hours and stored in sealed polythene bags for subsequent use.

2.3. Collection and Preparation of Biosorbent

Samples were collected from wastewater discharges originating from the textile industry using a ten-liter plastic jerry can. Collection occurred between 9 AM and 1 PM, representing peak flow periods due to high production levels. The samples were transported to the laboratory for heavy metal and biosorption studies, with pH and temperature measured at the point of collection.

2.4. Characterization of Biosorbents

The surface area, pore size distribution, and pore volume were measured using the Brunauer-Emmett-Teller (BET) analysis method, based on nitrogen adsorption-desorption at liquid nitrogen temperature, conducted with Quantachrome NovaWin version 11.3. The surface morphology of both loaded and unloaded SCB, LM, and their composites was examined before and after Cr (VI) uptake using Scanning Electron Microscopy (SEM, Thermo Scientific Quanta 650). The existing chemical functional groups involved in the biosorption of Cr (VI) onto SCB, LM, and their blend were detected by Fourier Transform Infrared (FTIR) spectroscopy (240FS, Agilent) before and after uptake, with samples analyzed in the range of 4000-500 cm⁻¹ at room temperature.

2.5. Batch Sorption Experiment

2.5.1. Optimization Conditions for Biosorption

The optimum conditions for the biosorption of Cr (VI) ions onto SCB, LM, and their blend were determined using Central Composite Design (CCD). CCD is commonly employed under Response Surface Methodology (RSM) due to its suitability for fitting quadratic surfaces. It involves a combination of factorial points, center points, and axial points, which are effective for process optimization. Optimization studies investigated the effects of experimental factors, such as contact time and adsorbent dosage, on the adsorption capacity of Cr (VI) ions using SCB, LM, and their blend. The effect of contact time was explored within the range of 20-120 min, while the effect of adsorbent dosage was studied within the range of 0.1-0.9 g.

2.5.2. Biosorption Experiment

Batch experiments were carried out in 50 mL beakers. A specific amount of SCB, LM, and their blend, according to the design formulation of CCD, was added to 25 mL of the Cr (VI) wastewater solution. The resulting solutions were stirred vigorously with a magnetic stirrer at 150 rpm for a predetermined period until equilibrium was reached. After equilibrium was achieved, the biomasses were separated from the solutions using Whatman filter paper, and the concentration of the supernatant was determined using Atomic Absorption Spectrometry (AAS). The quantity of metals adsorbed was calculated using Equation 1:

$$q_e = \frac{c_0 - c_f}{m} V \tag{1}$$

where: q_e is the adsorption capacity (mg/g), C_o and C_e are the initial and equilibrium concentration (mg/L) of metal ions, respectively. V and m represent the solution volume and mass (q) of the adsorbent respectively.

2.6. Equilibrium Adsorption Isotherm Models

Adsorption isotherms describe the equilibrium relationship between the quantity of sorbate (metal ions) sorbed by the biosorbent and the concentration in the equilibrium solution at constant temperature [4]. They provide valuable information regarding the mechanism and nature of the adsorption process and facilitate the evaluation of the feasibility of the adsorption process for a given application. In this work, commonly used isotherm models, including Langmuir, Freundlich, and Temkin, were employed to interpret Cr (VI) ions sorption and understand the mechanism of biosorption on SCB, LM, and their blend. The experimental data were fitted into these equilibrium isotherm models.

2.6.1. Langmuir Isotherm Model

The Langmuir isotherm model is based on the assumption that sorption occurs over energetically homogeneous sites of the biosorbent, resulting in a monolayer coverage. The non-linear form of the Langmuir equation is given in Equation 2:

$$q_e = \frac{q_m b C_e}{1 + b C_e} \tag{2}$$

where: C_e is the equilibrium concentration of metal ion (mg/L); q_e is the amount of metal ion adsorbed per unit weight of adsorbent material at equilibrium (mg/g); b is the Langmuir constant (L/mg) which represents the adsorbate's degree of adsorption affinity, and q_m is the maximum adsorption capacity (mg/g) associated with full monolayer cover. The Langmuir isotherm is characterized by essential properties that can be related in terms of a dimensionless separation factor R_L . This factor allows the prediction of the form of adsorption isotherm, providing insights into whether the sorption process is favorable or not. Specifically, the process is considered unfavorable when $R_L > 1$, linear when $R_L = 1$, favorable in the interval $0 < R_L < 1$ and irreversible when $R_L = 0$ [19]. The separation factor R_L can be calculated using equation 3.

$$R_L = \frac{1}{1 + bC_0} \tag{3}$$

where: C₀ is the initial metal concentration (mg/L) and b is the Langmuir constant.

2.6.2. Freundlich Isotherm Model

The Freundlich isotherm model assumes an exponential decrease in the biosorption energy with increasing surface coverage. It is applicable to heterogeneous surfaces with negligible interactions between sorbed molecules. The model is expressed in Equation 4:

$$q_e = K_f C_e^{1/n}(4)$$

where: C_e is the equilibrium concentration (mg/L); q_e is the amount of metal ion adsorbed per unit weight (mg/g); K_f and n are Freundlich constants indicating the sorption capacity. The favorability of the Freundlich model was determined by n. Values of n in the range of 1-10 indicate favorable adsorption, while n<1 indicates unfavorable adsorption and the parameter 1/n is an empirical factor that relates to the biosorption intensity [20].

2.6.3. Temkin Isotherm Model

The Temkin isotherm model assumes a uniform distribution of binding energies over a number of adsorption sites [21]. The non-linear form of the Temkin is represented in Equation 5:

$$q_e = \frac{RT}{h_T} In(K_T C_e) \tag{5}$$

where: $B = \frac{RT}{b_T}$ with the universal gas constant, R = 8.314 J/mol.K, and T as the absolute temperature in Kelvin; b_T is the Temkin isotherm constant; q_e (mg/g) is the amount of metal ions absorbed onto the adsorbent at equilibrium. The Temkin parameters A and B are the equilibrium binding energy and constant heat of sorption respectively.

2.7. Adsorption Kinetic Models

Analyzing kinetic models in biosorption studies is critical for understanding the reaction pathways, mechanisms, and process dynamics. It aids in determining the physiochemical interactions, mass transport, and rate-determining phases in the biosorption process. Additionally, understanding the kinetics of metal sorption is essential for optimizing sorption processes, reactor dimensions, and residence times [6]. Therefore, to evaluate the rate and mechanism of metal biosorption, the experimental kinetic data were analyzed using various reaction rate and diffusion models, including the Pseudo-first-order, Pseudo-second-order, and Elovich kinetic models.

2.7.1. Pseudo-First-Order Kinetic Model

The Pseudo-first-order (PFO) kinetic model, proposed by Lagergren (1898), is based on the assumption that the sorption rate is proportional to the number of free available sites (Lee et al., 2014). It is typically employed to analyze kinetic behavior at the initial stages of the biosorption process, and its non-linear form is expressed in Equation 6:

$$q_t = q_e (1 - e^{-k_1 t}) (6)$$

where: k_1 is the PFO rate constant (min $^{-1}$); q_t and q_e are the amount of metal ion sorbed at time t and at equilibrium (mg/g), respectively.

2.7.2. Pseudo-Second-Order Kinetics

The Pseudo-second-order (PSO) model assumes that chemical reactions occur between the metal ions and the biosorbent, resulting in the formation of strong covalent bonds [14]. The non-linear PSO kinetic model is mathematically represented by Equation 7:

$$q_t = \frac{k_2 q_e^2 t}{1 + k_2 q_e} \tag{7}$$

where: k_2 is the PSO rate constant in g/(mg/min), qt and q_e are the amount of metal ion adsorbed at time (t), and at equilibrium in mg/g, respectively.

2.7.3. Elovich Kinetic Model

The Elovich kinetic model, which considers the surface as energetically heterogeneous, is frequently employed to interpret adsorption kinetics. It effectively describes second-order kinetics and was originally developed to explain the kinetics of gas chemisorption on solids [22]. The Elovich kinetic model can be expressed in Equation 8:

$$q_t = \frac{1}{h}\ln(ab) + \frac{1}{h}\ln(t) \tag{8}$$

where: a is the initial adsorption rate in $mg/(g \cdot min)$ and b is the constant.

2.8. Statistical Analysis

In general, the data were fitted into the respective models to obtain corresponding slopes and intercepts from the plot of q_t versus ln(t), by non-linear regression method using R-square values to ascertain to the suitability of the model to fit the adsorption experiment data.

3. Results and discussions

3.1. Characterization of the Biosorbent

3.1.1. Analysis of Brunauer-Emmet-Teller (BET)

The quality of biosorbents is strongly indicated by a high surface area as it correlates directly with the adsorption capacity. The Brunauer-Emmett-Teller (BET) technique was employed to quantify the surface area, pore diameter, and pore volume [23]. The average values for BET surface area, total pore volume, and pore size for SCB, LM and their blend are provided in Table 1. For SCB, the surface area, pore volume, and pore size were determined to be 501.999 m²/g, 0.253 cm³/g and 2.10 nm, respectively. These values were discovered to be considerably higher reported by [24] and [25], with the exception of the pore size, which closely aligned with the findings of [25]. LM exhibited a specific surface area of 811.761 m²/g, a pore volume of 0.406 cm³/g and a pore size of 2.125 nm. These values were in accordance with the findings of [26]. Comparatively, the blend of SCB and LM demonstrated a higher surface area and pore volume, measuring 1047.885 m²/g and 0.544 cm³/g, respectively. This implies that the composite may possess enhanced metal adsorption capabilities and increased metal uptake, attributed to its larger surface area [12].

Biosorbent surface area, pore volume, pore diameter

Biosorbent	BET Surface area (m²/g)	Pore volume (cm³/g)	Pore size (nm)		
Sugarcane bagasse	501.999	0.253	2.100		
Lemongrass	811.761	0.406	2.125		
Blend	1067.885	0.544	2.105		

3.1.2. Analysis of the Fourier Transform Infrared (FTIR) Spectra

The FTIR spectra of SCB, LM and their blend before and after Cr (VI) uptake were studied to qualitatively determine the major functional groups on the surface of the adsorbent. The spectral analysis covered a wavelength range from 4000 to 500 cm⁻¹ as shown in Figures 1 and 2 for SCB, LM and their blend respectively. The infrared (IR) spectrum obtained from FTIR of SCB displayed a number of different absorption peaks. Distinct peaks were identified in the FTIR spectra of SCB, specifically at 3292, 2906, 1603, 1379, 1259, 1036, and 916 cm⁻¹. The peak at 3292 cm⁻¹ corresponds to the O-H stretching of hydroxyl groups in Cellulose I, as reported by [27]. The presence of peak at 2906 cm⁻¹ indicates C-H stretching of alkane groups, while the increased intensity at 1603 cm⁻¹, associated with C=O stretching, suggests the uptake of Cr (VI) metals, potential pollutants in wastewater [14]. The peak at 1512 cm⁻¹ is linked to the C=C carboxylic groups of aromatic rings, and the range from 2311 to 1841 cm⁻¹ indicates C≡C stretching vibrations of lignin aromatic rings [12]. The intense 1036 cm⁻¹ peak represents C-O stretching vibration of cellulose, lignin, and hemicellulose [27]. According to the study, these major functional groups, which include hydroxyl, carbonyl, and aromatic rings, play an important role in Cr (VI) sorption. They are actively involved in binding interactions with metal ions, and the spectral changes imply the creation of metal

Table 1

complexes. Complexation interactions are seen as the primary driving factor underlying the sorption mechanism, as supported by [14, 27, 28].

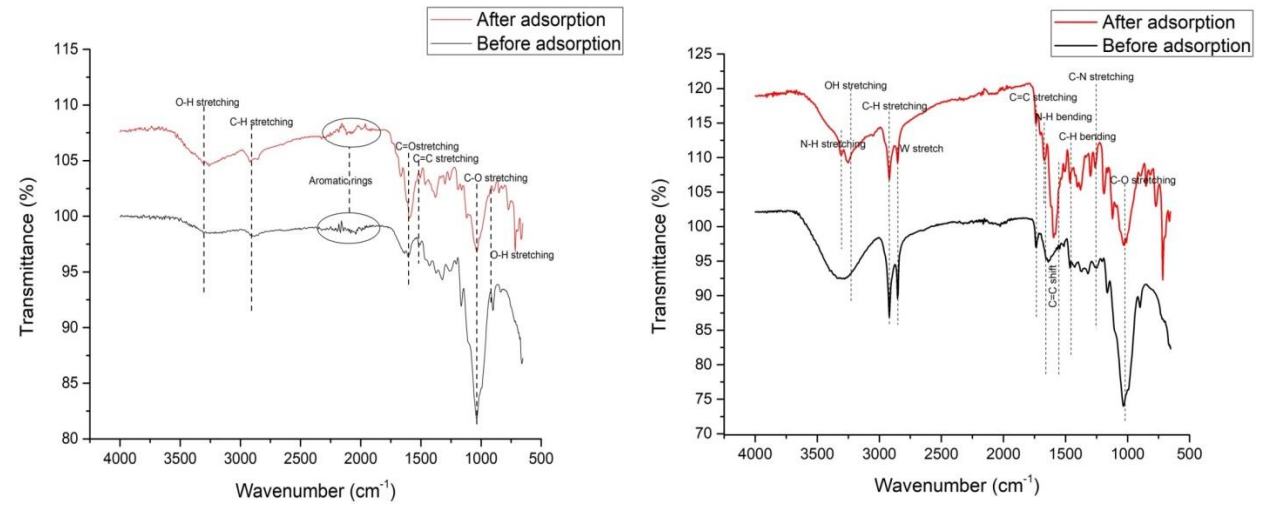


Figure 5. FTIR spectra obtained before and after adsorption of Cr (VI) using sugarcane bagasse (left) and lemongrass (right).

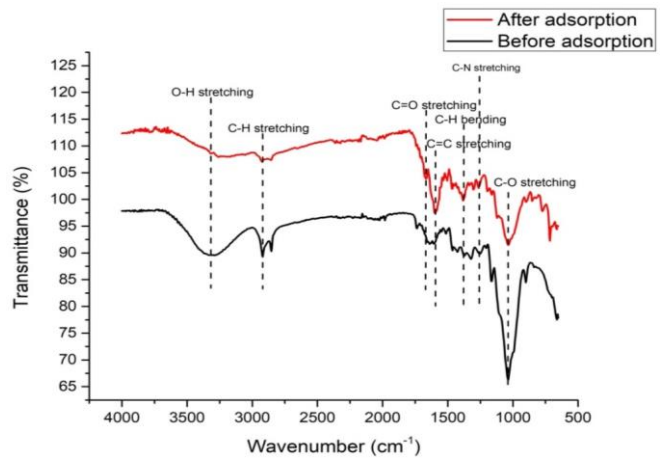


Figure 6. FTIR spectra of a blend derived from SCB and LM before and after adsorption of Cr (VI) ions.

3.1.3. Analysis of the Scanning Electron Microscopy (SEM) Images

Scanning electron microscopy (SEM) analysis was conducted on SCB, LM and their blend before and after the sorption of Cr (VI) ions to examine the resulting changes in the surface morphology. The observed changes are shown in Figures 3, 4 and 5 for SCB, LM and their blend, respectively. The figures illustrate the surface texture and porosity which include wide openings and large pores both before and after Cr (VI) ions uptake. The uneven surfaces are attributed to the presence of parallel grooves and cracks, and granules with irregularly shaped cavities and voids. The rough and porous surface before sorption may offer possible sorption sites for the uptake of Cr (VI) ions [29]. The analysis of surface morphology indicates that SCB exhibits larger pore sizes before Cr (VI) uptake (Figure 3 (LHS)) compared to SCB after Cr (VI) ions uptake, where fewer pores are observed (Figure 3 (RHS)). This reduction in pore size may be because the pores have been filled due to the uptake of Cr (VI) ions by the SCB [14]. The surface morphology of LM after Cr (VI) ions uptake, as shown in Figure 4 (RHS), reveals significant changes, transforming coarse particle sizes into finer ones, when compared to the rough and uneven surface before Cr (VI) ions uptake in Figure 4 (LHS). These

changes could be as a result of the deposition of Cr (VI) ions onto the surface of LM. Similar observation was reported in the work of [15]. The micrographs surface of the blend material in Figure 5 (LHS) exhibited larger pores, rough and uneven surface because of a hydrolysis reaction occurring on the surface of the blend material [15]. In Figure 5 (RHS), the surface became smoother with less porosity, which is likely attributed to the entrapment of Cr (VI) ions on the surface of the blend material [30].

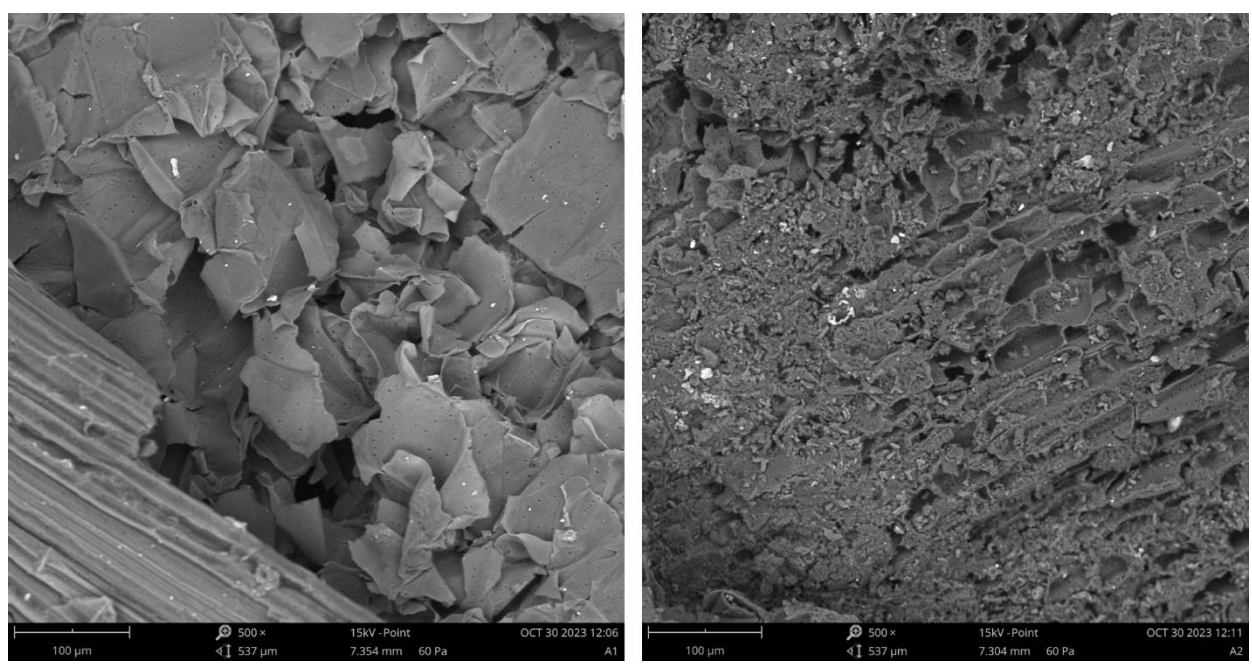


Figure 3. SEM micrographs of sugarcane bagasse before (left) and after (right) Cr (VI) uptake.

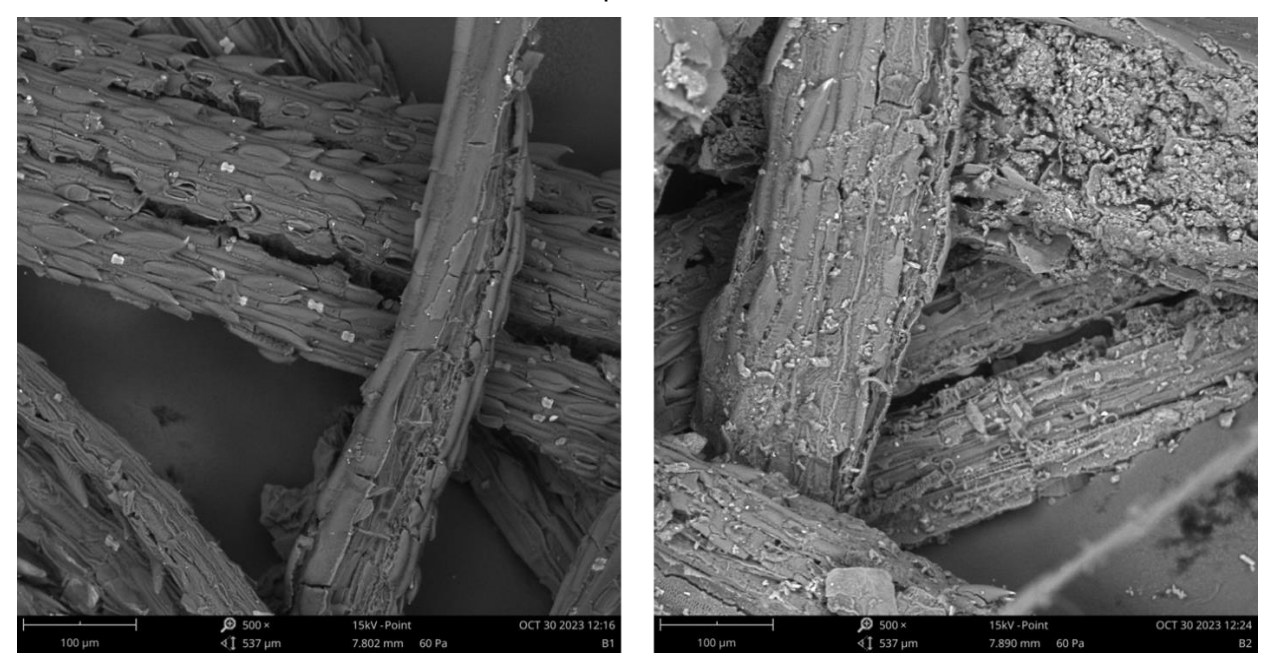


Figure 4. SEM micrographs of lemongrass before (left) and after (right) Cr (VI) uptake.

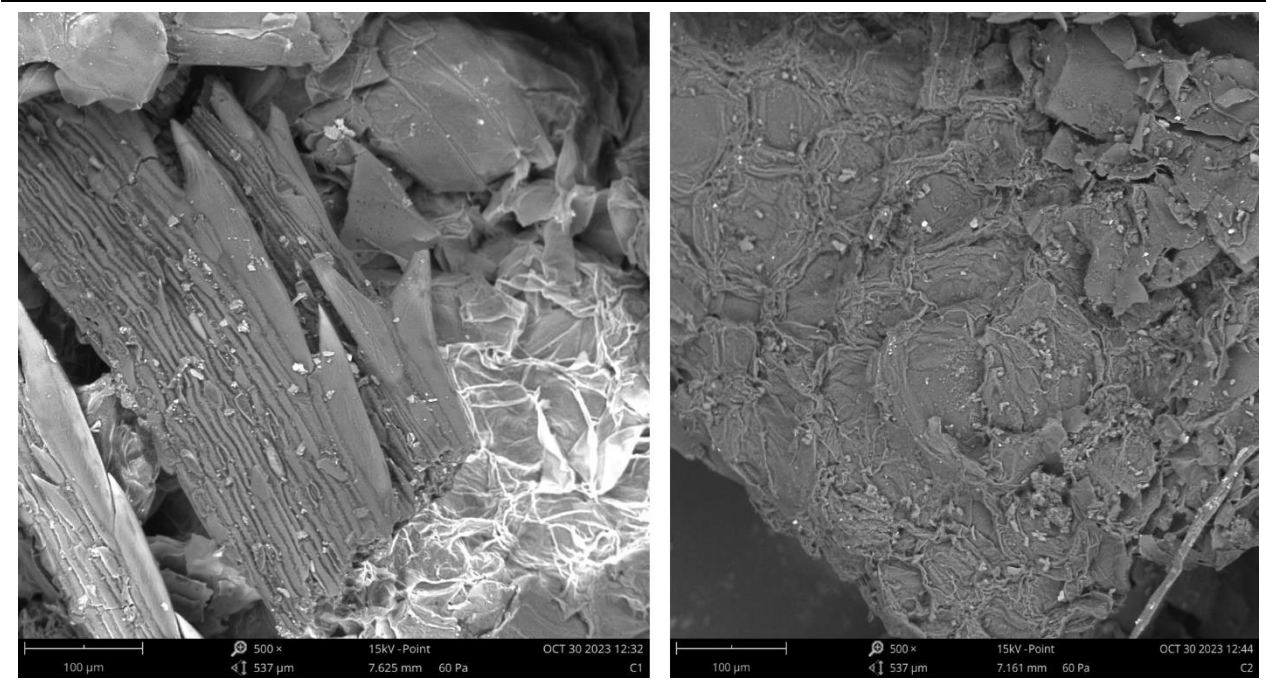


Figure 5. SEM micrographs of a composite derived from SCB and LM before (left) and after (right) Cr (VI) uptake.

3.2. Optimization studies of the metal removal

3.2.1. Fitting process model statistical analysis

The optimum level of process parameters, such as contact time and adsorbent dosage were obtained with the CCD experimental design. The interactive effect of contact time and adsorbent dosage on the adsorption capacity was subsequently studied. Statistical software, specifically design expert version 13.5, was used for the regression analysis of the data to evaluate the statistical significance of the quadratic model. The analysis of variance ANOVA for the response surface model of Cr (VI) ions adsorption on SCB, LM and their blend are presented in Table 2. The analysis of variance (ANOVA) results from Table 2 indicates that the analyzed variables fall within an acceptable range. ANOVA was used to verify the quadratic models, revealing the ability to predict Cr (VI) ions uptake. The equations of the models, generated after interpreting the experimental data for the biosorption Cr (VI) ions by SCB, LM and the blend are presented in Equations 9, 10 and 11, respectively.

 $qCr = 0.408865 + 0.003639A + 0.058496B + 0.000778AB - 0.000022A^2 - 0.042756B^2(9)$

$$qCr = 1.63198 - 0.007455A - 0.410243B - 0.001238AB + 0.000042A^2 + 0.362925B^2$$
 (10)

$$qCr = 0.369950 + 0.010817A + 2.31205B + 0.001132AB - 0.000059A^2 - 2.08442B^2$$
 (11)

where: qPb and qCr are the predicted adsorption capacities for Pb (II) and Cr (VI) ions respectively, the actual values of the test variables, contact time and adsorbent dosage are represented by A and B respectively. The coefficient involving two factors, namely (AB) and $(A^2 \text{ and } B^2)$ signifies the interaction between these two parameters and the quadratic effect. The negative sign in front of the term indicates an antagonistic effect, whereas the positive sign indicates a synergistic effect [31]. The correlation coefficient (R^2) was used to evaluate the model fitness. The closer the R^2 is to 1, the stronger the model and the better it predicts the response [25]. The P and F values indicate the significance of the regression coefficients and the overall significance of the model. The model term is considered significant if the P value is < 0.05 [32]. The results presented in Table 2 showed that the regression was

statistically significant for the adsorption of Cr (VI) ions using SCB, with an F value of 707.49 and prob > F (<0.0001).

Table 2
Summary of the ANOVA results for the adsorption of Cr (VI) ions using SCB, LM and their blend as an adsorbent

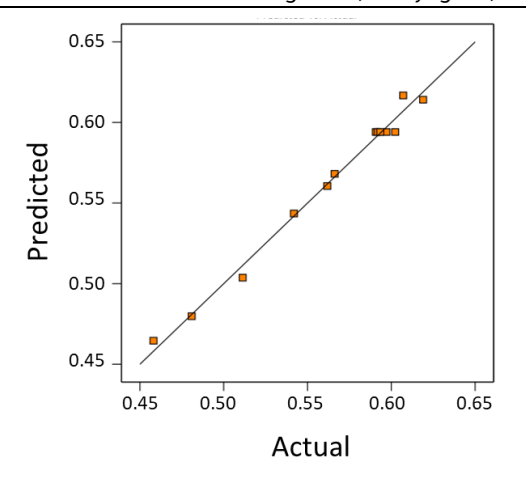
Parameters	Sugarcane bagasse	Lemongrass	Composite
Model	<0.0001	<0.0001	<0.0001
Standard deviation	0.0067	0.0101	0.0209
Mean	0.5632	1.25	1.28
Coefficient of variance	1.2000	0.8139	1.63
R^2	0.9898	0.9955	0.9959
Adjusted R ²	0.9825	0.9923	0.9930
Predicted R ²	0.9402	0.9783	0.9791
Adequate precision	33.2072	48.7025	51.7078
Lack of fit	0.1277	0.3357	0.2903

In equation 9, the correlation coefficient R^2 (0.9898) value for the adsorption of Cr (VI) using SCB, was found to be close to 1 and in reasonable agreement with the adjusted correlation coefficient (Adjusted R^2 =0.9825), indicating high model significance. While the predicted R^2 (0.9402) is not as high, but the model remains significant.

The term adequate precision (AP) ratio corresponds to the target's response variable under varying noise conditions. An AP value greater than 4 is desirable. The reproducibility of the model is indicated by the coefficient of variance (CV). It is calculated as the ratio of the stand error of the estimate to the mean value of the response. The model is deemed reproducible if the value is less than 10% [31]. The model F-value for the adsorption of Cr (VI) ions was found to be 310.19, implying that the model is significant. Additionally, Prob > F values less than 0.05 indicate that the model terms are significant at 95% confidence level. The R² value of Cr (VI) ions was found to be 0.9955, which is close to unity, is desirable and in reasonable agreement with the adjusted R2 value of 0.9923 for Cr (VI) ions. The term "adequate precision" (AP) ratio refers to the response variable concerning the target under varying noise conditions. The adequate precision (AP) obtained for the adsorption of Cr (VI) ions using LM was found to be 48.7025. An AP value higher than 4 is desirable [31]. The results also from Table 2, for the adsorption of Cr (VI) ions using the blend of SCB and LM indicate that the regression is statistically significant, with an F value of 343.43 for Cr (VI) ions, and a prob > F value less than 0.0001. The term is considered significant if the P value < 0.05. The R² value of Cr (VI) ions was found to be 0.9959, indicating that the values are desirable and are close to unity.

The value of R^2 for Cr (VI) ions (0.9959), and the predicted R^2 of 0.9197 for Cr (VI) ions adsorption are also in good agreement with the adjusted R^2 0.9930. The response variable in respect to the goal under changing noise levels is referred to as the "adequate precision" (AP) ratio.

The adequate precision (AP) for Cr (VI) ion adsorption using a blend from SCB and LM was 51.7078. An AP value greater than 4 is considered desirable [31]. According to the summary of ANOVA results presented in Table 2, the independent variable (contact time and adsorbent dosage) are significant terms for the adsorption of Cr (VI) ions from textile wastewater using SCB, LM and a blend derived from SCB and LM.



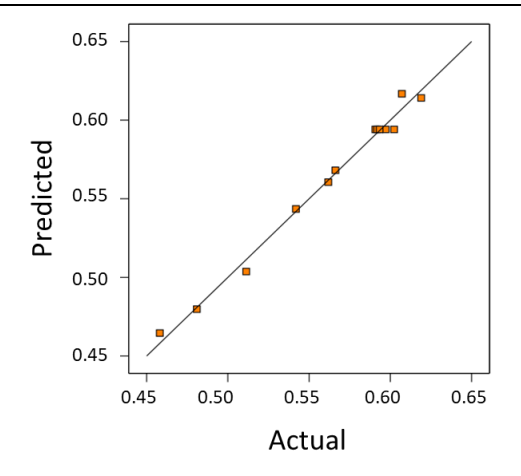


Figure 6. A parity plot showing the actual and predicted values for the adsorption of Cr (VI) ions using SCB as adsorbent.

Figure 7. A parity plot showing the actual and predicted values for the adsorption of Cr (VI) ions using LM as adsorbent.

To show the correlation between actual and predicted values, a parity plot is employed to show the relationship for the adsorption of Cr (VI) ions using SCB, LM, and the blend derived from SCB and LM in Figures 6, 7, and 8, respectively. For a model to be reliable, it should accurately predict the response when compared with the experimental data. As shown, there is a significant correlation between the actual and predicted values, suggesting that the generated models successfully capture the relationship between the adsorption variables (contact time and adsorbent dosage) and the metal uptake rate.

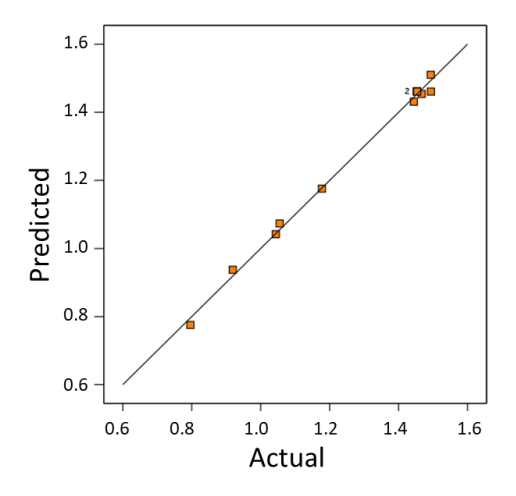


Figure 8. A parity plot showing the actual and predicted values for the adsorption of Cr (VI) ions using a blend derived from SCB and LM as an adsorbent.

The parity plots of SCB, LM, and their blend reveal that the data points cluster around the diagonal line, implying a satisfactory agreement between the predicted and the actual values. This suggests that the models generated successfully capture the relationship between the independent adsorption variables (contact time and adsorbent dosage) and the adsorption capacity. The model for SCB exhibits a high correlation coefficient (R²) of 0.9898 for Cr (VI) ions adsorption, indicating the suitability and accuracy of the models in predicting the adsorption capacity under variable conditions of contact time and adsorbent dosage. The model equation for Cr (VI) ions is statistically significant, as the Prob. >F values are less than 0.05, and the R² value is 0.9898. Similarly, the high correlation coefficient R² for LM in the adsorption of Cr (VI) ions indicates the suitability and accuracy of the model, being close to

unity. The closer the R² value is to unity, the stronger and better the model predicts the response. Moreover, the high correlation coefficient R² of 0.9959 for the adsorption of Cr (VI) ions using the blend further indicates a well-fitted model that can predict the adsorption capacity with reasonable certainty under independent variables such as contact and adsorbent dosage. In conclusion, the parity plots exhibit a satisfactory correlation between the actual and the predicted values for SCB, LM, and the blend derived from SCB and LM.

3.2.2. Effect of Model Variables and Their Interactions

The three-dimensional response surface plots are essential for determining the optimum values of the variables and illustrating the interaction between contact time (A) and adsorbent dosage (B) on the adsorption capacity (q, mg/g) of biosorbent during the adsorption of Cr (VI) ions from textile wastewater using SCB, LM and a blend derived from SCB and LM at room temperature, as presented in Figure 9 and Figure 10, respectively.

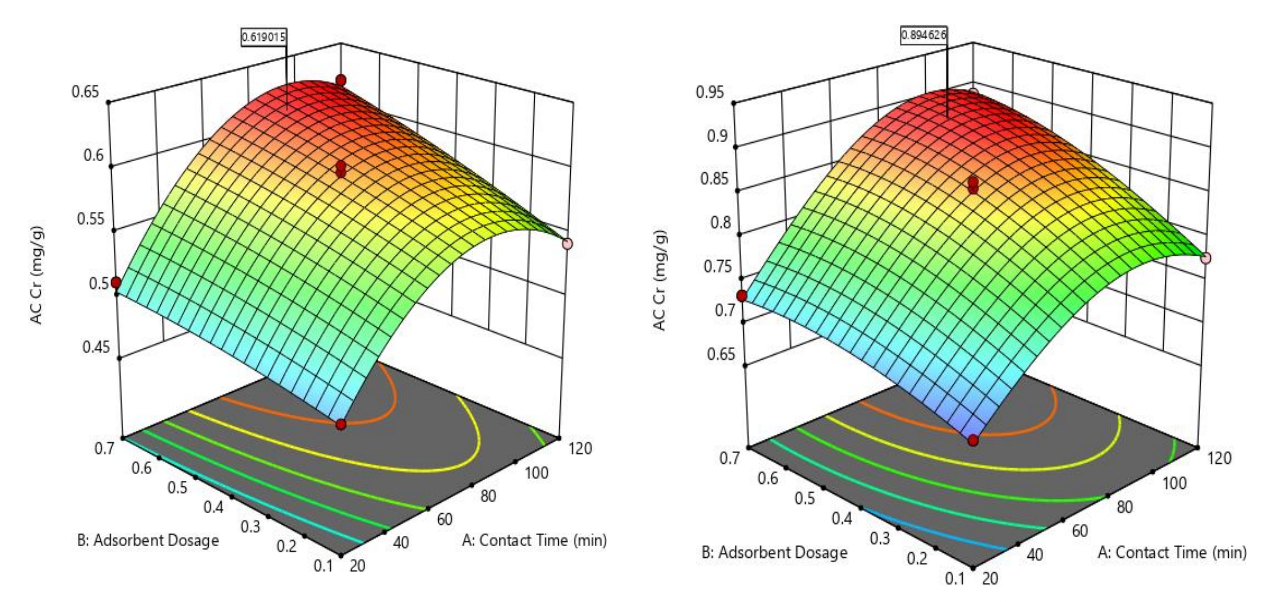


Figure 9. 3D response surface plot for the adsorption of Cr (V) ions on SCB (left) and LM (right).

In analyzing the objective functions in relation to the optimal operating conditions of the biosorption system, the variation of the process parameters were considered (independent variables) and the influence on the previously established experimental field, provided that the biosorption capacity (q, mg/g) are maximized. The primary goal of the response surface is to efficiently track the optimum values of variables, maximizing the response. Through the analysis of the plots, the best response range can be calculated. Each response plot represents an infinite number of combinations of two test variable with the other maintained constant [33]. Analyzing the 3D plots, the quantities of Cr (VI) adsorbed by SCB, LM and their blend per unit gram were 0.61, 0.89 and 1.56 mg/g, respectively.

Lemongrass demonstrated a greater absorption of Cr (VI) ions compared to sugarcane bagasse, attributed to the higher affinity of Cr (VI) ions towards the biosorbent. Significantly, the blend displayed enhanced performance, surpassing the individual materials, which indicates improved affinity for Pb (II) ions when the materials are combined. The plots show the optimal conditions for the adsorption of Cr (VI) ions from textile wastewater, using SCB, LM and their blend are observed at a contact time of 82, 69 and 71 min, respectively and at an adsorbent dosage of 0.62, 0.58 and 0.45 g. A desirability value of 1.00, 0.821 and 1.00 was obtained after optimizing both process variables i.e. contact time and adsorbent dosage. The

desired objective of this numerical optimization was to maximize the adsorption capacity too. The effect of contact time on the adsorption capacity of Cr (VI) using SCB, LM and their blend was studied within the range 20-120 min and the results presented in Figures 9 and 10 were analyzed. It shows that the adsorption of Cr (VI) using SCB increased with an increase in contact time and then slightly decreased after equilibrium was attained at 82 min of agitation. Subsequently, a decline in the adsorption capacity was observed.

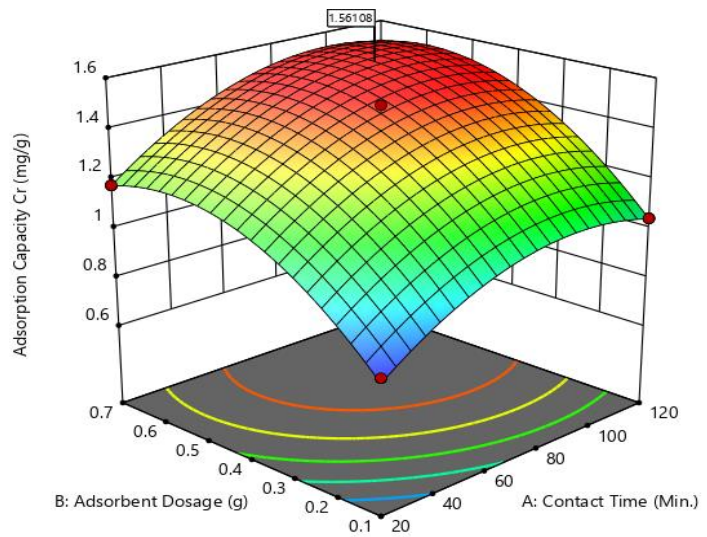


Figure 10. 3D response surface plot for the adsorption of Cr (VI) ions onto a blend derived from SCB and LM.

Similarly, using LM as a biosorbent for the adsorption of Cr (VI) ions, the adsorption capacity increased with an increase in contact time and then slightly decreased after which equilibrium was attained at 70 min of agitation. Subsequently, a decline in the adsorption capacity was observed. For the adsorption of Cr (VI) ions using the blend derived from SCB and LM, the adsorption capacity of Cr (VI) ions increased rapidly with an increase in contact time, reaching equilibrium at 71 min of agitation, however, beyond this point, there was no substantial change observed with further increase with time. This finding aligns with the result reported by [13, 20, 34, 35]. This trend may be attributed to the large number of vacant sites available at the beginning of the process, which eventually become saturated, resulting in a constant adsorption capacity. After attaining equilibrium, the adsorption process may slow down because of the saturation of binding sites on the adsorbent surface [36]. Generally, the uptake of metal increased with an increase in contact time and then ceased due to the saturation of the binding sites on the cell surface [37].

The effect of adsorbent dosage on the adsorption of Cr (VI) using SCB, LM, and their blend was studied by varying the dosage from 0.1 to 0.7 g, as illustrated in Figures 9 and 10. For the adsorption of Cr (VI) ions using SCB, it was observed that adsorption capacity increases with an increase in adsorbent dosage until an optimum dosage was reached at 0.62 g. Similarly, the adsorption of Cr (VI) ions using LM increases with an increase in the amount of adsorbent dosage until an equilibrium dosage is attained at 0.58. The adsorption capacity of Cr (VI) increases over time, reaching a plateau at an equilibrium dosage of 0.45 g, and then becoming constant with no notable changes observed upon increasing the dosage. This increase could be attributed to the overall increase in the surface area of the biosorbent, which in turn increased the number of available binding sites for adsorption [38]. However, as the initial adsorbent dose increases and the number of active sites for ion binding increases, providing easier penetration of metal into the active sites and consequently, the

resultant adsorption also increases, and after a certain value, the increase of the amount of the adsorbent does not affect the adsorption process because of saturation of active sites [39]. A similar results were reported by [1, 13, 19].

3.3. Adsorption Isotherm and Kinetic Models

The experimental data were fitted into the non-linear isotherms and kinetic models employed for this study, employing a non-linear curve fitting tool in OriginPro 9 software. In each case, the best model considered was the one with the highest correlation coefficient R² and lowest chi-square X² values. The closer the R² values are to unity, the higher the goodness of fit, and the lower the Chi-square values, the better the fit [14].

3.3.1. Adsorption Isotherms

The isotherm parameters, as well as the correlation coefficients (R²) and chi-square (X²) values derived from Figure 11 for the adsorption isotherms of Cr (VI) ions using SCB, as shown in Table 3, indicating that all three models fit the experimental data. The Langmuir isotherm offers the best fit among the models, with low reduced chi-square values of 0.00027 for Cr (VI) ions, and large adjusted R² values of 0.9873. This suggests that the Langmuir isotherm is more suitable for describing the adsorption of Cr (VI) ions using sugarcane bagasse than the other two isotherm models. This implies that Cr (VI) ions adsorption follows the monolayer adsorption, in which all metal binding sites have the same energy levels and there are no interactions between the adsorbed metals, nor is there any transmigration of sorbate within the surface area plane [40]. Similar results were reported by Pagala on the adsorption of Pb (II) and Cr (VI) ions using sugarcane bagasse [41]. Additionally, Kumar et al. reported similar results for the adsorption of Cr (VI) ions onto groundnut shells [42].

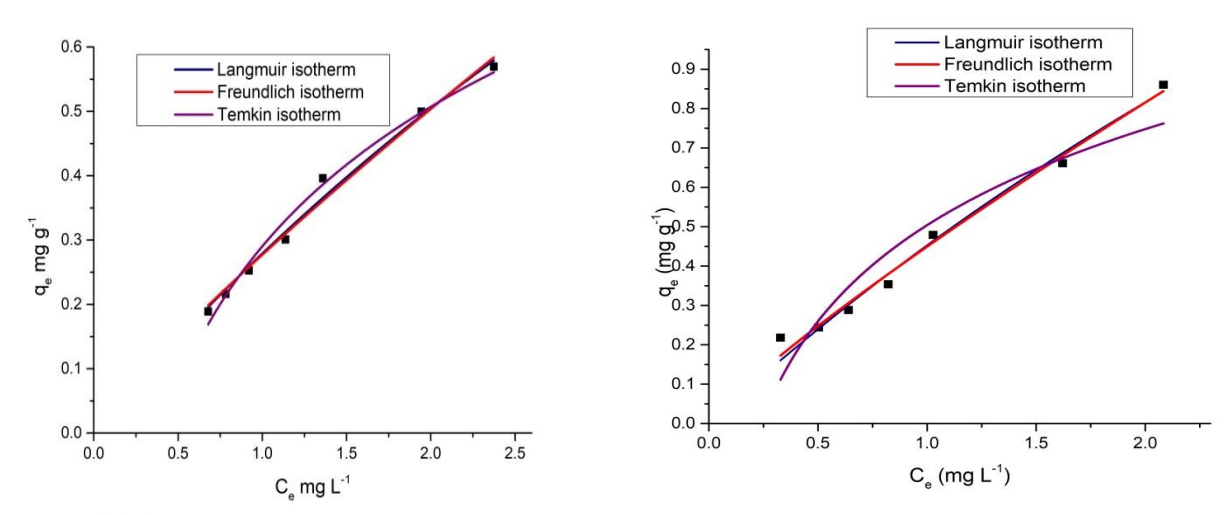


Figure 11. Non-linear models for the adsorption isotherm of Cr (VI) ions using SCB (left) and LM (right).

The maximum adsorption capacities for Cr (VI) ions were estimated using Langmuir isotherm and were found to be 2.68 mg/g, with a Langmuir constant of 0.1160 L/mg. The dimensionless separation factor R_L is used to analyze the adsorption process's favorability, with Cr (VI) values of 0.7455. These values describe a favorable adsorption isotherm. The R_L values indicate the order of isotherm: R_L >1signifies an unfavorable isotherm, R_L =1 indicates linear isotherm, R_L <1 denotes favorable isotherm while R_L =0 signifies an irreversible isotherm [43].

Similarly, the adsorption isotherm parameters reported in Table 3 show that Cr (VI) biosorption follows the Freundlich isotherm as evident by higher values of R² (0.9858) and

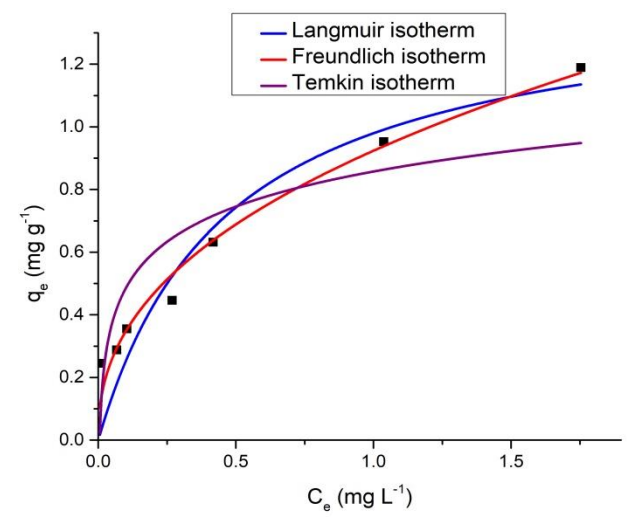


Figure 12. Non-linear models for the adsorption isotherm of Cr (VI) using a blend derived from sugarcane bagasse and lemongrass.

lower reduced chi-square (0.00082) values when compared to other isotherms. It means that the fitted model followed heterogeneous and multilayer adsorption of Cr (VI) ions on the surface of the LM. The findings were consistent with those previously reported by El Dean et al.'s work on Cr (VI) ions adsorption on SCB [20]. The maximum adsorption capacities (q_m), for Cr (VI) ions were estimated using Langmuir and found to be 4.153 mg/g, as indicated in Table 3. The separation factor R_L ranges from 0 to 1, indicating favorable biosorption of Cr (VI) ions on LM with values 0.7355. The R_L values imply that Langmuir adsorption is reversible (R_L =0), favorable (R_L <1), linear (R_L =1) or unfavorable (R_L >1) [17].

Adsorption isotherm constants for adsorption of Cr (VI) ions

Table 3

	/ tase: ption :	30 ti i Ci i i i Co i i Sc	units for ausorpt	.0 0. 0. (1.) .0	119
	Biosorbent	$(\frac{Q_m}{mg})$	$\frac{K_L}{(\frac{L}{mg})}$	\mathbf{R}^2	X ²
Langmuir	SCB	2.6750	0.1160	0.9873	0.00027
	LM	4.153	0.1222	09813	0.001
	Blend	1.4397	2.1289	0.8698	0.0169
		¹ /n	$K_f(\frac{mg}{g})$	R ²	X^2
Freundlich	SCB	0.8630	0.2760	0.9835	0.00035
	LM	0.8601	0.4492	0.9858	0.00082
	Blend	0.4246	0.9237	0.9679	0.0055
		$b\left(\frac{J}{mol}\right)$	$K_{T}(\frac{L}{g})$	R^2	X^2
Temkin	SCB	3.195	2.526	0.9852	0.00032
	LM	2.838	4.1776	0.8867	0.0065
	Blend	6.1777	3.1396	0.6954	0.0396

Note: Q_m = maximum monolayer adsorption capacity; K_L = Langmuir Constant; K_f = Freundlich constant; R^2 = correlation coefficient; X^2 = Chi square; n is the adsorption intensity; K_T binding energy; b = heat of adsorption; L = Liter; mg/g = Milligram per gram; J/mol = joule per mole.

For the blend material, the reduced chi-square and adjusted correlation coefficient (R^2) values obtained from Figure 12 for Cr (VI) ions adsorption using a blend formed from SCB and LM, as shown in Table 3, indicate that all three models show a good fit with the experimental data. Freundlich shows the best fit with a higher R^2 value of 0.9679 and a low reduced chi-square 0.0055. This shows that the Freundlich isotherm is more suitable for describing the

adsorption of Cr (VI) ions. This implies the fitted model followed heterogeneous and multilayer adsorption of Cr (VI) ions on the surface of the adsorbent. Similar results were previously reported by [20] in their work on the adsorption of Cr (VI) ions on SCB. The maximum adsorption capacities (q_m), as calculated by Langmuir were determined to be 1.4397 mg/g Cr (VI) ions, as shown in Table 3. The dimensionless separation factor R_L as indicated in Table 3, falls within the range of 0-1, showing favorable Cr (VI) ions biosorption on the blend derived from SCB and LM, with values 0.1376. The value of R_L indicates the type of isotherm to be either unfavorable (R_L >1), linear (R_L =1), favorable (0< R_L <1) or irreversible (R_L =0) [20]. The Temkin isotherm has the least fit among the three isotherms as shown in Table 3 for Cr (VI) adsorption using SCB, LM and their blend.

3.3.2. Adsorption Kinetics

To further understand the adsorption mechanism of Cr (VI) on SCB, LM and their blend, the kinetic models used in this work were applied to the experimental data. Non-linear fits of these models are illustrated in Figures 13 and 14, while Table 4 presents the parameters obtained from the model fits.

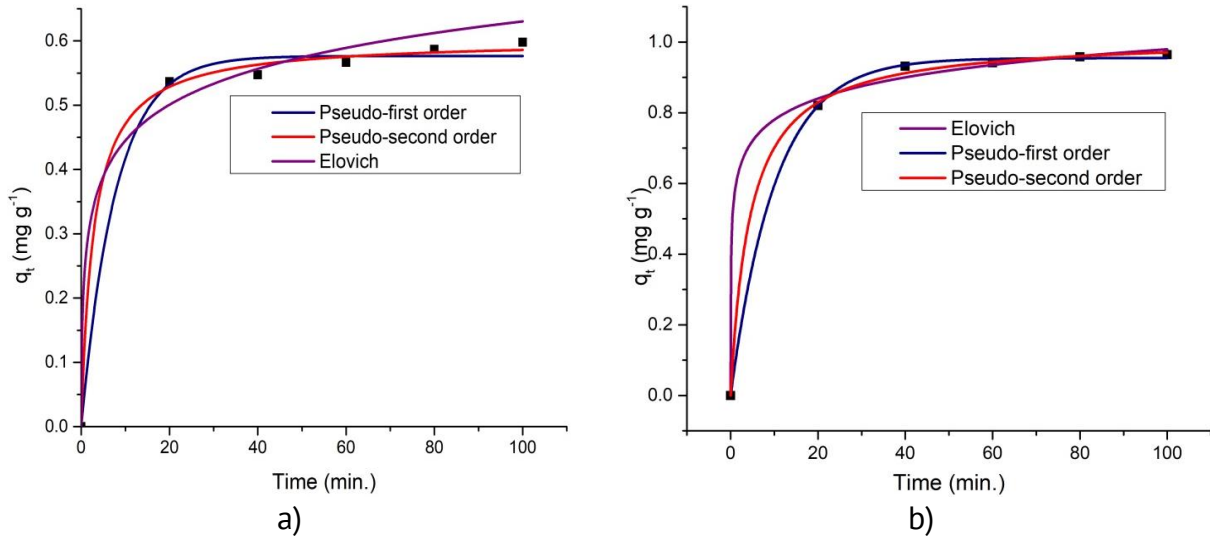


Figure 13. Non-linear adsorption kinetics models applied for the adsorption of Cr (VI) ions onto SCB (a) and LM (b).

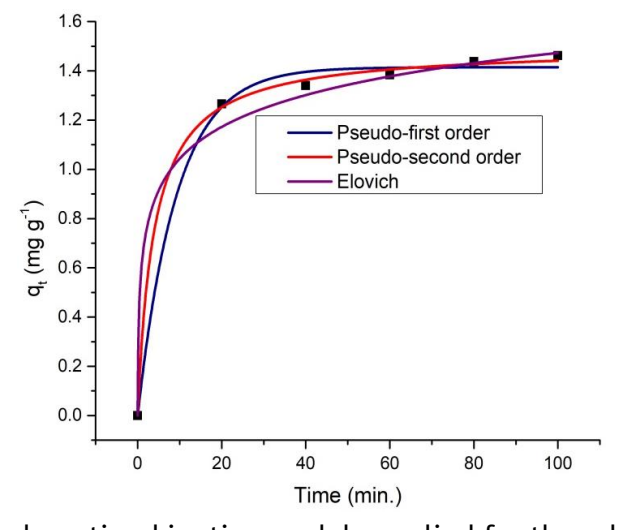


Figure 14. Non-linear adsorption kinetics models applied for the adsorption of Cr (VI) onto a blend derived from sugarcane bagasse and lemongrass.

The parameters extracted from Figure 13 and presented in Table 4 reveal that the correlation coefficient R² and reduced chi-square X² values for PFO, PSO, and Elovich kinetic models indicate that all kinetic models showed a good fit. However, for Cr (VI) ions adsorption using SCB, the PSO, exhibiting the highest correlation coefficient of 0.9975 for Cr (VI), which is closer to unity, shows a better fit. This model predicts an equilibrium Cr (VI) ions uptake of 0.57655 mg/g, which is in agreement with the experimentally obtained value of 0.62 mg/g. The PSO kinetic model shows the best fit with the adjusted R² value of 0.9996, along with a low chi-square value of 0.00013 for Cr (VI) ions adsorption using LM. This model predicts an equilibrium uptake of 1.01404 mg/g for Cr (VI), closely aligning with experimentally obtained values.

Adsorption kinetic model constants for Cr (VI) ions

Table 4

	Biosorbent	K ₁	Q _e	Q _p	\mathbb{R}^2	X ²
PFO	SCB	0.1286	0.62	0.576	0.9939	0.0003
	LM	0.097	0.89	0.954	0.9991	0.0006
	blend	0.108	1.49	1.414	0.9947	0.0017
	Biosorbent	K^2	$Q_{\rm e}$	Q_p	R^2	X^2
PSO	SCB	0.595	0.62	0.602	0.9975	0.00013
	LM	0.220	0.89	1.014	0.9996	0.0001
	Blend	0.1699	1.49	1.498	09987	0.0004
	Biosorbent	Α	β	-	R^2	X^2
Elovich	SCB	2.001	12.402	-	0.9834	0.0009
	LM	69.95	11.53	-	0.9971	0.0004
	Blend	4.904	5.344	-	0.9918	0.00262

Note: Q_e = experimental adsorption capacity; Q_p = predicted adsorption capacity; K_1 = PFO constant; K^2 PSO constant; R^2 = correlation coefficient; X^2 = Chi-square; L = Liter; mg/g = Milligram per gram; J/mol = joule per mole.

Similarly, the PSO kinetic model exhibits adjusted R² values of 0.09987, along with reduced chi-square values of 0.00043 for Cr (VI) ions adsorption using the blend material. This model predicts equilibrium Cr (VI) ions uptake of 1.497 mg/g which closely aligns with the experimentally obtained value of 1.49 mg/g. The closer the R² value is to unity, the better the fit. Notably, The PSO stands out as the best fit among the three models tested (in Figures 13 and 14) for Cr (VI) ions adsorption using SCB, LM, and their blend, implying that the active sites on the adsorbent surface significantly influence the adsorption capacity. The findings obtained were in good agreement with previous studies, which also reported that the adsorption process of Cr (VI) ions followed the PSO kinetic model following the literature [41, 42,44,45].

4. Conclusions

This study has demonstrated the significant potential of sugarcane bagasse (SCB) and lemongrass (LM) as effective biosorbents for the removal of chromium (VI) ions from textile wastewater. The results indicate that both materials exhibit substantial adsorption capacities, with their blend demonstrating superior performance. Characterization techniques, including BET analysis and FTIR, provided critical insights into the biosorbents' properties. The BET analysis revealed high surface areas for SCB (501.999 m²/g), lemongrass (811.761 m²/g), and their blend (1047.885 m²/g), which are essential for maximizing adsorption efficiency. The FTIR analysis identified significant functional groups, such as hydroxyl and carbonyl, crucial

for binding Cr (VI) ions, suggesting strong chemical interactions that enhance biosorption effectiveness.

In addition to the characterization results, the kinetic studies showed that the adsorption of Cr (VI) ions followed the Pseudo-second order model for all biosorbents, indicating that the process is significantly influenced by the availability of active sites on the adsorbent surfaces. This model's high correlation coefficients suggest that chemisorption is the dominant mechanism for Cr (VI) ions uptake. Moreover, isotherm analysis revealed that the Langmuir isotherm provided the best fit for SCB, indicating monolayer adsorption on homogeneous sites, while the Freundlich isotherm was more appropriate for lemongrass and the blend, suggesting heterogeneous and multilayer adsorption. These findings highlight the complexity of the interactions between the biosorbents and chromium (VI) ions, underscoring the diverse mechanisms involved in the adsorption process.

Overall, the findings of this research contribute significantly to the understanding of biosorption technology and promote the use of sustainable materials in wastewater treatment processes. SCB and LM emerge as viable options for the remediation of chromium (VI) ions, paving the way for further investigations into their application for other heavy metals. This study encourages a shift towards environmentally friendly practices in wastewater management, reinforcing the potential of natural biosorbents in mitigating pollution and protecting water resources.

Conflicts of Interest: The author declares no conflict of interest.

References

- 1. Balarak, D.; Jaafari, J.; Hassani, G. The use of low-cost adsorbent (Canola residues) for the adsorption of methylene blue from aqueous solution: Isotherm, kinetic and thermodynamic studies. *Colloids and Interface Science Communications* 2015, 7, pp. 16-19.
- 2. Ameen, H.S.A.; Yub, H.N.; Mahmoud, N.M.; Al-Fakih, A.; Abdulhakim, S.G.A.; Kolawole, A.H. Removal of cadmium from aqueous solution by optimized rice husk biochar using response surface methodology. *Ain Shams Engineering Journal* 2022, 13(1), pp. 101516.
- 3. Rizvi, A.; Ahmed, B.; Zaidi, A.; Khan, M.S. Biosorption of heavy metals by dry biomass of metal tolerant bacterial biosorbents: an efficient metal clean-up strategy. *Environ Monit Assess.* 2020, 192, pp.1-21
- 4. Oyegoke, T.; Adnan, A. Impact of Selected Adsorbent Functional Groups on Chromium Sorption Capacities In An Effluent Treatment: A DFT Study. *The Journal of Engineering Research* [TJER] 2024, 21(1), pp. 59-70.
- 5. Zhao, Y.; Yang, S.; Ding, D.; Effective adsorption of Cr (VI) from aqueous solution using natural Akadama clay. *J Colloid Interface Sci.* 2013, 395, pp. 198-204.
- 6. Agarwal, A.; Upadhyay, U.; Sreedhar, I.; Singh, S.A.; Patel, C.M. A review on valorization of biomass in heavy metal removal from wastewater. *Journal of Water Process Engineering* 2020, 38, p.101602.
- 7. Oyegoke, T.; Igwebuike, C.M.; Oyegoke, A. Unraveling the influence of biomaterial's functional groups in Cd biosorption: a density functional theory calculation. *Pure and Applied Chemistry* 2024, 96(3), pp. 399-412.
- 8. Sen, S.; Nandi, S.; Dutta, S. Application of RSM and ANN for optimization and modeling of biosorption of chromium (VI) using cyanobacterial biomass. *Appl Water Sci.* 2018, 8, pp.1-12.
- 9. Yous, R.; Mohellebi, F.; Cherifi, H.; Amrane, A. Competitive biosorption of heavy metals from aqueous solutions onto Streptomyces rimosus. *Korean Journal of Chemical Engineering* 2018, 35, pp.890-899.
- 10. Abdelfattah, I.; Ismail, A.A.; Sayed, F.; Almedolab, A.; Aboelghait, K.M. Biosorption of heavy metals ions in real industrial wastewater using peanut husk as efficient and cost-effective adsorbent. *Environ Nanotechnol Monit Manag.* 2016, 6, pp.176-183.
- 11. Martini, S.; Afroze, S.; Ahmad, R.K. Modified eucalyptus bark as a sorbent for simultaneous removal of COD, oil, and Cr(III) from industrial wastewater. *Alexandria Engineering Journal* 2020, 59(3), pp.1637-1648.
- 12. Molaudzi, N.R.; Ambushe, A.A.; Sugarcane Bagasse and Orange Peels as Low-Cost Biosorbents for the Removal of Lead Ions from Contaminated Water Samples. *Water*, 2022, 14(21), p.3395.

- 13. Aminu, Z.I.; Galadima, M.S.; Isa, M.T.; Ameh, A.O.; Sanni, M.I. Application of Response Surface Methodology in Adsorption of Lead Ion from Laboratory Simulated Wastewater Using Eucalyptus Tereticornis Leaves. *Nigerian J. Mater. Sci. Eng.* 2016, 6(1), pp. 1-10.
- 14. Ezeonuegbu, B.A.; Machido, D.A.; Whong, C.M.Z. Agricultural waste of sugarcane bagasse as efficient adsorbent for lead and nickel removal from untreated wastewater: Biosorption, equilibrium isotherms, kinetics and desorption studies. *Biotechnology Reports* 2021, 30, pp. e00614.
- 15. Homagai, P.L.; Ghimire, K.N.; Inoue, K. Preparation and characterization of charred xanthated sugarcane bagasse for the separation of heavy metals from aqueous solutions. *Separation Science and Technology* 2010, 46(2), pp. 330-339.
- 16. Aruna-Bagotia, N.; Sharma, A.K.; Kumar, S. A review on modified sugarcane bagasse biosorbent for removal of dyes. *Chemosphere* 2021, 268, pp. 129309.
- 17. Babarinde, A.; Ogundipe, K.; Sangosanya, K.T.; Akintola, B.D.; Hassan, E. Comparative study on the biosorption of Pb(II), Cd(II) and Zn(II) using Lemon grass (Cymbopogon citratus): Kinetics, isotherms and thermodynamics. *Chem. Int.* 2016, 2(2), pp. 89-102.
- 18. Zein, R.; Satrio-Purnomo, J.; Ramadhani, P.; Safni-Alif, M.F.; Putri, C.N. Enhancing sorption capacity of methylene blue dye using solid waste of lemongrass biosorbent by modification method. *Arabian Journal of Chemistry* 2023, 16(2), pp. 104480.
- 19. Silva, C.E.; Gama, B.M.V.; Gonçalves, A.H.; Medeiros, J.A.; Abud, A.K.S. Basic-dye adsorption in albedo residue: Effect of pH, contact time, temperature, dye concentration, biomass dosage, rotation, and ionic strength. *Journal of King Saud University Engineering Sciences* 2020, 32(6), pp. 351-359.
- 20. Kamal-El-Dean, A.M.; Hashem, E.Y.; Ahmed, M.M.; Mohamed, M.A.; Hussain, S.M. Removal of chromium(VI) from wastewater using citric acid modified sugarcane bagasse. *European Chemical Bulletin* 2019, 8(5), pp. 141-149.
- 21. Darweesh, M.A.; Elgendy, M.Y.; Ayad, M.I.; Ahmed, A.M.M.; Elsayed, N.M.K.; Hammad, W.A. Adsorption isotherm, kinetic, and optimization studies for copper (II) removal from aqueous solutions by banana leaves and derived activated carbon. *S Afr J Chem Eng.* 2022, 40, pp. 10-20.
- 22. Sahoo, T.R.; Prelot, B. Adsorption processes for the removal of contaminants from wastewater: the perspective role of nanomaterials and nanotechnology. *Micro and Nano Technologies* 2020, pp. 161-222.
- 23. Dwiyaniti, M.; Elang-Barruna, A.G.; Muhamad-Naufal, R.; Subiyanto, I.; Setiabudy, R.; Hudaya, C. Extremely high surface area of activated carbon originated from sugarcane bagasse. *IOP Conf Ser Mater Sci Eng.* 2020, 909(1), 012018.
- 24. Darla, U.R.; Lataye, D.H.; Kumar, A.; Pandit, B.; Ubaidullah, M. Adsorption of phenol using adsorbent derived from Saccharum officinarum biomass: optimization, isotherms, kinetics, and thermodynamic study. *Sci Rep.* 2023, 13(1), 18356.
- 25. Ogundeji, O.J.; Jimoh, A. Characterization of sugarcane bagasse as a potential treatment of heavy metal effluents by the response surface methodology. *Int. J. Pure Appl. Sci.* 2021, 20(9), pp. 1-24.
- 26. Ahmad, M.A.; Ahmed, N.B.; Adegoke, K.A.; Bello, O.S. Sorption studies of methyl red dye removal using lemon grass (Cymbopogon citratus). *Chemical Data Collections* 2019, 22, 100249.
- 27. Harripersadth, C.; Musonge, P.; Makarfi-Isa, Y.; Morales, M.G.; Sayago, A. The application of eggshells and sugarcane bagasse as potential biomaterials in the removal of heavy metals from aqueous solutions. *S Afr J Chem Eng.* 2020, 34(1), pp. 142-150.
- 28. Bernal-Jácome, L.A.; Olvera-Izaguirre, L.; García, M.G.; Delgado-Delgado, R.; Rodríguez, M.Á.E. Adsorption of Lead (II) from Aqueous Solution Using Adsorbents Obtained from Nanche Stone (Byrsonima Crassifolia). *J Mex Chem Soc.* 2021, 64(4), pp. 301-315.
- 29. Lee, L.Y.; Lee, X.J.; Chia, P.C.; Tan, K.W.; Gan, S. Utilisation of Cymbopogon citratus (lemon grass) as biosorbent for the sequestration of nickel ions from aqueous solution: Equilibrium, kinetic, thermodynamics and mechanism studies. *J Taiwan Inst Chem Eng.* 2014, 45(4), pp. 1764-1772.
- 30. Abdolali, A.; Ngo, H.H.; Guo, W. Characterization of a multi-metal binding biosorbent: Chemical modification and desorption studies. *Bioresour Technol.* 2015, 193, pp. 477-487.
- 31. Isam, M.; Baloo, L.; Chabuk, A.; Majdi, A.; Al-Ansari, N. Optimization and modelling of Pb (II) and Cu (II) adsorption onto red algae (Gracilaria changii)-based activated carbon by using response surface methodology. *Biomass Convers Biorefin.* 2024, 14(15), pp. 16799-16818.
- 32. Amini, M.; Younesi, H.; Bahramifar, N. Application of response surface methodology for optimization of lead biosorption in an aqueous solution by *Aspergillus niger*. *J Hazard Mater* 2008, 154(1-3), pp. 694-702.

- 33. Fertu, D.I.; Dragoi, E.N.; Bulgariu, L.; Curteanu, S.; Gavrilescu, M. Modeling the Biosorption Process of Heavy Metal Ions on Soybean-Based Low-Cost Biosorbents Using Artificial Neural Networks. *Processes* 2022, 10(3), 603.
- 34. Amode, J.O.; Santos, J.H.; Alam, Z.; Mirza, A.H.; Mei, C.C. Adsorption of methylene blue from aqueous solution using untreated and treated (Metroxylon spp.) waste adsorbent: equilibrium and kinetics studies. *International Journal of Industrial Chemistry* 2016, 7, pp. 333-345.
- 35. Kerrou, M.; Bouslamti, N.; Raada, A.; Elanssari, A.; Mrani, D.; Slimani, M.S. The Use of Sugarcane Bagasse to Remove the Organic Dyes from Wastewater. *Int J Anal Chem.* 2021, 1, 5570806.
- 36. Ashfaq, A.; Nadeem, R.; Bibi, S. Efficient adsorption of lead ions from synthetic wastewater using agrowaste-based mixed biomass (Potato peels and banana peels). *Water* 2021, 13(23), 3344.
- 37. Hauwa, H.; Whong, .C.M.Z.; Ado, S.A.; Abdulmumin, A.N. Optimization of Culture Condition for Biosorption of Lead using Pseudomonas aeruginosa isolated from Gold Mining Site of Anka, Zamfara State. *Journal of Microbiology Research* 2020, 5(1), pp. 43-48.
- 38. Al-Homaidan, A.A.; Alabdullatif, J.; Al-Hazzani, A.A.; Al-Ghanayem, A.A.; Alabbad, A.F. Adsorptive removal of cadmium ions by Spirulina platensis dry biomass. *Saudi J Biol Sci.* 2015, 22(6), pp. 795-800.
- 39. Kaya, N.; Arslan, F.; Yildiz Uzun, Z. Production and characterization of carbon-based adsorbents from waste lignocellulosic biomass: their effectiveness in heavy metal removal. *Fullerenes Nanotubes and Carbon Nanostructures*, 2020, 28(10), pp. 769-780.
- 40. Kalantari, K.; Ahmad, M.B.; Masoumi, H.R.F.; Shameli, K.; Basri, M.; Khandanlou, R. Rapid adsorption of heavy metals by Fe3O4/talc nanocomposite and optimization study using response surface methodology. *Int J Mol Sci 2014*, 15(7), pp. 12913-12927.
- 41. Pagala, B. Biosorption of Chromium and Lead from Electroplating Industry Effluent Using Modified Cane Bagasse. *Journal of The Institution of Engineers* 2023, 1, pp. 1-12.
- 42. Kumar, H.; Kumara Jawa, G.; Rai, A. Removal of Cr(VI) using citric acid and phosphoric acid-modified groundnut shells. *IJCCE* 2024, 43(3), pp. 1045-1059.
- 43. Naseem, K.; Huma, R.; Shahbaz, A. Extraction of Heavy Metals from Aqueous Medium by Husk Biomass: Adsorption Isotherm, Kinetic and Thermodynamic study. *Zeitschrift fur Physikalische Chemie* 2019, 233(2), pp. 201-223.
- 44. El Yakoubi, N.; El Ansari, Z.N.; Ennami, M.; El Kbiach, M.L.; Bounab, L.; El Bouzdoudi, B.; Biosorption of Hexavalent Chromium Cr(VI) onto Ziziphus Lotus Fruits Powder: Kinetics, Equilibrium, and Thermodynamics. *Journal of Ecological Engineering* 2024, 25(2), pp. 321-332.
- 45. Mousavi, S.A.; Almasi, A.; Navazeshkh, F.; Falahi, F. Biosorption of lead from aqueous solutions by algae biomass: optimization and modeling. *Desalination Water Treat*. 2019, 148, pp. 229-237.

Citation: Dangamba, A.S.; Oyegoke, T.; Ocheje, F.E.; Dikko, M.A.; Galadima, M.S. Evaluating the adsorption potential of sugarcane bagasse and lemongrass for chromium (VI) removal in wastewater treatment. *Journal of Engineering Science* 2024, XXXI (3), pp. 96-116. https://doi.org/10.52326/jes.utm.2024.31(3).09.

Publisher's Note: JES stays neutral with regard to jurisdictional claims in published maps and institutional affiliations.



Copyright:© 2024 by the authors. Submitted for possible open access publication under the terms and conditions of the Creative Commons Attribution (CC BY) license (https://creativecommons.org/licenses/by/4.0/).

Submission of manuscripts:

jes@meridian.utm.md

Vol. XXXI, no. 3 (2024), pp. 117 - 129 ISSN 2587-3474 eISSN 2587-3482

https://doi.org/10.52326/jes.utm.2024.31(3).10 UDC 663.257:665.939.14





INFLUENCE OF POTATO AND PEA PROTEIN FINING ON THE CHROMATIC PROFILE FEATURES OF RARA NEAGRA WINE

Natalia Vladei *, ORCID: 0000-0003-1094-6812, Alexandra Arseni, ORCID: 0009-0002-0166-4215

Technical University of Moldova,168 Stefan cel Mare Blvd., Chisinau, Republic of Moldova

* Corresponding author: Natalia Vladei, natalia.vladei@ffta.utm.md

Received: 07. 28. 2024 Accepted: 08. 31. 2024

Abstract. Due to food security issues associated to use of animal proteins and the rising demand for non-animal-based fining agents, the wine industry is becoming more interested in developing alternatives to conventional protein fining. This study evaluated the effects of several protein fining agents on the color and phenolic content of Rara Neagra red wine. Wines that were fined with proteins from potatoes and peas were contrasted with gelatin treated wines and untreated control wines. Variations in color and phenolic content revealed that plant and animal proteins had different capacities for clarification and interaction with colorless phenolics and anthocyanins, which had significant effects on color characteristics. The experimental study revealed that, in comparison to gelatin, potato and pea protein extracts were more protective in lowering the overall polyphenol level of Rara Neagra wines. Similar to other proteinaceous fining agents, the acquired data demonstrated a minor decrease in color intensity and a low decrease in the quantity of total anthocyanins. Overall, results showed that potato protein and pea protein could be used as effective fining alternatives to animal proteins, and their effectiveness should be researched in different variations depending on the chemical composition or variety of the wines.

Keywords: clarification, chromatic indices, plant protein, stabilization.

Abstract. Preocuparea tot mai mare a industriei vinului cu privire la dezvoltarea alternativelor de tratare complexa a vinurilor se datorează problemelor de siguranță alimentară asociate utilizării proteinelor animale și a cererii pentru agenți de tratare de origine ne animalieră. Acest studiu a evaluat efectele mai multor agenți de tratare proteici asupra culorii și conținutului de compuși fenolici al vinului Rara Neagră. Vinurile tratate cu proteine din cartofi și mazăre au fost comparate cu vinurile tratate cu gelatină și vinurile martor netratate. Variațiile de culoare și conținutul de polifenoli au arătat că proteinele vegetale și animale au capacități diferite de limpezire și interacțiune cu polifenolii incolori și antocieni, având efecte semnificative asupra caracteristicilor culorii. Studiul experimental a arătat că, în comparație cu gelatina, extractele proteice de cartofi și mazăre au fost mai protectoare în scăderea nivelului general de polifenoli din vinurile Rara Neagră. Similar altor agenți de limpezire proteici, datele obținute au demonstrat o scădere minoră a intensității culorii și o scădere

nesemnificativa a cantității de antocieni. În ansamblu, rezultatele au arătat că proteina din cartofi și proteina din mazăre ar putea fi folosite ca alternative eficiente de limpezire, iar eficacitatea acestora ar trebui cercetată în diferite variații, în funcție de compoziția chimică sau soiul de struguri.

Cuvinte-cheie: limpezire, caracteristici cromatica, proteine vegetale, stabilizare.

1. Introduction

Wine is an extremely complex medium, where polyphenols have a crucial impact on its final physicochemical and sensory properties [1]. The chemical diversity of polyphenols in grapes and wines is countless. With varying degrees of hydroxylation, substitutions, and even the formation of adducts between them, any family can exist in free or conjugated forms [2,3]. The primary chemical components that give wines their organoleptic qualities—such as color, bitterness, and astringency—especially in red wines, are phenolic compounds [4]. Since red wine's color is the first thing people notice about it, it has a significant impact on consumer preferences and purchasing decisions, making it one of the most crucial factors in determining its quality [5].

Anthocyanins are responsible of the diversity of red wines color, and their profile can be utilized as an analytical method to verify authenticity. Condensed tannins and flavan-3-ols, on the other hand, are important substances because of their effects on color stabilization as well as their astringent and bitterness qualities [6,7]. The primary function of other phenolics, such as flavonols and hydroxycinnamic acids, may be considered that of copigmentation, which aids in color evolution and stabilization, is directly tied to the anthocyanin composition of wine and the interactions between them or with other wine components (mostly colorless phenolics) [8,9].

Numerous factors influence the types and quantities of the various phenolic compounds found in grapes [1–4]. In particular, viticulture methods, environmental factors (soil, climate), and disease diseases all have a significant impact on the polyphenolic composition of grapes [10]. However, the winemaking technique and varietal or genetic variances [11] are certainly among the most significant variables. Controlling and regulating the phenolic composition during vinification is therefore essential to producing full-bodied red wines with stable, rich colors and balanced bitter and astringent characteristics [9,12].

The presence of microorganisms (bacteria and yeast), tartrate crystals, remaining grape peel and pulp, and aggregation of macromolecules (mostly pectin and protein components) produced during the fermentative maceration process are the main causes of wines' turbidity and instability after fermentation [13]. Wine's natural slow precipitation and sedimentation are determined by the presence of colloidal unstable molecules at advanced stages of vinification, which are linked to the formation of less soluble phenolic compounds that tend to co-aggregate gradually over time [14]. In order to prevent changes in taste, flavor, or color before bottling and consumption, the variety of particles that cause hazes and deposits must be eliminated or stabilized. These particles can aggregate coloring matter and uncolored phenolics, affecting the wines' sensory quality [13,14].

In oenology, fining agent clarification is a widespread procedure that involves adding an exogenous material to a turbid wine that uses flocculation or adsorption to precipitate other suspended particles [15]. By removing or lowering content of certain phenolic components of colloidal type linked to oxidation processes or harsh taste sensations, the primary advantages focus on improving the wine's limpidity, color stability, and mouthfeel

perception [16,17]. Nevertheless, this is a significant problem for red wines with low phenolic content since excessive clarifying might harm the stabilizing processes linked to tiny solutes and macromolecules that mostly affect color [18-20].

The tendency of protein fining agents to interact with wine phenolics and their varied affinity for various phenolic classes make them highly desirable among clarifying additives for wine fining [13,14,17,21,22]. Different studies show that certain phenolic compounds may be significantly reduced by commonly used fining agents in the wine sector, such as bentonite, gelatine, casein, egg albumin, and PVPP [5,15–22]. However, it has also been shown that gelatine fining treatments had no noticeable effect on the phenolic level and composition of wine. Yet due to their potential for causing allergies or food intolerance, conventional animal-derived fining agents, such as milk and egg proteins, have been more strictly regulated by the European Union in the past ten years, even though their effectiveness [14,23,24]. This is why alternative approaches for clarifying white, rose, and red wines have been recently suggested as plant-derived macromolecules including proteins, cell wall material, or fiber from various vegetal sources [13,14,19,23–27].

In the last decades, socioeconomic changes and globalization have led the industrial environment to develop products adapted to the changing interests of consumers. This new generation has more options and access to information, which means they have access to good products with a higher value. Growing consumers concern about health and environmental issues is leading to increased interest in the use of alternative food additives. In the wine industry, the preference for ecological, "vegan", bio-dynamic, alternative and more sustainable wines is getting popular [24,27].

The International Organization of Vine and Wine reports that currently around 53 million tons of grapes are processed globally, and global wine production is estimated at an average value of 244.1 million hectoliters [24,28]. According to the data of the National Vine and Wine Office of the Republic of Moldova, in 2022, 280 thousand tons of grapes were processed, which were converted into about 1.9 million hectoliters of wine, and about 55% were destined for export [29]. These data demonstrate that the wine industry is a primary one with potential for development, therefore it becomes even more important to connect the quality of wine to the demands of consumers [30], thus contributing to the harmlessness and sustainability of the food industry. For this reason, there is a growing interest in finding alternative wine fining agents to replace potentially allergenic animal-derived proteins and to avoid the legal obligation of indicating their presence on the label [27,30]. Moreover, some diets, such as vegetarians or vegans, do not accept foods or beverages treated with animal products [27].

The innovative solutions currently proposed for the fining of wines with materials of plant origin are in the sights of wine producers and consumers for various reasons. They certainly solve some of the problems that have led to the need for plant-based treatment agents, such as the lack of labeling requirements for animal-based adjuvants, and provide a solution to consumer demands for products that are vegetarian/vegan friendly [24,30].

Considering the allergenic issues with using animal proteins in order to clarify the wines and the increased demand for vegan wines, new researches are needed to promote alternative wine fining agents like plant extracted proteins.

The purpose of this research was to investigate the effects of alternative oenological additives: use of plant-based fining agents (patatin and pea protein) compared to gelatin (pork origin) and their action on the phenolic compounds content and color indices of Rara

Neagra red dry wine using spectrophotometric method, as well as the physical-chemical and sensorial assessment.

2. Materials and Methods

The Rara Neagra variety belongs to the group of autochthonous (Moldovan-Romanian) varieties and represents a major interest for oenologists [31].

Grapes of Rara Neagra variety from Purcari region, harvest 2023, were technologically processed according to the classic vinification scheme under micro winery conditions at the Department of Oenology and Chemistry, Technical University of Moldova. At the completion of the fermentation-maceration process, the must was pressed in a pneumatic press and the young wine was directed to post-fermentation. After the post-fermentation period, the dry red wines were added 40 mg/L of SO_2 and subjected to physicochemical analyses.

The research focused on the influence of protein fining agents of vegetable origin from potatoes (Vegecoll, Laffort) and from peas (Clear V, Perdomini IOC) on the evolution of the phenolic complex of the studied wine. For comparison, a preparation of animal origin was also used (gelatin – ErbiGel, Erbslöh Geisenheim GmbH). The principle of the method consisted in the fact that the protein adjuvant interacts with the tannins present in the wine, canceling the electric charge of these substances [13,32]. This process causes the formation of insoluble flocs, for the efficient sedimentation of which bentonite (GranuBent, Erbslöh Geisenheim GmbH) was used. The optimal doses of administered adjuvants were determined empirically, the samples were refrigerated and analyzed for the presence of disorders, as well as subjected to the tannin test [13].

The physico-chemical and quality indices of the grapes and raw material wines were established by modern analysis methods recommended in the national [33] and international official International Organization of Vine and Wine (OIV) practices [34].

The sensory analysis of the samples was carried out by a group of 12 tasters, which provided the description of the sensorial profile. Each descriptor was scored by points between 1 (least felt) and 10 (most felt) and then recorded in a special descriptive evaluation sheet [35].

The content of total phenolic substances was determined by the UV-Vis spectrophotometry method with the Folin-Ciocalteu reagent [36], gallic acid (Sigma-Aldrich) being used as a calibration substance. Prior to determination of phenolic compounds, the red wines were centrifuged at 8000 rpm for 15 min. The calibration curve and the regression equation (y = 1.378x + 0.0423) were used to determine the concentrations of total phenolic substances in the studied wines. There were no essential deviations from the calibration curve, which is also demonstrated by the coefficient $R^2 = 0.9898$.

The total content of anthocyanins was determined spectrophotometrically by the method of dilution in ethyl alcohol acidified with HCl and measuring the absorbance at wavelength 520 nm. The method is based on the principle of balance between the colored and colorless forms of anthocyanins present in an acidic environment. Anthocyanin content was calculated based on the difference in optical absorbance at a wavelength of 520 nm, which is obtained by adding two buffer solutions (pH 0.6 and 3.5) and an alcoholic solution of HCl 0.1 % in the sample [37,38].

Chromatic features were measured spectrophotometrically using quartz cuvettes with 1 mm optical length. The UV-Vis spectrophotometer was used to measure the absorption and transmission of light in the UV spectrum and the visibility of samples. The phenomenon of

light radiation adsorption by its passage through adsorbent media is governed by the fundamental Lambert-Beer law expressed as follows: the intensity of a monochromatic flux of a certain wavelength passing through a colored solution decreases proportionally with the concentration and the thickness of the layer of liquid [39].

The analysis of the color parameters of Rara Neagra red wines samples subjected to treatment with protein additives of different origin was carried out by the usual spectrophotometric method recommended by the OIV [34]. The intensity of the color results from the summation of the absorbances of the red, yellow and blue pigments which have a maximum absorption at the wavelengths 520 nm, 420 nm and 620 nm, respectively Eq. (1). The color hue results from the overlap of the red color measured at 520 nm over the yellow color measured at 420 nm Eq. (2). The color composition represents the percentage contribution of each of the three components and is given by A_{420} , A_{520} and A_{620} Eq. (3-5) from the coloring intensity (I_c). The proportion of the red color, produced by free and bound anthocyanins in the spectrum form of flavylium cations (dA) Eq. (6), was calculated using the formula described by Glories [10]:

$$I_c = A_{420} + A_{520} + A_{620} (1)$$

$$H_c = \frac{A_{420}}{A_{520}} \tag{2}$$

$$Y = \frac{A_{420}}{I_c} \times 100\% \tag{3}$$

$$Y = \frac{A_{420}}{I_c} \times 100\%$$

$$R = \frac{A_{520}}{I_c} \times 100\%$$
(4)

$$B = \frac{A_{620}}{I_c} \times 100\% \tag{5}$$

$$B = \frac{A_{620}}{I_c} \times 100\%$$

$$dA = \left[1 - \frac{A_{420} + A_{620}}{2 \times A_{520}}\right] \times 100\%$$
(5)

where:

A420 – the absorbance value at 420 nm, characterizes the yellow (Y) component of the colour:

A520 - the absorbance value at 520 nm, characterizes the red (R) component of the colour;

A620 - the absorbance value at 620 nm, characterizes the blue (B) component of the colour.

The statistical processing and mathematical modeling of the experimental results was carried out to exclude the results with accidental errors and those with a high level of uncertainty [40]. For this purpose, 3-4 parallel measurements were performed, the results were subjected to dispersion and correlative statistical processing, which was carried out through the MS Excel and ANOVA programs with the statistical significance threshold of p < p0.05, and the Q test was used to establish the degree of conformity of the experimental results.

3. Results and Discussion

The experimental study carried out allowed determining the influence of fining treatment operations on specific physicochemical indices. The results of the physicochemical analyzes of the investigated wines obtained under micro vinification conditions and with the addition of fining agents of different origins are presented in Table 1.

Table 1

The variation of the	nhysicochemical	narameters of the	Rara Neadi	a wine samnles
THE VAHIALION OF LINE	priysicociiennicat	parameters or the	: Itala Itcayi	a wille salliples

Physicochemical parameter	Control	Vegecoll	Clear-V	ErbiGel
Concentration of alcohol, % vol.	13.95± 0.11	13.90±0.12	13.90±0.11	13.85±0.11
Mass concentration of titratable acids, g/L	5.78±0.12	5.33±0.10	5.39±0.08	5.6±0.12
Mass concentration of volatile acids, g/L	0.64±0.08	0.61±0.08	0.66±0.11	0.62±0.06
рН	3.91±0.01	3.901±0.01	3.901±0.01	3.904±0.01

Thus, it was found that depending on the fining agent used, the physicochemical parameters of the Rara Neagra wine also vary. The concentration of the volume alcohol, expressed in %vol in the treated samples showed insignificant deviations from the control sample ranging 0.05- 0.1 units. The mass concentration of titratable acids in the treated wine samples decreases between 0.18-0.45 units. The mass concentration of volatile acids in the control sample is 0.64 g/L, after treatment with Vegecoll this indicates a decrease of 0.03 g/L, with ErbiGel 0.02 g/L, and in the case of treatment with Clear-V volatile acidity increased by 0.02 g/L. Regarding the pH value, the values are approximately the same with unsignificant deviations.

The results of the wine samples organoleptic analysis demonstrated that the average notes obtained by the wines treated in laboratory conditions vary depending on the clarification agent used (Figure 1).

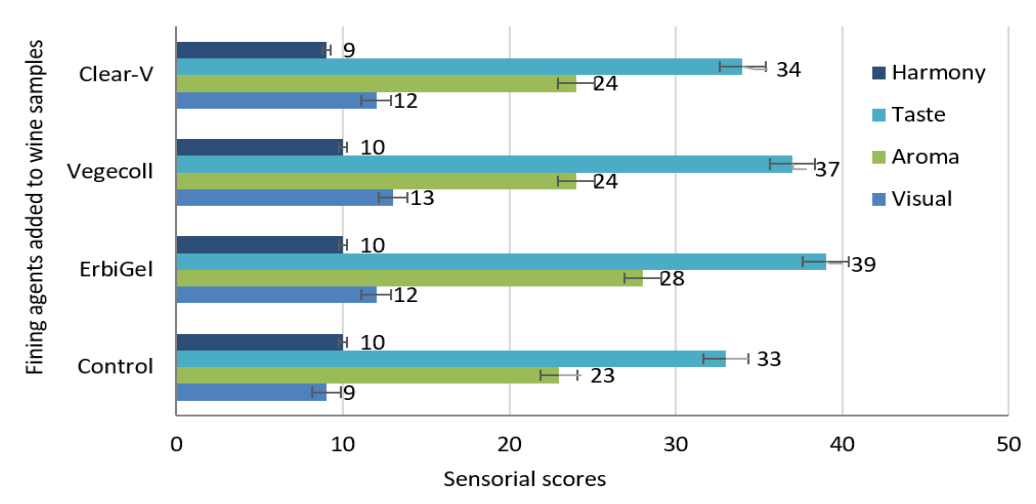


Figure 1. The sensorial scores for the Rara Neagra wine samples.

From the above diagram it can be concluded that visually, the highest score was given to the wine sample treated with Vegecoll (13 points), the lowest score to the untreated control sample. Clarifying agents have proven their effectiveness by significantly improving wine clarity. The highest score for the aromatic profile was given to the sample treated with ErbiGel (28 points), also the highest score was given to the sample treated with ErbiGel (39 points) for the taste parameter. The lowest score for harmony descriptor was given to the sample treated with Clear-V (9 points), the other samples accumulated equal scores - 10 points. Overall, the best score was given to the Rara Neagră wine sample treated with ErbiGel (89 points), and the lowest score to Vegecoll (79 points).

In order to evaluate the phenolic compounds features of Rara Neagra wine, the samples treated with vegetable and animal fining agents were subjected to UV-Vis analysis (Figure 2).

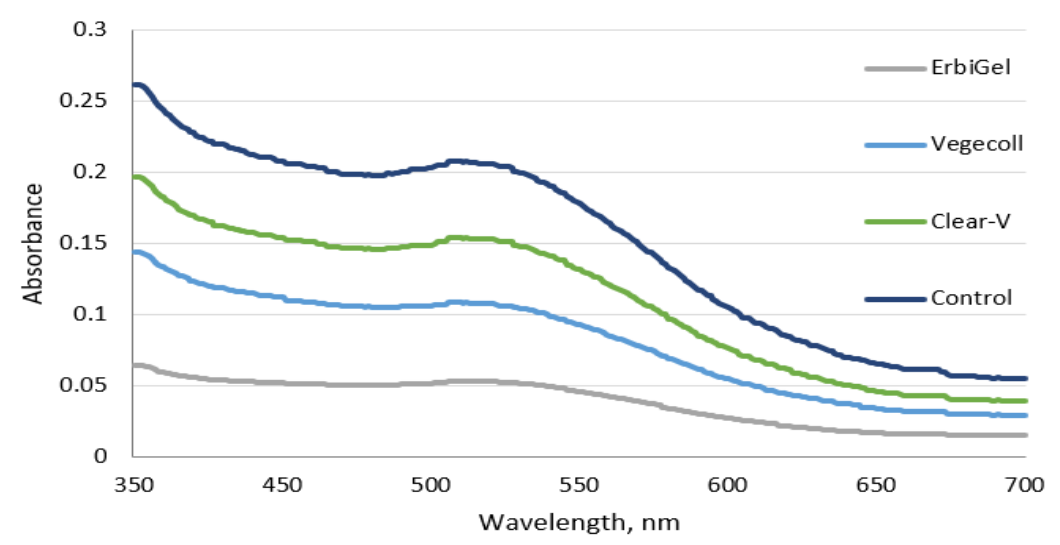


Figura 2. UV/VIS spectra of studied Rara Neagra wine samples.

From Figure 2 it can be observed that the maximum absorption of the analyzed samples is at the wavelength of 524 nm. The sample with the highest absorption is the sample where was used the pea protein fining agent (Clear-V), and the sample treated with ErbiGel (pork protein) recorded the lowest absorbance values.

The chromatic characteristics of the wines refer to the color of the wines, pointing out the intensity and hue of the color that reproduce the "appearance" and the brilliance of the color of the wine [39]. Based on the results obtained from the spectrophotometric analysis, the chromatic parameters of the wines were calculated: the color intensity and the color hue. The hue is related to the nature of the flavonic and anthocyanin pigments that give the wine its color, age and degree of technological treatments of the wine [10].

According to Ribéreau-Gayon, a young red wine's hue value ranges from 0.5 to 0.7, although it can rise to 1.3 as it ages [10]. In fact, the presence of anthocyanins in young wine gives it a vivid crimson color with violaceous reflections [6]. Because of increased content of tannins in an aged red wine, the color has an orange reflection [9].

Depending on the wine type, color intensity levels typically range from three to eighteen [10]. The anthocyanins in red wines have a strong correlation with the visible spectra of absorption. These anthocyanins contribute significantly to the wine's aging process by polymerizing with tannins [6,8,9]. We determined the values that characterize red wine color based on the absorption spectra, the obtained results were within the typical hue value range.

From the results shown in Figure 3, where the values of the chromatic parameters in dynamics is represented, we notice that during technological processing, both the color intensity and the color hue decrease. Color intensity ranges between 5.08-7.20, which is a lower content compared to other researches carried out on Rara Neagra wines [41-43].

Regarding the color hue, the values are in the range 0.6720-0.6943, being consistent with data provided by other researches on the color intensity of Rara Neagra wines [41-43].

Analyzing the average data obtained for the coloring intensity Figure 3, it can be observed that the reported differences between the applied treatment agents are insignificant from a statistical point of view (decrease by 3.2% for adjuvants of vegetable origin and 2.5% for gelatin). In case of color hue, the decrease is much significant: 34.4% for gelatin use and 29.5% for patatin and pea protein.

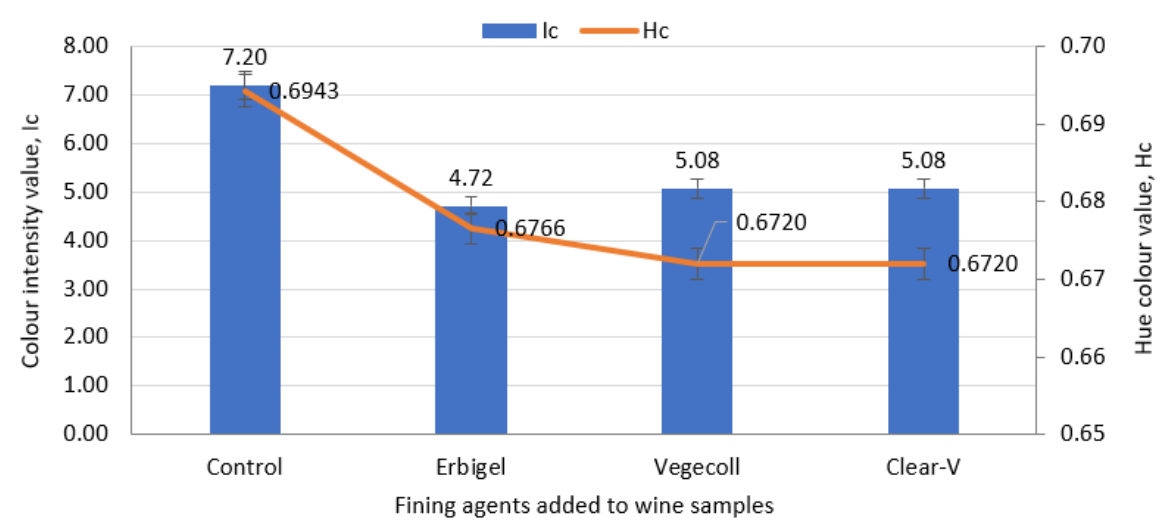


Figure 3. Variation of chromatic parameters I_c and H_c in dependance of fining agent.

Thus, it can be stated that fining treatment doesn't have significant influence on the color intensity, although an important decrease is noticed for the color hue, which mean that fining treatments reduced the compounds that give orange reflections to wine (i.e. flavones, tannins), giving the wine a bright red colour due to the anthocyanins. Our results confirmed previous findings that reported color parameters in Rara Neagra dry red wines [41-43], even though individual variations that could be attributed to the fining technique, selected dose and nature of fining agent.

The colour parameters were calculated according to Eq. 3-5, the results are illustrated in Figure 4. Yellow-colored components (A_{420}) varied between 44.09% for wines treated with vegetal protein, 44.92% for wines treated with gelatin compared to 45.00% in control sample (Figure 4).

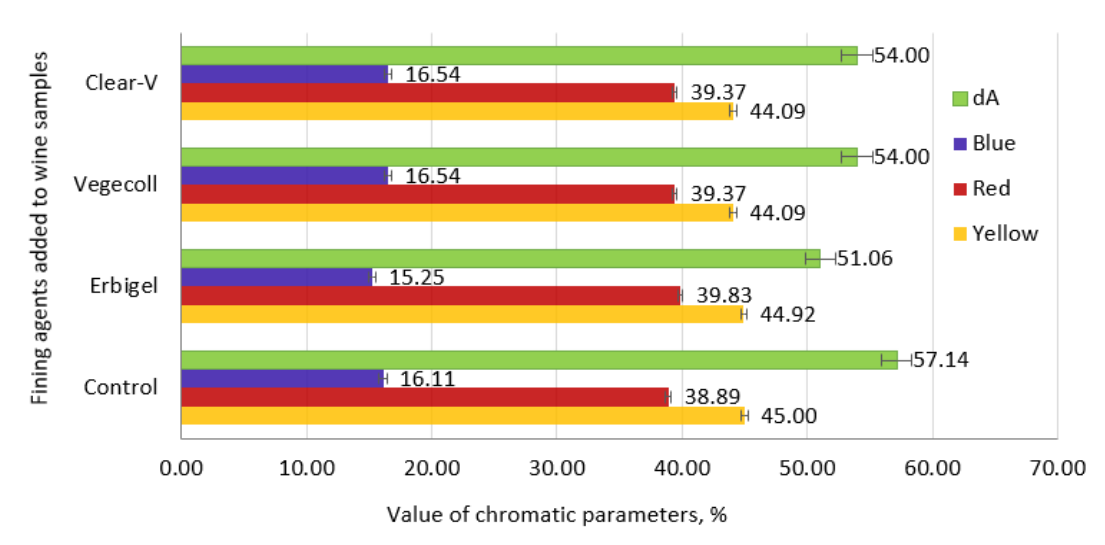


Figure 4. Intensity of yellow (A_{420}), red (A_{520}), blue (A_{620}) colours, and spectrum form (dA) of Rara Neagră wine with different fining agents.

The red-colored phenolic components (A_{520}) ranged between and 39.37% and 39.83% compared to the control sample – 38.89%, which demonstrates unsignificant statistical changes of red-coloured components (i.e. anthocyanins).

Regarding the spectrum form (dA), which describes the proportion of the red color, produced by flavylium cations of free and bound anthocyanins, from Figure 4 we can notice

a 10.6% decrease in case of gelatin fining treatment and 5.5% lower values for wines treated with vegetal proteins. The spectrum form (dA) of red wines has values ranging between 40 and 60% for young wines, which implies that the higher the value, the more predominant the red color of the wine is. Normally, in red wines, the concentration of total phenolic compounds can be mostly up to 2.5 g/L [10]. More than 200 phenolic compounds have been found, and they are thought to be the fundamental ingredients of wines. Flavonoids and nonflavonoids are the two main phenolic groups found in grapes and wine [1,2].

From Figure 5 it can be observed that, through the Rara Neagra wine samples treated with different types of fining agents, the highest amount of total polyphenolic content is in the sample treated with pea protein Clear-V (787.37 mg GAE/L), and it decreased the most in the sample treated with gelatin ErbiGel (642.24 mg GAE/L).

The obtained results confirm a variation in the polyphenolic content amongst tested wines, which can be explained by the different technological treatment applied, as expected. Comparisons with other data of wines from Moldova and Romania is difficult since only phenolic content, antioxidant proprieties and chromatic characteristics of Rara Neagra wines are available [41-45], but no information regarding influence of plant derived fining agents on chromatic profile of the wines, except studies on other varieties [15-19,20,22,26]. However, the obtained concentration ranges are in agreement with the values reported in available literature [41-46], i.e., numerous factors, including variety, harvesting method, winemaking, meteorological and ecological factors, influence the variation in total phenol content.

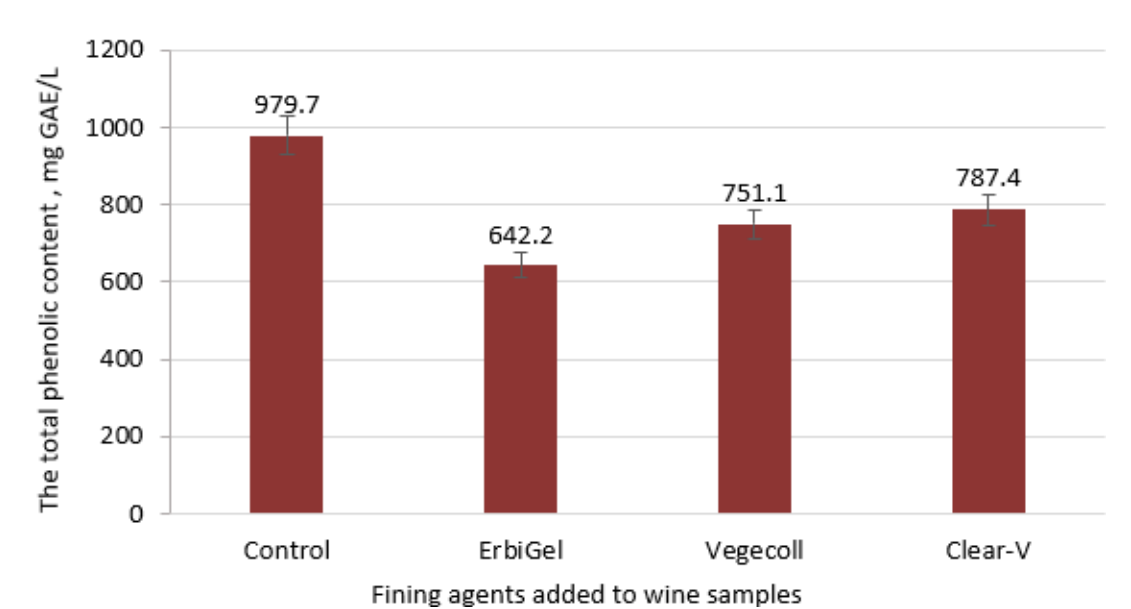


Figure 5. The polyphenolic content of Rara Neagră wine treated with different fining agents.

Analyzing the average data obtained for the total phenolic content in Rara Neagra dry red wine, the biggest difference is recorded in the case of the sample treated with gelatin - 34.4%. In the samples treated with adjuvants of vegetal origin, there is a lower decrease: - 23.3% in the case of patatin and -19.6% in the case of pea protein.

Gathering the color of red wines is a much more complex process compared to the process of the white wines; not only the flavones, phenolic acids and tannins participate in obtaining the color, but also important and diversified amounts of anthocyanins. The most important are the anthocyanins that give the red-blue color of the wines [10,12].

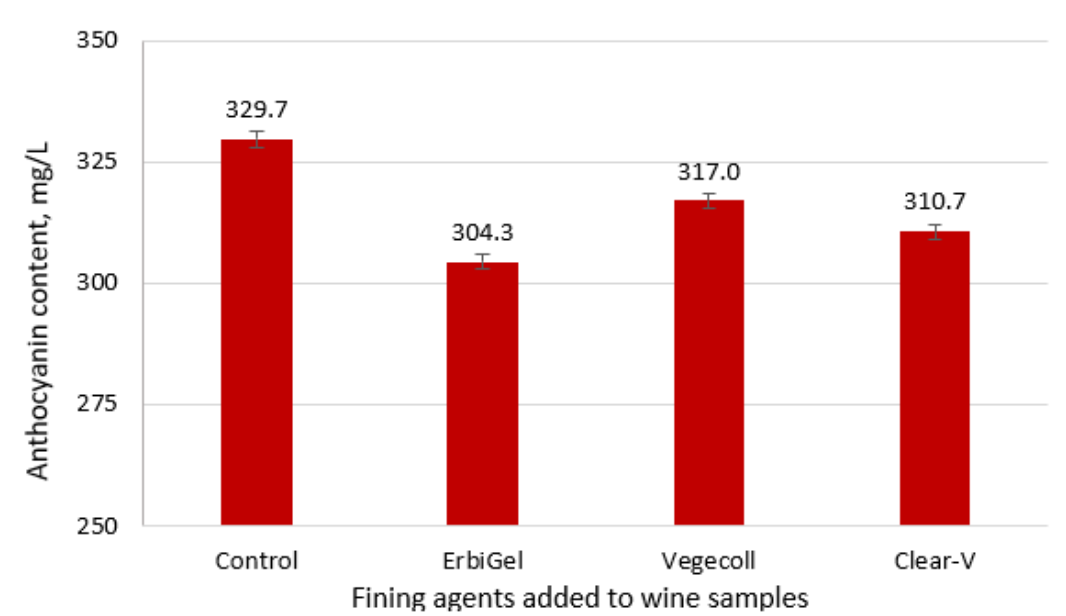


Figure 6. The anthocyanin content of Rara Neagră wine treated with different fining agents.

Anthocyanins, the visible phenolic compounds (pigments), accumulate in grapes skin and give the color of red wines. The Rara Neagra variety is characterized by an average containing of phenolic compounds which can be processed in order to obtain light red wines [44]. From the data presented in Figure 6, we can see that the most significant decrease in anthocyanins was recorded for the version where it was treated with gelatin - by 7.7% compared to the control, meanwhile the additives of vegetable origin showed a smaller decrease of anthocyanins: patatin - with 3.8% and pea protein - with 5.8%.

Previous studies reported Rara Neagra wine to have lower anthocyanins content than wines from other red varieties [41-45], nevertheless all values are within the normal range of anthocyanins (200-500 mg CE/L).

4. Conclusions

As a result of the experimental research, it was found that dry red wines obtained from the Rara Neagra grape variety are characterized by a relatively low content of phenolic substances and, although the wines are young, an intensive oxidation reaction took place with the accumulation of oxidized compounds. The treatment with protein agents of various origin had a positive impact on the structure of the polyphenolic complex, the treated wines being described by a more advanced content in anthocyanins and a lower content in oxidized and condensed compounds compared to the control sample.

The wine samples physicochemical parameters didn't show significant deviations and the organoleptic analysis demonstrated that the average scores obtained by the treated wines varied depending on the clarification agent used, the best score was given to the sample treated with gelatin, while the lowest score was given to the sample treated with patatin.

Potato and pea protein extracts were more protective in reducing the total polyphenol content of Rara Neagra wines compared to gelatin. Treatments with these two plant proteins showed a lower decrease of total anthocyanins content and slightly decreased the color intensity similar to other proteinaceous fining agents. Meanwhile, although it was stated that fining treatment doesn't have significant influence on the color intensity, an important decrease is noticed for the color hue, which mean that fining treatments reduced the

compounds that give orange reflections to wine (i.e. flavones, tannins), giving the wine a bright red color due to the anthocyanins.

Overall, results showed that potato protein and pea protein could be used as effective fining agents alternatives to animal proteins such as gelatin, and their effectiveness should be researched in different variations depending on the chemical composition or variety of the wines.

Acknowledgments: The research was supported by Institutional Project, subprogram 02.04.05 Optimizing food processing technologies in the context of the circular bioeconomy and climate change, Bio-OpTehPAS, being implemented at the Technical University of Moldova.

Conflicts of Interest: The authors declare no conflict of interest.

References

- 1. Dias, M.C.; Pinto, D.C.G.A.; Silva, A.M.S. Plant Flavonoids: Chemical Characteristics and Biological Activity. *Molecules* 2021, *26*, 5377. https://doi.org/10.3390/molecules26175377
- 2. Garrido, J.; Borges, F. Wine and grape polyphenols—A chemical perspective. *Food Res. Int.* 2013, 54, pp. 1844-1858. https://doi.org/10.1016/j.foodres.2013.08.002
- 3. Sturza, R.; Scutaru, Iu.; Duca, G. Redox Processes in Grapes Processing. In: *Environmental and Technological Aspects of Redox Processes*; Duca, G., Vaseashta, A., Eds.; IGI Global Engineering Science Reference, USA, 2023, 1, pp. 276-306. ISBN: 9798369305140.
- 4. Hornedo-Ortega, R.; Reyes González-Centeno, M.; Chira, K.; Jourdes, M.; Teissedre, P.L. Phenolic compounds of grapes and wines: key compounds and implications in sensory perception, In *Chemistry and biochemistry of winemaking, wine stabilization and aging*. IntechOpen; London, UK, 2020, 1, pp. 1-26. https://doi:10.5772/intechopen.93127
- 5. Vecchio, R.; Decordi, G.; Grésillon, L.; Gugenberger, C.; Mahéo, M.; Jourjon, F. European consumers' perception of moderate wine consumption on health. *Wine Econ. Policy* 2017, 6, pp. 14–22, https://doi.org/10.1016/j.wep.2017.04.001
- 6. de Freitas, V. A. P.; Fernandes, A.; Oliveira, J.; Teixeira, N.; Mateus, N. A review of the current knowledge of red wine colour. *OENO One* 2017, 51(1), pp. 1001-1021. https://doi.org/10.20870/oeno-one.2017.51.1.1604
- 7. Basalekou, M.; Kyraleou, M.; Pappas, C.; Tarantilis, P.; Kotseridis, Y.; Kallithraka, S. Proanthocyanidin content as an astringency estimation tool and maturation index in red and white winemaking technology. *Food Chem.* 2019, 299, pp. 125-135. https://doi:10.1016/j.foodchem. 2019.125135.
- 8. Boulton, R. The copigmentation of anthocyanins and its role in the color of red wine: A critical review. *Am. J. Enol. Vitic.* 2001, 52, pp. 67–87. https://doi:10.5344/ajev.2001.52.2.67
- 9. Sun, B.; Neves, A.; Fernandes, T.; Fernandes, A.; Mateus, N.; de Freitas, V.; Leandro, C.; Spranger, M. Evolution of phenolic composition of red wine during vinification and storage and its contribution to wine sensory properties and antioxidant activity. *J. Agric. Food Chem.* 2011, 59 (12), pp. 6550-6557. https://doi:10.1021/jf201383ePMID:21561162
- 10. Ribereau-Gayon, P.; Glories, Y.; Maujean, A.; Dubourdieu, D. The chemistry of wine stabilization and treatments. In: *Handbook of Enology*, John Wiley & Sons Ltd., Southern Gate, Chichester, UK, 2021, 2, pp. 231-428. ISBN: 978-0-470-01037-2.
- 11. Geana, E.I.; Marinescu, A.; Iordache, A.M.; Sandru, C.; Ionete, R.E.; Bala, C. Differentiation of Romanian Wines on Geographical Origin and Wine Variety by Elemental Composition and Phenolic Components. *Food Anal. Methods* 2014, 7, pp. 2064–2074.
- 12. Gutiérrez-Escobar, R.; Aliaño-González, M.J.; Cantos-Villar, E. Wine polyphenol content and its influence on wine quality and properties: A review. *Molecules* 2021, 26, 718. https://doi.org/10.3390/molecules26030718
- 13. Cosme, F.; Fernandes, C.; Ribeiro, T.; Filipe-Ribeiro, L.; Nunes, F.M. White Wine Protein Instability: Mechanism, Quality Controland Technological Alternatives for Wine Stabilisation—An Overview. *Beverages* 2020, 6, 19. https://doi.org/10.3390/beverages6010019
- 14. Kemp, B.; Marangon, M.; Curioni, A.; Waters, E.; Marchal, R. New Directions in Stabilization, Clarification, and Fining. In: *Managing Wine Quality*. 2nd Ed., Reynolds, A. G., Eds., Elsevier Publishing, Elsevier: Berlin/Heidelberg, Germany, 2022, pp. 245-301. https://doi.org/10.1016/B978-0-08-102065-4.00002-X

- 15. Kumar, Y.; Suhag, R. Impact of Fining Agents on Color, Phenolics, Aroma, and Sensory Properties of Wine: A Review. *Beverages* 2024, 10(3), 71. https://doi.org/10.3390/beverages10030071
- 16. González-Neves, G.; Favre, G.; Gil, G. Effect of fining on the colour and pigment composition of young red wines. *Food Chem.* 2014, 157, pp. 385–392.
- 17. Rihak, Z.; Prusova, B.; Prokes, K.; Baron, M. The Effect of Different Fining Treatments on Phenolic and Aroma Composition of Grape Musts and Wines. *Fermentation* 2022, 8(12), 737. https://doi.org/10.3390/fermentation8120737
- 18. Kang, W.; Niimi, J.; Putnam Bastian, S. E. Reduction of Red Wine Astringency Perception Using Vegetable Protein Fining Agents. *Am. J. Enol. Vitic.* 2018, 69, pp. 22-31. https://doi.org/10.5344/ajev.2017.17054
- 19. Noriega-Domínguez, M. J.; Durán, D. S.; Vírseda, P.; Marín-Arroyo, M. R. Non-animal proteins as clarifying agents for red wines. *OENO One* 2010, 44(3), pp. 179–189. https://doi.org/10.20870/oeno-one.2010.44.3.1472
- 20. Gordillo, B.; Chamizo-González, F.; González-Miret, M. L.; Heredia, F. J. Impact of alternative protein fining agents on the phenolic composition and color of Syrah red wines from warm climate, *Food Chem.* 2021, 342, 128297, ISSN 0308-8146, https://doi.org/10.1016/j.foodchem.2020.128297.
- 21. Lisanti, M.T.; Gambuti, A.; Genovese, A.; Piombino, P.; Moio, L. Treatment by fining agents of red wine affected by phenolic off-odour. *Eur. Food Res. Technol.* 2017, 243, pp. 501–510. https://doi.org/10.1007/s00217-016-2763-4
- 22. Río Segade, S.; Paissoni, M. A.; Vilanova, M.; Gerbi, V.; Rolle, L.; Giacosa, S. Phenolic Composition Influences the Effectiveness of Fining Agents in Vegan-Friendly Red Wine Production. *Molecules* 2020, 25(1), 120. https://doi.org/10.3390/molecules25010120
- 23. Silva-Barbieri, D.; Salazar, F.N.; López, F.; Brossard, N.; Escalona, N.; Pérez-Correa, J.R. Advances in White Wine Protein Stabilization Technologies. *Molecules* 2022, 27, 1251. https://doi.org/10.3390/molecules27041251
- 24. State of the World Vine and Wine Sector in 2022. Available online: https://www.oiv.int/sites/default/files/documents/OIV_State_of_the_world_Vine_and_Wine_sector_in_2022_2.pdf (accessed on 23 September 2024).
- 25. Marangon, M.; Vincenzi, S.; Curioni, A. Wine Fining with Plant Proteins. *Molecules* 2019, 24(11), 2186. https://doi.org/10.3390/molecules24112186
- 26. Noriega-Domínguez, M.J.; Durán, D.S.; Vírseda, P.; Marín-Arroyo, M.R. Non-animal proteins as clarifying agents for red wines. *J. Int. des Sci. la vigne du vin* 2010, 44, 179. https://doi.org/10.20870/oeno-one.2010.44.3.1472
- 27. OIV Guide for the Implementation of Principles of Sustainable Vitiviniculture. Resolution OIV-VITI 641-2020. Available online: https://www.oiv.int/node/2777/download/pdf (accessed on 28 September 2024).
- 28.In 2023, world wine production is expected to be the smallest in the last 60 years. Available online: https://www.oiv.int/press/2023-world-wine-production-expected-be-smallest-last-60-years (accessed on 12 October 2024).
- 29. Economic export of wine production in 2022. Available online: https://wineofmoldova.com/wp-content/uploads/2023/01/Raport-Export-12-luni-2022-1.pdf (accessed on 20 September 2024).
- 30. Wine sector in the Republic of Moldova. WINET BSB-638 Project: Trade and Innovation in Wine Industry. Available online: https://blacksea-cbc.net/wp-content/uploads/2020/02/BSB638_WINET_Study-on-the-wine-sector-in-the-Republic-of-Moldova_EN.pdf (accessed on 18 September 2024).
- 31. Cornea, V.; Savin, G. Exploration and revaluation of old autochthonous varieties in the Republic of Moldova. *Vitis* 2015, 54, pp. 115–119. ISSN 0042-7500.
- 32. Technical regulation "Analytical methods in wine production" approved by Republic of Moldova Government Decision no. 708 from 20.09.2011. Chişinău, Republic of Moldova. Available online: https://www.legis.md/cautare/getResults?doc_id=114344&lang=ro (accessed on 08 June 2024).
- 33. Compendium of international methods of analysis-OIV, Paris: Organisation Internationale de la Vigne et du Vin, 2021. OIV-MA-INT-00-2021. Available online: https://www.oiv.int/standards/compendium-of-international-methods-of-wine-and-must-analysis (accessed on 08 June 2024).
- 34. Lambri, M.; Colangelo, D.; Dordoni, R.; Torchio, F.; De Faveri, D. M. Innovations in the Use of Bentonite in Oenology: Interactions with Grape and Wine Proteins, Colloids, Polyphenols and Aroma Compounds. In: *Grape and Wine Biotechnology*; Morata, A. Loira, I., Eds.; IntechOpen, Rijeka, Croatia, 2016. pp. 381-400. https://doi:10.5772/64753

- 35. Regulation Evaluation Method of the Organoleptic Characteristics of Wine Products through Sensory Analysis approved by Republic of Moldova Government Decision no.810. Chisinau, Republic of Moldova. Available online: https://www.legis.md/cautare/getResults?doc_id=114817&lang=ro (accessed on 18 September 2024).
- 36. Singleton, V. L.; Rossi, J. A. Colorimetry of total phenolics with phosphomolybdic-phosphotungstic acid reagents. *Am. J. Enol. Vitic.* 1965, 16, pp. 144-158. https://doi.org/10.1515/10.5344/ajev.1965.16.3.144
- 37. Constantin, O. E.; Skrt, M.; Poklar Ulrih, N.; Râpeanu, G. Anthocyanins profile, total phenolics and antioxidant activity of two Romanian red grape varieties: Fetească neagră and Băbească neagră (Vitis vinifera)" *Chem. Pap.* 2015, 69 (12), pp. 573-1581. https://doi.org/10.1515/chempap-2015-0163
- 38. Avula, B.; Katragunta, K.; Osman, A. G.; Ali, Z.; John Adams, S.; Chittiboyina, A. G.; Khan, I. A. Advances in the Chemistry, Analysis and Adulteration of Anthocyanin Rich-Berries and Fruits: 2000–2022. *Molecules* 2023, 28(2), 560. https://doi.org/10.3390/molecules28020560
- 39. Fan, S.; Liu, C.; Li, Y.; Zhang, Y. Visual Representation of Red Wine Color: Methodology, Comparison and Applications. *Foods* 2023, 12(5), 924. https://doi.org/10.3390/foods12050924.
- 40.ISO 5725-1:2023 Accuracy (trueness and precision) of measurement methods and results. Available online: https://www.iso.org/obp/ui/#iso:std:iso:5725:-1:ed-2:v1:en (accessed on 08 June 2024).
- 41. Bora, F. D.; Bunea, C. I.; Călugăr, A.; Donici, A. Phenolic, anthocyanin composition and color measurement at red wines from Dealu Bujorului vineyard, *Agricultura* 2019, 109 (1–2), pp. 14-28. https://doi.org/10.15835/agrisp.v109i1-2.13256.
- 42. Odageriu, G.; Niculaua, M.; Cotea, V.; Zamfir, C.; Nechita, B. Time variation of anthocyans profile specific to some red wines. In: *Proceedings of XXXI-th OIV World Congress*, Verona, Italy 15-22 June 2008, P. II. 100. https://doi:10.13140/2.1.2768.4163.
- 43. Bora, F. D.; Bunea, C. I.; Coldea, T. E.; Călugăr, A.; Iliescu, M.; Donici, A. The Analyse of Physicochemical Composition, Total Phenolic Content and Colour of Some Red Wines From Dealu Bujorului Vineyard, *Agricultura* 2018, 107 (3-4), pp. 98–104. https://doi.org/10.15835/agrisp.v107i3-4.13071.
- 44. Vladei, N.; Covaci, E. Assessment the potential of biologically active substances of young red wine produced from Rară Neagră (local grape variety). In: *Ecological and environmental chemistry*, Centrul Editorial-Poligrafic USM, Chisinau, RM, 2022, 1, 168. ISBN 9789975159074.
- 45. Banc, R.; Loghin, F.; Miere, D.; Ranga, F.; Socaciu, C. Phenolic composition and antioxidant activity of red, rosé and white wines originating from Romanian grape cultivars. *Not. Bot. Horti Agrobot.* 2020, 48, pp. 716–734. https://doi.org/10.15835/nbha48211848.
- 46. Diblan, S.; Özkan, M. Effects of various clarification treatments on anthocyanins, color, phenolics and antioxidant activity of red grape juice. *Food Chem.* 2021, 352, 129321 .https://doi.org/10.1016/j.foodchem.2021.129321.

Citation: Vladei, N.; Arseni, A. Influence of Potato and Pea Protein Fining on the Chromatic Profile Features of Rara Neagra Wine. *Journal of Engineering Science* 2024, XXXI (3), pp. 117-129. https://doi.org/10.52326/jes.utm.2024.31(3).10.

Publisher's Note: JES stays neutral with regard to jurisdictional claims in published maps and institutional affiliations.



Copyright:© 2024 by the authors. Submitted for possible open access publication under the terms and conditions of the Creative Commons Attribution (CC BY) license (https://creativecommons.org/licenses/by/4.0/).

Submission of manuscripts:

jes@meridian.utm.md

https://doi.org/10.52326/jes.utm.2024.31(3).11 UDC 664.6/.7:664





INTEGRATION OF SPENT GRAIN INTO FOOD PRODUCTS

Svetlana Erşova ¹, ORCID: 0009-0006-8723-7095, Olesea Saitan ^{1*}, ORCID: 0000-0001-8814-1825, Ruslan Tarna ¹, ORCID: 0000-0001-5488-7506, Iurie Rumeus ^{1,2}, ORCID: 0000-0002-6392-7343, Georgiana Gabriela Codină ³, ORCID: 0000-0002-6575-0078, Aliona Ghendov-Mosanu ¹, ORCID: 0000-0001-5214-3562

¹ Technical University of Moldova, 168 Stefan cel Mare Blvd., Chisinau, Republic of Moldova ² Cahul State University "Bogdan Petriceicu Hasdeu", 1 Independence Square, Cahul, Republic of Moldova ³ "Stefan cel Mare" University, 720229 Suceava, Romania * Corresponding author: Olesea Saitan, olesea.saitan@tpa.utm.md

> Received: 08. 19. 2024 Accepted: 09. 28. 2024

Abstract. Spent grain is a component of grain that consists primarily of its shells and is a byproduct of the production of beer or ethyl alcohol. It is characterized by a diverse chemical composition, mainly composed of proteins and dietary fibers and, to a lesser extent, lipids, minerals, phenolic compounds, as well as B vitamins and vitamin E. In its native form, it is a product with a high moisture content, which makes it unsuitable for long-term storage. In this connection, several problems arise that worsen the economic and environmental situation at the global level. This article presents effective methods of processing spent grain to prevent negative consequences associated with its irrational use. Possibilities for the application of used spent grain in the food industry are also presented: bakery and pasta, confectionery, the meat and dairy industry, as well as the production of beverages. Thus, the integration of spent grain in the food composition will lead to solving the economic and environmental difficulties that have appeared in the last decades; it will allow the development of a functional food market, which will lead to the improvement of the quality of the population life by strengthening the trend of good nutrition and reducing the negative impact on the environment.

Keywords: spent grain, waste, biological value, bioprocessing, food products.

Rezumat. Borhotul este o componentă a cerealelor, care constă în principal din coaja acestora și este un subprodus al producției de bere sau etanol. Se caracterizează printr-o compoziție chimică diversă, alcătuită în principal din proteine și fibre alimentare și, într-o mai mică măsură, din lipide, minerale și compuși fenolici, precum și din vitaminele grupei B și vitamina E. În forma sa nativă, prezintă un produs cu un conținut ridicat de umiditate, ceea ce îl face nepotrivit pentru depozitarea pe termen lung. Acest fapt ridică o serie de probleme care agravează situația economică și de mediu la nivel global. În acest articol sunt prezentate

metode eficiente de prelucrare a borhotului pentru a preveni consecințele negative asociate cu utilizarea lui irațională. De asemenea, sunt prezentate posibilități de aplicare ale borhotului în industria alimentară: panificație și paste făinoase, cofetărie, industria cărnii și a produselor lactate, precum și producția de băuturi. Astfel, integrarea borhotului în compoziția alimentelor va conduce la rezolvarea dificultăților economice și de mediu care au apărut în ultimele decenii; va permite dezvoltarea unei piețe de alimente funcționale, ceea ce va duce la îmbunătățirea calității vieții populației prin consolidarea tendinței de bună nutriție și reducerea impactului negativ asupra mediului.

Cuvinte cheie: borhot, deseuri, valoare biologică, bioprocesare, produse alimentare.

1. Introduction

Every year the world population increases, which, in turn, directly affects all spheres of human life, in particular, nutrition, both individual and whole social groups, as well as countries and continents. According to the World Bank, in the period from 2000 to 2022, the population growth varies from year to year in the range from 0.8 to 1.4% worldwide [1]. On this basis, not only the need for food but also the quantity of production at the industrial level is increasing. Along with the augmentation in population and annual volumes of produced and consumed products, there is also an increase in food waste, which has recently been considered a global environmental and economic problem that has affected the whole world and every part of it.

It is generally accepted that annually about 1/3 (30%) of the manufactured food products do not find their direct use, i.e., are lost, which is approximately more than one billion tonnes of products annually [2]. Also, if we consider the annual food waste per capita, in industrialized countries this figure is 95-115 kg/year, while in African and South Asian countries food waste per person is much lower (more than 10 times) and ranges from 6-11 kg/year [3]. In developing countries, the causes of food losses and waste are financial, technical, production, and organizational constraints, which are caused by the weak economies of the countries. At the same time, the listed constraints contribute to the aggravation of the current economic situation. In countries with developed economies and food industries, the cause of food waste is the human factor, i.e. consumers who buy excessive quantities of products daily, which are then thrown away, but this also affects the economic component of the countries.

In addition to the economic problem, it should be noted that unused food has a detrimental effect on the global ecological system. This entails a number of changes: climate restructuring, deterioration of air quality, water quality, and other vital components. These changes lead to a lower quality of life in general.

In addition, it should be noted that food loss and waste generation can occur at different stages of the production chain, which is based on the "farm to fork" strategy:

- In the fields, farms, and other components of agriculture.
- During the processing of raw materials into finished products.
- At the point of Retailing directly to the consumer or wholesale to intermediary organizations.
- At the point of storage and domestic use by consumers.

According to the Food and Agriculture Organization of the United Nations, the percentage of food waste at the mentioned sites in Europe is 23% for the agricultural sector,

17% is due to waste resulting from the processing of raw materials, 9% is due to losses at the point of sale and the highest percentage is due to consumer losses (52%) [4].

In this way, there is a need to find solutions to minimize all kinds of losses in the industrial process of food products, which is rapidly developing every year within the food industry. This is reflected in various developments related to zero-waste production, which implies the use of by-products of food processing, such as fruit and vegetable pomace, press cake and grist, spent grain, and other things that can be reused in food production.

The above is one side of the current situation in the food industry and the food market. The other side is represented by the increasing demand for healthy and improved products. This can be explained both by the above-mentioned problems and personal preferences, most of which are aimed at taking care of one's health through proper and, importantly, safe nutrition. It follows that a manufacturer interested in selling its goods will look for ways and methods that will allow it to produce appropriate food products without incurring material losses. One such solution may be the use of edible by-products in the technology of certain products, which will reduce production costs and, in some cases, increase the nutritional value of the product. As this trend grows, there is a high probability that over time the amount of food waste will be significantly lower. This fact will have a direct favorable impact on the ecological state of our planet and the health of the population, as well as on the economic performance of countries.

Referring to the points mentioned above, the main objective of this work was to choose a bibliographic analysis of waste-free technologies, namely the possibility of using spent grain in food products, which can contribute to the reduction of production waste and increase the biological value of the food into which it will be integrated.

2. Definition and classification

Spent grain is a by-product of beer, ethanol, and other alcoholic beverages such as whisky production [5,6]. Spent grain is the components of grain consisting mainly of its shells which are not soluble [7]. To date, it is brewer's spent grain that has gained the most popularity, as evidenced by a significant number of scientific papers [5-7]. This type of waste is formed after malt mashing, i.e. at the stage of mixing milled malt with drinking water and soaking at certain temperatures, with further filtration. Therefore, the water-insoluble fraction is the brewer's spent grain, and the liquid part is wort, which is directed to further technological operations for beer production [7].

The spent grain produced at the initial stages of beer production accounts for 85% of the total amount of secondary products that are generated during all the technological stages of production of this beverage, which indicates a high level of losses and the corresponding economic and environmental problems associated with its utilization [7]. Other sources mention that when producing beer in quantities equal to 1000 t, the numerical value of solid waste generated varies from 137 to 173 t. However, solid brewing waste includes not only brewer's spent grain but also a certain amount of yeast, which at the end of its life activity has precipitated [8]. In any case, unused components account for approximately one-sixth of the product produced, reflecting significant technological losses that directly affect the economy of the enterprise, reducing its efficiency.

Thus, for example, in the period from 2020 to 2022, the production of beer from malt in the Republic of Moldova averaged 8372 thousand dal, distributed by year as follows: 2022-8418.3 thousand dal, 2021-8790.8 thousand dal and 2020-7901.1 thousand dal [9]. Based

on the above information, it can be assumed that the amount of solid waste averaged 14511.5 t for the mentioned years. The numerical values of solid waste and beer from 2020 to 2022 are displayed in Figure 2.

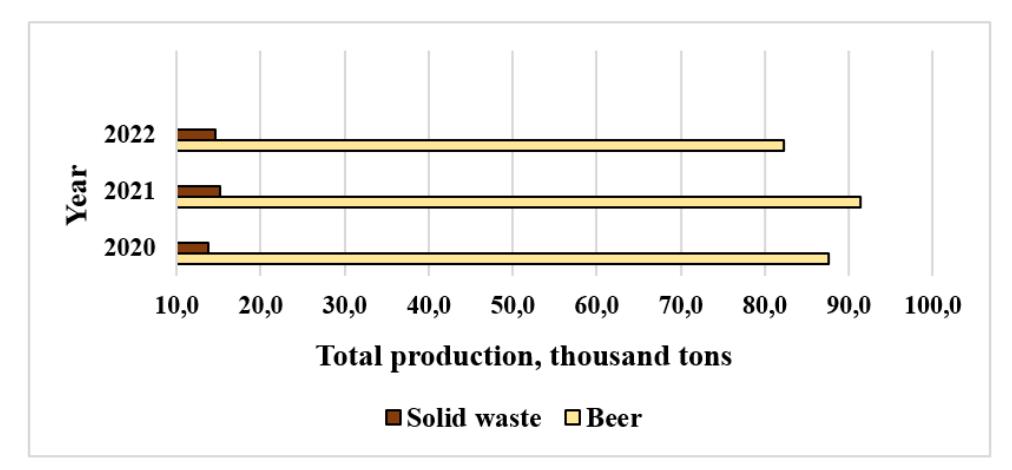


Figure 1. Production of beer and solid waste, thousand tons (2020-2022) [8,9].

The spent grain can also be obtained in whisky production at the end of the malt mashing step. Due to the expansion of the range and variety of raw materials used (different types of cereal crops and their mixtures) for beer making, the number of types of spent grain obtained is also increasing. Thus, it can be obtained from barley and rye, oats, maize, wheat, and rice [6].

In the case of the alcohol industry, the appropriately named spent grain is a secondary raw material or a waste product resulting from ethanol production. The production of alcoholic spent grain is similar to the above type. It is formed during the filtration of mash, which is a mixture of the initial grain raw materials with water, which has undergone the stages of cooking and saccharification. The spent grain obtained during alcohol production has a dense, homogeneous consistency with specific organoleptic indicators such as taste and smell, as well as color from dark yellow to brown. The percentage of spent grain obtained during ethanol production is also quite high. It varies from 60 to 65% of the original grain weight, which in physical units can be represented as 18-19.5 kg/day of alcohol produced [10].

3. Chemical composition

Referring to the above-mentioned, spent grain has interested researchers from different parts of the world, because, being a by-product of brewing and ethyl alcohol production, they are not used further in production, but represent production waste and have some negative consequences: a decrease in the output of finished products and, accordingly, the profit of producers and, no less importantly, affect the environmental situation of both individual countries and the world. It is stated that 70% is distributed for animal feed as an alternative to zero-waste production, 10% is processed into biogas and the remaining 20% is disposed of in landfills [11]. In addition, it was found that spent grain has a rich chemical composition, which provoked even more interest in this secondary product. The chemical composition of spent grain can vary depending on the quality and type of grain raw material used, the time of harvest, and the malting and mashing conditions. Nevertheless, spent grain contains a high amount of macro- and micronutrients such as proteins and, respectively, substitutable and essential amino acids in their composition, fats and fatty acids, polyphenolic compounds, vitamins and minerals, and at the same time dietary fiber [12]. For this reason,

new research work is increasingly being observed in the food and agricultural industries, medicine, and other fields to determine the potential of recycling this type of waste with maximum benefits for people and the environment.

Due to the structure of the raw material used in beer production and alcohol production, namely malt, the chemical composition of the resulting spent grain is due to its high biological value and it is common to consider this by-product as a lignocellulosic material. This is since the spent grain is predominantly the outer component of the grain (the shell), from which follows an increased content of dietary fibers such as cellulose (a polysaccharide of a linear structure consisting of glucose residues), hemicellulose and lignin (a phenolic polymer), which are insoluble dietary fibers. Their quantity can reach up to 50% of the total weight of the spent grain. Regarding hemicellulose, it should be mentioned that in spent grain it is contained in the form of arabinoxylans, non-starch biopolymers, which are present in all parts of cereals and consist of arabinose and xylose. In brewer's spent grain, the arabinoxylan content can reach up to 40 percent of the total dry matter. In addition, the spent grain has a high monosaccharide content in terms of dry matter, in particular glucose, xylose, and arabinose. In addition to fiber, spent grains are also rich in proteins, the content of which varies from 15 to 25%, and to a lesser extent in fats and residual endosperm starch [13,14]. The proteins of spent grain include about 30% of essential amino acids, which cannot be synthesized by the animal organism, but play an important role in the life support of these organisms, including the human organism. The most common essential amino acid included in the composition of spent grain is lysine. In addition to lysine, essential amino acids in spent grain include leucine and isoleucine, methionine, tryptophan, phenylalanine, and threonine, while non-essential amino acids include cysteine, glycine, proline, tyrosine, serine and others [7]. The most common lipids found in the composition of spent grain are triglycerides and their content varies from 55 to 67% (in the case of brewer's spent grain), the content of free fatty acids is inferior to triglycerides and is 18-30% (typical for brewer's spent grain). Free fatty acids include linoleic acid, which is an essential fatty acid (ω -6), as well as oleic acid (ω -9), stearic acid, and palmitic acid. In addition, lipid composition acts as a source of volatile compounds, including acetic acid, butyric and propionic acids [15]. Moreover, compounds of phenolic origin can be found in the composition of spent grain, which is most represented in the form of ferulic and p-Coumaric acids [16].

Other elements included in spent grain include vitamins and minerals-microelements required by the human body in milligrams and micrograms to support its vital functions. The minerals include silicon, calcium, cobalt, copper, iron, magnesium, phosphorus, potassium, selenium, sodium, sulfur, and manganese. The vitamin composition is mainly represented by water-soluble B vitamins (for example, biotin, pantothenic and folic acids, thiamin, riboflavin, and others) and fat-soluble tocopherols (vitamin E) [14].

4. Biological value

Having considered the chemical composition of spent grain and its peculiarities, it is possible to assert the high biological importance of this by-product, which should not be ignored, but on the contrary to consider in more detail and determine the possible favorable effects on the health and life activity of the population. With its high fiber and protein content, as well as the presence of essential amino acids and fatty acids, vitamins, minerals, and phenolic components, spent grain can be analyzed as a potential ingredient in food products.

Hence a need to investigate the health benefits to the human body of both spent grain as a whole and its constituent components [11-14].

4.1 Dietary fiber

Dietary fiber is a class of substances in which polysaccharides, specifically carbohydrates with three or more monomers, occupy the major part. However, the exception is lignin, which refers to phenolic compounds. A distinctive feature of this class is that they are resistant to the influence of endogenous enzymes of the digestive tract, as a consequence of which they are not broken down and assimilated by the small intestine, but still fulfill their role affecting the organism [17].

The composition of spent grain consists largely of insoluble dietary fiber, which includes cellulose, hemicellulose, and lignin, and to a lesser extent, soluble fiber. A major part of soluble fiber is identified as θ -glucans, which range from 4.7 to 13.4% of all carbohydrates in barley brewer's spent grain [15].

Research has been conducted for many years related to dietary fibers and their effects on the human body. They have the potential to reduce low-density cholesterol [18], to minimize the risk associated with diseases such as coronary heart disease, diabetes mellitus, and obesity, and also dietary fiber can improve intestinal peristalsis, which has a beneficial effect on the entire gastrointestinal tract [19, 20]. Regarding the differentiation of fiber into soluble and insoluble fiber, some differences have also been found in their effects on the body: soluble dietary fiber has immunomodulatory and anti-inflammatory effects, while insoluble fiber stimulates the intestine, being the main source of energy for its microbiota [21-23].

4.2 Proteins and amino acids

Proteins are biopolymers whose monomers are amino acids linked by peptide bonds. These substances play an integral part in the formation and repair of cells and tissues and are part of salts that are involved in maintaining osmotic balance. Also, amino acids form various complex protein molecules (glycoproteins, nucleoproteins, lipoproteins), hormones, enzymes, antibodies, and other protective components of the immune system, which allow our body to function normally [24].

Traditionally, the biological value of protein is determined based on its amino acid composition (qualitative and quantitative, as well as the ratio of essential to substituted amino acids), while taking into account individual human needs and the degree of digestibility and bioavailability of this type of protein by the body [25]. Despite the lack of precise data concerning the quality of spent grain proteins, we should not neglect the fact that in its composition the percentage of protein can reach 30%, which is not inferior to some types of food products of animal origin. It should also be added that brewer's spent grain from barley contains 7 essential amino acids (lysine and leucine have the highest proportion) and 11 non-essential amino acids in varying amounts, of which histidine and glutamic acid are predominant [7].

In turn, in addition to the fact that amino acids are part of proteins and fulfill a building function in the human body, the deficiency of each of them leads to a number of negative consequences that can be avoided with proper nutrition, which includes not only the necessary qualitative composition of amino acids but also a sufficient amount of them. For example, lysine has an antiviral effect, is able to reduce the level of triglycerides, and ensures the growth of bone tissue. Its deficiency contributes to a decrease in the number of red blood

cells and hemoglobin, provokes a lack of calcification of bones, and degenerative changes in muscles, liver, and lungs can be observed. Considering the fact that it is found in relatively small amounts in cereals and the daily requirement is high, its elevated content in brewer's spent grain may be one of the solutions to this problem [26].

4.3 Lipids and fatty acids

Lipids are organic high molecular-weight substances consisting of fatty acids and glycerol esters. One of the main functions of these nutrients is to saturate the body with energy, as well as the ability to reserve it. Other functions include plastic (they are part of cell membranes), thermal insulation, and regulatory functions (fats are precursors of steroid hormones), in addition to being carriers of fat-soluble vitamins [24].

The biological value of fats, as well as proteins, is directly related to their constituent parts, i.e. it is determined by the presence of essential fatty acids, both quantitatively and qualitatively, as well as their bioavailability [24].

Based on the lipid composition of spent grain, in which triglycerides and a smaller amount of free fatty acids predominate, it can be concluded that this product has a fairly high energy value directly due to neutral fats (triglycerides) and nutritional value due to free essential fatty acids (ω -6), as well as monounsaturated fatty acids [15,24]. Several studies have shown that consumption of foods containing linoleic acid leads to a reduction in low-density lipoprotein levels, consequently minimizing the risks of cardiovascular disease [15,24,27]. In addition, linoleic acid can reduce the level of triglycerides in the blood consumed with food and restrain the occurrence of cardiac arrhythmias [27]. In addition to the above, ω -6 fatty acids preserve the integrity of cell membranes, intensify the synthesis of hormone-like substances, reduce psycho-emotional stress, and strengthen the functional state of the dermis [28].

Despite the fact that oleic acid, which is a part of spent grain is not an essential fatty acid, it, as a monounsaturated acid, has a number of positive effects on the body: it has a preventive effect against heart attacks, regulates blood cholesterol and carbohydrate metabolism, improves memory, and has anti-inflammatory effects [28].

4.4 Phenolic compounds

Phenolic substances are the most widespread group of natural biologically active substances, the number of which exceeds 8000 compounds. They also belong to the main classes of secondary metabolites of plants [29]. From the chemical point of view, phenolic compounds are substances consisting of a benzene (aromatic) ring and one or more hydroxyl groups (-OH), in particular their derivatives [30]. This class of compounds is widely known for its biological properties, which include: antioxidant, anti-inflammatory, and antimicrobial abilities, can act as cardiovascular and neuroprotective agents, and helps to reduce the risk of cancer and diabetes [29].

Ferulic and *p*-coumaric acids have been identified as the main phenolic compounds in the composition of spent grain, which belong to the hydroxycinnamic acid group, formed from cinnamic acid, and, most often in a bound state [16,31]. Hydroxycinnamic acids have a simple chemical structure with a C6-C3 phenylpropanoid at the base and the carboxyl group located in the side chain [29].

In turn, hydroxycinnamic acids, as phenolic compounds, have all the above physiological properties and contribute to the quality of life. For example, these acids play

an important role in the prevention of coronary heart disease due to their ability to inhibit oxidative changes in low-density lipoproteins and total cholesterol [32].

So, the presence of hydroxycinnamic acids in the composition of spent grain also suggests an increased biological value of this industrial waste, which raises even more interest for further research on its integration into food products.

4.5 Vitamins and minerals

Micronutrients, which include vitamins and minerals, are essential substances for maintaining the normal functioning of all body systems, i.e. they are biologically important elements for humans [33]. Although a small number of micronutrients is sufficient to maintain the vital activity of the organism relative to the needs for proteins, fats, or carbohydrates, their deficiency can lead to serious disorders, some of which cannot be determined at the initial stages. For example, vitamin E deficiency can provoke the development of Bassen-Kornzweig syndrome (a disorder in which fats and fat-soluble vitamins from food cannot be absorbed), leading to ataxia and systemic pathology-mucoviscidosis. Alternatively, potassium deficiency is one of the causes of cardiac dysfunction [33].

Based on all of the above, it is appropriate to conclude that in terms of its functional features, spent grain is of great importance for the health and normal functioning of the human body, which is explained by the main components included in its composition. However, since this type of by-product is not recommended for human consumption in its native state, it is possible to ensure its maximum nutritional value through the production of certain food products - foods enriched with spent grain. In this case, the biological value will not only not be lost or reduced, but, on the contrary, may even be increased.

5. Spoilage and preservation methods

Despite the above-mentioned advantages of the composition of spent grain as a potential ingredient in the food industry and concerning the human body, the peculiarities of the chemical composition also generate several difficulties that can induce serious problems. In such cases, not only the quality of the waste but also its quantity plays a role. Thus, based on the previous information, malt processing generates a significant amount of spent grain as waste: per 100 kg of malt, approximately 100-130 kg of spent grain with a high water content (70-80%) are generated. Due to high moisture content during storage, the spent grains sour and lose their nutritional value [34]. In addition to high moisture content, spent grains are rich in polysaccharides and proteins, which makes them more vulnerable to microorganisms and becomes an attractive growth medium for them. In one study, spent grain was stored for thirty days at room temperature, and eight isolates of some fungal genera, including Aspergillus, Fusarium, Penicillium, Rhizopus, and Mucor, were found [7]. This fact hurts the safety and stability of the spent grain, as high concentrations of these fungi contribute to the accumulation of mycotoxins with strong toxicity. Also, despite its microbiological stability after production, the spent grain is subject to rapid multiplication of microaerophilic and anaerobic microorganisms, which reduces both the stability and safety of the waste. In addition to the reduced shelf life in native form, the transport of wet spent grain is also difficult and materially expensive [7]. Accordingly, when considering spent grain as a component of food products, their stabilization and optimization of storage conditions are necessary.

One of the directions of spent grain stabilization is the reduction of moisture content, which can be achieved by drying. In some countries, beer-producing companies use special

installations that allow to reduce the moisture level in the spent grain and this is done in two stages. In the first stage, the moisture level is reduced to 65% and below by pressing, while the second stage reduces the moisture content to below 10% [13]. The mechanical dewatering of the spent grain in the first stage can be done in two ways: using a press-screw separator or a hydrocyclone thickener [34].

As a second step, that is drying, several methods have been proposed: freeze-drying, drying oven, and superheated steam drying [7]. The analysis of the chemical composition of the spent grain after lyophilization application did not reveal significant changes, which may indicate that the nutritional value of the secondary product is preserved. However, freeze-drying of the spent grain was not economically efficient. The drying oven also showed no changes in the chemical composition of the spent grain and is considered to be a fairly acceptable method of drying them, despite its energy intensity. It should be noted that the temperature in the chamber oven should not exceed 60 °C, as higher temperatures can lead to an unpleasant taste and a strong color change (darkening). There is also a risk of increasing the temperature of the grain as it approaches the exit of the drying chamber, which may contribute to the burning of the dried sample [7].

As an alternative method of drying, superheated steam has started to be used. By its specificity, it is more economical and effective, because this method uses less energy due to the circulation of steam in a closed circuit than in a drying oven, but the degree of extraction of organic compounds increases. In addition, the use of superheated steam reduces carbon emissions into the environment and minimizes the risk of explosion [13]. When using this method, attention should be paid to the rate at which the steam passes through the material and the temperature inside the unit, as excessively high temperatures (around 180 °C) have been shown to affect starch gelatinization [7, 13].

Other methods to extend the shelf life of spent grain include the following: cold preservation and preservation with food acids [7,13]. Freezing or cold preservation was found to be impractical because freezing requires large production areas and significant energy costs to maintain a certain sub-zero temperature. Also, changes in the quantitative content of arabinose have been found during freezing [7,13,14].

Solutions of lactic, acetic, formic, and benzoic acids were used for the preservation of spent grain with food acids. Increased efficiency of benzoic and methanoic acids application is highlighted.

Despite the positive results in increasing shelf life, the application of this technology may affect the demand for the product in which the acid-treated spent grain will be used. This is because there is currently a trend towards the consumption of products based on natural ingredients, with so-called "clean labeling" [7].

Summarizing the above, we can conclude that the most attractive method of extending the shelf life of spent grain is drying, which allows us to obtain a fairly stable product with minimal changes in composition and with acceptable energy costs. However, given that the drying process has several variations, it is necessary to choose the most appropriate method for a particular case in order to achieve the highest results from the process.

6. Nutrient extraction

Based on the chemical composition analysis and the conclusions drawn earlier, it is necessary to consider ways of extracting those nutrients contained in the spent grain for their further use for various purposes, such as food fortification the creation of bioactive supplements, and so on. This will not only diversify the market but also allow to use of food

industry waste, which will have a favorable impact on the environmental situation in the countries and will have a positive impact on the economic component of individual industries that generate this type of waste [34,35].

6.1 Protein extraction

One of the peculiarities of spent grain at the time of its obtaining is its high moisture content (70-80%), which makes it necessary to perform an additional operation. This treatment includes the drying process and allows for prolonging the stability of the product, reduces its volume, and facilitate the processing of the material for the extraction of protein substances [34,35]. After the initial processing of the component used, a number of methods are applied to allow the extraction of protein products, of which alkaline extraction is the most widely used. In addition to drying, prior to the extraction process, the spent grain may be subjected to various pre-treatments to facilitate the release of protein from the spent grain structure. These can include degreasing, particle size reduction by grinding, enzymatic hydrolysis, and ultrasound. In addition, enzymatic hydrolysis and ultrasound can be applied as independent extraction methods [35].

Alkaline extraction is a sufficiently studied method for protein extraction not only from spent grain but also from other agricultural products. The essence of the method is that the alkaline medium provides solubilization of protein, thus changing its configuration, charge, and, accordingly, interaction with other substances [35]. One of the most used alkalis is sodium hydroxide in the obtaining of protein components. The main parameters of this method that determine its efficiency are the type and concentration of the alkali used, the extraction temperature, the ratio of solid and liquid phases, as well as the values of the isoelectric point at which protein precipitation occurs. By modifying the above conditions of the method, a rather wide range of protein extraction yields (18-82%) was obtained, and the values of its purity varied from 37 to 69% [35].

Since the composition of spent grain, in addition to large amounts of protein, also contains significant concentrations of hemicellulose, the method of extraction with the help of acids and reducing agents, such as sulfuric acid and sodium bisulfite, is used. This increases the solubility of proteins and facilitates their release by hydrolysis of the said polysaccharide and breaking disulfide bonds in proteins [38]. In addition to acids, this extraction method involves autoclaving the material at temperatures ranging from 121 to 130 °C and lasting 30-60 min, resulting in an accelerated process of decomposition of cell wall components. When acid extraction was used, the yield of protein substances was 63-90%, which is superior to the previous method, but the protein purity was reduced and was 24-39% [35].

Another method of protein extraction from the composition of spent grain is solvent extraction. Among the tested methods, the following two methods were considered specifically for spent grain: deep eutectic solvents (DES) and extraction in the presence of pressurized solvents. Deep eutectic solvents simplify the process of protein extraction due to the possibility of fractionating and dissolving lignin and starch, which are part of the material used [37]. When deep eutectic solvents are used, the heating parameters include a temperature of 80 °C for 4 h (low temperatures and long-time intervals), while if solvents are used in combination with pressure, the heating is carried out at higher temperatures (150 °C) and the duration is shortened accordingly. The proteins are then separated into a liquid fraction. The disadvantage of these methods may be the violation of functional characteristics of proteins due to the impact of high temperatures, as well as the need to analyze the

maximum permissible concentrations of each type of solvent and additional studies of their toxicity and impact on the human body. At the same time, the degree of protein extraction by these methods varies from 69-79% depending on the solvents used [35].

Hydrothermal and subcritical methods, which use water as a solvent, can be considered environmentally friendly and chemical-free methods of protein extraction from spent grain. In the case of hydrothermal extraction, high or low temperatures are applied at short and long-time intervals, respectively, to facilitate protein extraction. Subcritical extraction uses water brought to a temperature above 100 °C and not converted to vapor by a special pressurized system. According to the results of the analyses carried out, the protein yields were similar and, in some cases, higher than those of acid and alkaline extractions. For example, using hydrothermal protein release, 66% of the protein compounds were extracted and the protein purity was 53%. The treatment was carried out for 24 h at 60 °C [35, 38]. Subcritical extraction conditions allowed the colloidal dissolution of about 78% of proteins from the spent grain. These conditions implied a temperature regime of 180-185 °C maintained for 150 min [39].

Enzymatic extraction is designed to solubilize protein by breaking down carbohydrates and proteins in their matrix, resulting in partially degraded protein in the process of hydrolysis (protein hydrolysate). Carbohydrase and protease enzymes are used to perform the above actions. The yield of extracts in this method is quite wide and ranges from 31-86%, and protein purity is mostly equated to 40% [35].

It was also found that the use of ultrasound treatment had a positive effect on the amount of protein released. In one study, the yield increased from 46 to 86% after ultrasound treatment with a power of 250 W and a duration of 20 min at the time of alkaline extraction [40]. The use of microwave radiation during alkaline extraction also helps to increase the extraction rate of protein compounds. In addition, the use of microwaves during hydrothermal extraction provided an extract yield of about 90%. These values were achieved as a result of a ten-minute exposure at 110 °C and a maximum microwave power of 1800 W [35, 41].

6.2 Extraction of carbohydrates

As for the extraction of proteins, so for the extraction of polysaccharides from spent grain, chemical and enzymatic extraction methods with or without primary treatment are mainly used, less often combined, as the full range of their action is not yet fully understood [7, 42]. To date, when choosing a method of extraction of components that will later become part of the technological chain for the production of food items, preference is given to enzymatic methods. This is due to a number of factors related to the safety of the extract obtained. Firstly, the use of enzymes allows for closer monitoring of the process and the nature of the components released. Secondly, it will allow for greater preservation of nutritional value and environmental friendliness, which will present food products containing extracts obtained by this method in a more favorable light to consumers. Thirdly, the enzymatic extraction process does not generate potentially toxic by-products, which also makes it more stable and environmentally friendly [43].

However, difficulty arises during extraction due to the complexity of the structure of the polymers comprising the spent grain, hence a complex of enzymes must be used to fully hydrolyze them. For example, the final degradation of hemicelluloses will require the use of several different enzymes, which are of the following types: xylanase, θ -xylosidase, feruloyl esterase, acetyl esterase, glucuronidase, glucuronoyl esterase and α -L-arabinofuranosidase [7].

In addition to studies on the extraction processes of components from spent grain, various methods are also being investigated to facilitate the extraction of these components. These include the use of microwave radiation or ultrasound, as well as extrusion processing [7]. Thus, one of the works considered the effect of physical and thermal primary treatments, relying on the improvement of extraction yield and efficiency. These treatments were represented by grinding and exposure to microwaves. Microwave treatment combined with acids and alkalis proved to be the most effective method. In this type of treatment at a temperature of 160 °C for 10 min and in the presence of sodium hydroxide, the polysaccharide yield was 49%, while the physical treatment by grinding did not significantly change the monosaccharide yield [44].

Ultrasound can also be used as a stand-alone method, which is used for the isolation of arabinoxylans. When comparing this method with alkaline extraction, it was observed that the use of ultrasound waves helps to shorten the process time and is consequently a less energy-intensive method [7].

6.3 Extraction of phenolic compounds

Phenolic compounds, being natural biologically active substances, are components that can significantly increase the functional value of products, which is currently one of the directions in the creation of innovative food items. Therefore, there is a need to search for new methods of their production and growing interest in the study of alternative sources of phenols and their derivatives. One of the solutions may be the extraction of phenolic compounds from spent grain, which is carried out by various methods, each of which has a number of its features. Modern developments are based on the use of advanced extraction methods: microwave radiation, hydrolysis in the presence of acids, saponification with sodium hydroxide, as well as liquid and solid-liquid extraction. Most often the isolation of phenolic acids from the composition of spent grain resorts to solid-liquid extraction, which is due to the convenience of its implementation, a significant degree of efficiency, and a wide range of applications [13]. The methods of obtaining phenolic compounds from spent grain by solidliquid extraction include extraction in a hot water bath using different solvents: methanol, acetone, ethanol, hexane, ethyl acetate, and direct water separately, as well as a mixture of methanol, ethanol, and acetone with water. From all the experiments carried out, the highest yield of phenols was found in the extract obtained using 60% acetone as solvent. At the same time, all the extracts obtained irrespective of the solvents used showed antioxidant activity to different degrees, which can be considered as a positive aspect of the method. Another method of solid-liquid extraction of phenolic components, as well as other constituents of spent grain, is enzymatic hydrolysis. As mentioned above, this method can preserve the bioactive capacity of the extracted components and at the same time will be more environmentally friendly compared to chemically extracted substances [13,45].

The next extraction method can be identified as high-intensity ultrasound, which improves the release of complex chemicals found in plants, particularly phenols, through cavitation [46]. This method uses high sound power at low frequencies, which favors compression and decompression of the liquid medium, from which follows the destruction of the cell wall, which in turn increases mass transfer [47]. Also, microwave technology can contribute to the efficiency of extraction of polyphenols from spent grain by heating the internal water molecules. The superheating of the molecules leads to the destruction of the cell wall of the sample, which helps to facilitate the release of the associated compounds [48].

Other methods by which phenolic compounds can be extracted from spent grain include high-pressure methods. In combination with pressure, different solvents are used, which differ in their physicochemical characteristics such as viscosity, density and dielectric constant. Also, by modifying the pressure and temperature parameters, it is possible to achieve different polarity of the solvent and, consequently, influence its ability to solvate ions or molecules of the soluble components [49]. The ohmic heating technology can also be considered as a method for extraction of phenolic compounds from spent grain. The method is based on the supply of electricity through the extraction medium, which is dispersed as heat due to the electrical resistance of its components, which promotes electroporation and electrical destruction of cell structures. This in turn promotes better mass transfer between sample and solvent [47].

In this way, among the current technologies for extraction of phenolic components, ultrasound and high-pressure fluid extraction are popular methods. However, methods such as microwave radiation extraction, ohmic heating and pulsed electric field are less well studied, hence there is an additional need to analyze them for further insights and data to draw appropriate conclusions on their feasibility and effectiveness for extraction of phenolic compounds [47].

6.4 Lipid extraction

As mentioned above, spent grain has various chemical compositions, which also include free fatty acids in sufficient quantities [15]. In addition, fatty acids can be essential, i.e. substances necessary for the human body, which it cannot synthesize on its own, but must be obtained from food. This fact is important for the food industry, as the extraction of free essential fatty acids inherent in spent grain can be a good solution for food fortification and additional utilization of by-products.

In its essence, the extraction of lipid compounds is a method aimed at breaking ester bonds with other material components, such as proteins or phenolic substances. Consequently, it is predominantly a method to be performed in an integrated manner, i.e. to affect not only lipid fractions but also related substances [42]. At the same time, despite the complexity of the spent grain fraction matrix, one work attempted to extract fats by simple extraction. For this purpose, an alcohol solution with a volume fraction of 20 vol.% was used and the extraction was carried out for 24 h at room temperature. As a result, the authors were able to extract 5 fatty acids, of which 2 were essential fatty acids. These fatty acids included: palmitic, stearic, oleic, linoleic, and linolenic acids [50].

Extraction in the presence of a mixture consisting of chloroform and methanol in a ratio 2:1 was also applied. The spent grain was previously ground into fine particles of small size, and after the addition of the mixture, extraction was carried out for 30 s under conditions of high-speed homogenizer. According to the results of the experiment, the composition of fatty acids that were able to be released into the extract was presented in the following proportions: polyunsaturated fatty acids made up the majority of the extract (50-55%), followed by saturated acids in the amount of 25-30% and a smaller proportion was occupied by monounsaturated fatty acids (15-20%). The qualitative composition was represented by linoleic (50%), palmitic (25%), oleic (15%), linolenic (5%) and stearic (<5%) acids and traces of docosahexaenoic, eicosapentaenoic and arachidonic acids (ω -3 and ω -6) were also found [42,51].

An enzymatic method of lipid extraction from spent grain was also tested, in which the spent grain sample was fermented with *Bacillus subtilis* culture for two days at 37 °C. The data collected were analyzed in comparison with the extract obtained from unfermented spent grain, after which the authors found that the amount of palmitic and linolenic acids extracted was independent of the treatment under the influence of biological catalysts (in this case, microorganisms), while oleic and stearic acids were dependent (the yield of oleic fatty acid increased after biocatalytic treatment, while that of stearic acid decreased) [42,52].

Referring to the above-mentioned, it can be concluded that spent grain is a good material for efficient extraction of its macronutrients as well as phenolic compounds, which forms an additional area of application of this by-product. Expanding the scope of use will reduce the amount of utilized waste and consequently reduce the negative impact on the environment.

7. Disposal methods and other applications

Given the volumes of spent grain produced in the beer or ethanol production process, there is increasing talk about the need to dispose of them without landfilling in huge quantities or to recycle them to minimize environmental pollution [53]. As discussed above, one alternative would be to use the spent grain as a material for extracting useful substances, but either way, some of the waste is left behind and eventually disposed of in landfills. Thus, today the most frequently used methods of utilization of spent grain are: disposal in landfills, use in its initial state in animal husbandry, production of various feed mixtures with high protein content using starter, preservation for extending shelf life by silage, drying or mechanical dehydration, as well as the use of spent grain as organic fertilizer and soil ameliorant [53].

For example, raw brewer's spent grain without additional treatment has been used for feeding both domestic animals and poultry for quite a long time, but as a rule, their purpose is narrowed down to feeding ruminants. However, as a result of special treatment, brewer's spent grain can become an excellent feed additive for other mammals and birds. Today there is a demand for a feed additive called "Probiocel", which is used as an additional source of nutrients for fattening piglets, broilers, and laying hens. This additive is produced by homogenizing brewer's spent grain with bran, digesting the resulting mixture with especially isolated Bacillus subtilis bacteria, which in turn partially process dietary fiber into digestible carbohydrates. Selenium is then added and after fermentation, the resulting mixture is dried to extend the shelf life of this supplement. In this form, it can be stored for a year. It also has a positive effect on the animal, both on its health and physiological features [54]. Despite the positive aspects, in some countries the feeding of spent grain to animals is being minimized due to some restrictions, for example, a reduction in the number of farms and people involved in animal husbandry, and stricter legislation that requires spent grain producers to have a certificate of quality and appropriate documentation that allows them to distribute spent grain as an alternative livestock nutritional supplement [16].

Another method of spent grain utilization is disposal to landfills or special polygons (about 20% of the amount of spent grain produced). However, this method is one of the least preferable, as it is associated with numerous environmental problems: air and water pollution, unpleasant odors, and associated health hazards [11,16]. It has been noted that the disposal of one tonne of brewer's spent grain releases an equivalent of 513 kg of CO_2 into the atmosphere [55]. Such indicators are disappointing and even dangerous for the ecology of the

world and, therefore, require measures to eliminate this problem, which is caused by the amount of waste produced, its increased moisture and reduced shelf life, and costly conservation. Thus, it is necessary to consider the concept of bioprocessing of brewing and distillery by-products (spent grain) to ensure environmental and economic prosperity [16].

As an example of bioprocessing of spent grain, its application as a solid biofuel for energy generation can be considered, but for this purpose, the spent grain needs to be dried beforehand [16]. Also, in one study, bio-oil, hydrogen, and ethane were produced by pyrolysis of spent grain [56]. Another study reported the use of spent grain to produce bio-oil and bio-coal by hydrothermal liquefaction [57]. In addition, the spent grain can be modified by biological processes (e.g., anaerobic digestion or fermentation) into biogas and bioethanol appropriately [58, 59].

Also due to its high content of polysaccharides, proteins, vitamins, and minerals, spent grain can be an optimal medium for the cultivation of various microorganisms such as fungi and bacteria [16]. Experiments have been repeatedly carried out to grow different microorganisms using spent grain, aiming to produce a range of enzymes: amylase, cellulase, hemicellulase, protease, and enzymes that promote lignin degradation [60]. In addition to the production of enzymes, during the cultivation of microorganisms, spent grain can be transformed into the following chemical components: lactic and succinic acid, itaconate, and xylitol [16].

It can be added that spent grain can be used to produce building materials for wooden buildings, such as bricks, or the production of pulp and paper, due to its rich chemical composition, namely fibers [61]. In many studies, brewer's spent grain has been able to produce paper towels, business cards, and cellulose pulp properly [62,63]. In addition, the spent grain has been tested as an adsorbent for the removal of pollutants from wastewater, for example, synthetic dyes used in the textile and pulp and paper industries have been removed [64].

Thus, the problem of utilization of spent grain, as well as other by-products of production, is at the peak of discussions and search for solutions, since the increase in discarded waste is directly related to the worsening environmental situation in the world. This is why it is necessary to expand the use or utilization of spent grain, which will reduce the carbon dioxide emissions generated during the decomposition of spent grain when they are buried.

8. Application in the food industry

For many reasons, it was proposed to study the properties of spent grain concerning food products in different areas: bakery, pasta and confectionery products, milk and dairy products, meat products, etc. This is explained by the chemical composition of spent grain, which allows it to be classified as a biologically valuable product but is not sufficiently acceptable for human consumption as an independent product in its native form, in terms of its taste, which creates the need for its integration into other food products, as auxiliary raw materials. Given the limited shelf life and the need for large spaces for its storage, various methods for its processing are also being developed to obtain optimal moisture levels to extend shelf life and further use in the food industry, as already mentioned earlier. Also, population growth and the corresponding expansion of the food industry sector are becoming compelling reasons to search for alternative technologies, which will make it possible to

obtain highly nutritious products at fairly low prices and without harm to human health and the environment [6].

In this case, the purpose of this chapter and the work as a whole is to consider the currently known ways of the use of spent grain in various products suitable for human nutrition, with its technological properties and behavior at the time of processing of products into which spent grain were introduced.

8.1. Production of bakery, pasta, and confectionery products

The production of bread and other bakery products is one of the main areas of the food industry, which ensures the daily satisfaction of the needs of the majority of the population [66]. The variety of these products is becoming wider every year, which is associated with the dietary characteristics of consumers or their taste needs (for example, gluten intolerance or lack of desire to eat products with chemically derived additives). It follows that the addition of spent grain in the production of baked items can make them competitive and bring innovative food products with increased nutritional value to the market, which is a desirable aspect in the development of the food sector and, in particular, the bakery industry [67].

In one of the studies, two types of bread were produced using spent grain. In the first case, the spent grain was added directly to the dough; in the second case, at the initial stage, a sourdough was produced from the spent grain, which was subsequently added to the dough. In both cases, the spent grain content was 15%, and the samples were characterized by a high fiber content: 11.9% in the spent grain flour added to the dough and 12.1% in the sourdough flour. In terms of mineral composition, sourdough bread made from spent grain turned out to be more enriched compared to bread with the addition of flour from the same spent grain. For example, the calcium content in sourdough bread was 107.9 mg/100 g, while in bread without sourdough this figure was 98.9 mg/100 g, magnesium values were 12.7 mg/100 g and 11.6 mg/100 g, respectively, and potassium - 100.4 mg/100 g and 98.9 md/100 g. Bread acidity was also higher in the sample using sourdough (pH 5.3 versus 5.8) [65]. It was also noted that with an increase in the percentage of spent grain from 0 to 20% with its further use in the production of bread, the content of some mineral compounds also increases: the amount of calcium increased from 76.44 mg/100g to 150.93 mg/100 g, magnesium - from 87.12 mg/100 q to 176.81 mg/100 q and potassium - from 116.04 mg/100 q to 225.49 mg/100 g [66].

Another study analyzed bread made from spent grain starter through fermentation for eight days. The content of spent grain in the sourdough was 25, 50, 75% and the sourdough was exclusively based on spent grain (100%). Based on the results of the experiment, it was determined that sourdough bread with low concentrations of spent grain (25 and 50%) was distinguished by relatively high porosity, acidity, and corresponding moisture content when compared with a sample made from 100% sourdough. In addition, the bacteriostatic properties of the product were revealed due to the addition of spent grain, which is due to the presence of early signs of spoilage in the sample without the addition of spent grain (control sample). And the introduction of spent grain into bread made it possible to increase its shelf life by 1-2 days, due to a decrease in the activity of microorganisms that cause spoilage of bread [67].

However, it was found that replacing wheat flour with spent grain flour causes some technological deterioration: a decrease in gluten yield with a worsening of its quality and, as a consequence, a reduction in the sedimentation ability and stability of the dough along with

an increase in its softening. These negative aspects were justified by the duration of kneading the dough (longer than kneading wheat dough), the increased content of protein and dietary fiber, as well as the increased force to stretch the dough, which was increased. Based on this, the authors identified the optimal content of spent grain in bread made from wheat flour, at which the bread will not differ significantly in appearance, crust condition, and crumb properties. This can be achieved by adding 10% spent grain, however, in any case, color changes in the product are observed, which is associated with the characteristics of the raw materials used (from the usual light cream color, the sample moved to a brown color, the intensity of which directly depended on the concentration of the added spent grain: darker with increasing and lighter when decreasing) [6,68].

The following studies demonstrated the relationship between the amount of spent grain used and the physical properties of the resulting bread. Thus, the water absorption capacity of the product increased with increasing concentration of the introduced by-product: at 0% this value was equal to 58.40 mL/100 g, and at 20% the content was already 66.67 mL/100 g. Experts argued this by the composition of the raw materials, that is, the increased content of protein substances and non-starch polysaccharides, which are capable of absorbing large amounts of moisture [68]. High concentrations of proteins and dietary fiber also affected the duration of the kneading, increasing it several times (from 3.43 min to 17.57 min) [69]. Changes in the weight and volume of the finished product were also demonstrated: with an increase in the added spent grain, the weight of the bread increased from 127.58 q to 148.85 g, while the volume decreased from 2.92 cm³/g to 2.46 cm³/g. This is again due to the spent grain's richness in protein and fiber, which absorb large volumes of water, giving the product a firmer and more durable structure. According to organoleptic characteristics, the same trend is observed, that is a lower acceptability of the product with growing concentration of spent grain in it. This is justified by the darker color, malt aroma and, as well as crumb texture [6,66,69].

As for pasta products, the addition of spent grain is a good option to increase the nutritional value with minimal changes in functional properties, despite the concentration of 25% [6]. One study analyzed pasta recipes with the addition of two types of spent grain: einkorn and tritordeum. The resulting pasta had a higher content of protein and dietary fiber, in particular θ -glucans, and some changes in antioxidant activity were also detected, with its increase. From an organoleptic point of view, these products turned out to be very acceptable [70].

Just like for the production of bread, when developing fortified pasta, two different fractions of spent grain were used: one containing 10-20% dietary fiber and the second containing 5-10% protein. Their quality was assessed based on a number of characteristics: relative chemical composition, optimal cooking time, sensory indicators. Thus, the addition of the protein fraction contributed to the production of pasta with a protein component content of about 18%, and fiber values exceeding 8%. In both cases, the color of the paste was significantly darker than the control sample. The optimal cooking time until the products were ready varied from 11 min to 13.5 min. In terms of the degree of elasticity when bitten, these pasta products were rated adequately [71].

Another similar study, based on the development of pasta by adding the protein and fiber fraction of spent grain products has been created with stronger gluten structure and binding characteristics, high hardness and elasticity, as well as dough viscosity, which is characterized by tensile strength, while glycemic index indicators were reduced. In addition, pasta products into which spent grain fiber was integrated showed lower cooking loss values

(3.47%), which was due to the amount of spent grain used in their production, according to the authors [72].

As a new direction in the pasta industry, we can highlight the work of Romanian researchers who tested the use of flour from spent grain and spelled flour (a type of dinkel wheat), which currently has low demand in the production of these flour-based products. The spent grain used in the study is a by-product of whiskey production, which was subsequently dried at 50 °C for 24 h, then crushed and sifted to a particle size of less than 200 µm. The goal of the work of Romanian experts was to increase the nutritional value of pasta through the introduction of two new types of flour: spent grain and hulled wheat. When mixing the dough, different amounts of spent grain were used to determine the optimal concentration based on sensory and physicochemical quality indicators. In conclusion, the authors finalized that from all analyses performed, the most acceptable results were achieved in the case of the sample that was produced by adding 10% spent grain [73].

Regarding the introduction of spent grain into the cookie dough composition, work was carried out aimed at determining the relationship between the size of the introduced particles and the quality of the finished product. As a result, medium- and large-sized particles demonstrated higher quality indicators compared to the fine fraction. For example, the distribution coefficient of raw materials in the mass of cookies was higher, as well as the organoleptic characteristics were more acceptable [74].

In one of the works, in the production of biscuits, replacing part of the wheat flour with spent grain in various ratios (0, 10, 20, and 30%). Samples containing a 20% concentration of spent grain tended to reduce hydrolysis and glycemic index, as well as a decrease in total starch when compared to the reference sample. In addition, changes in the percentage of dough composition, reducing the amount of wheat flour and replacing it with spent grain, contributed to an increase in the nutritional value of the finished products such as a significant growth in the content of proteins and bioactive compounds (phenolic acids) [75].

Among other things, the mechanism of the effect of thermally and mechanically untreated raw spent grain on the quality of biscuits was analyzed. Wheat flour in the dough was replaced by 15, 25, and 50% brewer's spent grain, the purpose of which was to evaluate the effect of concentrations on the content of nutrients (protein and dietary fiber), microbiological stability, and the sensory characteristics of the finished product. The authors recommend using spent grain to increase the nutritional value of cookies but in conditions of maintaining optimal replacement percentages, which should not exceed 25%. This will preserve acceptable organoleptic characteristics without compromising microbiological stability [76].

In the technology for the production of sugar cookies, wheat flour was replaced with spent grain obtained as a by-product during the production of ethyl alcohol in different ratios, which varied from 5 % to 12%. At the same time, the density of the dough changed from 1.32 g/cm³ to 1.26 g/cm³, and the humidity increased from 16.6% to 19%, since raw spent grain with a high moisture content was used. However, the authors note improvements in the quality indicators of the finished product: the density of the cookies decreased by 17.4%, the swelling capacity increased by 18.3% with a dosage of spent grain from ethanol production equal to 10%. In terms of physiological value, experimental examples are superior to control samples due to the content of essential amino acids represented by threonine, valine, isoleucine, leucine, and lysine, mineral compounds, such as calcium and phosphorus, as well as an increase in the concentrations of protein, fat and dietary fiber. Raising the fat content is a

positive aspect of this technology since it will reduce the amount of additional fat, and this, in turn, contributes to the production of a more affordable product [10].

In other work, spent grain flour was also used to partially replace wheat flour and increase the nutritional value of the finished muffins. Flour was added when forming the emulsion in various quantities: 5, 10, 15, and 20% of the total raw material content. The quality indicators of the finished products are represented by physicochemical (alkalinity, moisture content, weight loss of the product during baking, and specific volume) and sensory characteristics. Researchers recommend that to preserve organoleptic and physicochemical parameters, as well as to increase the nutritional value of muffins, a 15% concentration of brewer's spent grain flour should be used as the maximum amount [77].

Also, an attempt was made to introduce raw crushed brewer's spent grain into the recipe for gingerbread products in order to enrich the product. The quantitative content of spent grain, which replaced 1st grade wheat flour, was 5, 10, 15, 20 and 25%. Based on the results of the analysis, it was found that an increase in the dosage of spent grain leads to a gradual improvement in the firmness properties of the dough due to protein substances, which enhance the strength of the flour and result in greater firmness of the dough. From the point of view of sensory characteristics, the resulting products with the additive differed from the control sample without the addition of spent grain: they acquired a darker shade, malt flavor, and aroma. In terms of nutritional value, the experimental samples are superior to the control sample, since the addition of spent grain contributed to an increase in the content of protein, dietary fiber, mineral compounds (iron, zinc, manganese), and vitamins (mainly group B and vitamin E). From a microbiological point of view, no violations of requirements and standards were identified. As a result of the experiments, researchers recommend replacing 1st-grade wheat flour with crushed raw brewer's spent grain in an amount equal to 20% when producing gingerbread [78].

8.2. Dairy food production

In the production technology of dairy products, in comparison with bakery and other flour products, cereal crops are quite rare, which makes the use of spent grain more difficult [79]. However, despite this fact, many studies have been carried out aimed at using spent grain in the production of yogurt and cheese, to obtain a more enriched food item and expand the range of dairy products.

Thus, spent grain in various proportions was used as a substitute for fermentation in the production of yogurt. At the same time, a significant decrease in syneresis of the product was noted, a reduction in the duration of fermentation with an increase in the viscosity of yogurt. Products with the addition of 5% and 10% spent grain were characterized as maximum quality yoghurt, taking into account acidity and the development of lactic acid bacteria during storage, as well as rheological properties. However, higher byproduct concentrations (15-20%) resulted in a more stable dispersion system with reduced liquid separation and flowability of the finished product. In conclusion, the authors recommend the use of 10% spent grain in yogurt as the optimal amount, which will maintain fluidity and other physicochemical indicators at a good level, but with further study of its sensory characteristics, in particular the taste of yogurt [79].

Spent grain was used as an additive in the production of yoghurt in percentages of 2, 4, 6, 8, and 10%, and yoghurt without added brewer's spent grain was chosen as a reference sample. With an increase in the concentration of applied spent grain, significant changes were

noted in the chemical composition, microbiological component, as well as in sensory characteristics. The sample with 10% added brewer's spent grain showed the highest quantitative contents of protein, fat, fiber, ash, and pH, but at the same time had the lowest values of titratable acidity, the number of lactic acid bacteria, and organoleptic parameters. The product remained organoleptically acceptable when the spent grain concentration was increased to a maximum of 8% (at 8% and 10% there were reduced sensory scores). Thus, researchers recommend the use of spent grains to fortify yogurt [80].

In another study, spent grain was used to add processed cheese to Karish cheese. Replacement was made out in the following sizes: 10, 20, 30, 40 and 50%. The analysis was carried out to evaluate the physicochemical, microbiological, and organoleptic characteristics of processed cheeses with the addition of various amounts of brewer's spent grain. The indicators were determined both for a freshly prepared product and during storage for 3 months, monthly. As in the previous experiment, significant changes were observed in the listed indicators with an increase in the percentage of spent grain in the processed cheese. The sample consisting of 50% brewer's spent grain was determined to be the sample with the highest dry matter content, pH value, and the best rheological properties, but relative to other samples it demonstrated lower titratable acidity and oil separation. Moreover, according to sensory analyses, all samples were assessed as acceptable, based on which the authors concluded that the use of brewer's spent grain is a good way to obtain a functional food product with beneficial properties for consumer health [81].

8.3. Manufacture of meat and fish products

Today, products of animal origin, such as meat of animals, poultry, and fish, are characterized by frequent price increases, which in developing countries becomes a problem and leads to a reduction in consumption of this type of food. This in turn contributes to the development of various deficiencies and subsequent diseases caused by a lack of macro- and microelements present in meat (for example, iron deficiency anemia). Based on this, manufacturers are looking for ways to reduce the cost of meat products by replacing the components of the recipe with cheaper raw materials, which provide the necessary technological characteristics of the products. However, replacing raw materials (meat) with components of plant or synthetic origin leads to a decrease in the nutritional value and quality of manufactured products. Thus, the use of spent grain can become an alternative to currently available meat substitutes and at the same time maintain or increase the biological value of the product and reduce cost.

For example, in one of the works, the recipe for minced meat semi-finished products was optimized by introducing dry and frozen brewer's spent grain. The dry brewer's spent grain was used without preliminary hydration and substituted the bread according to the recipe in various proportions. Kyiv cutlets were chosen as a reference sample. The frozen spent grain was not subjected to defrosting or hydration and was introduced at the last stage of adding raw materials, based on the recipe. Three types of meat products were produced: Kyiv cutlets, rump steaks, and beefsteaks, in the compositions of which a certain type of raw material was replaced with frozen brewer's spent grain in different quantities. As in the case of dry spent grain, frozen spent grain served as a substitute for wheat bread in Kyiv cutlets. In rump steaks spent grain replaced hydrated soy protein and in beefsteaks-parts of beef and lard were substituted [82].

Based on the data obtained on sensory quality indicators and amino acid composition, experts recommend introducing into production activities samples with improved taste and external characteristics, as well as a higher amino acid balance, which is represented by the following experimentally obtained samples:

- Kyiv cutlets with a quantitative content of dried brewer's spent grain of 4%.
- Kyiv cutlets with frozen brewer's spent grain in the amount of 4%.
- Beefsteaks using frozen brewer's spent grain in an amount equal to 6.9% [82].

Next, an analysis was carried out of the chemical composition, nutritional value, and shelf life of the above-recommended semi-finished meat products with the addition of brewer's spent grain. Based on the results of the entire research work, the authors have not changed their recommendations for the use of brewer's spent grain in dried and frozen form. The percentage of dry and frozen spent grain equal to 4% in Kyiv cutlets, as well as frozen spent grain of 6.9% in beefsteaks, will increase the biological value of finished meat products, improve their organoleptic characteristics, increase product yield by reducing losses during heat treatment, and also minimize costs the listed semi-finished products [82].

The goal of the next work was to develop a new recipe and corresponding technology for the production of a meat product from chilled chicken using spent grain. Based on this, in further development, the dried spent grain was ground using a laboratory mill, followed by sifting to obtain flour. In this investigation, the most acceptable concentration of brewer's spent grain flour in a chicken meat and lard product was determined and was 3%. A similar product was chosen as a comparison sample, in which wheat flour took the place of spent grain flour. According to the results, the control sample was inferior to the product with the addition of spent grain according to several criteria: paler color, less pleasant taste, and weakly perceptible aroma, as well as a small amount of carbohydrates and dietary fiber [83].

In the production of fish items, attempts have also been made to integrate spent grain into their composition. Thus, in one of the works, to improve the functional, technological, and sensory properties of minced fish, it was proposed to use dry brewer's spent grain in molded fish products, as a raw material that can enrich the products with protein, carbohydrates, in particular dietary fiber, some minerals and vitamins, as well as lipids. During the study, it was noted that an increase in the concentration of brewer's spent grain in the minced fish system leads to an improvement in its water-holding capacity. When analyzing losses during heat treatment of minced meat, there was a tendency to reduce them with a growth in the percentage of spent grain, which increases the yield of the finished product. In terms of sensory characteristics, the highest scores were received by samples containing 3 and 4% dry spent grain. Tasters noted the presence in these samples of a color similar to pork meat, the absence of a fishy smell, and the appearance of a bready aroma. As for the finished products made from this type of minced meat, a regular, round shape with an even contour was noted, but in products with the addition of 8 and 10% spent grain, small cracks and inclusions of brewer's spent grain were observed. The color of the products, similar to the previous indicators, changed as the dosage of spent grain increased: 1% - unattractive appearance due to the gray color on the surface, but when cut, white meat was observed, 3 and 4% - yellowbrown crust with light meat on the cut, 5 and 6% - gray color on the section. In conclusion, the researchers noticed that the introduction of dried and ground brewer's spent grain into fish products has a beneficial effect on their functional and technological properties. The values of 3 and 4% by weight of the mixture were taken as the optimal percentage of spent grain in minced fish [84].

The general idea of all conducted works is to increase the nutritional value of food items while simultaneously maintaining all quality indicators and reducing the price of finished products. The authors of the mentioned studies demonstrated that the use of brewer's spent grain in the technology of these products can serve as an integral part of the food industry. It should be noted that the successful implementation of this direction requires additional research and development aimed at optimizing technology and creating new formulations, and it is also important to ensure high-quality control of spent grain to avoid adverse consequences associated with product safety. Consequently, the use of spent grain, in particular brewer's spent grain, in the production technology of food items is a promising direction for increasing the functional value of products while simultaneously reducing cost and maintaining quality indicators. Successful implementation of this area can ensure the development of the food industry and sustainable public health by improving the quality of nutrition.

9. Conclusions

Spent grain, a byproduct of beer and alcohol production is rich in nutrients but poses storage and disposal challenges due to its high moisture and protein content. These factors lead to rapid spoilage and environmental issues, such as CO_2 emissions and unpleasant odors during inadequate storage. Effective storage methods include refrigeration, chemical treatment, and dehydration, with drying emerging as the most promising approach to extend shelf life and preserve nutritional value.

The disposal of spent grain primarily impacts the agricultural sector, as it is commonly used in livestock feed. However, declining farm numbers and regulatory changes are complicating this use, often resulting in landfill disposal, which raises environmental concerns. Bioprocessing spent grain for biofuels and food products offers a sustainable alternative, expanding the potential for functional foods that improve public health.

Particularly promising is the use of spent grain in flour products like bread, pasta, and pastries, where it can replace part of traditional flour, enhancing product quality and nutritional content. Additionally, spent grain can be incorporated into meat and dairy, products, improving their nutritional profiles and reducing costs, especially in economically disadvantaged regions.

Overall, spent grain presents a multifaceted solution to environmental, economic, and nutritional challenges. Continued research, educational initiatives, and international collaboration will be crucial in maximizing its potential, promoting sustainable development, and enhancing public health.

Acknowledgments. This work was supported by a grant from the Ministry of Research, Innovation and Digitization, CNCS-UEFISCDI, project number PN-IV-P8-8.3-ROMD-2023-0078, within PNCDI IV and Institutional Project 020405 "Optimizing food processing technologies in the context of the circular bioeconomy and climate change", Bio-OpTehPAS, being implemented at the Technical University of Moldova.

Conflicts of Interest: The authors declare no conflict of interest.

References

1. World Bank. Available online: https://databank.worldbank.org/source/world-development-indicators/Series/SP.POP.GROW (accessed on 02.08.2024).

- 2. WHO/ FAO. Technical Platform on the Measurement and Reduction of Food Loss and Waste. Available online: https://www.fao.org/platform-food-loss-waste/ru/ (accessed on 02.08.2024).
- 3. Gustavsson, J.; Cederberg, C.; Sonesson U.; Van Otterdijk, R.; Meybeck, A. Global Food Losses and Food Waste-Extent, Causes and Prevention. *FAO* 2011. Available online: https://www.fao.org/sustainable-food-value-chains/library/details/en/c/266053/ (accessed on 02.08.2024).
- 4. Storup, K.; Mattfolk, K.; Voinea, D.; Jakobsen, B.; Bain, M.; Reverte i Casas, M.E.; Oliveira, P. Combating Food Waste: An Opportunity for the EU to Improve the Resource-Efficiency of the Food Supply Chain. *European Court of Auditors* 2016, 34. Available online: https://www.eca.europa.eu/Lists/ECADocuments/SR16_34/SR_FOOD_WASTE_EN.pdf (accessed on 02.08.2024).
- 5. Kasatkina, A. Zernovaya drobina kak osnova dlya polucheniya biologicheski aktivnyh dobavok s probioticheskimi svojstvami. Disss. Rossíjskij hímiko-tehnologícheskij universitét ímeni D. I. Mendeléeva, 2008, p. 146.
- 6. Chetrariu, A.; Dabija, A. Spent Grain: A Functional Ingredient for Food Applications. Foods 2023, 12(7), 1533.
- 7. Lynch, K.; Steffen, E.J.; Arendt, E.K. Brewer's spent grain: A review with an emphasis in food and health. *Journal of the Institute of Brewing* 2016, 122(4), pp. 553-568.
- 8. Kazimirova, E.A.; Ljutova, E.V. Ispol'zovanie pivnoj drobiny v pishhevoj promyshlennosti. *Vestnik molodezhnoj nauki* 2015, 1, pp. 3-5.
- 9. Statistical data bank: Agriculture. Available online: https://statistica.gov.md/ (accessed on 21.08.2024).
- 10. Orlova, O.L.; Lisavtova, L.V. Svojstva spirtovoj drobiny i eyo ispolzovanie v proizvodstve pechenya. Tambovskij gosudarstvennyj tehnicheskij universitet, 2010, p. 3.
- 11. Bianco, A.; Budroni, M.; Zara, S.; Mannazzu, I.; Fancello, F.; Zara G. The role of microorganisms on biotransformation of brewers' spent grain. *Applied Microbiology and Biotechnology* 2020, 104, pp. 8661-8678.
- 12. Lisci, S.; Tronci, S.; Grosso, M.; Karring, H.; Hajrizaj, R.; Errico, M. Brewer's Spent Grain: its Value as Renewable Biomass and its Possible Applications. *Chemical Engineering Transactions* 2022, 92, pp. 259-264.
- 13. Ikram, S.; Huang, L.Y.; Zhang, H.; Wang, J.; Yin, M. Composition and Nutrient Value Proposition of Brewers Spent Grain: Composition and preservation of BSG. *Journal of Food Science* 2017, 82(3), 11.
- 14. Bouillon, M.E. Brewers Spent Grain: its chemical composition, potential applications and source of value-added products. Bangor University 2016, 12, DOI:10.13140/RG.2.2.31341.82400.
- 15. Naibaho, J.; Korzeniowska, M. Brewers' spent grain in food systems: Processing and final products quality as a function of fiber modification treatment. *Journal of Food Science* 2020, 86(5), pp. 1532-1551.
- 16. Parchami, M. Unlocking the Potential of Brewer's Spent Grain: A Sustainable Biorefinery Approach to Value-Added Product Generation. Diss. PhD, University of Borås, 2023, p. 91.
- 17. Guan, Z.; Yu, E.; Feng, Q. Soluble Dietary Fiber, One of the Most Important Nutrients for the Gut Microbiota. *Molecules* 2021, 26 (22), 6802, doi: 10.3390/molecules26226802.
- 18. Andreasen, M. F.; Landbo, A. K.; Christensen, L. P.; Hansen, Å.; Meyer, A. S. Antioxidant effects of phenolic rye (Secale cereale L.) extracts, monomeric hydroxycinnamates, and ferulic acid dehydrodimers on human low-density lipoproteins. *Journal of Agricultural and Food Chemistry* 2001, 49, pp. 4090-4096.
- 19. Schweizer, T. F.; Wursch, P. Dietary fibre and prevention of cancer. Nestle Research News 1986, pp. 43-52.
- 20. Telrandhe, U. B.; Kurmi, R.; Uplanchiwar, V.; Mansoori, M. H.; Raj, V. J.; Jain, K. Nutraceuticals A phenomenal resource in modern medicine. *International Journal of Universal Pharmacy and Life Sciences* 2012, 2, pp. 179-195.
- 21. Peters, U.; Sinha, R.; Chatterjee, N.; Subar, A. F.; Ziegler, R. G.; Kulldorff, M.; Bresalier, R.; Weissfeld, J. L.; Flood, A.; Schatzkin, A.; Hayes, R. B. Dietary fire and colorectal adenoma in a colorectal cancer early detection programme. *Lancet* 2003, 361, pp. 1491–1495.
- 22. Macfarlane, G. T.; Steed, H.; Macfarlane, S. Bacterial metabolism and health-related effects of galacto-oligosaccharides and other prebiotics. *Applied Microbiology* 2008, 104, pp. 305–344.
- 23. David, L. A.; Maurice, C. F.; Carmody, R. N.; Gootenberg, D. B.; Button, J. E.; Wolfe, B. E.; Ling, A.V.; Devlin, A.S.; Varma, Y.; Fischbach, M.A.; Turnbaugh, P. J. Diet rapidly and reproducibly alters the human gut microbiome. *Nature* 2014, 505, pp. 559–563.
- 24. Rospotrebnadzor. Biologicheskaya cennost pitaniya. Available online: https://cqon.rospotrebnadzor.ru/ofitsialno/roditelyam-o-zdorovom-pitanii-detey/ (accessed on 25.08.2024)
- 25. Moore, D.R.; Soeters, P.B. the Biological Value of Protein. Nestlé Nutrition Institute Workshop series 2015, 82, pp. 39-51, DOI:10.1159/000382000.

- 26. Lysikov, Yu. A. Amino Acids in Human Nutrition. *Experimental and Clinical Gastroenterology* 2012, 2, pp. 88-105.
- 27.International Food Information Council Foundation. Omega-6 Fatty Acids and Health Fact Sheet, 2009. Available online: https://foodinsight.org/wp-content/uploads/2012/04/Omega-6_Fact_Sheet_6-5-09-2_pdf. (accessed on 30.08.2024).
- 28. Volovik, V.T.; Leonidova, T.V.; Korovina, L.M.; Blokhina, N.A.; Kasarina, N.P. Sravnenie zhirnokislotnogo sostava razlichnyh pishevyh masel. *Mezhdunarodnyj zhurnal prikladnyh i fundamentalnyh issledovanij* 2019, 5, pp. 147-152. https://doi.org/10.17513/mjpfi.12754.
- 29. Vinholes, J.; Silva, B.M.; Silva, L.R. Hydroxycinnamic acids (HCAS): Structure, biological properties and health effects. *Advances in Medicine and Biology* 2015, 88, 33.
- 30. Polyarkova, N.M.; Saparklycheva, S.E. Fiziologicheskaya rol fenolnyh soedinenij. *Agrarnoe obrazovanie i nauka* 2019, 4, 14.
- 31. Abdrakhimova, Y.R.; Valieva, A.I. Vtorichnye metabolity rastenij: fiziologicheskie i biohimicheskie aspekty. Fenolnye soedineniya. Uchebno-metodicheskoe posobie. Kazanskij universitet, 2012, 40 p.
- 32. El-Seedi, H.; Taher, E.; Sheikh, B.Y.; Anjum, S.; Saeed, A.; AlAjmi, M.F.; Moustafa, M.S.; Al-Mousawi, S.M.; Farag, M.A.; Hegazy, M.F.; Khalifa, S.A.M.; Göransson, U. Hydroxycinnamic Acids: Natural Sources, Biosynthesis, Possible Biological Activities, and Roles in Islamic Medicine. *Studies in Natural Products Chemistry* 2018, 8, pp. 269-292, DOI:10.1016/B978-0-444-64068-0.00008-5.
- 33. Onyekere, P.F.; Egbuna, C.; Munir, N.; Daniyal, M. Vitamins and Minerals: Types, Sources and their Functions. *Functional Foods and Nutraceuticals* 2020, pp. 149-172, DOI:10.1007/978-3-030-42319-3 9.
- 34. Batishcheva, N.V. Innovacionnye sposoby utilizacii pivnoj drobiny. Tehnicheskie nauki 2016, 6, pp. 10-14.
- 35. Devnani, B.; Moran, G.C.; Grossmann L. Extraction, Composition, Functionality, and Utilization of Brewer's Spent Grain Protein in Food Formulations. *Foods* 2023, 12(7), 1543, https://doi.org/10.3390/foods12071543.
- 36.He, Y.; Kuhn, D.D.; Ogejo, J.A.; O'Keefe, S.F.; Fraguas, C.F.; Wiersema, B.D.; Jin, Q.; Yu, D.; Huang, H. Wet Fractionation Process to Produce High Protein and High Fiber Products from Brewer's Spent Grain. *Food Bioprod. Process.* 2019, 117, pp. 266–274.
- 37. Wahlström, R.; Rommi, K.; Willberg-Keyriläinen, P.; Ercili-Cura, D.; Holopainen-Mantila, U.; Hiltunen, J.; Mäkinen, O.; Nygren, H.; Mikkelson, A.; Kuutti, L. High Yield Protein Extraction from Brewer's Spent Grain with Novel Carboxylate Salt—Urea Aqueous Deep Eutectic Solvents. *Chemistry Select* 2017, 2, pp. 9355–9363.
- 38. Qin, F.; Johansen, A.Z.; Mussatto, S.I. Evaluation of Different Pretreatment Strategies for Protein Extraction from Brewer's Spent Grains. *Ind. Crops Prod* 2018, 125, pp. 443–453.
- 39. Alonso-Riaño, P.; Sanz, M.T.; Benito-Román, O.; Beltrán, S.; Trigueros, E. Subcritical Water as Hydrolytic Medium to Recover and Fractionate the Protein Fraction and Phenolic Compounds from Craft Brewer's Spent Grain. *Food Chem.* 2021, 351 (1), 129264, DOI: 10.1016/j.foodchem.2021.129264.
- 40.Li, W.; Yang, H.; Coldea, T.E.; Zhao, H. Modification of Structural and Functional Characteristics of Brewer's Spent Grain Protein by Ultrasound Assisted Extraction. *LWT* 2021, 139, 110582.
- 41. Barrios, C.; Fernández-Delgado, M.; López-Linares, J.C.; García-Cubero, M.T.; Coca, M.; Lucas, S. A. Techno-Economic Perspective on a Microwave Extraction Process for Efficient Protein Recovery from Agri-Food Wastes. *Ind. Crops Prod.* 2022, 186 (3), 115166, DOI: 10.1016/j.indcrop.2022.115166.
- 42. Gribkova, I.N.; Kharlamova, L.N.; Sevostianova, E.M.; Lazareva, I.V. Extracting Organic Compounds from Brewer's Spent Grain by Various Methods. *Food Processing: Techniques and Technology* 2022, 52(3), pp. 469-489, DOI:10.21603/2074-9414-2022-3-2383.
- 43. Mussatto, S. I. Brewer's spent grain: A valuable feedstock for industrial applications. *J. Sci. Food Agric*. 2014, 94, pp. 1264–1275, DOI: 10.1002/jsfa.6486.
- 44. Macheiner, D.; Adamitsch, B. F.; Karner, F.; Hampel, W. A. Pretreatment and hydrolysis of brewer's spent grains. *Eng. Life Sci.* 2003, 3, pp. 401–405, DOI:10.1002/elsc.200301831.
- 45. Meneses, N.G.T.; Martins, S.; Teixeira, J.; Mussatto, S. Influence of extraction solvents on the recovery of antioxidant phenolic compounds from brewer's spent grains. *Sep Purif Technol* 2013, 108, pp. 152–158.
- 46. Chemat, F.; Rombaut, N.; Sicaire, A.-G.; Meullemiestre, A.; Fabiano-Tixier, A.-S.; Abert-Vian, M. Ultrasound Assisted Extraction of Food and Natural Products. Mechanisms, Techniques, Combinations, Protocols and Applications. A Review. *Ultrason. Sonochem.* 2017, 34, pp. 540–560.
- 47. Cerqueira e Silva, K.F.; Strieder, M.M.; Carvalhal Pinto, M.B.; Rostagno, M.A.; Hubinger, M.D. Processing Strategies for Extraction and Concentration of Bitter Acids and Polyphenols from Brewing By-Products: A Comprehensive Review. *Processes* 2023, 11(3), 921, https://doi.org/10.3390/pr11030921.

- 48. Osorio-Tobón, J.F. Recent Advances and Comparisons of Conventional and Alternative Extraction Techniques of Phenolic Compounds. *J. Food Sci. Technol.* 2020, 57, pp. 4299–4315.
- 49. Zielinski, A.A.F.; Sanchez-Camargo, A.D.P.; Benvenutti, L.; Ferro, D.M.; Dias, J.L.; Ferreira, S.R.S. High-Pressure Fluid Technologies: Recent Approaches to the Production of Natural Pigments for Food and Pharmaceutical Applications. *Trends Food Sci. Technol.* 2021, 118, pp. 850–869.
- 50. Tang, D-S.; Yin, G-M.; He, Y-Z.; Hu, S-Q.; Li, B.; Li, L.; Liang, H-L.; Borthakur D. Recovery of protein from brewer's spent grain by ultrafiltration. *Biochemical Engineering Journal* 2009, 48(1), pp. 1–5.
- 51. Thavasiappan, V.; Nanjappan, K.; Ezakial Napolean, R.; Visha, P.; Selvaraj, P.; Doraisamy, K.A. Fatty acid profile of wet brewer's spent grain. *International Journal of Science, Environment and Technology* 2016, 5(4), pp. 2516–2521.
- 52. Tan, Y.X.; Mok, W.K.; Lee, J.; Kim, J.; Chen, W.N. Solid state fermentation of Brewers' spent grains for improved nutritional profile using Bacillus subtilis WX-17. *Fermentation* 2019, 5(3), 52.
- 53. Petrov, S.M.; Filatov, S.L.; Pivnova, E.P.; Shibanova, V.M. K voprosu o sposobah utilizacii pivnoj drobiny. *Tehnologiya* 2014, 6, pp. 32-37.
- 54. Chechina, O.N.; Zyuzina, A.V.; Zimichev, A.V. Perspektivy utilizacii pivnoj drobiny. *Pishevaya promyshlennost* 2010, 7, pp. 17-19.
- 55. Kavalopoulos, M.; Stoumpou, V.; Christofi, A.; Mai, S.; Barampouti, E.M.; Moustakas, K.; Malamis, D.; Loizidou, M. Sustainable valorisation pathways mitigating environmental pollution from brewers' spent grains. *Environmental Pollution* 2021, 270, 116069, DOI:10.1016/j.envpol.2020.116069.
- 56. Ashman, C.H.; Gao, L.; Goldfarb, J.L. Silver nitrate in situ upgrades pyrolysis biofuels from brewer's spent grain via biotemplating. *Journal of Analytical and Applied Pyrolysis* 2020, 146 (5760), 104729.
- 57. Lorente, A.; Remón, J.; Budarin, V.L.; Sánchez-Verdú, P.; Moreno, A.; Clark, J.H. Analysis and optimisation of a novel "bio-brewery" approach: Production of bio-fuels and bio-chemicals by microwave-assisted, hydrothermal liquefaction of brewers' spent grains. *Energy Conversion and Management* 2019, 185, pp. 410-430.
- 58. Carlini, M.; Monarca, D.; Castellucci, S.; Mennuni, A.; Casini, L.; Selli, S. Beer spent grains biomass for biogas production: Characterization and anaerobic digestionoriented pre-treatments. *Energy Reports* 2021, 7(1), pp. 921-929, DOI: 10.1016/j.egyr.2021.07.049.
- 59. Wilkinson, S.; Smart, K.A.; James, S.; Cook, D.J. Bioethanol Production from Brewers Spent Grains Using a Fungal Consolidated Bioprocessing (CBP) Approach. *BioEnergy Research* 2017, 10(1), pp. 146-157.
- 60. Xiros, C.; Christakopoulos, P. Biotechnological Potential of Brewers Spent Grain and its Recent Applications. *Waste and Biomass Valorization* 2012, 3, pp. 213-232, DOI:10.1007/s12649-012-9108-8.
- 61. Pabbathi, N.P.P.; Velidandi, A.; Pogula, S.; Gandam, P.K.; Baadhe, R.R.; Sharma, M.; Sirohi, R.; Thakur, V.K.; Gupta, V.K. Brewer's spent grains-based biorefineries: A critical review. *Fuel* 2022, 317, 123435.
- 62. Ishiwaki, N.; Murayama, H.; Awayama, H.; Kanauchi, O.; Sato, T. Development of high value uses of spent grain by fractionation technology. *Technical quarterly-Master Brewers Association of the Americas* 2000, 37(2), pp. 261-265.
- 63. Mussatto, S.I.; Rocha, G.J.M.; Roberto, I.C. Hydrogen peroxide bleaching of cellulose pulps obtained from brewer's spent grain. *Cellulose* 2008, 15, pp. 641-649.
- 64. Pedro Silva, J.; Sousa, S.; Rodrigues, J.; Antunes, H.; Porter, J.J.; Gonçalves, I.; Ferreira-Dias, S. Adsorption of acid orange 7 dye in aqueous solutions by spent brewery grains. *Separation and Purification Technology* 2004, 40(3), pp. 309-315.
- 65. Ktenioudaki, A.; Alvarez-Jubete, L.; Smyth, TJ.; Kilcawley, K.; Rai, D.K.; Gallagher, E. Application of Bioprocessing Techniques (Sourdough Fermentation and Technological Aids) for Brewer's Spent Grain Breads. *Food Res. Int.* 2015,73, pp. 107–116.
- 66. Yitayew, T.; Moges, D.; Satheesh, N. Effect of Brewery Spent Grain Level and Fermentation Time on the Quality of Bread. *Int. J.Food Sci.* 2022, 704684,10, DOI:10.1155/2022/8704684.
- 67. Şaitan, O.; Tarna, R.; Ghendov-Moşanu A. Influence of brewer's spent grain on qualitative indicators of bread from wheat flour. *MTFI* 2022, 5, 53.
- 68. Czubaszek, A.; Wojciechowicz-Budzisz, A.; Spychaj, R.; Kawa-Rygielska, J. Effect of Added Brewer's Spent Grain on the Baking Value of Flour and the Quality of Wheat Bread. *Molecules* 2022, 27, 1624.
- 69. Stojceska, V.; Ainsworth, P. The Effect of Different Enzymes on the Quality of High-Fibre Enriched Brewer's Spent Grain Breads. *Food Chem.* 2008, 110, pp. 865–872.
- 70. Nocente, F.; Natale, C.; Galassi, E.; Taddei, F.; Gazza, L. Using Einkorn and Tritordeum Brewers' Spent Grain to Increase the Nutritional Potential of Durum Wheat Pasta. *Foods* 2021, 10, 502.

- 71. Cuomo, F.; Trivisonno, M.C.; Iacovino, S.; Messia, M.C.; Marconi, E. Sustainable Re-Use of Brewer's Spent Grain for the Production of High Protein and Fibre Pasta. *Foods* 2022, 11, 642.
- 72. Sahin, A.W.; Hardiman, K.; Atzler, J.J.; Vogelsang-O'Dwyer, M.; Valdeperez, D.; Münch, S.; Cattaneo, G.; O'Riordan, P.; Arendt, E.K. Rejuvenated Brewer's Spent Grain: The Impact of Two BSG-Derived Ingredients on Techno-Functional and Nutritional Characteristics of Fibre-Enriched Pasta. *Innov. Food Sci. Emerg. Technol.* 2021, 68, 102633.
- 73. Chetrariu, A.; Dabija, A. Quality Characteristics of Spelt Pasta Enriched with Spent Grain. *Agronomy* 2021, 11, 1824.
- 74. Öztürk, S.; Özboy, Ö.; Ox, D.; Köksel, H.; Brew, J.I. Effects of Brewers Spent Grain on the Quality and Dietary Fibre Content of Cookies. *J. Inst. Brew.* 2002, 108, pp. 23–27.
- 75. Heredia-Sandoval, N.G.; del Carmen Granados-Nevárez, M.; de la Barca, A.M.C.; Vásquez-Lara, F.; Malunga, L.N.; Apea-Bah, F.B.; Beta, T.; Islas-Rubio, A.R. Phenolic Acids, Antioxidant Capacity, and Estimated Glycemic Index of Cookies Added with Brewer's Spent Grain. *Plant Foods Hum. Nutr.* 2020, 75, pp. 41–47.
- 76. Petrovic, J.; Pajin, B.; Tanackov-Kocic, S.; Pejin, J.; Fistes, A.; Bojanic, N.; Loncarevic, I. Quality Properties of Cookies Supplemented with Fresh Brewer's Spent Grain. *Food Feed Res.* 2017, 44, pp. 57–63.
- 77. Rogovaya, A.L.; Choni, I.V.; Shidakova-Kamenyuka, E.G. Ispolzovanie pivnoj drobiny v tehnologii muchnyh konditerskih izdelij. BGATU, 2021, pp. 51-53.
- 78. Lesnikova, N.A.; Lavrova, L. Yu.; Bortsova, E.L. Ispolzovanie pivnoj drobiny v proizvodstve pryanichnyh izdelij. *Hleboprodukty* 2015, 7, pp. 44-46.
- 79. Naibaho, J.; Butula, N.; Jonuzi, E.; Korzeniowska, M.; Laaksonen, O.; Föste, M.; Kütt, M.L.; Yang, B. Potential of Brewers' Spent Grain in Yogurt Fermentation and Evaluation of Its Impact in Rheological Behaviour, Consistency, Microstructural Properties and Acidity Profile during the Refrigerated Storage. *Food Hydrocoll.* 2022, 125, 107412.
- 80. Abd EL-Moneim, R.; Shamsia, S.; EL-Deeb, A.; Ziena, H. Utilization of brewers spent grain (BSG) in making functional yoghurt. *Journal of Food and Dairy Sciences* 2015, 6(10), pp. 577-589.
- 81. Abd El-Moneim, R.; Shamsia, S.; EL-Deeb, A.; Ziena, H. Utilization of brewers spent grain (BSG) in producing functional processed cheese 'Block'. *Journal of Food and Dairy Sciences* 2018, 3, pp. 103-109.
- 82. Menuhov, N.V. Tovarovednaya ocenka myasnyh rublenyh polufabrikatov s primeneniem pivnoj drobiny. Diss. Kemerovskij tehnologicheskij institut pishevoj promyshlennosti, 2006, 163 p.
- 83. Belokurova, E.S.; Shirokova, N.M. Pivnaya drobina kak istochnik cennyh veshestv pri razrabotke receptur kombinirovannyh pishevyh produktov. Yugo-Zapadnyj gosudarstvennyj universitet, 2021, pp. 43-46.
- 84. Volotka, F.B.; Bogdanov, V.D. Vliyanie suhoj pivnoj drobiny na funkcionalno-tehnologicheskie svojstva rybnogo farsha. *Nauchnye trudy DALRYBVTUZA* 2013, 28, pp. 10-106.

Citation: Erşova, S.; Saitan, O.; Tarna, R.; Rumeus, Iu.; Codină, Ge. G.; Ghendov-Mosanu, A. Integration of spent grain into food products. *Journal of Engineering Science* 2024, XXXI (3), pp. 130-155. https://doi.org/10.52326/jes.utm.2024.31(3).11.

Publisher's Note: JES stays neutral with regard to jurisdictional claims in published maps and institutional affiliations.



Copyright:© 2024 by the authors. Submitted for possible open access publication under the terms and conditions of the Creative Commons Attribution (CC BY) license (https://creativecommons.org/licenses/by/4.0/).

Submission of manuscripts:

jes@meridian.utm.md

https://doi.org/10.52326/jes.utm.2024.31(3).12 UDC 663.2/.5:[005.936.5:504.6]





CHARACTERISTICS OF BIOMASS RESULTING FROM AGRO-INDUSTRIAL PROCESSES AND POSSIBILITIES OF ITS EVALUATION IN THE CONTEXT OF THE CIRCULAR BIOECONOMY

Corina Taşca 1,2*, ORCID: 0000-0003-3359-3490

¹ State University of Moldova, Institute of Chemistry, 3 Academiei Str., Chisinau, Republic of Moldova * Corresponding author: Corina Taşca, zubic.corina@gmail.com

Received: 07. 11. 2024 Accepted: 09. 12. 2024

Abstract. Waste management in the agro-industrial sector is a significant issue that demands a thoughtful and multifaceted approach, not only to prevent environmental contamination with harmful substances but also to produce value-added products. The selection of waste treatment technology should be based on the waste's nature, composition, and initial quantities, which are determined by the primary production cycle, raw materials, and applied conditions. This study focuses on exploring innovative methods to enhance the conversion rate and efficiency of organic waste biomass by incorporating small amounts of biologically active substances into the fermentation mix. The research also examines the impact of natural plant-based additives on various types of biomass within the agro-industrial sector. In agricultural areas where industries produce wine, spirits, beer, and juices, liquid waste is continuously produced in a state of ongoing digestion. This requires strict measures to prevent its direct disposal into landfills, water bodies, or other environmental compartments, as such actions could disrupt the natural balance of soil microorganisms, plants, and other organisms. Present-day methods for handling solid organic waste often include its application in agriculture, incineration, anaerobic digestion, composting, and related processes. Liquid waste from the agro-industrial sector can be treated through processes like sedimentation, settling, and anaerobic fermentation.

Keywords: waste, agro-industrial sector, management, value-added products, wine, spirits, beer.

Rezumat. Gestionarea deșeurilor din sectorul agroindustrial este o problemă importantă care necesită o abordare inteligentă și complexă, pentru a preveni poluarea mediului cu componente toxice, dar și pentru a obține produse cu valoare adăugată. Tehnologia de tratare a deșeurilor trebuie selectată în funcție de natura, compoziția și cantitățile inițiale ale deșeurilor, care depind de ciclul principal de producție, de materiile prime și de condițiile aplicate. Prezentul studiu se concentrează pe investigarea metodelor originale de creștere a ratei de conversie și a gradului de conversie a biomasei deșeurilor organice, utilizarea unor cantități mici de substanțe biologic active introduse în amestecul fermentat. S-a urmărit efectul unor aditivi de origine vegetală naturală, introduși în diferite tipuri de biomasă din sectorul agroindustrial. Concret, în regiunile agricole cu industrii producătoare de vin, băuturi

spirtoase, bere și sucuri, deșeurile lichide sunt generate în stare de digestie continuă, ceea ce înseamnă prevenirea strictă a deversărilor direct în gropile de gunoi, apă sau alte compartimente de mediu, deoarece pot încălca normele naturale. echilibrul microbiotei solului, al plantelor și al altor organisme vii. Metodele existente de gestionare a deșeurilor organice solide își asumă aplicarea în agricultură, ardere, digestie anaerobă, compostare etc. Deșeurile lichide din sectorul agroindustrial pot fi tratate prin sedimentare, decantare, fermentare anaerobă etc.

Cuvinte cheie: deșeuri, sector agroindustrial, management, produse cu valoare adăugată, vin, băuturi spirtoase, bere.

1. Introduction

In recent years, the food industry has experienced unprecedented development, which is correlated with the rapid increase in the quantity of agricultural waste. Clearly, environmental issues and the negative impact of agricultural waste have become a major concern. Agricultural waste has considerable applicability due to its high resilience, low costs, availability, and ease of reuse. One of the primary environmental challenges facing today's society is the ongoing rise in the volume of organic waste. These alarming aspects have led to the necessity of designing sustainable development that suggests maintaining harmony and balance between humans and nature while promoting socio-economic progress. The circular bioeconomy for producing high-value products has attracted interest due to emerging policies focused on the reuse and sustainable recovery of underutilized local raw materials in various countries.

Beer, a fermented beverage with ancient origins, is currently the fifth most consumed drink worldwide. In 2018, global beer consumption across 170 major countries and regions was approximately 1.8879 billion hL [1]. According to reports [2], global beer production in the same year surpassed 1.94 billion hL, highlighting the significant economic impact of the beer manufacturing industry. Modern beer production is largely conducted on a large scale, yielding substantial amounts of beer and by-products.



Figure 1. Beer production process [3,4].

The larger red arrows indicate the steps where the main brewery by-products are removed.

The beer production process involves several sequential steps: grinding grains, mashing, filtering, boiling, fermenting, maturation, and packaging (Figure 1) [3,4]. The primary objective of this process is to convert starch from grains into simple sugars, extract these sugars, and ferment them using yeast to produce a lightly carbonated beverage with varying alcohol content. The first and most abundant by-product in the brewing process is generated after mashing. During this stage, spent grains are separated and removed once the liquid produced in mashing, known as wort, is extracted. Another type of waste is created after the wort boiling stage, where the thermal denaturation of proteins occurs, causing high molecular weight proteins to precipitate, forming a waste product known as hot trub. This hot trub, which contains spent hops, is separated and removed from the wort. Following this, yeast is added to initiate fermentation. Once fermentation is complete, most of the yeast is removed from the young beer, producing another by-product called spent beer yeast. Before the beer is packaged, it is typically filtered through diatomaceous earth or cellulose filters to eliminate any remaining yeast residues [3, 4].

2. Characteristics of biomass resulting from the brewing industry and reuse possibilities

Brewer's spent grain (BSG) is a low-value by-product of the brewing industry, generated in substantial quantities each year. BSG is the solid residue left from barley malt after wort production and represents around 85% of all residues produced by breweries [4].

This solid by-product contains water-insoluble proteins, along with the pericarp hull and seed coating from the original barley grain [5]. The dry matter of BSG consists of approximately 20% proteins and 70% fibers, with a negligible starch content. Due to its high protein content, BSG has potential applications similar to whey proteins, offering various health benefits to consumers. Additionally, BSG is rich in phenolic compounds, particularly ferulic acid and p-coumaric acid [6], as well as oligosaccharides and polysaccharides. Recent research suggests that dietary phenolic compounds may have anticancer, anti-inflammatory, and antioxidant properties [7,8], which has sparked significant interest in plant phenolics among the food industry, scientists and consumers.

BSG contains hydroxycinnamic acids such as ferulic acid, p-coumaric acid, and caffeic acid, all of which possess bioactive properties like antioxidant, anti-inflammatory, anti-atherogenic and anticancer effects [8]. Research shows that adding BSG to animal feed can boost milk production, increase milk fat content, and supply essential amino acids [9]. In human food applications, incorporating BSG into items like cakes and snacks has been shown to raise protein and fiber levels, although it can also significantly alter taste and texture [10]. BSG is increasingly recognized as a valuable source of fiber, protein and phenolic compounds like ferulic, p-coumaric, and caffeic acids [11].

As a complex material made up of lignocellulosic biomass, BSG is rich in proteins (20-30%), fibers (30-70%), lipids, vitamins and minerals and contains around 12-28% lignin, 12-25% cellulose and 28% non-cellulosic polysaccharides, primarily arabinoxylans [12,13]. Previous studies have thoroughly reviewed and documented the chemical composition of BSG [9]. On average, around 14 kg of BSG is produced per hectoliter of wort, with a moisture content ranging between 75% and 90% [14]. The ash content in spent brewer's grains typically ranges from 2% to 7.9% [9]. BSG also contains vitamins, minerals, a variety of amino acids, oligo- and polysaccharides and a rich array of phenolic compounds [15]. Among the phenolic acids, BSG has particularly high levels of ferulic acid (1860-1948 mg/g) and *p*-coumaric acid (565-794 mg/g) [16], as well as sinapic, caffeic and syringic acids.

According to Mussatto et al. [10], BSG can be classified as a lignocellulosic material, composed of cellulose (a linear homopolymer of glucose units), hemicellulose, and lignin (a polyphenolic macromolecule), which together make up nearly 50% of the BSG by weight, as shown in Table 1. On a dry weight basis, BSG contains a considerable amount of monosaccharides, including significant quantities of glucose, xylose and arabinose. Hemicellulose, primarily composed of arabinoxylan (AX), is the dominant component of BSG, constituting up to 40% of its dry weight [16].

Table 1

Composition of BSG

Components of BSG (g/kg dry mass)

Destrict	A . I.	1	Cellulose	Hemice	ellulose	Research
Proteins	Ash	Lignin	(glucose)	Xylose	Arabinose	conducted
153	46	278	168	199	85	[10]
240	24	119	254	-	-	[17]
246	12	217	219	206	90	[18]
-	46	169	253	-	-	[19]
247	42	194	217	136	56	[20]

Phenolic profile of BSG. Phenolic acids, primarily hydroxybenzoic acids and hydroxycinnamic acids, are secondary metabolites in plants, predominantly found in vegetables. These compounds have gained considerable research attention due to their anticancer, anti-inflammatory and antioxidant properties [10].

BSG is considered a significant source of phenolic acids, as the outer layers of barley grains contain substantial amounts of these compounds [10]. Notably, p-coumaric and ferulic acids (Figure 2) [23] are present in high concentrations in BSG. So, p-coumaric acid is present in both forms, with a free concentration of 0.48 ± 0.06 and a much higher bound concentration of 652.27 ± 160.5 and ferulic acid shows a minimal free form concentration of 0.072 ± 0.51 but exhibits a significantly high bound concentration of 3739.42 ± 270.80 [21, 23]. Research indicates that the ferulic acid content in BSG ranges from 1860 to $1948 \mu g/g$, while p-coumaric acid content varies between 565 and $794 \mu g/g$ [21]. The total phenolic content in BSG can also vary depending on the type of malt used [20, 22]. Recent studies have revealed that the majority of bioactive phenolic acids in BSG are found in bound form [23]. A different study also found that ferulic acid and p-cumaric acid were detected in elevated concentrations compared to AX and BSG includes substantial quantities of other bioactive compounds such as catechin, quinic acid and syringic acid [23].

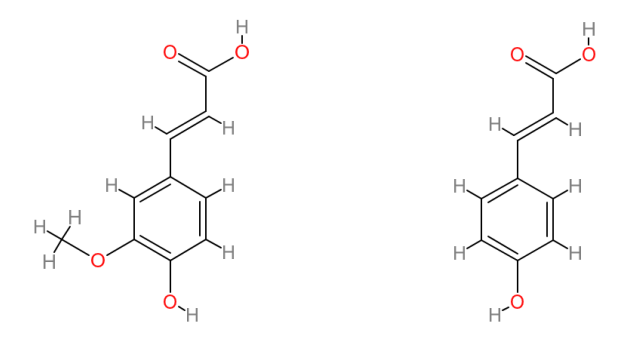


Figure 2. Structure of p-coumaric and ferulic acids $(C_{10}H_{10}O_4)$.

Chen and Ho [24] demonstrated the antioxidant potential of ferulic acid using the DPPH and Rancimat methods. Their findings showed that although ferulic acid possesses antioxidant properties, it is less potent than caffeic acid and α -tocopherol [25]. Caffeic acid, in particular, has been identified as a powerful in vitro antioxidant and radical scavenger, effectively neutralizing DPPH and superoxide anions [25]. Furthermore, research using the DPPH assay has ranked several hydroxycinnamic acids by their antioxidant effectiveness in the following order: caffeic acid > sinapic acid = ferulic acid > ferulates > p-coumaric acid [26].

Both ferulic and caffeic acids exhibit strong antioxidant potential at low concentrations, with the ability to neutralize various free radicals. These phenolic acids scavenge reactive oxygen and nitrogen species, showing concentration-dependent activity against NO, superoxide, and ABTS (2,2'-azino-bis(3-ethylbenzothiazoline-6-sulfonic acid)) radicals. While caffeic acid was found to be more effective in scavenging DPPH radicals, ferulic acid performed better at scavenging ABTS and NO radicals [27].

In addition to their antioxidant properties, growing evidence suggests that phenolic acids may have anticancer effects. Caffeic acid, for instance, has shown antiproliferative activity against various cancer cell lines, including breast gland adenocarcinoma, lymphoblastic leukemia [28], and cervical cancer cells [28, 29]. The COX-2 (cyclooxygenase-2) assay has been used to assess the anticancer potential of these compounds. Overexpression of COX-2, which converts arachidonic acid to prostaglandins, serves a crucial role in inflammation and cancer development. Researc has demonstrated that phenolic acids such as caffeic acid [30] and vanillic acid [31], along with polyphenols like epigallocatechin-3-gallate [32] and quercetin [33], inhibit COX-2 expression, potentially lowering cancer risk.

Incorporation of Brewer's Spent Grain (BSG) in Animal Feed and Food. As previously mentioned, BSG contains approximately 20% protein and 70% fiber, making it a valuable raw material or food ingredient [10]. It is especially beneficial in animal feed, particularly for ruminants. When paired with cost-effective nitrogen sources like urea, BSG can supply all essential amino acids required by ruminants [34]. This high nutritional value makes BSG a significant component in animal feed formulations.

Beyond its use in animal feed, BSG has been successfully incorporated into various human food products due to its low cost and rich nutritional profile. BSG is especially suitable for products like cookies and ready-to-eat snacks, where an increase in dietary fiber is desired [10]. In 1978, researchers explored the use of BSG in cookies by replacing flour with BSG at levels ranging from 5% to 60% [35]. It was found that adding 40% BSG significantly enhanced the cookies' physical qualities. This level of supplementation resulted in a 74% increase in nitrogen and a tenfold increase in crude fiber content. A study published in 2002 supported these findings, demonstrating that adding BSG (at 5-25%) to cookies significantly boosted the dietary fiber content [36].

However, it was concluded that 20% BSG was the optimal level for maintaining the sensory and structural properties of commercially available snacks. When BSG protein hydrolysates are incorporated into food, there may be concerns about the bitter taste of certain peptides, caused by their hydrophobic amino acid content [37].

Hot Trub. Another byproduct of beer production is hot trub, which refers to the sediments formed during wort boiling. The particle size of hot trub is between 30 and 80 μ m [38, 39]. This insoluble precipitate is mainly made up of colloidal proteins that solidify during the boiling process, forming complexes with the polyphenols naturally found in the wort. Hot trub also includes complex carbohydrates, lipids, minerals, tannins, hop remnants, and

smaller malt particles [40]. These residues make up approximately 0.2-0.4% of the wort volume and are generally removed prior to fermentation. It's worth noting that hops, which contribute to the trub, are added and removed at various stages of brewing, with approximately 85% of hops used in beer production ending up as byproducts [41].

Hot trub contains a high level of moisture (80-90%), a dry matter content of about 15-20%, and a low ash content (2-5%) [41]. While its primary component is high molecular weight proteins, it also has a high carbon content due to the significant amount of reducing sugars (20%) present [39]. The protein content of hot trub can vary depending on the brewery but generally ranges from 40% to 70% [41, 42].

The formation of trub is an essential step in brewing, as removing polyphenols and soluble proteins is crucial to prevent the formation of insoluble complexes. These precipitates are undesirable in filtered pale beers, which are expected to be bright and clear [40].

Spent Brewer's Yeast (BSY). Residual brewer's yeast, also known as BSY, is the second largest byproduct in the beer manufacturing process, comprising up to 15% of total byproducts generated [42]. This yeast is recovered through sedimentation before beer maturation in the final stage of secondary fermentation [43]. Yeast can be reused up to six times in the brewing process. The Saccharomyces cerevisiae yeast, introduced at the start of fermentation, undergoes numerous divisions, resulting in a significant increase in yeast biomass. The growth rate of yeast depends on fermentation conditions in the brewery, with BSY contributing to beer losses ranging from 1.5% to 3% of the total beer volume produced [44]. On average, 0.6–0.8 lb/bbl (2.7 kg/m³) of yeast residue is generated from lager fermentation [41].

Yeast cells are rich in proteins (49%), carbohydrates (40%), minerals, vitamins (7%) and lipids (4%) [45]. BSY typically has a moisture content of 74%-86% and its dry matter content ranges from 10% to 16%, depending on the brewery [39]. The mineral residue (ash) content in spent yeast varies from 2% to 8.5%, with yeast richer in phosphate when it has been reused fewer times. Additionally, BSY is abundant in polyphenolic compounds and B vitamins, particularly B_1 , B_2 , B_3 , B_6 , and B_8 [46]. The carbon content in BSY is high, accounting for 45%-47% of the dry matter, and the carbon-to-nitrogen ratio of the residue is around 5.1-5.8 [39].

3. Characteristics of biomass resulting from the wine industry and reuse possibilities

Grapes are one of the most important fruit crops grown worldwide [47]. Grape production was estimated at approximately 77.8 million tons in 2018 [49]. According to FAO statistics, grapes are the most widespread fruit crop in the world [49].

Reports from the International Organization of Vine and Wine (OIV) show that 292 million L of wine were produced globally in 2018 [48]. The United States, Australia, Italy, Spain, France, and Germany are the main grape-producing countries [48]. Spain, China, Italy, Turkey, and France collectively contribute 50% of the total wine production worldwide [48].

In recent years, there has been a drastic shift in consumer demand. There is a growing preference for naturally processed products without additives and those that are safe [49]. Consumers prefer safer, tastier, and traditional products that are accepted as natural without other additives [49]. Therefore, replacing currently used synthetic food antioxidants (many of which are suspected of being carcinogenic) with natural ones is of interest to food technologists. Grape waste can be used to extract polyphenols for use in foods [50, 51]. Polyphenols not only exhibit antioxidant activity but also have other properties such as anticancer, antiallergic, antimutagenic, and anti-aging activities [52, 53].

Grape pomace, skins, stems, and seeds are among the major wastes generated by the wine industry. In addition, significant amounts of wastewater, wine yeast, shoots, and some filter residues generated by the wine industry are among the major causes of environmental degradation [54], as they lead to the emission of volatile organic compounds (VOCs), increased chemical oxygen demand infiltration of complex effluents with varied physicochemical properties into soils [55].

The toxicological effects of winemaking byproducts have been reported on terrestrial plants and aquatic organisms even at high dilutions, implying the need for proper treatment of wine industry waste [56]. Currently, wine industry waste is directed by producers either towards composting or disposal, but it could serve as a source for producing many bioproducts [57, 58, 59] (Figure 3).

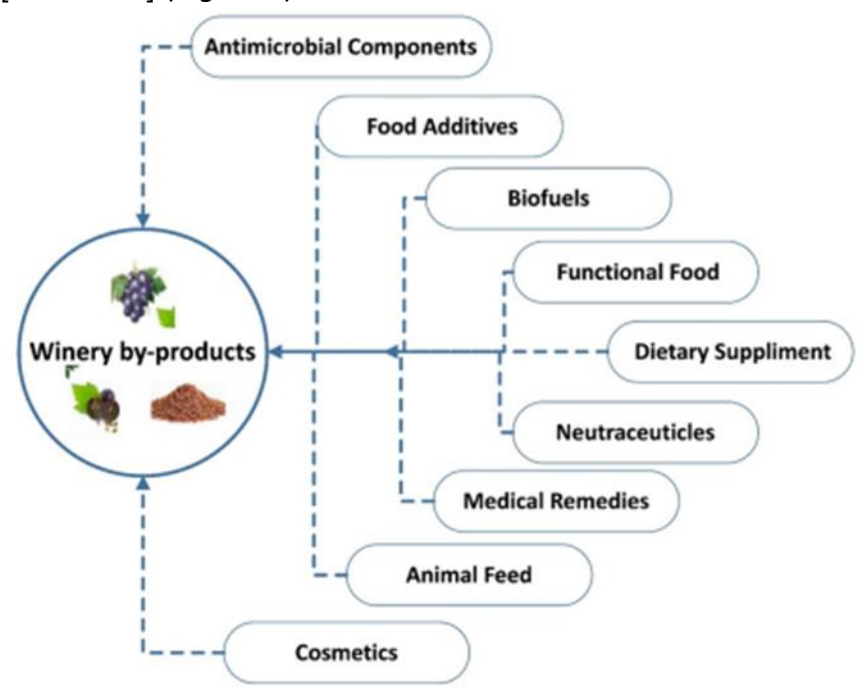


Figure 3. Valorization options for wine byproducts [57-59].

In addition to traditional uses limited to the fertilizer and biofuel industries, these byproducts could serve for obtaining food additives, including compounds with antimicrobial properties, preservatives, antioxidants for the production of functional foods, dietary supplements, nutraceuticals, medical remedies, and cosmetic products (Figure 3). The increasing need for energy and waste valorization through eco-friendly processes is pushing the transition from general practices to sustainable circular approaches [60].

Several recent studies have highlighted these wine byproducts as a good opportunity for recovering antioxidant compounds, which could subsequently be used as nutraceuticals and ingredients for functional foods [61-64]. Polyphenol-rich extracts obtained from grape skins and seeds [65-68] can also be sourced from grape pomace for polysaccharides and fibers [55,69,70]. Similarly, grape stems, obtained after destemming, emerge as an important source of phenolic compounds [71-74], particularly stilbenes [55,75,76].

Several in vivo and in vitro studies with phenolic compounds present in wine and grape pomace have demonstrated significant health-promoting effects, such as neuroprotection for preventing cognitive and mental disorders [77, 78], prevention of cardiovascular diseases [80, 81], reduction of insulin resistance [82], and antiproliferative action against cancer cells [83].

Functional ingredients are obtained through aqueous or alcoholic solvent extraction processes [65,66,71,82,84], and more recently, through supercritical CO_2 extraction [85, 86]. These processes present technical difficulties for industrial scaling, especially due to the perishability of these products and waste logistics.

Considering the issue of winemaking waste, the search for a viable solution for utilizing byproducts to obtain ingredients with enhanced biological value necessitated conducting a study on processing winemaking waste to preserve their functionality through dehydration processes, which will allow for their further valorization. Additionally, it is necessary to develop efficient extraction techniques to achieve good recoveries of the compounds.

Chemical composition of grape pomace. Grape pomace represents the dehydrated byproduct from the pressing of grapes (*Vitis vinifera* L.) during the wine and grape juice production process. It contains the pulp, skins, seeds, peduncles, and possibly fragments of stems (the woody support of the grape cluster) [77]. Grape pomace contains a high concentration of phenolic compounds, as not all of these substances are fully extracted during winemaking [88]. These phenolic compounds, which are secondary plant metabolites, are known for their potential health benefits, including antioxidant, antimicrobial, antiviral, and anti-inflammatory properties [76]. Due to these attributes, grape pomace offers an affordable source of valuable phytochemicals, which can be utilized across various sectors such as pharmaceuticals, cosmetics, and the food industry [88]. With increased attention to the sustainability of agricultural practices, efforts have been made to utilize extracts from grape pomace in various industry fields. It has been demonstrated that spent grape pomace, after the extraction of bioactive compounds, can undergo procedures for the extraction of condensed tannins, recommended for adhesive production [87]. The elemental composition of grape pomace is presented in Figure 4.

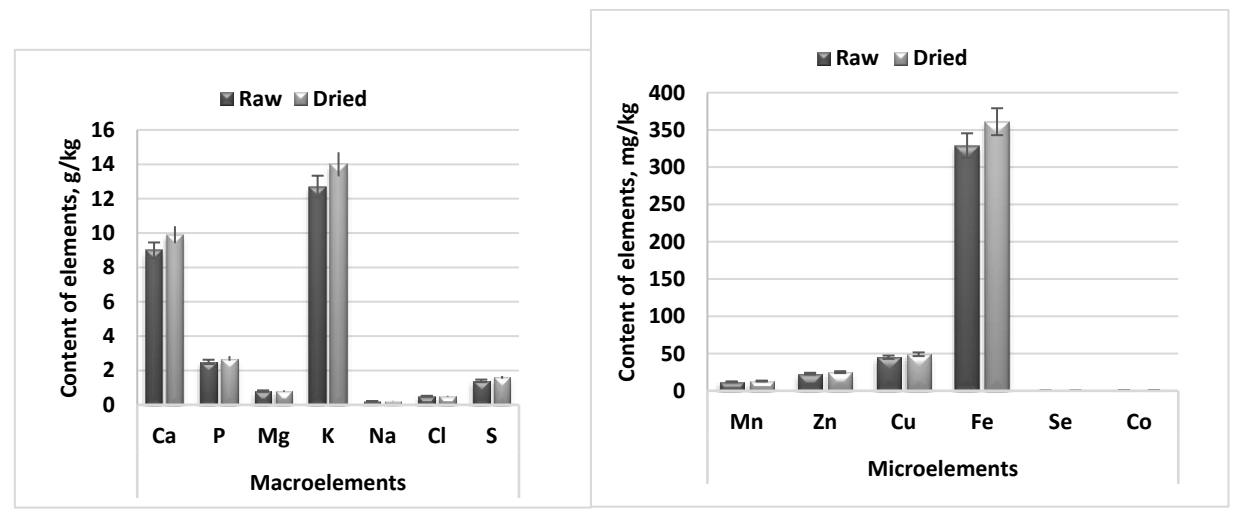


Figure 4. Elemental composition of grape pomace, macroelements and microelements. *Composed by the author based on bibliographic sources [88,89].

As shown in Figure 4, grape pomace is an important source of iron, potassium, and manganese, as well as copper and zinc. It is low in elements such as sodium and calcium. Grape pomace can serve as a good source of essential minerals, as it does not accumulate elements that pose health risks.

The fatty acid composition of grape pomace is presented in Table 2 [90 - 94].

Table 2

Fatty Acid Composition of Grape Pomace*													
<u>-</u>	Fatty acids, g/kg												
Grape Pomace	Palmitic C16:0	Palmitoleic C16:1	Stearic C18:0	Oleic C18:1	Linoleic C18:2	Linolenic C18:3	Arachidic C20:0	Eicosenoic C20:1	Myristic C14:0	Vitamine E, mg/kg			
Raw	2.9	0.06	1.8	6.6	29	0.2	0.07	0.07	0.02	4.4	_		
Dried	3.2	0.07	1.9	7.2	31.8	0.2	0.08	0.08	0.03	4.9			

^{*}Composed by the author based on bibliographic sources [90-94]

According to the data presented in Table 2, grape pomace primarily contains linoleic acid (70.9%), oleic acid (16.1%), palmitic acid (7.1%), and stearic acid (4.3%) [92]. Erucic acid is absent. There is a significant amount of vitamin E (4.4 mg/kg in raw pomace, 4.9 mg/kg in dried pomace)[94]. It was found that the total fatty acid content in grape pomace constitutes 75% [90, 91].

The amino acid composition of grape pomace is presented in Table 3 [90-96].

Table 3

Amino acid	composition	of grape	pomace

Grape Pomace	Lysine	Threonine	Cysteine	Isoleucine	Valine	Leucine	Phenylalanine	Tyrosine	Phenylalanine + Tyrosine	Arginine	Alanine	Aspartic Acid	Glutamic Acid	Glycine	Serine	Proline
Raw, g/kg	4.9	4.3	1.3	4.5	4.7	8.1	4.2	2.5	6.8	6.5	5.5	6.3	5.5	8	4.5	4.4
Dried, _g/kg	5.4	4.7	1.4	4.9	5.2	8.9	4.6	2.8	7.4	7.1	6	6.9	21.4	8.7	4.9	4.8

^{*}Composed by the author based on bibliographic sources [90-96]

Grape pomace has a significant content of glutamic acid (19.5 g/kg raw pomace, 21.4 g/kg dried pomace) and aspartic acid (6.3 g/kg and 6.9 g/kg, respectively) [92]. It also contains a notable amount of essential amino acids. However, most studies demonstrate that the nitrogen digestibility of grape pomace is moderate, varying from 16.3% in rabbits to 82.1% in fish [94]. In pigs, this indicator ranges from 47.7% to 68.1%, and for poultry, it is between 61% and 78% [91].

Polyphenol composition of grape pomace. Research suggests that the chemical makeup of grapes is shaped by both environmental conditions and grape varieties [55]. Various studies have explored the characteristics of carbohydrate polymers found in grape skins [95] and grape stems [96]. Grape pomace, known for its high polyphenol content, has been studied as a source of antioxidants. Since the "French paradox" was observed [97], numerous studies have emphasized the positive effects of grape or wine polyphenols on human health [98]. he general composition of several grape pomaces has also been

documented [95, 99]. Grape pomace contains components that inhibit the proliferation of Caco-2 and HT-29 cancer cells by inducing apoptosis, has potent free radical scavenging activity, and may provide protection against certain cancers [100].

Chemical characterization of grape pomace is necessary to evaluate their potential, determine extraction yields, and ensure quality control. Various phenolic compounds, representative of different structural types, have been identified. Profiles of phenolic compounds recovered from different winery wastes are dominated by gallic acid, catechin, and epicatechin. Additionally, hydroxytyrosol, tyrosol, cyanidin glycosides, and various phenolic acids such as caffeic, protocatechuic, syringic, vanillic, o-coumaric, and p-coumaric acids have been identified [101]. Different extraction systems quantitatively but not qualitatively alter the phenolic composition of grape pomace extracts.

Biological characterization involves antioxidant and antimicrobial tests for all extracts and seed oil, with the ability to inhibit α -glucosidase, α -amylase, α -tyrosinase, and ChE enzymes, along with anti-inflammatory activity and macrophage release stimulation [103].

The content of anthocyanins and flavan-3-ols in grape phenolic extracts varies depending on the grape variety and whether the extract comes from whole fruit or fermented pomace. However, all grape phenolic extracts significantly inhibit glucosyltransferases B and C (70-85% inhibition) at concentrations up to 62.5 μ g/mL (P < 0.01) [102]. Additionally, these extracts reduce the glycolytic pH drop caused by *Streptococcus mutans* without affecting bacterial viability, likely due to partial inhibition of F-ATPase activity (30-65% inhibition at 125 μ g/mL; P < 0.01) [102]. Notably, fermented pomace extracts displayed similar or superior biological activity compared to whole fruit extracts [104]. These findings suggest that grape phenolic extracts, particularly from pomace, are highly effective against specific virulence traits of *S. mutans*, even with significant variations in their phenolic content.

Phenolic compounds are primarily synthesized from carbohydrates via the shikimic acid and acetate pathways. Shikimic acid leads to cinnamic acids and their derivatives through transamination and deamination. Acetates lead to polyketides or polyacetates (malonate). The structure of phenolic compounds ranges from a single aromatic nucleus with low molecular weight to complex tannins with very high molecular weight, depending on the nature of the carbon skeleton and the length of the aliphatic chain attached to the benzene nucleus [105]. Phenolic compounds are capable of conjugation with sugars or organic acids. Phenolic compounds can be divided into two major groups: flavonoids and non-flavonoids.

Flavonoids are a group of polyphenolic compounds consisting of 15 carbon atoms arranged in a C6-C3-C6 structure, where two aromatic rings are linked by a three-carbon bridge. They are the most abundant among all phenolic compounds. They are the most prevalent phenolic compounds and serve various functions in plants as secondary metabolites, including roles in UV protection, pigmentation, nitrogen fixation, and resistance to diseases. This C6-C3-C6 structure results from two synthetic pathways of phenolic compounds (Figure 5) [105]. The B ring and the three-carbon bridge form a phenylpropanoid unit, produced from phenylalanine through the shikimic acid pathway, while the A ring is derived from the condensation of three acetate units via the malonic acid pathway. The fusion of these two parts involves the condensation of a phenylpropanoid, 4-coumaroyl, with three malonyl-CoA, each contributing two carbon atoms. The reaction is catalyzed by chalcone synthase, thus generating tetrahydroxychalcone, which can subsequently generate all flavonoids [105].

Figure 5. Flavonoid structure.

There are several groups of flavonoids, the main ones being flavones, flavonols, flavan-3-ols, isoflavones, flavanones, and anthocyanidins (Figure 6) [106]. Isoflavones are not present in grapes. The basic structure of flavonoids can undergo many substitutions, with hydroxyl groups typically at positions 4, 5, and 7. Most flavonoids exist as glycosides, varying greatly depending on the species and the nature of the sugars. Substitutions alter the solubility of flavonoids; hydroxylations and glycosylations generally make the compounds more hydrophilic, while other substituents, such as methylation, make them more lipophilic [106].

Flavonols are often highly widespread compounds. Flavonols such as myricetin, quercetin, and kaempferol are usually present as O-glycosides. The bond is most frequently at position 3 of the aromatic C ring, though substitutions at positions 5, 7, 4', 3', and 5' are possible [106]. The number of aglycones is limited, but there is a substantial number of derivatives. For example, kaempferol alone has over 200 conjugates with different osidic fragments. There is strong variability in flavonol concentration depending on the season and the grape variety considered. Their structure is planar. Four flavonols are predominantly present in grapes: kaempferol, quercetin (5-10 mg/kg), myricetin, and isorhamnetin. Quercetin derivatives are always predominant. The average maximum flavonol content in grapes is around 50 mg/kg but varies between 10 and 285 mg/kg [105].

Flavanones are the first products of the flavonoid biosynthesis pathway. They are characterized by the absence of double bonding between C2 and C3 and by the presence of a chiral center at C2. Most naturally occurring flavanones have the B ring attached to the aromatic C ring. The structure of flavanones is highly reactive, leading to hydroxylation, Omethylation, and glycosylation reactions. Flavanones are present in grapes at concentrations of a few mg/kg [106].

Polymeric polyphenol (Condensed tannin, n= no. Of monomeric units)

Figure 6. Main classes of flavonoids.

Flavan-3-ols are the most structurally complex group of flavonoids. They include simple monomers like (+)-catechin and its isomer (-)-epicatechin, as well as larger oligomers and polymers known as proanthocyanidins [107]. Proanthocyanidins are formed from catechin and epicatechin with oxidative couplings between C4 positions of the heterocycle and C6 or C8 of the adjacent monomer. Procyanidin oligomers consist of 2 to 5 catechin or epicatechin units, while polymers contain 6 or more units. Additionally, flavan-3-ols can be esterified with gallic acid or, alternatively, hydroxylated to form gallo-catechins and gallotannins. Flavan-3-ols in grapes are primarily found as polymers. Seed tannins are composed of proanthocyanidins (polymers of catechin and epicatechin), partially galloylated, while those in grape skins also contain prodelfinidins (polymers of gallo-catechin and epigallocatechin) [108]. The average number of monomer units, defined as the average degree of polymerization (DPm), can reach up to 18 in a seed-derived fraction and approaches 30 units in a grape skin extract [108].

Flavones are structurally very similar to flavonols, with the difference being the absence of a hydroxyl group at C3. There are also many possible substitutions for flavones, such as hydroxylation, methylation, O- and C-alkylation, and glycosylation. Flavones are mainly present as glycosides. Grapes contain very small amounts of flavones [106, 107].

Anthocyanidins are widely present in the plant kingdom, primarily as glycosides, and are found exclusively in the skins of black grapes (absent in white grapes) [109]. They are responsible for red, blue, and purple colors depending on the pH of the environment [110]. These compounds are involved in protecting plants against excessive sunlight. The most common anthocyanidins are pelargonidin, cyanidin, delphinidin, peonidin, and malvidin, but these compounds are present only as glycosylated conjugates, anthocyanins. Anthocyanidins can form conjugates with hydroxycinnamic acids and organic acids (malic acid and acetic acid) [111]. Unlike other species (hybrids) with high levels of diglucosylated anthocyanins at C-3' and C-5', Vitis vinifera contains only traces of these compounds. This is due to the

predominant presence of 3-monoglucoside anthocyanidins, especially malvidin 3-O-glucoside and its acyl derivatives [112]. Anthocyanins are present in grapes with average contents ranging from 500 to 3,000 mg/kg, but can reach up to 5,000 mg/kg [110].

Non-flavonoids. The main non-flavonoids of nutritional importance are phenolic acids, hydroxycinnamic acids, and stilbenes (Figure 7) [113].

Figure 7. Structure of main non-flavonoids.

Phenolic acids. Hydroxybenzoic acids have a C6-C1 structure, consisting of a benzene ring attached to an aliphatic chain. These include vanillic acid, syringic acid, gentisic acid, and gallic acid [114]. The primary compound is gallic acid, which is found in grapes between 100 and 230 mg/kg [105, 109].

Hydroxycinnamic acids. Cinnamic acid is a C6-C3 compound formed through the deamination of phenylalanine, a process catalyzed by phenylalanine ammonia-lyase. This reaction produces p-coumaric acid through the hydroxylation of cinnamic acid. Both cinnamic acid and hydroxycinnamic acids are commonly referred to as phenylpropanoids. Their basic structure consists of a benzene ring attached to a 3-carbon aliphatic chain, often featuring one or more hydroxyl groups that may be esterified with an aliphatic alcohol [115]. The most common hydroxycinnamic acids include caffeic, p-coumaric, ferulic, and sinapic acids. These compounds are produced through a series of hydroxylation and methylation reactions. They often accumulate in plants as esters of tartaric acid, forming compounds such as coutaric (an ester of p-coumaric acid), caftaric (an ester of caffeic acid), and fertaric acid (an ester of ferulic acid). These esters play significant roles in plant metabolism and contribute to the antioxidant properties of various foods and beverages [115]. These constituents are primarily found in the pulp of grape berries. The major hydroxycinnamic acid in grapes is caftaric acid (caffeoyl tartaric ester), which can be found at levels of approximately 200 mg/kg [116].

Stilbenes are polyphenolic compounds with a C6-C2-C6 structure, two benzene rings linked by a methylene bridge. They are produced by plants in response to fungal, bacterial, or viral attacks, as demonstrated for trans-resveratrol [117]. Resveratrol is synthesized by condensing 4-coumaroyl with 3 malonyl CoA, each providing 2 carbon atoms. The reaction is catalyzed by stilbene synthase, with the products being the same as for flavonoid synthesis, the only difference being the enzyme that catalyzes the reaction. Resveratrol in its cis- and trans- forms is found in plant tissues, mainly as trans-resveratrol-3-O-glucoside [118]. Oligomeric forms of stilbenes, such as pallidol and viniferin, have also been identified in grapes, and more recently, a tetramer of resveratrol, hopeaphenol [119].

The content of catechins and proanthocyanidins (catechin oligomers) varies depending on the type of grape. In table grapes, the content of these compounds ranges from 243 to 1,108 mg/kg, with over 89% generally located in the seeds [120]. Table 4 presents the distribution of polyphenolic compounds according to the different parts of red grape berries.

C. Tașca 169

Table 4
Distribution of polyphenolic compounds in grapes (mg/kg)

Compounds	Pulp	Skin	Seeds
Tannins	Traces	100-500	1000-6000
Anthocyanins	-	500-3000	-
Phenolic Acids	20-170	50-200	-

^{*}Composed by the author based on bibliographic sources [120-123]

This distribution confirms that the grape pomace resulting from the winemaking process is an extremely concentrated source of bioactive compounds.

Tannins in grape pomace are primarily composed of proanthocyanidins or catechin tannins. These compounds are made up of monomeric or polymeric units of flavan-3-ols [61].

Proanthocyanidins, also known as condensed tannins, are synthesized as secondary polyphenolic metabolites through the flavonoid biosynthetic pathway. Discovered in 1947 by Jacques Masquelier, who developed and patented techniques for extracting oligomeric procyanidins from pine bark and grape seeds, proanthocyanidins continue to attract attention due to their biological and physiological properties [121]. They are composed of procyanidin and prodelfinidin units linked together by a C4-C8 bond (Figure 8) [122,123].

However, the high polyphenol content is a disadvantage for using pomace as animal feed and may pose potential pollution issues when used as soil fertilizer.

Antioxidant and microbiostatic properties of CBA from grape pomace. Numerous studies demonstrate the effectiveness of CBA extracted from grape pomace on health, particularly due to their antioxidant, anti-inflammatory, and microbiostatic effects related to the significant CBA content [124]. The antioxidant activity of grape pomace extracts was evaluated in obese male mice with diet-induced obesity (ODI) by measuring their oxygen radical absorption capacity (ORAC) [125]. Male ODI mice were randomly assigned to one of three treatment groups (n = 12): a normal diet group (DN), a high-fat diet group (Gr), and a high-fat diet group supplemented with grape pomace extracts (GrTS). After 12 weeks of treatment, the mice in the high-fat diet groups gained 29% more weight compared to those in the DN group. Supplementation with grape pomace extracts, estimated at 250 mg/kg/day (GrTS group), reduced plasma levels of C-reactive protein by 15.5% in mice fed a high-fat diet, suggesting a potential anti-inflammatory effect [125]. Grape pomace extracts (GPE) demonstrate anti-inflammatory effects in diet-induced obesity, largely due to their high content of polyphenolic compounds and anthocyanins, measured at 475.4 mg of gallic acid equivalent/q and 156.9 mg of cyanidin 3-glucoside equivalent/g, respectively [124, 125]. GPE also contains catechin (28.6 mg/g) and epicatechin (24.5 mg/g), as well as other antioxidants, including quercetin (1.6 mg/g), trans-resveratrol (60 μg/g), gallic acid (867.2 μg/g), coutaric acid (511.8 μg/g), p-hydroxybenzoic acid (408.3 μg/g), and protocatechuic acid (371.5 μg/g). The antioxidant activity, as measured by the ORAC assay, was 4133 µmol TE/g [125].

A recent study examined the effectiveness of antioxidant supplements in reducing oxidative stress [126], particularly focusing on the impact of grape beverages and extracts on oxidative stress markers in athletes. The study detailed the polyphenolic doses, participant demographics, and exercise protocols used [126].

Grape pomace extracts were also tested for their antibacterial properties against several strains, including *Bacillus cereus*, *Bacillus coagulans*, *Bacillus subtilis*, *Staphylococcus*

Figure 8. Structures of flavan-3-ols and proanthocyanidins – main constituents of grape seed extract: (+)-catechin (1), (-)-epicatechin (2), proanthocyanidin B1 (3), B2 (4), B3 (5), B4 (6), and C1 (7)

aureus, strains of *Escherichia coli* and *Pseudomonas aeruginosa* [53]. The results showed that Gram-positive bacteria were inhibited at concentrations of 850-1000 ppm, while Gram-negative bacteria required 1250-1500 ppm for inhibition [52].

Additionally, since a significant amount of polyphenols are not absorbed in the small intestine, their interaction with colonic microbiota was studied. The influence of polyphenolic extracts on the growth of *Lactobacillus acidophilus* CECT 903 was investigated in vitro through agar diffusion tests and liquid medium cultures. Grape phenolic extracts and some standard phenolic compounds (caffeic, gallic, tannic acids, catechin, epicatechin, and quercetin) were tested. None of the tested phenolic compounds exerted an inhibitory effect on *Lactobacillus acidophilus* growth at a maximum concentration of 5000 µg/disk diffusion tests in agar. It was found that the phenolic extract from grape pomace (1 mg/mL) induced a significant increase in *Lactobacillus acidophilus* biomass in liquid culture media [127].

Phenolic compounds in grape pomace undoubtedly have therapeutic properties, particularly for certain chronic conditions such as atherosclerosis, diabetes, hypertension, and some types of cancer [128]. Among the mechanisms of action of phenolic compounds involved in the prevention of chronic pathologies are:

- 1. Grape pomace demonstrates significant antioxidant activity, as measured by ABTS• and DPPH• assays, as well as H_2O_2 scavenging tests. This high level of antioxidant activity is strongly associated with the presence of flavan-3-ols, phenolic acids, and ethyl gallate. Additionally, grape skin has been shown to exert cellular antioxidant effects on adenocarcinoma cells, with an EC₅₀ value of 56.4 mg total phenolic content (TPC)/mL, which is closely linked to the presence of flavonols and anthocyanins [129].
 - 2. A saving effect on endogenous antioxidants (vitamin E, vitamin C, ß-carotene, etc.) [130].
- 3. A saving effect on antioxidant enzymes (SOD superoxide dismutase, catalase, SeGSHPx glutathione peroxidase) [131].
- 4. A significant effect on reducing cholesterol and rebalancing blood lipids high density lipoproteins (HDL) and low density lipoproteins (LDL) [132].
- 5. Chelation effect on oxidation cofactors, fatty acids, and certain metal ions (Fe^{2+} , Cu^{2+}) [133].
- 6. An inhibitory effect on oxidative enzymes such as cyclooxygenases and lipoxygenases [102].
- 7. Effect on NO synthesis in endothelial cells of the arterial wall, leading to vasorelaxation and membrane hyperpolarization through extracellular potassium release [134].
- 8. An inhibitory effect on the genesis of NADPH oxidase production in vascular wall cells (thoracic aorta and heart), resulting in a reduction in free radical production [135].
- 9. A significant effect is the presence of trans-resveratrol. Trans-resveratrol has been shown to have beneficial effects on diseases related to oxidative and/or inflammatory processes and extends lifespan. A study aimed at estimating the dietary intake of four stilbenes in the Spanish adult population allowed for the mediation of intake and their sources [136]. Among the four stilbenes studied, trans-piceid was the most abundant, accounting for 53.6% of the total, followed by trans-resveratrol at 20.9%, cis-piceid at 19.3%, and cis-resveratrol at 6.2%. The majority of the research and development on these compounds focused on wines (98.4%), with only 1.6% attributed to grapes and grape juices, while contributions from sources like nuts, pistachios, and berries were negligible, making up less than 0.01% [136].

As a natural food ingredient, resveratrol possesses significant antioxidant potential, antitumor activity, and is considered a potential candidate for the prevention and treatment of various types of cancer [137]. The anticancer properties of resveratrol have been confirmed in numerous *in vitro* and *in vivo* studies, demonstrating its ability to inhibit all stages of carcinogenesis, including initiation, promotion, and progression. In addition to its anticancer effects, resveratrol exhibits a wide range of bioactive properties, such as anti-inflammatory, cardioprotective, vasorelaxant, phytoestrogenic, and neuroprotective effects. Despite these promising benefits, the pharmaceutical application of resveratrol faces challenges due to its poor solubility, low bioavailability, and potential adverse effects. As a result, numerous studies have focused on estimating the resveratrol content in wines and grape pomace from various sources in an effort to improve its therapeutic potential [138-141]. The general conclusion is that this component accumulates depending on plant metabolism, agroclimatic conditions, and other difficult-to-predict factors.

4. Conclusions

Managing waste in the agro-industrial sector is critical for preventing environmental pollution while simultaneously capitalizing on opportunities to obtain value-added products. Waste from industries like wine, spirits, beer, and juice production can have harmful effects on ecosystems if not properly managed. For example, improper disposal of liquid waste can damage soil chemical composition, disrupt the balance of microorganisms, and negatively affect plants and other living organisms. Solid organic waste is often managed through agricultural application, anaerobic digestion, composting, and incineration—though incineration is costly and linked to air emissions. Liquid waste, on the other hand, is treated via methods like sedimentation, decantation in stabilization ponds, and anaerobic fermentation to reduce its environmental impact. The key challenge is that agro-industrial waste often contains toxic components harmful to plants and ecosystems, making direct soil disposal unsuitable. However, this waste can be repurposed as a renewable source of value-added products, offering potential for sustainable development within the agro-industrial sector.

Conflict of Interest: The author declares no conflict of interest.

References

- 1. Swinnen, J. Beer consumption and trade in an era of economic growth and globalization. *Choices* 2017, 32 (3), pp. 1–6.
- 2. Sganzerla, W. G.; Ampese, L. C.; Mussatto, S. I.; Forster-Carneiro, T. A bibliometric analysis on potential uses of brewer's spent grains in a biorefinery for the circular economy transition of the beer industry. *Biofpr* 2021, 15(6), pp. 1965-1988.
- 3. dos Santos Mathias, T. R.; de Mello, P. P. M.; Sérvulo, E. F. C. Solid wastes in brewing process: A review. *J. Brew. Distill* 2014, 5(1), pp. 1-19.
- 4. Rachwal, K.; Wasko, A.;, Gustaw, K., Polak-Berecka, M. Utilization of brewery wastes in food industry. *PeerJ* 2020, vol. 8.
- 5. Townsley, P.M. Preparation of commercial products from brewer's waste grain and trub. *MBAA Tech Quarterly* 1979, 16, pp. 130–134.
- 6. Bartolomè, B.; Santos, M.; Jimenez, J.J.; del Nozal, M.J.; Gomez-Cordoves, C. Pentoses and hydroxycinnamic acids in brewers' spent grain. *J. Cereal Sci* 2002, 36, pp. 51-58.
- 7. Sajib, M.; Falck, P.; Sardari, R.R.R; Mathew, S.; Grey, C.; Karlsson, E.N.; Adlercreutz, P. Valorization of Brewer's spent grain to prebiotic oligosaccharide: Production, xylanase catalyzed hydrolysis, in-vitro evaluation with probiotic strains and in a batch human fecal fermentation model. *J. Biotech* 2018, 268, pp. 61-70.
- 8. Nagasaka, R.; Chotimarkorn, C.; Shafiqul, I. M.; Hori, M.; Ozaki, H.; Ushio, H. Antiinflammatory effects of hydroxycinnamic acid derivatives. *BBRC* 2007, 358, pp. 615–619.
- 9. Aliyu, S.; Bala, M. Brewer's spent grain: a review of its potentials and applications. *Afr J Biotech* 2011, 10(3), pp. 324–331.
- 10. Mussatto, S.; Dragone, G.; Roberto, I. Brewers' spent grain: generation, characteristics and potential applications. *J Cereal Sci* 2006, 43, pp. 1–14.
- 11. Ikram, S.; Huang, L.; Zhang, H.; Wang, J.; Yin, M. Composition and Nutrient Value Proposition of Brewers Spent Grain. *J Food Sci* 2017, 82(10), pp. 2232-2242.
- 12. Mussatto, S.I.; Roberto, I.C. Acid hydrolysis and fermentation of brewers' spent grain to produce xylitol. J. Sci. Food Agric., 2005, vol. 85, pp. 2453-2460.
- 13. Lynch, K.M.; Steffen, E.J.; Arendt, E.K. Brewers' spent grain: a review with an emphasis on food and health. *JIB* 2016, 122, pp. 553-568.
- 14. Robertson, J.A.I.; Anson, K.J.A.; Treimo, J.; Faulds, C.B.; Brocklehurst, T.F.; Eijsink, V.G.H.; Waldron, K.W. Profiling brewer's spent grain for composition and microbial ecology at the site of production. *LWT-Food Science and Technology* 2010, 43, pp. 890-896.
- 15. Cooray, S.T.; Lee, J.J.L.; Chen, W.N. Evaluation of brewers' spent grain as a novel media for yeast growth. *AMB Express* 2017, 7, pp. 1-10.

C. Tașca 173

- 16. Stefanello, F.S.; Dos Santos, C.O.; Bochi, V.C.; Fruet, A.P.B.; Soquetta, M.B.; Dörr, A.C.; Nörnberg, J.L. Analysis of polyphenols in brewer's spent grain and its comparison with corn silage and cereal brans commonly used for animal nutrition. *Food Chem* 2018, 239, pp. 385-401.
- 17. Kanauchi, O.; Mitsuyama, K.; Araki, Y. Development of a functional germinated barley foodstuff from brewer's spent grain for the treatment of ulcerative colitis. *J Am Soc Brew Chem* 2001, 59(2), pp. 59–62.
- 18. Carvalheiro, F.; Esteves, M.P.; Paraj'o, J.C.; Pereira, H.; Gırio, F.M. Production of oligosaccharides by autohydrolysis of brewery's spent grain. *Bioresour. Technol* 2004, 91(1), pp. 93–100.
- 19. Silva, J.P.; Sousa, S.; Rodrigues, J.; Antunes, H.; Porter, J.J.; Gonc, alves, I.; Ferreira-Dias, S. Adsorption of acid orange 7 dye in aqueous solutions by spent brewery grains. *Sep Purif Technol* 2004, 40(3), pp. 309–315.
- 20. Moreira, M.M.; Morais, S.; Carvalho, D.O.; Barros, A.A.; Delerue-Matos, C.; Guido, L.F. Brewer's spent grain from different types of malt: evaluation of the antioxidant activity and identification of the major phenolic compounds. *Food Res Int* 2013, 54(1), pp. 382–388.
- 21. Hernanz, D.; Nunez, V.; Sancho, A.I.; Faulds, C.B.; Williamson, G.; Bartolome, B.; Gomez-Cordoves, C. Hydroxycinnamic acids and ferulic acid dehydrodimers in barley and processed barley. *J Agr Food Chem* 2001, 49(10), pp. 4884–4888.
- 22.McCarthy, A.L.; O'Callaghan, Y.C.; Neugart, S.; Piggott, C.O.; Connolly, A.; Jansen, M.A.K.; Krumbein, A.; Schreiner, M.; FitzGerald, R.J.; O'Brien, N.M. The hydroxycinnamic acid content of barley and brewers' spent grain (BSG) and the potential to incorporate phenolic extracts of BSG as antioxidants into fruit beverages. *Food Chem* 2013, 141(3), pp. 2567–2574.
- 23. Ktenioudaki, A.; Alvarez-Jubete, L.; Smyth, T.J.; Kilcawley, K.; Rai, D.K.; Gallagher, E. Application of bioprocessing techniques (sourdough fermentation and technological aids) for brewer's spent grain breads. *Food Res Int* 2015, 73, pp. 107–116.
- 24. Chen, J.H.; Ho, C.T. Antioxidant activities of caffeic acid and its related hydroxycinnamic acid compounds. *J Agric Food Chem* 1997, 45, pp. 2374–2378.
- 25. Gulcin, I. Antioxidant activity of caffeic acid (3, 4-dihydroxycinnamic acid). *Toxicology* 2006, 217, pp. 213–220.
- 26. Kikuzaki, H.; Hisamoto, M.; Hirose, K.; Akiyama, K.; Taniguchi, H. Antioxidant properties of ferulic acid and its related compounds. *J Agric Food Chem* 2002, 50(7), pp. 2161–2168.
- 27. Maurya, D.K.; Devasagayam, T.P.A. Antioxidant and prooxidant nature of hydroxycinnamic acid derivatives ferulic and caffeic acids. *Food Chem Toxicol* 2010, 48(12), pp. 3369–3373.
- 28. Gomes, C.A.; da Cruz, T.G.; Andrade, J.L.; Milhazes, N.; Borges, F.; Marques, M.P. Anticancer activity of phenolic acids of natural or synthetic origin: a structure activity study. *J Med Chem* 2003, 46 (25), pp. 5395 5401.
- 29. Chang, W.-C.; Hsieh, C.-H.; Hsiao, M.-W.; Lin, W.-C.; Hung, Y.-C.; Ye, J.-C. Caffeic acid induces apoptosis in human cervical cancer cells through the mitochondrial pathway. *TJOG* 2010, 49(4), pp. 419–424.
- 30. Kang, NJ.; Lee, K.W.; Shin, BJ.; Jung, S. K.; Hwang, M. K.; Bode, A. M.; Dong, Z. Caffeic acid, a phenolic phytochemical in coffee, directly inhibits Fyn kinase activity and UVB-induced COX-2 expression. *Carcinogenesis* 2009, 30(2), pp. 321–330.
- 31. Kim, M.C.; Kim, S.J.; Kim, D.S.; Jeon, Y.-D.; Park, S. J.; Lee, H. S.; Hong, S.-H. Vanillic acid inhibits inflammatory mediators by suppressing NF-B in lipopolysaccharide-stimulated mouse peritoneal macrophages. *Immunopharmacol Immunotoxicol* 2011, 33(3), pp. 525–532.
- 32. Hussain, T.; Gupta, S.; Adhami, V.M.; Mukhtar, H. Green tea constituent epigallocatechin 3 gallate selectively inhibits COX 2 without affecting COX 1 expression in human prostate carcinoma cells. *Int J Cancer* 2005, 113(4), pp. 660–669.
- 33. Garcı'a-Mediavilla, V.; Crespo, I.; Collado, P.S.; Esteller, A.; Sánchez-Campos, S.; Tuñón, M. J.; González-Gallego, J. The anti-inflammatory flavones quercetin and kaempferol cause inhibition of inducible nitric oxide synthase, cyclooxygenase-2 and reactive C-protein, and down-regulation of the nuclear factor kappaB pathway in Chang Liver cells. *Eur J Pharmacol* 2007, 557(2-3), pp. 221–229.
- 34. Tang, D.-S.; Yin, G.-M.; He, Y.-Z.; Hu, S.-Q.; Li, B.; Li, L.; Liang, H.- L.; Borthakur, D. Recovery of protein from brewer's spent grain by ultrafiltration. *Biochem Eng J* 2009, 48(1), pp. 1–5.
- 35. Prentice, N.; Kissell, L. T.; Lindsay, R.C.; Yamazaki, W.T. High-fiber cookies containing brewers' spent grain. *Cereal Chem* 1978, 55(5), pp. 712–721.
- 36. Ozturk, S.; Özboy, Ö.; Cavidoğlu, I.; Köksel, H. Effects of brewers' spent grains on the quality and dietary fibre content of cookies. *J Inst Brew* 2002, 108(1), pp. 23–27.

- 37. Clemente, A. Enzymatic protein hydrolysates in human nutrition. *Trends Food Sci Technol* 2000, 11(7), pp. 254–262.
- 38. Kühbeck, F.; Back, W.; Krottenthaler, M.Influence of lauter turbidity on wort composition, fermentation performance and beer quality –a review. *JIB* 2006, 112, pp. 215-221.
- 39. dos Santos Mathias, T. R.; Alexandre, V. M. F.; Cammarota, M. C.; de Mello, P. P. M.; Sérvulo, E. F. C. Characterization and determination of brewer's solid wastes composition. *JIB 2015*, 121(3), pp. 400-404.
- 40. Sterczyńska, M.; Zdaniewicz, M.; Wolny-Koładka, K. Rheological and Microbiological Characteristics of Hops and Hot Trub Particles Formed during Beer Production. *Molecules* 2021, 26(3), pp. 681.
- 41. Huige, N. Brewery by-products and effluents. In: Priest FG, Stewart GG, eds. Handbook of brewing (2nd edition). *CRC Press, Boca Raton: Taylor & Francis Group* 2006, pp.656-707.
- 42. Kerby, C.; Vriesekoop, F. An overview of the utilisation of brewery by-products as generated by british craft breweries. *Beverages* 2017, 3(2), pp.24.
- 43. Olajire, A.A. The brewing industry and environmental challenges. J. Clean. Prod 2012, 30, pp. 1-21.
- 44. Fillaudeau, L.; Blanpain-Avet, P.; Daufin, G. Water, wastewater and waste management in brewing industries. *J. Clean. Prod* 2006, 14(5), pp. 463-471.
- 45. Rachwał, K.; Waśko, A.; Gustaw, K.; Polak-Berecka, M. Utilization of brewery wastes in food industry. *FS& Techn* 2020, PeerJ8:e9427.
- 46. Podpora, B.; Swiderski, F.; Sadowska, A.; Rakovska, R.; Wasiak-Zys, G. Spent brewer's yeast extracts as a new component of functional food. *Czech J. Food Sci* 2016, 34, pp. 554-563.
- 47. Gómez-Brandón, M.; Lores, M.; Insam, H.; Domínguez, J. Strategies for recycling and valorization of grape marc. *Crit. Rev. Biotechnol* 2019, 39(4), pp. 437–450.
- 48. Hussain, M.; Cholette, S.; Castaldi, R. M. An Analysis of Globalization Forces in the Wine Industry: Implications and Recommendations for Wineries. J. *Glob. Mark* 2008, 21(1), pp. 33–47.
- 49. Bianco, A.; Uccella, N. Biophenolic components of olives. Int. Food Res 2000, 33(6), pp. 475-485.
- 50. Lapornik, B.; Lapornik, B.; Prosek, M.; Wondra, A.G. Comparison of extracts prepared from plant by-products using different solvents and extraction time. *J. Food Eng* 2005, 71(2), pp. 214-222.
- 51. Yilmaz, Y.; Toledo, R. Antioxidant activity of water-soluble Maillard reaction products. *Food Chem* 2005, 93(2), pp. 273-278.
- 52. Jayaprakasha, G.K.; Singh, R.P.; Sakariah, K.K. Antioxidant activity of grape seed (Vitis vinifera) extracts on peroxidation models in vitro. *Food Chem* 2001, 73(3), pp. 285-290.
- 53. Jayaprakasha, G.K.; Selvi, T.; Sakariah, K.K. Antibacterial and antioxidant activities of grape (Vitis vinifera) seed extracts. *Food Res Intern* 2003, 36, pp. 117-122.
- 54. Musee, N.; Lorenzen, L.; Aldrich, C. Cellar waste minimization in the wine industry: a systems approach. J. *Clean. Prod* 2007, 15(5), pp. 417-431.
- 55. Rondeau, P.; Gambier, F.; Jolibert, F.; Brosse, N. Compositions and chemical variability of grape pomaces from French vineyard. *Ind. Crop. Prod* 2013, 43, pp. 251-254.
- 56. Sousa, R.M.O.F.; Amaral, C.; Fernandes, J.M.C.; Fraga, I.; Semitela, S.; Braga, F.; Coimbra, A.M.; Dias, A.A.; Bezerra, R. M.; Sampaio, A. Hazardous impact of vinasse from distilled winemaking by-products in terrestrial plants and aquatic organisms. *Ecotoxicol. Environ. Saf* 2019, 183, 109493.
- 57. Amulya, K.; Jukuri, S.; Venkata Mohan, S. Sustainable multistage process for enhanced productivity of bioplastics from waste remediation through aerobic dynamic feeding strategy: Process integration for upscaling. *Bioresour. Technol* 2015, 188, pp. 231-239.
- 58. Ping, L.; Brosse, N.; Sannigrahi, P.; Ragauskas, A. Evaluation of grape stalks as a bioresource. *Ind. Crops Prod* 2011, 33 (1), pp. 200-204.
- 59. Spigno, G.; De Faveri, D. M. Antioxidants from grape stalks and marc: Influence of extraction procedure on yield, purity and antioxidant power of the extracts. *J. Food Eng* 2007, 78 (3), pp. 793-801.
- 60. Venkata, S.; Nikhil, G.N.; Chiranjeevi, P.; Nagendranatha Reddy, C.; Rohit, M.V.; Naresh Kumar, A. Omprakash Sarkar, Waste biorefinery models towards sustainable circular bioeconomy: Critical review and future perspectives. *Bioresour Technol* 2016, 215, pp. 2-12.
- 61. Alonso, Á.M.; Domínguez, C.; Guillén, D.A.; Barroso, C.G. Determination of Antioxidant Power of Red and White Wines by a New Electrochemical Method and Its Correlation with Polyphenolic Content. *J. Agric. Food Chem* 2002, 50 (11), pp. 3112–3115.
- 62. Barcia, M. T.; Pertuzatti, P. B.; Gómez-Alonso, S.; Godoy, H. T.; Hermosín-Gutiérrez I. Phenolic composition of grape and winemaking by-products of Brazilian hybrid cultivars BRS Violeta and BRS Lorena. *Food Chem* 2014, 159, pp. 95-105.

63. Beres, C.; Costa, G.N.S.; Cabezudo, I.; da Silva-James, N.K.; Teles, A.S.C.; Cruz, A. P.G.; Mellinger-Silva, C.; V. Tonon, R.; Cabral, L. M.C.; Freitas, S. P. Towards integral utilization of grape pomace from winemaking process: A review. *Waste Manag* 2017, 68, pp. 581-594.

- 64. Vanessa, S.; Igrejas, G.; Falco, V.; Santos, T. P.; Torres, C.; Oliveira, A.M.P.; Pereira, J. E.; Amaral, J.S.; Poeta, P. Chemical composition, antioxidant and antimicrobial activity of phenolic compounds extracted from wine industry by-products. *Food Control* 2018, 92, pp. 516-522.
- 65. Marwa, B.; Gambier, F.; Brosse, N. Optimization of polyphenols extraction from grape residues in water medium. *Ind. Crops Prod* 2014, 52, pp. 18-22.
- 66. Caldas, T.W.; Karen E.L. Mazza; Aline S.C., Teles; Gabriela N., Mattos; Ana Iraidy, S. Brígida; Carlos A., Conte-Junior; Renata G., Borguini; Ronoel L.O., Godoy; Lourdes M.C., Cabral; Renata V., Tonon. Phenolic compounds recovery from grape skin using conventional and non-conventional extraction methods. *Ind. Crops Prod* 2018, 111, pp. 86-91.
- 67. Thorsten, M.; Schieber, A.; Kammerer, D. R.; Carle, R. Residues of grape (Vitis vinifera L.) seed oil production as a valuable source of phenolic antioxidants. *Food Chem* 2009, 112(3), pp. 551-559.
- 68. Medouni-Adrar, S.; Boulekbache-Makhlouf, L.; Cadot, Y.; Medouni-Haroune, L.; Dahmoune, F.; Makhoukhe, A.; Madani, K. Optimization of the recovery of phenolic compounds from Algerian grape by-products. *Ind. Crops Prod* 2015, 77, pp. 123-132.
- 69. Beres, C.; Suely Pereira, F.; Ronoel Luiz de Oliveira, G.; Denize Cristine, Rodrigues de Oliveira; Rosires D.; Marcello, I.; Caroline, M-S.; Lourdes, Maria C. C. Antioxidant dietary fibre from grape pomace flour or extract: Does it make any difference on the nutritional and functional value? *J. Funct. Foods* 2019, 56.
- 70. Mendes, Joana A.S.; Xavier, Ana M.R.B.; Evtuguin, Dmitry V.; Lopes, Luísa P.C. Integrated utilization of grape skins from white grape pomaces. *Ind. Crops Prod* 2013, 49, pp. 286-291.
- 71. Anastasiadi, M.; Pratsinis, H.; Kletsas, D.; Skaltsounis, A.-L.; Haroutounian, S.A. Grape stem extracts: Polyphenolic content and assessment of their in vitro antioxidant properties. *LWT Food Science and Technology* 2012, 48(2), pp. 316-322.
- 72. Barros, A.; Gironés-Vilaplana, A.; Teixeira, A.; Collado-González, J.; Moreno, D.A.; Gil-Izquierdo, A.; Rosa, E.; Domínguez-Perles, R. Evaluation of grape (Vitis vinifera L.) stems from Portuguese varieties as a resource of (poly)phenolic compounds: A comparative study. *Int. Food Res* 2014, 65(c), pp. 375-384.
- **73.**González-Centeno, M. R.; Jourdes, M.; Femenia, A.; Simal, S.; Rosselló, C.; Teissedre, P.-L. Characterization of Polyphenols and Antioxidant Potential of White Grape Pomace Byproducts (Vitis vinifera L.). *J. Agric. Food Chem* 2013, 61(47), pp. 11579–11587.
- 74. Spatafora, C.; Barbagallo, E.; Amico, V.; Tringali, C. Grape stems from Sicilian Vitis vinifera cultivars as a source of polyphenol-enriched fractions with enhanced antioxidant activity. *LWT Food Science and Technology* 2013, 54(2), pp. 542-548.
- 75. Ewald, P.; Delker, U.; Winterhalter, P. Quantification of stilbenoids in grapevine canes and grape cluster stems with a focus on long-term storage effects on stilbenoid concentration in grapevine canes. *Int. Food Res* 2017, 100(3), pp. 326-331.
- 76. Prozil, Sónia O.; Evtuguin, D.V.; Cruz Lopes, L. P. Chemical composition of grape stalks of Vitis vinifera L. from red grape pomaces. *Ind. Crops Prod* 2012, 35(1), pp. 178-184.
- 77. Gomez-Pinilla, F.; Nguyen, T. T. J. Natural mood foods: The actions of polyphenols against psychiatric and cognitive disorders. *Nutr. Neurosci* 2012, 15 (3), pp. 127–133.
- 78. Zorraquín-Peña, I.; Esteban-Fernández, A.; González de Llano, D.; Bartolomé, B.; Moreno-Arribas, M.V. Wine-Derived Phenolic Metabolites in the Digestive and Brain Function. *Beverages* 2019, 5, pp. 7.
- 79.de Oliveira, V.S.; Ferreira, F.S.; Cople, M.C.R.; Labre, T.d.S.; Augusta, I.M.; Gamallo, O.D.; Saldanha, T. Use of Natural Antioxidants in the Inhibition of Cholesterol Oxidation: A Review. *C.R. Food Sci. Food Saf* 2018, 17, pp. 1465-1483.
- 80. Chacar, S.; Hajal, J.; Saliba, Y.; Bois, P.; Louka, N.; Maroun, Richard G.; Faivre, J-F.; Fares, N. Long-term intake of phenolic compounds attenuates age related cardiac remodeling. *AgingCell* 2019, 189(2):e12894.
- 81. Herrera-Bravo, J.; Beltrán-Lissabet, J. F.; Saavedra, K.; Saavedra, N.; Hevia, M.; Alvear, M.; Lanas, F.; Salazar, L. A. Protective effect of Pinot noir pomace extract against the cytotoxicity induced by polycyclic aromatic hydrocarbons on endothelial cells. *Food and Chem. Toxicol* 2021, 148:111947.
- 82. Costa, M.D.; Davis, R.B.; Goldberger, A.L. Heart Rate Fragmentation: A Symbolic Dynamical Approach. *Front. Physiol* 2017, 8:827.

- 83. Raquel Del, P.-G.; González-SanJosé, María L.; Rivero-Pérez, María D.; García-Lomillo, J.; Muñiz, P. The effects of heat treatment on the phenolic composition and antioxidant capacity of red wine pomace seasonings. Food Chem 2017, 221, pp. 1723-1732.
- 84. Rodríquez-Esparza, E.; Zanella-Calzada, L. A.; Oliva, D.; Heidari, A. A.; Zaldivar, D.; Pérez-Cisneros, M.; Kok Foong, L. An efficient Harris hawks-inspired image segmentation method. Expert Syst. Appl 2020, 155, 113428.
- 85. Barajas-Álvarez, P.; González-Avila, M.; Espinosa-Andrews, H. Recent Advances in Probiotic Encapsulation to Improve Viability under Storage and Gastrointestinal Conditions and Their Impact on Functional Food Formulation. *Food Rev. Int* 2021, 39(2), pp.1-22.
- 86. Cañadas, R.; González-Miquel, M.; González, E. J.; Díaz, I.; Rodríguez, M.; Hydrophobic eutectic solvents for extraction of natural phenolic antioxidants from winery wastewater. Separation and Purification. Technology 2021, 254, 117590.
- 87. Gambier, F. Valorisation des marcs de raisins épuisés: vers un procédé d'éxtraction de tannins condensés à grande échelle pour la production d'adhesifs pour panneaux de particules. Thèse présentée à, pour l'obtention du grade de docteur Université de Lorraine, 2014.
- 88. Apolinar-Valiente, R.; Romero-Cascales, I.; Gómez-Plaza, E.; López-Roca, J. M.; Ros-García J. M. The composition of cell walls from grape marcs is affected by grape origin and enological technique. Food Chem 2015, 167, pp. 370-377.
- 89. Patti, A.-F.; Issa, G. (Jason); Smernik, R.; Wilkinso, K. Chemical composition of composted grape marc. Water *Sci Technol* 2009, 60 (5), pp. 1265–1271.
- 90. Carmona-Jiménez, Y.; Igartuburu, J.M.; Guillén-Sánchez, D.A.; García-Moreno, M.V. Fatty Acid and Tocopherol Composition of Pomace and Seed Oil from Five Grape Varieties Southern Spain. Molecules 2022, 27(20):6980.
- 91. Lutterodt, H.; Slavin, M.; Whent, M.; Turner, E.; Yu, L. Fatty acid composition, oxidative stability, antioxidant and antiproliferative properties of selected cold-pressed grape seed oils and flours. Food Chem 2011, 128(2), pp. 391-399.
- 92. Baca-Bocanegra, B.; Nogales-Bueno, J.; Hernández-Hierro, J.M.; Heredia, F.J. Optimization of Protein Extraction of Oenological Interest from Grape Seed Meal Using Design of Experiments and Response Surface Methodology. Foods 2021, 10, pp. 79.
- 93. Yu, J.; Ahmedna, M. Functional components of grape pomace: their composition, biological properties and potential applications. Int J Food Sci Technol 2013, 48, pp. 221-237.
- 94. Monteiro, G.C.; Minatel, I.O.; Pimentel, A.; Gomez, H.A.G.; de Camargo, J.P.C.; Diamante, M.S.; Pereira Basílio, L.S.; Tecchio, M.A.; Pereira Lima, G.P., Bioactive compounds and antioxidant capacity of grape pomace flours. LWT 2021, 135, 110053.
- 95. Llobera, A.; Cañellas, J. Dietary fibre content and antioxidant activity of Manto Negro red grape (Vitis vinifera): pomace and stem. Food Chem 2007, 01(2), pp. 659-666.
- 96. Ping, L.; Brosse, N.; Chrusciel, L.; Navarrete, P.; Pizzi, A. Extraction of condensed tannins from grape pomace for use as wood adhesives. Ind. Crops Prod 2011, 33(1), pp. 253-257.
- 97. Renaud, S.; De Lorgeril, M. Wine, alcohol, platelets, and the French paradox for coronary heart disease. *Lancet* 1992, 339(8808), pp.1523-1526.
- 98.de Gaetano, G.; Di Castelnuovo, A; Donati, M.B.; Iacoviello, L. The mediterranean lecture: wine and thrombosis--from epidemiology to physiology and back. Pathophysiol Haemost Thromb 2003, 33(5-6), pp.466-471.
- 99. Llobera, A.; Canellas, J. Antioxidant Activity and Dietary Fibre of Prensal Blanc White Grape (Vitis vinifera) By-Products. Int. J. Food Sci. Technol 2008, 43(11), pp. 1953-1959.
- 100. Parry, J.W.; Haiwen, L.; Jia-Ren, L.; Kequan, Z.; Lei, Z.; Shuxin, R. Antioxidant Activity, Antiproliferation of Colon Cancer Cells, and Chemical Composition of Grape Pomace. Food and Nutr Sci 2011, 2(6).
- 101. Lafka, T.-I.; Sinanoglou, V.; Lazos, E.S. On the extraction and antioxidant activity of phenolic compounds from winery wastes. *Food Chem* 2007, 104, pp. 1206–1214.
- 102. Mollica, A.; Scioli, G; Della Valle, A.; Cichelli, A.; Novellino, E.; Bauer, M.; Kamysz, W.; Llorent-Martínez, E.J.; Fernández-de Córdova, M.L.; Castillo-López, R.; Ak, G.; Zengin, G.; Pieretti, S.; Stefanucci, A. Phenolic Analysis and In Vitro Biological Activity of Red Wine, Pomace and Grape Seeds Oil Derived from Vitis vinifera L. cv. Montepulciano d'Abruzzo. Antioxidants 2021, 10(11), pp. 1704.
- 103. Peixoto, C.M.; Dias, M.I.; Alves, M.J.; Calhelha, R.C.; Barros, L.; Pinho, S.P.; Ferreira, I.C.F.R. Grape pomace as a source of phenolic compounds and diverse bioactive properties. Food Chem 2018, 253, pp.132-138.

C. Tașca 177

- 104. Thimothe, J.; Bonsi, I.A.; Padilla-Zakour, O.I.; Koo, H. Chemical characterization of red wine grape (Vitis vinifera and Vitis interspecific hybrids) and pomace phenolic extracts and their biological activity against Streptococcus mutans. *J. Agric Food Chem* 2007, 55(25), pp.10200-10207.
- 105. Chira, K.; Suh, J.-H.; Saucier, C.; Teissedre, P.-L. Les polyphénols du raisin. *Phytotherapie* 2008, 6(2), pp. 75-82.
- 106. Panche, A.N.; Diwan, A.D.; Chandra, S.R. Flavonoids: an overview. J. Nutr. Sci 2016, 5, e47.
- 107. Pietta, P.-G. Flavonoids as Antioxidants. J. Nat. Prod 2000, 63(7), pp. 1035-1042.
- 108. Gudej, J.; Tomczyk, M. Determination of Flavonoids, Tannins and Ellagic acid in leaves from Rubus L. species. *Arch Pharm Res* 2004, 27, pp. 1114–1119.
- 109. Amendola, D.; De Faveri, D.M.; Spigno, G. Grape marc phenolics: Extraction kinetics, quality and stability of extracts. *J. Food Eng* 2010, 97(3), pp. 384-392.
- 110. Muñoz, P.; Pérez, K.; Cassano, A.; Ruby-Figueroa, R. Recovery of Anthocyanins and Monosaccharides from Grape Marc Extract by Nanofiltration Membranes. *Molecules* 2021, 26, pp. 2003.
- 111. Holton, T.A.; Cornish, E.C. Genetics and Biochemistry of Anthocyanin Biosynthesis. *Plant Cell* 1995, 7(7), pp.1071-1083.
- 112. Welch, Cara R.; Wu, Q.; Simon, James E. Recent Advances in Anthocyanin Analysis and Characterization. *Curr. Anal. Chem* 2008, 4(2), pp. 75-101(27).
- 113. Rentzsch, M.; Wilkens, A.; Winterhalter, P. Non-flavonoid Phenolic Compounds. In: Moreno-Arribas. M.V., Polo, M.C. (eds) Wine Chemistry and Biochemistry. *Springer, New York* 2009, pp. 509-527.
- 114. Robbins, R.J. Phenolic Acids in Foods: An Overview of Analytical Methodology. *J. Agric. Food Chem* 2003, 51(10), pp. 2866–2887.
- 115. Taofiq, O.; González-Paramás, A.M.; Barreiro, M.F.; Ferreira, I.C.F.R. Hydroxycinnamic Acids and Their Derivatives: Cosmeceutical Significance, Challenges and Future Perspectives. a Review. *Molecules* 2017, 22, pp. 281.
- 116. Rivera-Dominguez, M.; Yahia, E.M.; Wlodarchak, N.; Kushad, M. Identification and quantification of phenolic compounds in grapes. *Acta Hortic* 2010, 877, pp. 1233-1240.
- 117. Teka, T.; Zhang, L.; Ge, X.; Li, Y.; Han, L.; Yan, X. Stilbenes: Source plants, chemistry, biosynthesis, pharmacology, application and problems related to their clinical Application-A comprehensive review. *Phytochemistry* 2022, 197, pp. 113-128.
- 118. Blackburn, E. V.; Timmons, C. J. The photocyclisation of stilbene analogues. *Q. Rev. Chem. Soc* 1969, 23(4), pp.482-503.
- 119. Guebailia, H.A.; Chira, K.; Richard, T.; Mabrouk, T.; Furiga, A.; Vitrac, X.; Monti, J.-P.; Delaunay, J.-C.; Mérillon, J.-M. Hopeaphenol: the first resveratrol tetramer in wines from North Africa. *J Agric Food Chem* 2006, 54(25), pp. 9559-9564.
- 120. Revilla, E.; Alonso, E.; Kovac, V. The content of catechins and procyanidins in grapes and wines as affected by agroecological and technological practices. *J. Am. Chem. Soc* 1997, 7, pp 69-80.
- 121. Rauf, A.; Imran, M.; Abu-Izneid, T.; Iahtisham-Ul-Haq; Patel, S.; Pan, X.; Naz, S.; Sanches-Silva, A.; Saeed, F.; Suleria, H.A.R. Proanthocyanidins: A comprehensive review. *Biomed. Pharmacother* 2019,116: 108999.
- 122. de Sá, M.; Justino, V.; Spranger, M.I.; Zhao, Y.Q.; Han, L.; Sun, B.S. Extraction Yields and Anti-oxidant Activity of Proanthocyanidins from Different Parts of Grape Pomace: Effect of Mechanical Treatments. *Phytochem. Anal* 2014, 25, pp. 134-140.
- 123. Freitas, V.A.D.; Glories, Y. Concentration and compositional changes of procyanidins in grape seeds and skin of white Vitis vinífera varieties. *J. Sci. Food Agric* 1999, 79, pp. 1601-1606.
- 124. Rzeppa, S.; Bittner, K.; Doll, S.; Danicke, S.; Humpf, H.-U. Urinary excretion and metabolism of procyanidins in pigs. *Mol. Nutr. Food Res* 2012, 56, pp. 653–665.
- 125. Hogan, S.; Canning, C.; Sun. S.; Sun, X.; Zhou, K. Effects of grape pomace antioxidant extract on oxidative stress and inflammation in diet induced obese mice. *J Agric Food Chem* 2010, 58(21), pp. 11250-11256.
- 126. Elejalde, E.; Villarán, MC.; Alonso, R.M. Grape polyphenols supplementation for exercise-induced oxidative stress. *J Int Soc Sports Nutr* 2021, 18(1), pp. 3.
- 127. Hervert-Hernández, D.; Pintado, C.; Rotger, R.; Goñi, I. Stimulatory role of grape pomace polyphenols on Lactobacillus acidophilus growth. *Int. J. Food Microbiol* 2009, 136(1), pp. 119–122.
- 128. Al-Awwadi, N.A.; Araiz, C.; Bornet, A.; Delbosc, S.; Cristol, J.-P.; Linck, N.; Azay, J.; Teissedre, P.-L.; Cros, G. Extracts enriched in different polyphenolic families normalize increased cardiac NADPH oxidase expression

- while having differential effects on insulin resistance, hypertension and cardiac hypertrophy in high fructosefed rats. *J Agric Food Chem* 2005, 53(1), pp. 151-157.
- 129. Milinčić, D.D.; Stanisavljević, N.S.; Kostić, A.Ž.; Soković Bajić, S.; Kojić, M.O.; Gašić, U.M.; Barać, M.B.; Stanojević, S.P.; Tešić, Ž.L.; Pešić, M.B. Phenolic compounds and biopotential of grape pomace extracts from Prokupac red grape variety. *LWT* 2021, 138, pp. 110739.
- 130. Brenes, A.; Viveros, A.; Goñi, I.; Centeno, C.; Sáyago-Ayerdy, S.G.; Arija, I.; Saura-Calixto, F. Effect of grape pomace concentrate and vitamin E on digestibility of polyphenols and antioxidant activity in chickens. *Poult Sci* 2008, 87(2), pp. 307-316.
- 131. Ribeiro, V.M.; Bede, T.P.; Rocha, G.S.; Barroso, S.; Valença, S.; Azeredo, V.B. High fat diet and high polyphenols beverages effects in enzymatic and non-enzymatic antioxidant activity. *Nutr. Hosp* 2017, 35(1), pp. 169-175.
- 132. Lupoli, R.; Ciciola, P.; Costabile, G.; Giacco, R.; Minno, M.; Capaldo, B. Impact of Grape Products on Lipid Profile: A Meta-Analysis of Randomized Controlled Studies. *J. Clinical Med* 2020, 9(2), pp. 313.
- 133. Sri Harsha, P.S.C.; Lavelli, V. Use of Grape Pomace Phenolics to Counteract Endogenous and Exogenous Formation of Advanced Glycation End-Products. *Nutrients* 2019, 11(8), pp. 1917.
- 134. Asbaghi, O.; Nazarian, B.; Reiner, Ž.; Amirani, E.; Kolahdooz, F.; Chamani, M.; Asemi, Z. The effects of grape seed extract on glycemic control, serum lipoproteins, inflammation, and body weight: A systematic review and meta-analysis of randomized controlled trials. *Phytother. Res* 2020, 34, pp. 239–253.
- 135. Chedea, V.S.; Tomoiagă, L.L.; Macovei, Ş,O.; Măgureanu, D.C.; Iliescu, M.L.; Bocsan, I.C.; Buzoianu, A.D.; Voşloban, C.M.; Pop, R.M. Antioxidant/Pro-Oxidant Actions of Polyphenols From Grapevine and Wine By-Products-Base for Complementary Therapy in Ischemic Heart Diseases. *Front. Cardiovasc Med* 2021, 3, 8:750508.
- 136. Zamora-Ros, R.; Andres-Lacueva, C.; Lamuela-Raventós, R.M.; Berenguer, T.; Jakszyn, P.; Martínez, C.; Sánchez, M.J.; Navarro, C.; Chirlaque, M.D.; Tormo, M.J.; Quirós, J.R.; Amiano, P.; Dorronsoro, M.; Larrañaga, N.; Barricarte, A.; Ardanaz, E.; González, C.A. Concentrations of resveratrol and derivatives in foods and estimation of dietary intake in a Spanish population: European Prospective Investigation into Cancer and Nutrition (EPIC)-Spain cohort. *Br J Nutr* 2008, 100(1), pp. 188-196.
- 137. Salehi, B.; Mishra, A. P.; Nigam, M.; Sener, B.; Kilic, M.; Sharifi-Rad, M.; Fokou, P.; Martins, N.; Sharifi-Rad, J. Resveratrol: A Double-Edged Sword in Health Benefits. *Biomedicines* 2018, 6(3), pp. 91.
- 138. Rathburn, H.; Bell, P.; Cook, S.; Mayberry, D. D.; Geye, E.; Goodrich, R. A statistical analysis of transresveratrol in grape cane from ten varieties of cultivated wine grapes (vitis spp.). *Tex. J. Sci* 2020, 72(1), art.3.
- 139. Romero-Pérez, A.I.; Lamuela-Raventós, R.M.; Waterhouse, A.L.; De La Torre-Boronat, M.C. Levels of cis- and trans-resveratrol and their glucosides in white and rosé Vitis vinifera wines from Spain. *J Agric Food Chem* 1996, 44, pp. 2124–2128.
- 140. Feijóo, O.; Moreno, A.; Falqué, E. Content of trans- and cis-resveratrol in Galician white and red wines. *J Food Compos Anal* 2008, 21, pp. 608–613.
- 141. Nour, V.; Trandafir, I.; Muntean, C. Ultraviolet irradiation of trans-resveratrol HPLC determination of trans-resveratrol cis-resveratrol in Romanian red wines. *J. Chromatogr Sci* 2012, 50, pp. 920–927.

Citation: Taşca, C. Characteristics of biomass resulting from agro-industrial processes and possibilities of its evaluation in the context of the circular bioeconomy. *Journal of Engineering Science* 2024, XXXI (3), pp. 156-178. https://doi.org/10.52326/jes.utm.2024.31(3).12.

Publisher's Note: JES stays neutral with regard to jurisdictional claims in published maps and institutional affiliations.



Copyright:© 2024 by the authors. Submitted for possible open access publication under the terms and conditions of the Creative Commons Attribution (CC BY) license (https://creativecommons.org/licenses/by/4.0/).

Submission of manuscripts:

jes@meridian.utm.md

Topic

Biotechnologies, Food Chemistry and Food Safety

https://doi.org/10.52326/jes.utm.2024.31(3).13 UDC 547.973:634.7





eISSN 2587-3482

ANTHOCYANINS – METHODS OF EXTRACTION AND STABILIZATION

Olga Smerea *, ORCID: 0009-0004-2520-439X, Viorica Bulgaru, ORCID: 0000-0002-1921-2009

Technical University of Moldova, 168 Stefan cel Mare Blvd., Chisinau, Republic of Moldova * Corresponding author: Olga Smerea, olga.smerea@doctorat.utm.md

Received: 08. 22. 2024 Accepted: 09. 28. 2024

Abstract. Anthocyanins, natural pigments present in plants which are of interest among researchers due to their antioxidant qualities and potential therapeutic advantages in certain contexts. Their occurrence in fruits, vegetables, and blossoms attributes to their unique hues. Once obtained, the dyes extracted from berries can serve as natural coloring agents in a variety of food items, displacing artificial dyes. Moreover, the antioxidative characteristics of anthocyanins position berry dyes as potential sources of functional components for creating healthier food alternatives. Overall, the extraction of pigments from berries shows considerable promise for both the food sector and health-conscious consumers. In this context, emphasis is placed on the identification of advantageous extraction methods from the point of view of the quality of the biologically active compounds obtained, the extraction yield and the impact of the respective methods on the environment. Directing the technological parameters for obtaining storage-stable phytochemical compounds is also important. The purpose of this paper is to deepen the methods of anthocyanin extraction, their advantages and disadvantages together with the condition of the berries subjected to the extraction processes. Moreover, it analyzes the stabilization methods of phytochemical compounds during storage and their use in the food industry.

Keywords: anthocyanins, antioxidant properties, berries, extraction methods.

Rezumat. Antocianinele, pigmenți naturali prezenți în plante, prezintă un interes considerabil datorită proprietăților lor antioxidante și a potentialelor avantaje terapeutice. Prezența lor în fructe, legume și flori se atribuie nuanțelor lor unice. Odată obținuți, coloranții extrași din fructe de pădure pot servi ca agenți de colorare naturali într-o varietate de produse alimentare, înlocuind coloranții artificiali. În plus, caracteristicile antioxidante ale antocianilor poziționează coloranții de fructe de pădure ca surse potențiale de componente funcționale pentru crearea de alternative alimentare mai sănătoase. În general, extracția pigmenților din fructe de pădure este importantă atât pentru sectorul alimentar, cât și pentru consumatorii în căutare de opțiuni naturale și sănătoase. În acest context se pune accent pe identificarea metodelor de extracție avantajoase din punct de vedere a calității compușilor biologic activi obținuți, a randamentului de extracție și a impactului metodelor respective asupra mediului înconjurător. De asemenea, este important de a dirija parametrii tehnologici pentru obținerea compușilor fitochimici stabili la păstrare. Scopul acestei lucrări a costat în evaluarea metodelor de extracție a antocianilor, avantajele și dezavantajele acestora, precum și metodele de stabilizare a compușilor fitochimici în timpul depozitării și utilizării în industria alimentară.

Cuvinte cheie: antociani, proprietăți antioxidante, fructe de pădure, metode de extracție.

1. Introduction

Horticultural resources containing abundant anthocyanins, like blueberries, blackberries, jostaberry and beetroot, have become popular for their antioxidative characteristics. These flavonoid compounds not only impart vivid hues to fruits and veggies but also shield cells from oxidative stress and harm caused by free radicals [1,2]. Regular intake of anthocyanin-rich foods can promote overall well-being and ward off diverse aliments. The advantages of consuming horticultural resources abundant in anthocyanins:

- Shielding against cardiovascular aliments: Anthocyanins aid in preserving heart and circulatory system health by decreasing "bad" LDL cholesterol levels and lessening artery inflammation [3]. Blueberries, abundant in anthocyanins, are frequently utilized in complementary treatments to stave off cardiovascular illnesses.
- Enhancing cognitive function: Anthocyanins can positively influence brain function and memory. Research indicates that these compounds enhance attention, focus, and cognitive stamina [4].
- Anti-inflammatory attributes: Anthocyanins exhibit robust anti-inflammatory properties, potentially lowering the likelihood of developing persistent inflammatory aliments like arthritis and inflammatory digestive disorders [5]. Due to its elevated anthocyanin content, beetroot can be included in an anti-inflammatory regimen, aiding in alleviating symptoms associated with such conditions [6].
- Boosting the immune system: Ingesting horticultural resources rich in anthocyanins can fortify the body's immunity, thanks to these compounds' capacity to combat free radicals and infections [7].

Raspberries, for instance, offer a rich reservoir of anthocyanins and vitamin C, bolstering immune system function and shielding the body from colds and infections [8]. Consuming anthocyanin-rich horticultural resources provides benefits such as safeguarding against cardiovascular aliments, supporting cognitive function, anti-inflammatory traits, and enhancing the immune system [9]. Fruits like blueberries, blackberries, jostaberry, beetroot, and raspberries exemplify foods abundant in anthocyanins that confer these advantages. Certain horticultural resources teeming with anthocyanins and antioxidative properties encompass:

- **Blueberries**. With their intense blue color derived from anthocyanins, blueberries are famed for their high anthocyanin content. They also boast other antioxidants such as vitamin C and vitamin E [10].
- **Blackberries.** Another anthocyanin-rich fruit, blackberries also offer a rich source of vitamins A and C, along with fiber.
- **Red cabbage.** A cruciferous vegetable brimming with anthocyanins, red cabbage also packs a punch with additional antioxidants, vitamins, and minerals.
- **Purple sweet potatoes**. These vibrant tubers owe their hue to anthocyanins and are rich in fiber, vitamins, and minerals.
- **Red grapes.** Particularly abundant in anthocyanins in their skin, red grapes also supply resveratrol, another potent antioxidant.
- **Elderberries.** Renowned for their copious anthocyanin content and medicinal properties, elderberries are also rich in vitamin C and dietary fiber.

- **Blackcurrants.** Small berries rich in anthocyanins and other antioxidants, blackcurrants are also laden with vitamin C and potassium.
- **Cherries.** Especially tart cherries, high in anthocyanins, also possess other antioxidants and anti-inflammatory characteristics. These anthocyanin-rich resources can be integrated into various dishes like smoothies, salads, desserts, or enjoyed as a snack to harness their antioxidative advantages [11].
- **Jostaberry.** The jostaberry hybrid (*Ribes* × *nidigrolaria*) is a fruiting shrub obtained by crossing the following species: the blackcurrant *Ribes nigrum*, the black gooseberry *Ribes divaricatum*, and the European gooseberry. The jostaberry hybrid varieties, are sources of notable nutritional value, due to their increased content of biologically active compounds, such as fiber, carbohydrates, phenolic compounds, vitamins, and minerals [2].

2. Berries pretreatment before hue extraction

Berries are known for their vibrant colors and delicious flavors, but they also pack a powerful punch when it comes to health benefits. Anthocyanins, the pigments that give berries their hues, are potent antioxidants with anti-inflammatory properties that may help reduce the risk of chronic diseases [12]. Berries can be used in various extraction processes to obtain juices, concentrates, bioactive compounds, extracts for food supplements, and others in fresh or pretreated form (Table 1).

Fresh. Ideal for ready-to-eat products, juices and smoothies.

Frozen. Good for processed foods and extracts of bioactive compounds.

Dried. Optimal for food supplements, tinctures and infusions.

Freeze-dried. Excellent for premium health and cosmetic products [13].

Depending on the final purpose of the product and the available resources, the choice of condition in which the pads are used will vary. Each method has its own advantages, and the right choice can optimize the quality and efficiency of the extraction process [14].

Pretreatment methods of fruits and berries

Table 1

State of berry	Advantages	Disadvantages	References
Fresh	High water content, which facilitates the extraction of soluble compounds. High extraction yield. The natural chemical composition is intact, without distortion.	High perishability, which can affect yield if not processed quickly. Seasonal variability and limited accessibility, that could influence the yield	[15,16]
Frozen	Preserves bioactive compounds, including anthocyanins, with minimal changes. Availability throughout the year.	freezing and thawing process,	[17,18]
	Freezing preserves the structural integrity and chemical composition of the berries, allowing a good extraction yield.	Need equipment for freezing and storage.	

	Continuation Table				
Dried	Stability and long storage life Possibility of transport and easy handling.	Significant loss of anthocyanins and other phenolic compounds due to oxidation and high temperature used in the drying process, which lowers the extraction yield. The need for rehydration before extraction, which can complicate the process reduce efficiency.	[19,20]		
Freeze-dried	Excellent preservation of bioactive compounds, including anthocyanins, due to the low temperatures and absence of oxygen in the freeze-drying process. High extraction yield due to the porous structure that facilitates the access of solvents.	High costs of the freeze- drying equipment and process. Requires carefully controlled storage conditions to prevent rehydration.	[21,22]		

The extraction of anthocyanins from berries can vary significantly depending on the state in which they are used (fresh, frozen, dried or freeze-dried). Each preservation method has its own advantages and disadvantages in terms of anthocyanin extraction yield [23].

Side-by-Side Comparison of Extraction Methods [24]

Table 2

State of berry	Anthocyanin Levels	Preparation Time	Extraction Difficulty		
Fresh	High	Short	Easy		
Frozen	High	Medium	Easy		
Dried	Moderate	Long	Moderate		
Freeze-Dried	High	Medium	Easy		

To achieve maximum anthocyanin extraction efficiency, it is recommended to use freeze-dried berries (Table 2). This preservation method ensures the preservation of bioactive compounds' integrity and allows for efficient extraction, although it involves higher costs and requires special equipment. If resources do not allow for freeze-drying, freezing can be a viable alternative, maintaining a good extraction yield at lower costs [25].

3. Phenolic Acids and Anthocyanidins in Red Fruits

In recent times, there has been a notable surge in research dedicated to the analysis of the composition and antioxidative characteristics of crimson fruits [26]. Scientists have

delved into diverse extraction techniques, encompassing traditional solvent extraction and innovative methods like ultrasound, microwave, and pressure-assisted extractions, to procure products abundant in antioxidants [27]. Furthermore, investigations have been conducted on the impact of cultivar types, storage conditions, and drying methodologies on the extraction and efficacy of antioxidants. This overview seeks to collate and present the most recent discoveries in this domain to offer a thorough insight into antioxidant extraction from crimson fruits [28].

These parameters aid in evaluating the strength and efficiency of anthocyanins concerning their antioxidative potential and overall health advantages [29]. Through the utilization of these parameters, researchers can precisely gauge and contrast the caliber of various origins of anthocyanins [30], ultimately fostering advancements in comprehending their plausible therapeutic uses.

Indices for the quality of anthocyanins provide a mechanism to scrutinize the attributes and efficacy of these substances. By comprehending the concentration, configuration, and biological functions of anthocyanins, informed choices can be made regarding which foods to ingest to optimize the health benefits linked with anthocyanins [31].

Moreover, the extraction technique, solvent, duration, temperature, and pH levels also exert a pivotal role in determining the attributes of the extract. These factors can impact the output, resilience, bioactivity, and composition of the extract, including specific bioactive components [32,33]. Hence, thoughtful consideration of these elements is imperative to procure extracts with desired features and potential health gains from berries.

To enhance the extraction of antioxidant compounds from berries, researchers concentrate on regulating extraction procedures due to the challenges in controlling climatic conditions, sunlight exposure, water uptake from plants, and maturation stage [34]. The incorporation of substances or exposure to diverse light treatments such as ultraviolet or blue light can boost antioxidant compounds and capacity. The extraction procedure encompasses the crimson fruit, technique (chemical or physical assistance) [35], and influential variables like duration and temperature.

Regarding extraction methodologies, the conventional solvent extraction remains the prevalent approach for extracting antioxidant compounds from crimson fruits, particularly on an industrial scale [36]. Nevertheless, this method engulfs a substantial amount of energy due to the heating process and solvents needed for solid-liquid extraction [37]. Novel non-conventional approaches have surfaced as eco-friendly alternatives to the former technique, such as ultrasound, microwave, and pressure-assisted extractions, either applied individually or in conjunction with solvent usage, to diminish the energy and solvent requisites [38].

3. Common Methods for the Extraction of Antioxidants from Berries

The use of emerging procedures for extracting biologically active compounds from plant raw materials remains a current technological problem, considering the importance of their use in different branches of industry. The correct choice of temperature and the appropriate solvent will ensure the complete extraction of biologically active compounds from the plant based materials, and the extraction time and the optimal hydromodule can save energy and expensive solvents, without the loss of the extracted compounds [39].

3.1. Mechanical Extraction

An ancient method of extraction known as cold press extraction is commonly used to extract antioxidant-rich inner fruit liquids without the use of heat or additional solvents. This

technique, widely employed in the production of fruit juices and oil extraction, involves a screw press to obtain the initial liquid, followed by multiple extractions of the residual press cake to enhance the overall extraction yield [40].

3.2. Traditional Extraction Methods

Within traditional extraction methods, two primary techniques are maceration and solvent extraction. Maceration involves the gradual release of substances into a solvent over extended periods without the application of heat [41]. Conversely, solvent extraction utilizes heat and various solvents to expedite the extraction process, with stirring often employed to enhance mass transfer. Soxhlet extraction, a cost-effective method commonly used at the laboratory scale, eliminates the need for subsequent filtration [42].

Solvents such as water, ethanol, methanol, and acetone, either individually or in combination, are typically utilized in these extraction processes [43]. Acidulated solvents, containing around 1% acid like HCl or acetic acid, may be employed to improve extraction efficiency. Water-alcohol mixtures have shown enhanced extraction efficiency compared to single-component solvents, with 50% ethanol demonstrating optimal results at different temperatures [44].

The solvent used will be chosen considering the following characteristics:

- Selectivity, which includes the solubility of target compounds and their purity.
- Reactivity, chemical interaction with target compounds is undesirable.
- Chemical and thermal stability under extraction conditions.
- Low viscosity, which increases substance transfer by increasing the diffusion coefficient.
- Low boiling point.
- Flammability, prohibited.
- Toxicity and environmental and health problems.
- The price of the solvent, which is directly exposed to the manufacturing costs on an industrial scale [39].

Numerous studies [45,46,47] have highlighted ethanol as the preferred solvent for extracting antioxidant compounds due to its effectiveness when compared to water, acetone, hexane, ethyl acetate, and methanol. The ideal composition of ethanol-water mixtures is generally found to be between 40% and 70%, as it is economically feasible and derived from a renewable source, aligning with green chemistry principles.

Traditional methods using ethanol, methanol or acetone give a good yield, but can be improved by optimizing the conditions (temperature, time, solvent/material ratio) [48].

3.2.1. Impact of Solid-to-Solvent Ratio

The solid-to-solvent ratio is crucial in extraction processes, as it influences the concentration of antioxidant compounds in the final extract. While a higher ratio results in increased compound concentration, an inadequate solvent volume can impede mass transfer, necessitating a balance between the two [49].

3.2.2. Influence of Temperature and Duration

Temperature and extraction time are interrelated factors affecting the extraction process. Elevated temperatures can reduce extraction time, leading to higher yields of antioxidants. However, excessive temperatures may cause thermal degradation of certain compounds, such as anthocyanins, impacting antioxidant content. The optimal balance

between temperature and time is essential to maximize extraction efficiency [50]. Currently, sustainable extraction methods, ultrasound-assisted extraction (UAE) and microwave-assisted extraction (MAE) could replace conventional methods, being sustainable extraction methods which are more efficient: economical, require less time, energy, and reagents. On the other hand, phytochemical compounds extracted by these methods are safe and harmless for the use in food industry.

3.3. Application of Ultrasound in Extraction (UAE)

UAE is a non-thermal technique utilizing frequencies above 20 kHz to disrupt cell walls and enhance mass transfer [51]. This environmentally friendly method has gained popularity for its cost-effectiveness and efficiency compared to traditional solvent extraction processes [52]. Ultrasound-induced cavitation aids in the extraction of intracellular compounds, such as anthocyanins, from plant material [53].

The efficacy of sonication has been demonstrated in improving extraction yields, although the frequency and duration of ultrasound exposure must be carefully controlled to prevent degradation of target compounds. While UAE has shown promising results in various studies [54,55], its impact on the extraction of antioxidant compounds may vary depending on the fruit type and processing conditions.

The use of ultrasonic waves can increase the extraction yield by effectively breaking the cells and releasing the anthocyanins. This method can reduce the extraction time and the amount of solvent required [56,57].

3.4. Microwave-Assisted Extraction (MAE)

MAE is characterized by rapid heating and reduced solvent usage, making it a favorable option for extraction processes. MAE's ability to utilize intrinsic moisture within fruits, coupled with its efficient heat transfer mechanism, results in shorter extraction times and lower environmental impact [54,55]. Optimal solid-to-solvent ratios are essential for maximizing extraction efficiency, with specialized techniques like Microwave Hydro diffusion and gravity offering enhanced extraction yields compared to traditional solvent extraction methods [58].

Microwaves heat the material quickly and evenly, facilitating the release of anthocyanins and increasing the extraction yield. This method is efficient and can reduce processing time. Main factors affecting yield are the microwave frequency, types of solvent and sample size [59].

The main steps of microwave enhanced extraction process included:

- Heat energy created by microwave radiation;
- Heat energy absorbed by samples;
- Creation of high vapor pressure due to moisture evaporation;
- Disruption of cell wall of matrices;
- Release of desired compound into solvents [60].

3.5. Pulsed electric Assisted Extraction

In order to increase the yield of biologically active compounds by increasing the permeability of the cell membranes of the raw material of vegetable origin, due to the phenomenon of electroporation, the extraction assisted by the pulsating electric field (Pulsed Electric Field - PEF) is used. It is an athermal method involving repeated high voltage pulses for several milliseconds on a plant sample placed between two electrodes [61]. Several authors have demonstrated the high efficiency of the extraction of biologically active

compounds, especially polyphenols, using PFE from raw and secondary plant materials [62,63], possibly due primarily to the temperatures of the process that varies between 20°C - 50°C, which contributes to the breaking of the cell membranes in the apple skin, allowing the extraction of soluble intracellular components due to increased diffusion [64].

3.6. Supercritical CO₂ extraction (SFE-CO₂)

Supercritical fluid extraction (SFE), a temperature- and pressure-dependent technique, is valued for the extraction yield and quality of natural chemical compounds obtained (flavonoids, essential oils, seed oils, carotenoids and fatty acids) from natural plant based materials. This technique is a sustainable alternative to traditional extraction systems. Research has shown the considerable benefits of SFE over conventional techniques. Carbon dioxide (CO_2) is a valued solvent in this technique because it is chemically inactive, economical, easily accessible, separable from extracts, non-toxic, approved as a food grade solvent.

Supercritical carbon dioxide is frequently used in SFE due to its gas-like and liquid-like properties, low critical temperature and pressure, and has the selectivity and potential to extract heat-sensitive compounds.

They can also extract compounds with different molecular sizes. Low polarity compounds and small molecules are easily dissolved in SC-CO₂, but large molecules and polar compounds are extracted with the addition of a co-solvent to improve the extraction yield, which can be ethanol, methanol or water [65]. Some authors [66, 67] used SC-CO₂ extraction of carotenoids, phenols and flavonoids from plant raw materials in combination with other methods of extraction, for example stage II including the use of pressurized ethanol extraction [68]. Qualitative comparison of extraction methods is shown in Table 3.

Qualitative comparison of extraction methods

Table 3

Extraction Method	Pros	Cons	References
Maceration	No additional energy needed	Very long extraction times.	
Solvent extraction	Easy industrial scale-up. Well known technique. One of the most prevalent approaches for anthocyanin extraction. Use of organic solvents. Adaptable for various plant sources.	Long extraction times. Potential flammability or toxicity of solvents necessitating specific safety precautions. Risk of losing valuable compounds due to solvent interactions	[3, 30, 69, 70-72]
Ultrasound assisted	Higher efficiency (less extraction time and solvent consumption requirements). Safe extraction of heat labile compounds.	Expensive scale-up	[73,74]

Continuation Tabl				
Microwave assisted	Quicker heating. Reduced equipment size. Cost-effective and straightforward technique. No added solvent needed. Higher efficiency (heat leads to the breaking of weak bonds that allow the release of bioactive components in the solvent).	Risk of burning the sample and denaturalizing compounds	[75-77]	
Aqueous extraction	Environmentally friendly and safe, using a common and harmless solvent. Minimizes the risk of adverse interactions between the solvent and pigments. Suitable for obtaining extracts rich in water-soluble anthocyanins.	Challenges in achieving high anthocyanin concentrations. Susceptibility to pigment degradation under specific conditions like high temperature and pH. Selective extraction of specific types of anthocyanins based on their water solubility.	[78-81]	
Supercritical CO ₂ extraction (SFE-CO ₂)	CO ₂ no toxicity, extraction in absence of air and light. Pure extracts.	The complexity of the extraction process	[65,82]	
Pulsed electric fields	Already acquired by some food industries to scale-up processes.	Need of specialized equipment	[30,69]	

The choice of extraction method and technology depends on the initial state of the berries and the resources available. Freeze-dried berries generally offer the highest anthocyanin extraction yield due to the preservation of structure and bioactive composition. Depending on the available equipment and costs. Ultrasound and microwave-assisted methods can also improve yield while reducing time and solvent quantity required. The optimal extraction method choice should consider both the desired yield and available resources [2,57].

4. Influence of technological regimes on anthocyanins antioxidant and coloring properties

Anthocyanins extracted from berries offer a wide range of applications in the food industry. These beneficial compounds can be incorporated into various food items such as juices, soft drinks, ice creams, and baked goods [83]. Consumption of foods enriched with berries anthocyanins can provide health benefits due to their antioxidant and anti-inflammatory properties [84].

The impact of technological factors, including temperature, pH, and ionic strength, on the antioxidant activity and color attributes of natural dyes is a crucial area of study. These variables can significantly influence the stability and functionality of natural dyes commonly utilized in different sectors like food, textiles, and cosmetics [85].

Temperature. Alterations in temperature can impact the antioxidant activity and color attributes of natural dyes. Higher temperatures may lead to the degradation or loss of antioxidant properties and changes in color intensity or hue. Conversely, lower temperatures can aid in preserving the antioxidant activity and color stability of natural dyes [86, 87].

pH. The pH level of a solution can profoundly affect the antioxidant activity and color properties of natural dyes. Different pH conditions can modify the chemical structure of dyes, influencing their stability and color characteristics [88,89]. Some natural dyes may exhibit enhanced antioxidant activity or color intensity at specific pH ranges, while others may demonstrate greater stability or vibrancy under different pH conditions [90,91]. Thus, controlling and optimizing pH conditions during the technological process is crucial to maximize the antioxidant potential of natural dyes [92].

lonic strength. The ionic strength of a solution, determined by the concentration of ions present, can impact the antioxidant activity and color attributes of natural dyes [93]. Changes in ionic strength can influence the solubility, stability, and interactions of dyes with other components in a system, thereby affecting their antioxidant capacity and color properties [94,95]. Increasing ion concentration in a solution can reduce the antioxidant activity of natural dyes. This reduction can occur through direct interaction with reactive oxygen molecules or by modifying the chemical environment where the antioxidant reaction occurs [96]. However, the effect of ionic strength on antioxidant activity can vary based on the specific dye and chemical system being used [97].

Comprehending the influence of these technological factors on natural dyes is crucial for optimizing their application in diverse industries. Researchers and manufacturers can leverage this knowledge to develop suitable processing conditions, storage methods, and formulation strategies to maximize the antioxidant activity and retain the desired color properties of natural dyes [98]. The examination of how technological factors impact the antioxidant activity and color attributes of natural dyes is particularly critical in the food industry [99]. As concerns over synthetic dye consumption grow, natural dyes are increasingly viewed as a safer and more consumer-accepted alternative [100].

5. Methods of stabilizing anthocyanin during storage

Manufacturers must focus on research and development to discover effective techniques for stabilizing dyes and prolonging their shelf life. This can involve selecting dyes with enhanced stability characteristics, incorporating protective coatings or additives, and implementing proper storage and handling practices [101]. By addressing this issue, manufacturers can ensure that their products retain their desired color and attractiveness, leading to increased customer satisfaction and product success.

- Incorporation of antioxidant additives. Antioxidant additives are capable of delaying
 or preventing product deterioration resulting from oxidative reactions [102]. Utilizing
 antioxidant additives can safeguard dyes against degradation processes that may
 occur during storage.
- Protective packaging. Packaging plays a crucial role in preserving dyes during storage.
 Opting for opaque packaging that shields against ultraviolet light can prevent dye damage due to light exposure [103]. Hermetic packaging can also aid in preventing oxidation and the ingress of oxygen into the product.

- **Control of temperature and humidity**. Proper regulation of temperature and humidity is essential for dye stabilization during storage [104]. Extreme temperatures can alter the chemical properties of dyes, leading to modification or discoloration. Excessive humidity levels can promote mold growth and other forms of damage.
- **Incorporation of preservatives.** In cases where the product containing dyes has an extended shelf life, the addition of preservatives can be considered [105]. This measure can inhibit the growth of bacteria and other microorganisms that could harm the dyes during storage.
- **Conducting stability assessments.** To validate the efficacy of the stabilization methods employed, conducting stability tests is imperative [106]. These tests aid in evaluating the resilience of dyes under various storage conditions, including temperature variations, humidity levels, light exposure, and oxidative environments [107].

To uphold the stability of dyes during storage, a range of strategies can be implemented. Incorporating antioxidant additives can counteract degradation due to oxidative reactions, while protective packaging, temperature and humidity control, and preservative incorporation can safeguard against chemical alterations, damage, and microbial growth. Furthermore, stability tests are essential for assessing the dyes' resilience to diverse storage conditions [108].

6. Conclusions

The extraction of anthocyanins from berries has shown promising potential in the food sector. Techniques such as soaking, fermenting, and pressing enable the production of concentrated extracts suitable for various food items. Anthocyanins possess antioxidant and anti-inflammatory properties, rendering them a valuable component in promoting consumer well-being. Consequently, berries are progressively gaining recognition as a significant source of anthocyanins in the contemporary food industry.

Solvent extraction entails utilizing organic solvents to extract anthocyanins, providing high extraction efficacy and adaptability in extracting anthocyanins from different plant sources. Nonetheless, it may necessitate additional steps to eliminate solvents from the extract and could lead to the loss of certain volatile compounds. Conversely, water extraction is a straightforward and eco-friendly approach applicable to specific plant materials. Nevertheless, it might exhibit lower extraction efficiency compared to solvent extraction and could be less suitable for plants with low water solubility of anthocyanins.

The selection of the extraction method should be meticulously assessed based on the specific requirements and characteristics of the anthocyanins to be extracted. The article underscores the importance of understanding anthocyanin extraction techniques, as it plays a crucial role in the processing of raw materials and acquiring valuable extracts utilized in the food, pharmaceutical, and cosmetic sectors.

As final thoughts, maintaining the stability of colorants during storage is crucial for the production of goods that rely on them. Techniques such as incorporating anti-oxidizing agents, appropriate packaging, regulation of temperature and moisture, and conducting endurance evaluations are essential in preserving the quality and hue of the colorants. These actions are imperative for meeting consumer demands and guaranteeing their contentment.

Anti-oxidizing agents aid in preventing the decomposition of colorants due to exposure to oxygen, whereas proper packaging, like hermetic containers or light-blocking materials, serves to shield colorants from external elements that could impact their stability.

Regulating temperature and humidity is vital to prevent colorants from deteriorating under extreme circumstances.

The addition of preservatives can hinder the proliferation of microorganisms that might lead to spoilage or deterioration of colorants. Endurance tests are carried out to evaluate the efficiency and durability of colorants under different storage conditions, ensuring that they uphold their intended hue and quality over time. By implementing these measures, producers can boost the stability of colorants, prolong their shelf life, and ultimately enhance consumer satisfaction by offering products with consistent and vivid hues.

The article provides a comprehensive and enlightening overview of the various technologies used in the extraction and stabilization of anthocyanins, highlighting their importance in research and development initiatives.

Acknowledgments. Institutional Project 020405 "Optimizing food processing technologies in the context of the circular bioeconomy and climate change", Bio-OpTehPAS, being implemented at the Technical University of Moldova.

Conflicts of Interest: The authors declare no conflict of interest.

References

- 1. Galván D'Alessandro, L.; Kriaa, K.; Nikov, I.; Dimitrov, K. Ultrasound assisted extraction of polyphenols from black chokeberry. *Sep. Purif. Technol.* 2012, 93, pp. 42–47.
- 2. Bulgaru, V.; Gurev, A.; Baerle, A.; Dragancea, V.; Balan, G.; Cojocari, D.; Sturza, R.; Soran, M.-L.; Ghendov-Mosanu, A. Phytochemical, Antimicrobial, and Antioxidant Activity of Different Extracts from Frozen, Freeze-Dried, and Oven-Dried Jostaberries Grown in Moldova. *Antioxidants* 2024, 13, 890.
- 3. Périno-Issartier, S.; Abert-Vian, M.; Chemat, F. Solvent Free Microwave-Assisted Extraction of Antioxidants from Sea Buckthorn (*Hippophae rhamnoides*) Food By-Products. *Food Bioprocess Technol.* 2011, 4, pp. 1020–1028
- 4. Paes, J.; Dotta, R.; Barbero, G.F.; Martínez, J. Extraction of phenolic compounds and anthocyanins from blueberry (*Vaccinium myrtillus* L.) residues using supercritical CO₂ and pressurized liquids. *J. Supercrit. Fluids* 2014, 95, pp. 8–16.
- 5. Häkkinen, S.H.; Törrönen, A.R. Content of flavonols and selected phenolic acids in strawberries and *Vaccinium* species: Influence of cultivar, cultivation site and technique. *Food Res. Int.* 2000, 33, pp. 517–524.
- 6. Ścibisz, I.; Mitek, M. The changes of antioxidant properties in highbush blueberries (*Vaccinium corymbosum* L.) During freezing and long-term frozen storage. *ACTA Acta Sci. Pol. Technol. Aliment* 2007, 6, pp. 75–82.
- 7. Chen, H.; Yang, H.; Gao, H.; Long, J.; Tao, F.; Fang, X.; Jiang, Y. Effect of hypobaric storage on quality, antioxidant enzyme and antioxidant capability of the Chinese bayberry fruits. *Chem. Cent. J.* 2013, 7(1), 4.
- 8. Wilkowska, A.; Ambroziak, W.; Czyzowska, A.; Adamiec, J. Effect of Microencapsulation by Spray-Drying and Freeze-Drying Technique on the Antioxidant Properties of Blueberry (*Vaccinium myrtillus*) Juice Polyphenolic Compounds. *Pol. J. Food Nutr. Sci.* 2016, 66, pp. 11–16.
- 9. Thi, N.D.; Hwang, E.S. Effects of drying methods on contents of bioactive compounds and antioxidant activities of black chokeberries (*Aronia melanocarpa*). Food Sci. Biotechnol. 2016, 25, pp. 55–61.
- 10. Dey, T.B.; Chakraborty, S.; Jain, K.K.; Sharma, A.; Kuhad, R.C. Antioxidant phenolics and their microbial production by submerged and solid state fermentation process: A review. *Trends Food Sci. Technol.* 2016, 53, pp. 60–74.
- 11. Galván D'Alessandro, L.; Dimitrov, K.; Vauchel, P.; Nikov, I. Kinetics of ultrasound assisted extraction of anthocyanins from *Aronia melanocarpa* (black chokeberry) wastes. *Chem. Eng. Res. Des.* 2014, 92, pp. 1818–1826.
- 12. Jiao, X.; Li, B.; Zhang, Q.; Gao, N.; Zhang, X.; Meng, X. Effect of *in vitro*-simulated gastrointestinal digestion on the stability and antioxidant activity of blueberry polyphenols and their cellular antioxidant activity towards HepG2 cells. *Int. J. Food Sci. Technol.* 2018, 53, pp. 61-71.

- 13. Herrera-Ramirez, J.; Meneses-Marentes, N.; Tarazona Diaz, M.P. Optimizing the extraction of anthocyanins from purple passion fruit peel using response surface methodology. *J. Food Meas. Char.* 2020, 14, pp. 72-79.
- 14. Azman, E.M.; Charalampopoulos, D.; Chatzifragkou, A. Acetic acid buffer as extraction medium for free and bound phenolics from dried blackcurrant (*Ribes nigrum* L.) skins. *J. Food Sci.* 2020, 85, pp. 3745-3755.
- 15. Pedro, A.C.; Granato, D.; Rosso, N.D. Extraction of anthocyanins and polyphenols from black rice (*Oryza sativa L.*) by modeling and assessing their reversibility and stability. *Food Chem.* 2016, 191, pp. 12-20.
- 16. Chen, L.; Yang, M.; Mou, H.; Kong, Q. Ultrasound-assisted extraction and characterization of anthocyanins from purple corn bran. *J. Food Process. Preserv.* 2017, 42, e13377.
- 17. Tian, Y.; Yang, Y.; Gao, P.; Wang, J.H.; Xu, Y.Q.; Yu, Z.Y. Optimization of ultrasonic-assisted extraction of flavonols and anthocyanins from blueberry using RSM. *Adv. Mater. Res.* 2012, 4, pp. 2423-2430.
- 18. Yang, Z.; Zhai, W. Optimization of microwave-assisted extraction of anthocyanins from purple corn (*Zea mays L.*) cob and identification with HPLC-MS. *Innov. Food Sci. Emerg* 2010, 11, pp. 470-476.
- 19. Liu, W.; Yang, C.; Zhou, C.; Wen, Z.; Dong, X. An improved microwave-assisted extraction of anthocyanins from purple sweet potato in favor of subsequent comprehensive utilization of pomace. *Food Bioprod. Process.* 2019, 5, pp. 1-9.
- 20. Xue, H.; Tang, J.; Fan, L.; Li, Q.; Cai, X. Optimization microwave-assisted extraction of anthocyanins from cranberry using response surface methodology coupled with genetic algorithm and kinetics model analysis. *J. Food Process. Eng.* 2021, 44, e13688.
- 21. Ahin, E.K., Bilgin, M.; Ahin, S. Recovery of anthocyanins from sour cherry (*Prunus cerasus L.*) peels via microwave assisted extraction: monitoring the storage stability. *Prep. Biochem. Biotechnol.* 2020, 5, pp. 1-11.
- 22. Tian, M.X.; Li, Y.D.; Hu, W.Z.; Wang, Y.Y.; Jiang, A.L.; Liu, J.A.C.H. Optimization of supercritical CO₂ extraction of blueberry anthocyanins using response surface methodology. *Sci. Tech. Food Ind.* 2016, 37, pp. 208-212.
- 23. Lauren Fresinghelli Ferreira. Renata Fritzsche Rodrigues. Roberson Pauletto. Citric acid water-based solution for blueberry bagasse anthocyanins recovery: optimization and comparisons with microwave-assisted extraction (MAE). *LWT–Food Sci. Tech.* 2020, 133, 11257.
- 24. Tan, J.; Li, Q.; Xue, H.; Tang, J. Ultrasound-assisted enzymatic extraction of anthocyanins from grape skins: optimization, identification, and antitumor activity. *J. Food Sci.* 2020, 85, pp. 3731-3744.
- 25. Xue, H.; Tan, J.; Li, Q.; Tang, J.; Cai, X. Ultrasound-assisted enzymatic extraction of anthocyanins from raspberry wine residues: process optimization, isolation, purification, and bioactivity determination. *Food Anal. Methods* 2021, 14, pp. 1-18.
- 26. Wu, X.; Beecher, G.R.; Holden, J.M.; Haytowitz, D.B.; Gebhardt, S.E.; Prior, R.L. Concentrations of anthocyanins in common foods in the United States and estimation of normal consumption. *J. Agric. Food Chem.* 2006, 54, pp. 4069–4075.
- 27. Skrovankova, S.; Sumczynski, D.; Mlcek, J.; Jurikova, T.; Sochor, J. Bioactive compounds and antioxidant activity in different types of berries. *Int. J. Mol. Sci.* 2015, 16, pp. 24673–24706.
- 28. Canuto, G.A.B.; Oliveira, D.R.; Da Conceição, L.S.M.; Farah, J.P.S.; Tavares, M.F.M. Development and validation of a liquid chromatography method for anthocyanins in strawberry (*Fragaria* spp.) and complementary studies on stability, kinetics and antioxidant power. *Food Chem.* 2016, 192, pp. 566–574.
- 29. Herrera, M.C.; de Castro, M.D.L. Ultrasound-assisted extraction of phenolic compounds from strawberries prior to liquid chromatographic separation and photodiode array ultraviolet detection. *J. Chromatogr.* A 2005, 1100, pp. 1–7.
- 30. Meyers, K.J.; Watkins, C.B.; Pritts, M.P.; Liu, R.H. Antioxidant and antiproliferative activities of strawberries. *J. Agric. Food Chem.* 2003, 51, pp. 6887–6892.
- 31. Golmohamadi, A.; Möller, G.; Powers, J.; Nindo, C. Effect of ultrasound frequency on antioxidant activity, total phenolic and anthocyanin content of red raspberry puree. *Ultrason. Sonochem.* 2013, 20, pp. 1316–1323.
- 32. Medina-Meza, I.G.; Boioli, P.; Barbosa-Cánovas, G.V. Assessment of the Effects of Ultrasonics and Pulsed Electric Fields on Nutritional and Rheological Properties of Raspberry and Blueberry Purees. *Food Bioprocess Technol.* 2016, 9, pp. 520–531.
- 33. Bulgaru, V.; Smerea, O., Gurev, A.; Ghendov-Moşanu, A. The effect of technological parameters on the stability of anthocyanins from forest fruits. In: National scientific conference "Innovation: Factor of social-economic development" December 15, 2023, State University "Bogdan Petriceicu Hasdeu" from Cahul, Republic of Moldova, pp. 116-121 [in Romanian].

- 34. Ştefănuţ, M.N.; Căta, A.; Pop, R.; Moşoarcă, C.; Zamfir, A.D. Anthocyanins HPLC-DAD and MS Characterization, Total Phenolics, and Antioxidant Activity of Some Berries Extracts. *Anal. Lett.* 2011, 44, pp. 2843–2855.
- 35. Piovezan, M.; García-Seco, D.; Micke, G.A.; Gutiérrez-Mañero, J.; Ramos-Solano, B. Method development for determination of (+)-catechin and (-)-epicatechin by micellar electrokinetic chromatography: Annual characterization of field grown blackberries. *Electrophoresis* 2013, 34, pp. 2251–2258.
- 36. Nour, V.; Trandafir, I.; Cosmulescu, S. Central Composite Design Applied to Optimize the Hydroalcoholic Extraction of Bilberry (*Vaccinium Myrtillus* L.) Fruits. *J. Food Biochem.* 2015, 39, pp. 179–188.
- 37. Borowska, E.J.; Mazur, B.; Kopciuch, R.G.; Buszewski, B. Polyphenol, anthocyanin and resveratrol mass fractions and antioxidant properties of cranberry cultivars. *Food Technol. Biotechnol.* 2009, 47, pp. 56–61.
- 38. Bessada, S.M.F.; Barreira, J.C.M.; Oliveira, M.B.P.P. Asteraceae species with most prominent bioactivity and their potential applications: A review. *Ind. Crops Prod.* 2015, *76*, 604–615. Rupasinghe, H.P.V.; Yu, L.J.; Bhullar, K.S.; Bors, B. Short Communication: Haskap (*Lonicera caerulea*): A new berry crop with high antioxidant capacity. *Can. J. Plant Sci.* 2012, 92, pp. 1311–1317.
- 39. Ghendov-Moşanu, A. Obtaining and stabilizing some colors, antioxidants and preservatives of vegetable origin for functional foods. Thesis of habilitated doctor, Chisinau, 2021. [in Roumanian].
- 40. Stoica, R.; Senin, R.M.; Ion, R. Ethanol Concentration Effect on the Extraction of Phenolic Compounds from *Ribes nigrum* Assessed by Spectrophotometric and HPLC-DAD Methods. *Rev. Chim.* 2013, 64, pp. 620–624.
- 41. Pantelidis, G.E.; Vasilakakis, M.; Manganaris, G.A.; Diamantidis, G. Antioxidant capacity, phenol, anthocyanin and ascorbic acid contents in raspberries, blackberries, red currants, gooseberries and Cornelian cherries. *Food Chem.* 2007, 102, pp. 777–783.
- 42. Deighton, N.; Brennan, R.; Finn, C.; Davies, H.V. Antioxidant properties of domesticated and wild *Rubus* species. *J. Sci. Food Agric*. 2000, 80, pp. 1307–1313.
- 43. Pisoschi, A.M.; Danet, A.F.; Kalinowski, S. Ascorbic Acid determination in commercial fruit juice samples by cyclic voltammetry. *J. Autom. Methods Manag. Chem.* 2008, 2008, 937651.
- 44. Prior, R.L.; Hoang, H.; Gu, L.; Wu, X.; Bacchiocca, M.; Howard, L.; Hampsch-Woodill, M.; Huang, D.; Ou, B.; Jacob, R. Assays for hydrophilic and lipophilic antioxidant capacity (oxygen radical absorbance capacity (ORAC(FL)) of plasma and other biological and food samples. *J. Agric. Food Chem.* 2003, 51, pp. 3273–3279.
- 45. Huang, D.; Ou, B.; Prior, R.L. The chemistry behind antioxidant capacity assays. *J. Agric. Food Chem.* 2005, *53*, pp. 1841–1856.
- 46. Goupy, P.; Dufour, C.; Loonis, M.; Dangles, O. Quantitative Kinetic Analysis of Hydrogen Transfer Reactions from Dietary Polyphenols to the DPPH Radical. *J. Agric. Food Chem.* 2003, 51, pp. 615–622.
- 47. Torres, J.L.; Lozano, C.; Julià, L.; Sánchez-Baeza, FJ.; Anglada, J.M.; Centelles, JJ.; Cascante, M. Cysteinyl-flavan-3-ol conjugates from grape procyanidins. Antioxidant and antiproliferative properties. *Bioorg. Med. Chem.* 2002, 10, pp. 2497–2509.
- 48. Xue, H., Tan, J.; Li, Q.; Tang, J.; Cai X. Optimization ultrasound-assisted deep eutectic solvent extraction of anthocyanins from raspberry using response surface methodology coupled with genetic algorithm. *Foods*, 2020, 9, 1409.
- 49. Zulueta, A.; Esteve, MJ.; Frasquet, I.; Frígola, A. Vitamin C, vitamin A, phenolic compounds and total antioxidant capacity of new fruit juice and skim milk mixture beverages marketed in Spain. *Food Chem.* 2007, 103, pp. 1365–1374.
- 50. Shahidi, F.; Ambigaipalan, P. Phenolics and polyphenolics in foods, beverages and spices: Antioxidant activity and health effects—A review. *J. Funct. Foods* 2015, 18, pp. 820–897.
- 51. Karadag, A.; Ozcelik, B.; Saner, S. Review of methods to determine antioxidant capacities. *Food Anal. Methods* 2009, 2, pp. 21–60.
- 52. Cao, S.; Hu, Z.; Zheng, Y.; Yang, Z.; Lu, B. Effect of BTH on antioxidant enzymes, radical-scavenging activity and decay in strawberry fruit. *Food Chem.* 2011, 125, pp. 145–149.
- 53. Bhat, R.; Stamminger, R. Impact of ultraviolet radiation treatments on the physicochemical properties, antioxidants, enzyme activity and microbial load in freshly prepared hand pressed strawberry juice. *Food Sci. Technol. Int.* 2015, 21, pp. 354–363.
- 54. Xu, F.; Shi, L.; Chen, W.; Cao, S.; Su, X.; Yang, Z. Effect of blue light treatment on fruit quality, antioxidant enzymes and radical-scavenging activity in strawberry fruit. *Sci. Hortic.* 2014, 175, pp. 181–186.
- 55. Teng, H.; Chen, L.; Huang, Q.; Wang, J.; Lin, Q.; Liu, M.; Lee, W.Y.; Song, H. Ultrasonic-Assisted Extraction of Raspberry Seed Oil and Evaluation of Its Physicochemical Properties, Fatty Acid Compositions and Antioxidant Activities. *PLoS ONE* 2016, 11, e0153457.

- 56. Liu, X.; Meng, L.; Xin, X. Optimization of ultrasonic-microwave assisted extraction of anthocyanin from *Lonicera caerulea* residue. *Food Res. Dev.* 2021, 42, pp. 50-54.
- 57. Dong, C.; Yan, X.; Li, X.; Liu, S.; Liu, C. Optimization of ultrasonic-microwave assisted extraction of anthocyanins from mulberry and their antioxidant activities. *China Cond* 2020, 45, pp. 172-178.
- 58. Wang, L.; Weller, C.L. Recent advances in extraction of nutraceuticals from plants. *Trends Food Sci. Technol.* 2006, 17, pp. 300–312.
- 59. Xiao, H.U.; Sun, A.D.; Zhang, D.Q. Separation of anthocyanins from *Perilla frutescens* by high speed counter-current chromatography. *J. Chin. Med. Mater.*, 2010, 33, 1586.
- 60. Berka-Zougali, B.; Hassani, A.; Besombes, C.; Allaf, K. Extraction of essential oils from Algerian myrtle leaves using instant controlled pressure drop technology. *J. Chromatogr. A* 2010, 1217, pp. 6134–6142.
- 61. Ghendov-Moşanu, A.; Sturza, A.; Patraş, A. Process for obtaining polyphenols from grape pomace. Short term patent. MD-825 Z, 2015a.05.31. [In Romanian].
- 62. Brianceau, S.; Turk, M.; Vitrac, X.; Vorobiev, E. Combined densification and pulsed electric field treatment for selective polyphenols recovery from fermented grape pomace. *Journal Innovative Food Science and Emerging Technologies* 2015, 29, pp. 2–8.
- 63. Cristea, E.; Ghendov-Moşanu, A. Utilization of grape pomace in the food industry. In: *Principles of development of modern oenology and the organization of the wine market*. Ed. Tehnica-UTM, Chisinau, RM, 2020, pp. 284-319 [in Romanian].
- 64. Muhlack, R.A.; Potumarthi, R.; Jeffery, D.W. Sustainable wineries through waste valorisation: a review of grape marc utilisation for value-added products. *Journal Waste Management* 2018, 72, pp. 99–118.
- 65. Herzyk, F.; PiłakowskaPietras, D.; Korzeniowska, M. Supercritical Extraction Techniques for Obtaining Biologically Active Substances from a Variety of Plant Byproducts. *Foods* 2024, 13, 1713.
- 66. Garcia-Mendoza, M.P.; Paula, J.T.; Paviani, L.C.; Cabral, F.A.; Martinez-Correa, H.A. Extracts from mango peel by-product obtained by supercritical CO2 and pressurized solvent processes. *LWT Food Sci. Technol.* 2015, 62, pp. 131–137.
- 67. Sánchez-Camargo, A.d.P.; Gutiérrez, L.F.; Vargas, S.M.; Martinez-Correa, H.A.; Parada-Alfonso, F.; Narváez-Cuenca, C.E. Valorisation of mango peel: Proximate composition, supercritical fluid extraction of carotenoids, and application as an antioxidant additive for an edible oil. *J. Supercrit. Fluids* 2019, 152, 104574.
- 68. Villacís-Chiriboga, J.; Voorspoels, S.; Uyttebroek, M.; Ruales, J.; Van Camp, J.; Vera, E.; Elst, K. Supercritical CO2 Extraction of Bioactive Compounds from Mango (Mangifera indica L.) Peel and Pulp. *Foods* 2021, 10, 2201.
- 69. Snoussi, A.; Haj, B.; Hayet, K.; Essaidi, I.; Zgoulli, S.; Moncef, C.M.; Thonart, P.; Bouzouita, N. Improvement of the Composition of Tunisian Myrtle Berries (*Myrtus communis* L.) Alcohol Extracts. *J. Agric. Food Chem.* 2012, 60, pp. 608–614.
- 70. Demirdoven, A.; Karabiyikli, S.; Tokatli, K.; Oncul, N. Inhibitory effects of red cabbage and sour cherry pomace anthocyanin extracts on food borne pathogens and their antioxidant properties. *LWT-Food Sci. Technol.* 2015, 63, pp. 8–13.
- 71. Wang, Y.; Zhao, L.; Wang, D.; Huo, Y.; Ji, B. Anthocyanin-rich extracts from blackberry, wild blueberry, strawberry, and chokeberry: Antioxidant activity and inhibitory effect on oleic acid-induced hepatic steatosis in vitro. *J. Sci. Food Agric.* 2016, 96, pp. 2494–2503.
- 72. Shortle, E.; O'Grady, M.N.; Gilroy, D.; Furey, A.; Quinn, N.; Kerry, J.P. Influence of extraction technique on the anti-oxidative potential of hawthorn (*Crataegus monogyna*) extracts in bovine muscle homogenates. *Meat Sci.* 2014, 98, pp. 828–834.
- 73. Rodrigues, S.; Fernandes, F.A.N.; de Brito, E.S.; Sousa, A.D.; Narain, N. Ultrasound extraction of phenolics and anthocyanins from jabuticaba peel. *Ind. Crops Prod.* 2015, 69, pp. 400–407.
- 74. Wang, Y.; Zhu, J.; Meng, X.; Liu, S.; Mu, J.; Ning, C. Comparison of polyphenol, anthocyanin and antioxidant capacity in four varieties of *Lonicera caerulea* berry extracts. *Food Chem.* 2016, 197, pp. 522–529.
- 75. De Cássia Rodrigues Batista, C.; De Oliveira, M.S.; Araújo, M.E.; Rodrigues, A.M.C.; Botelho, J.R.S.; Da Silva Souza Filho, A.P.; Machado, N.T.; Carvalho, R.N. Supercritical CO₂ extraction of açaí (*Euterpe oleracea*) berry oil: Global yield, fatty acids, allelopathic activities, and determination of phenolic and anthocyanins total compounds in the residual pulp. *J. Supercrit. Fluids* 2015, 107, pp. 364–369.
- 76. Babova, O.; Occhipinti, A.; Capuzzo, A.; Maffei, M.E. Extraction of bilberry (*Vaccinium myrtillus*) antioxidants using supercritical/subcritical CO₂ and ethanol as co-solvent. *J. Supercrit. Fluids* 2016, 107, pp. 358–363.

- 77. Martini, S.; D'Addario, C.; Colacevich, A.; Focardi, S.; Borghini, F.; Santucci, A.; Figura, N.; Rossi, C. Antimicrobial activity against *Helicobacter pylori* strains and antioxidant properties of blackberry leaves (*Rubus ulmifolius*) and isolated compounds. *Int. J. Antimicrob. Agents* 2009, 34, pp. 50–59.
- 78. Chon, S.U.; Kim, Y.M.; Park, Y.J.; Heo, B.G.; Park, Y.S.; Gorinstein, S. Antioxidant and antiproliferative effects of methanol extracts from raw and fermented parts of mulberry plant (*Morus alba* L.). *Eur. Food Res. Technol.* 2009, 230, pp. 231–237.
- 79. Dhar, R.S.; Khan, S.; Khajuria, R.K.; Bedi, Y.S. Dynamics of squalene content in different tissues of Ashwagandha (*Withania somnifera* L. Dunal) during its growth phases. *Ind. Crops Prod.* 2016, 84, pp. 375–380.
- 80. Mackėla, I.; Kraujalis, P.; Baranauskienė, R.; Venskutonis, P.R. Biorefining of blackcurrant (*Ribes nigrum* L.) buds into high value aroma and antioxidant fractions by supercritical carbon dioxide and pressurized liquid extraction. *J. Supercrit. Fluids* 2015, 104, pp. 291–300.
- 81. Dawidowicz, A.L.; Wianowska, D.; Baraniak, B. The antioxidant properties of alcoholic extracts from *Sambucus nigra* L. (antioxidant properties of extracts). *LWT-Food Sci. Technol.* 2006, 39, pp. 308–315.
- 82. Hangun-Balkir, Y.; McKenney, M.L. Determination of antioxidant activities of berries and resveratrol. *Green Chem. Lett. Rev.* 2012, 5, pp. 147–153.
- 83. Fuentes, L.; Valdenegro, M.; Gómez, M.G.; Ayala-Raso, A.; Quiroga, E.; Martínez, J.P.; Vinet, R.; Caballero, E.; Figueroa, C.R. Characterization of fruit development and potential health benefits of arrayan (*Luma apiculata*), a native berry of South America. *Food Chem.* 2016, 196, pp. 1239–1247.
- 84. Mikulic-Petkovsek, M.; Ivancic, A.; Schmitzer, V.; Veberic, R.; Stampar, F. Comparison of major taste compounds and antioxidative properties of fruits and flowers of different *Sambucus* species and interspecific hybrids. *Food Chem.* 2016, 200, pp. 134–140.
- 85. Cacace, J.E.; Mazza, G. Extraction of anthocyanins and other phenolics from black currants with sulfured water. *J. Agric. Food Chem.* 2002, 50, pp. 5939–5946.
- 86. Ayaz, F.A.; Hayirlioglu-Ayaz, S.; Gruz, J.; Novak, O.; Strnad, M. Separation, Characterization, and Quantitation of Phenolic Acids in a Little-Known Blueberry (*Vaccinium arctostaphylos* L.) Fruit by HPLC-MS. *J. Agric. Food Chem.* 2005, 53, pp. 8116–8122.
- 87. Bae, S.-H.; Suh, H.-J. Antioxidant activities of five different mulberry cultivars in Korea. *LWT-Food Sci. Technol.* 2007, 40, pp. 955–962.
- 88. Sharma, U.K.; Sharma, K.; Sharma, A.; Singh, H.P.; Sinha, A.K. Microwave-assisted efficient extraction of different parts of *Hippophae rhamnoides* for the comparative evaluation of antioxidant activity and quantification of its phenolic constituents by reverse-phase high-performance liquid chromatography (RP-HPLC). *J. Agric. Food Chem.* 2008, 56, pp. 374–379.
- 89. Wang, S.Y.; Camp, M.J.; Ehlenfeldt, M.K. Antioxidant capacity and α -glucosidase inhibitory activity in peel and flesh of blueberry (*Vaccinium* spp.) cultivars. *Food Chem.* 2012, 132, pp. 1759–1768.
- 90. Flores, F.P.; Singh, R.K.; Kerr, W.L.; Pegg, R.B.; Kong, F. Antioxidant and enzyme inhibitory activities of blueberry anthocyanins prepared using different solvents. *J. Agric. Food Chem.* 2013, 61, pp. 4441–4447.
- 91. Rugină, D.; Sconţa, Z.; Leopold, L.; Pintea, A.; Bunea, A.; Socaciu, C. Antioxidant Activities of Chokeberry Extracts and the Cytotoxic Action of Their Anthocyanin Fraction on HeLa Human Cervical Tumor Cells. *J. Med. Food* 2012, 15, pp. 700–706.
- 92. Dragišić Maksimović, J.J.; Milivojević, J.M.; Poledica, M.M.; Nikolić, M.D.; Maksimović, V.M. Profiling antioxidant activity of two primocane fruiting red raspberry cultivars (*Autumn bliss* and *Polka*). *J. Food Compos. Anal.* 2013, 31, pp. 173–179.
- 93. Bochi, V.C.; Barcia, M.T.; Rodrigues, D.; Godoy, H.T. Biochemical Characterization of *Dovyalis hebecarpa* Fruits: A Source of Anthocyanins with High Antioxidant Capacity. *J. Food Sci.* 2015, 80, pp. C2127 C2133.
- 94. Badhani, A.; Rawat, S.; Bhatt, I.D.; Rawal, R.S. Variation in Chemical Constituents and Antioxidant Activity in Yellow Himalayan (*Rubus ellipticus* Smith) and Hill Raspberry (*Rubus Niveus* Thunb.). *J. Food Biochem.* 2015, 39, pp. 663–672.
- 95. Mandave, P.C.; Pawar, P.K.; Ranjekar, P.K.; Mantri, N.; Kuvalekar, A.A. Comprehensive evaluation of in vitro antioxidant activity, total phenols and chemical profiles of two commercially important strawberry varieties. *Sci. Hortic.* 2014, 172, pp. 124–134.
- 96. Du, L.; Shen, Y.; Zhang, X.; Prinyawiwatkul, W.; Xu, Z. Antioxidant-rich phytochemicals in miracle berry (*Synsepalum dulcificum*) and antioxidant activity of its extracts. *Food Chem.* 2014, 153, pp. 279–284.
- 97. Duymuş, H.G.; Göger, F.; Başer, K.H.C. In vitro antioxidant properties and anthocyanin compositions of elderberry extracts. *Food Chem.* 2014, 155, pp. 112–119.

- 98. Güder, A.; Gür, M.; Engin, M.S. Antidiabetic and Antioxidant Properties of Bilberry (*Vaccinium myrtillus* Linn.) Fruit and Their Chemical Composition. *J. Agric. Sci. Technol.* 2015, 17, pp. 401–414.
- 99. Saini, R.; Dangwal, K.; Singh, H.; Garg, V. Antioxidant and antiproliferative activities of phenolics isolated from fruits of Himalayan yellow raspberry (*Rubus ellipticus*). *J. Food Sci. Technol.* 2012, 51, pp. 3369–3375.
- 100. Ag, S.; Wu, X.; Rl, P.; Ou, B.; Huang, D.; Owens, J.; Agarwal, A.; Gs, J.; Shanbrom, E. Antioxidant capacity and other bioactivities of the freeze-dried Amazonian palm berry, *Euterpe oleraceae* mart. (Acai). *J. Agric. Food Chem.* 2008, 54, pp. 8604–8610.
- 101. Kryzevicujte, N.; Kraujalis, P.; Venskutonis, R.P. Optimization of high pressure extraction processes for the separation of raspberry pomace into lipophilic and hydrophilic fractions. *J. Supercrit. Fluids* 2016, 108, pp. 61–68.
- 102. Cossuta, D.; Simandi, B.; Hohmann, J.; Doleschall, F.; Keve, T. Supercritical carbon dioxide extraction of sea buckthorn (*Hippophae rhamnoides* L.) pomace. *J. Sci. Food Agric.* 2007, 87, pp. 2472–2481.
- 103. Laroze, L.E.; Díaz-Reinoso, B.; Moure, A.; Zúñiga, M.E.; Domínguez, H. Extraction of antioxidants from several berries pressing wastes using conventional and supercritical solvents. *Eur. Food Res. Technol.* 2010, 231, pp. 669–677.
- 104. Cerón, I.X.; Higuita, J.C.; Cardona, C.A. Design and analysis of antioxidant compounds from Andes Berry fruits (*Rubus glaucus* Benth) using an enhanced-fluidity liquid extraction process with CO₂ and ethanol. *J. Supercrit. Fluids* 2012, 62, pp. 96−101.
- 105. Bobinaitė, R.; Pataro, G.; Lamanauskas, N.; Satkauskas, S.; Viskelis, P.; Ferrari, G. Application of pulsed electric field in the production of juice and extraction of bioactive compounds from blueberry fruits and their by-products. *J. Food Sci. Technol.* 2014, 52, pp. 5898–5905.
- 106. Sindhi, V.; Gupta, V.; Sharma, K.; Bhatnagar, S.; Kumari, R.; Dhaka, N. Potential applications of antioxidants—A review. *J. Pharm. Res.* 2013, 7, pp. 828–835.
- 107. Vauchel, P.; Galván D'Alessandro, L.; Dhulster, P.; Nikov, I.; Dimitrov, K. Pilot scale demonstration of integrated extraction-adsorption eco-process for selective recovery of antioxidants from berries wastes. *J. Food Eng.* 2015, 158, pp. 1–7.
- 108. Alvarez-Suarez, J.M.; Dekanski, D.; Ristić, S.; Radonjić, N.V.; Petronijević, N.D.; Giampieri, F.; Astolfi, P.; González-Paramás, A.M.; Santos-Buelga, C.; Tulipani, S.; Quiles, J.L.; Mezzetti, B.; Battino, M. Strawberry polyphenols attenuate ethanol-induced gastric lesions in rats by activation of antioxidant enzymes and attenuation of MDA increase. *PLoS ONE* 2011, 6, e25878.

Citation: Smerea, O.; Bulgaru, V. Anthocyanins – methods of extraction, stabilization and applications (review). *Journal of Engineering Science* 2024, XXXI (3), pp. 179-195. https://doi.org/10.52326/jes.utm.2024.31(3).13.

Publisher's Note: JES stays neutral with regard to jurisdictional claims in published maps and institutional affiliations.



Copyright:© 2024 by the authors. Submitted for possible open access publication under the terms and conditions of the Creative Commons Attribution (CC BY) license (https://creativecommons.org/licenses/by/4.0/).

Submission of manuscripts:

jes@meridian.utm.md

https://doi.org/10.52326/jes.utm.2024.31(3).14 UDC 665.3:633.85:664(478)





OIL CROP POMACE AS A POTENTIAL SOURCE OF PROTEIN AND DIETARY FIBER

Elena Sergheeva *, ORCID: 0000-0002-8563-0399, Natalia Netreba, ORCID: 0000-0003-4200-1303

Technical University of Moldova, 168, Stefan cel Mare Blvd., Chisinau, Republic of Moldova
* Correspondence author: Elena Sergheeva, elena.sergheeva1@tpa.utm.md

Received: 07. 24. 2024 Accepted: 08. 29. 2024

Abstract. The oil industry market is promising worldwide, including in the Republic of Moldova. The growth of vegetable oil production has led to the formation of a large amount of waste – oil crop pomace (meal), which is usually discarded or used in small quantities as animal feed and becomes a serious environmental problem. The aim of this work is to analyze and study different kinds of oil crop pomace, which can be used as a functional ingredient in product development due to its beneficial components, dietary fiber, and protein. This review presents the classification of meals, the methods of their production, chemical composition, protein, and dietary fiber extraction methods, also their characteristics are discussed. Harmless extraction methods are preferred as they reduce the number of reagents used, reduce waste, and increase the yield. The review presents physicochemical parameters of protein concentrates, isolates, and dietary fibers, which are actively used for valuable food additives production, used as low-calorie ingredients or texture stabilizers in the formulations of various food products.

Keywords: extraction, isolates, oilcake, pumpkin seed, rapeseed, soybean, squeeze, sunflower seed.

Rezumat. Piața industriei uleiului este promițătoare în toată lumea, inclusiv în Republica Moldova. Creșterea producției de uleiuri vegetale duce la formarea unei cantități mari de deșeuri de tip șroturi. Șroturile sunt de obicei aruncate sau folosite în cantități mici ca hrană pentru animale și devin o problemă gravă de mediu. Scopul lucrării este de a analiza și studia tipurile de șroturi care pot fi folosite ca ingrediente funcționale în dezvoltarea produselor alimentare datorită componentelor lor benefice, anume fibrele alimentare și proteinele. Acest studiu prezintă clasificarea șroturilor de oleaginoase, analiza metodelor de producere a acestora, compoziția chimică, metodele de extracție a proteinelor și fibrelor alimentare, precum și caracteristicile acestora. Metodele de extracție inofensive sunt binevenite, deoarece reduc cantitatea de reactivi utilizați, reduc deșeurile și cresc randamentul. Sunt prezentați indicatorii fizico-chimici ai concentratelor proteice, izolatelor și fibrelor alimentare, care sunt utilizate activ pentru producerea aditivilor alimentari valoroși, sunt utilizate ca ingrediente cu conținut scăzut de calorii sau stabilizatori de textură în formulările diferitor produse alimentare.

Cuvinte cheie: extracție, izolate, șroturi de oleaginoase, semințe de dovleac, rapiță, soia, tescovina, semințe de floarea soarelui.

1. Introduction

Nowadays, there are more and more problems with the availability of animal proteins because of environmental pollution, climate change, loss of biodiversity, etc. In addition, prices are also rising due to the increased demand for aliments and energy consumption. At the same time, the need to consume high-quality protein does not decrease. In this regard, research into the production of protein from other environmentally friendly sources is widely welcomed. Among them are plant sources rich in proteins with a good amino acid composition, which after extraction can be used in food as food additives. Plant proteins are easily absorbed by the organism, are not toxic, and are quite suitable for use as a substitute for animal protein [1,2].

In addition, there is the problem of utilization of food processing waste, which has an environmental impact. The Food Agriculture Organization reported that each year about 1.3 billion tons of food is lost, which is 1/3 of the global food production. This includes 20% of oilseeds, meat, and dairy products, 30% of cereals, 35% of fish, and 40-50% of fruits and vegetables. Of the total food waste, 54% occurs during cultivation and post-harvest stages, while 46% - during processing, distribution and consumption [3]. Residues after food processing contain precious compounds (pigments, minerals, fibers) that can be used in the food industry and other fields (agriculture, pharmaceutics, cosmetics) [4].

For these reasons, scientists, ecologists, and nutritionists welcome the recycling of food waste to obtain other products suitable for food or everyday use. This fact can also generate additional income for producers and processors. Agro-waste presents oilseed pomace, which remains after the production of vegetable oil. Residues after oil production contain valuable components such as fiber, antioxidants, pigments, and minerals, which after processing can be used in various industrial fields: food, pharmaceutical, agricultural, and cosmetic. This pomace is rich in protein, nitrogenous compounds, and minerals and is mainly used as cattle feed, but with proper processing can be a source of protein suitable for food [5]. Oilseed pomace has been found to increase the weight of young animals [6]. In this regard, oilseed pomace may become a raw material for protein preparations of plant-origin fabrication. Oilseed pomace has great potential to produce various value-added products with high nutritional value [5].

Soybean products remain the leader in processing, but such potential sources of protein as secondary products of melon seeds, flax, nuts, amaranth, and other oilseeds are also studied [5]. The main oilseed crops used for processing and rich in protein are sunflower, pumpkin, flax, rapeseed, soybean, poppy, and hemp.

The work aims to study the characteristics and origin of pomace of different oilseeds, methods of protein and dietary fiber extraction, and their characteristics.

2. Classification and characteristics of the oil crops

Oilseed crops are a large group of plants that include representatives of various families. From the point of view of their national economic importance, they contain 60-80% oil in their seeds or fruits and are one of the varieties of industrial crops [7]. The value of seed as a material for obtaining oil depends on the oil content of the seed, the price of the oil and its applicability, the difficulty of extracting the oil, and the value of the residue from the extraction [8].

The full list of families with high oil content includes more than 30 names. Oils produced from them make up 70% of the total volume of fats consumed in the world. Pomace

obtained during oil production becomes valuable feed for farm animals, but also, with proper processing, can be used for food purposes. The list of oil crops includes *Asteraceae*, *Lamiaceae*, *Umbelliferae*, palm, *Cucurbitaceae*, legumes, olive, *Euphorbiaceae*, and others [7].

2.1. Sunflower

The fat content of modern sunflower varieties reaches 52% of the dry matter weight of the seed. Sunflower oil refers to a semi-drying type and has excellent taste qualities. It is used for consumption, and food preparation and is also used in margarine production, canning, confectionery, etc. The main fatty acids of this product are oleic and linoleic. The linoleic acid content in the sunflower oil reaches 60% of the total fatty acids, oleic acid 30-35%. Sunflower oil contains vitamins A, D, E, and K, phosphatides, and other beneficial substances. Low-grade sunflower oil is used for soap, paints, linoleum, electrical fittings, and waterproof fabric production [9].

2.2. Rape

The botanical name is *Brassica napus L. ssp. Olivera Metzg.* (winter — *biennis*, spring — *annual*). It belongs to the annual herbaceous plants of the Cabbage family (*Brassicaceae*) [10]. Rapeseeds contain from 30 to 50% oil and up to 23% protein. Of all oilseed crops winter rape ranks first in terms of oil content in seeds (45-50%). The seeds of winter forms contain up to 20% protein and 17% carbohydrates. Semi-drying rapeseed oil can be used for food and technical purposes. Spring rapeseeds contain 35-45% oil, 21% protein and 17-18% carbohydrates. The oil is slightly drying and is used for food and technical purposes. Rapeseed oil is important in food, soap, polygraphy, and other industries. The output of pomace from seeds is 56%, and their protein content reaches 38-40% [11], according to other data, up to 45-49%, which is well balanced in the composition of amino acids. The pomace of erucic acid-free varieties serve as good fodder. The pomace of conventional rapeseed varieties contains 6-7% glycosinolates, whereas that of erucic acid-free varieties contains less than 0.5% and can therefore be compared with soybean oilcake. The pomace from the seeds of common varieties can be fed to animals, but in small quantities [12].

2.3. Other oil crops

Styrian oil pumpkin (*Cucurbita pepo var. Styriaca*) has rindless seeds with an oil content of up to 50%. Unlike other varieties of pumpkin, oil pumpkin varieties are cultivated to produce fruit with a large number of seeds and, respectively, a high total oil output. The seeds can be sold to the consumer as whole seeds or can be processed into oil. Pumpkin seed oil is considered beneficial due to its antioxidant properties (higher than olive oil, hemp, and sunflower oil) [9].

Flax seeds contain 30-50% oil, which includes up to 30-60% linolenic acid, 17-35% linoleic acid and 15-20% oleic acid. In terms of biological value, linseed oil takes one of the first places among other edible vegetable oils. In addition, linseed oil has a high specific energy content of 39.4 kJ/g, and the content of high molecular unsaturated fatty acids in the oil determines its ability to dry quickly and its value as a technical oil [10]. Linseeds contain 35-42% of the seed weight of well-drying oil, which is used in the production of paints, varnishes, drying oils, soap, paper, electrical, and other industries, as well as in medicine and perfumery. A small part of linseed oil is used for food purposes. Linseed pomace serves as a good concentrated feed for livestock. It contains 6-12 % fat and up to 30 % digestible protein [9].

Soybean (Glycine max) is a legume crop originating from East Asia. Because of its high oil content soya is classified as an oilseed. It is used as oil for consumption and for industrial applications as, for example, biodiesel. Soya accounts for about 60% of the total world production of oilseeds. However, in Europe, soya is considered a legume crop along with beans, lentils, and peas [9]. As a major source of vegetable protein and edible oil, soybean is a very important legume crop in the world. Although soya is produced mainly for its dry seeds, the widespread use of immature seeds, especially in eastern Asia, makes soya an important vegetable crop. The chemical composition of the seeds is as follows: 30-52% protein, 17-27% fats, 6-20% carbohydrates, minerals (potassium, phosphorus, calcium), and vitamins (C, B, E). Soy is recommended for the dietary nutrition of diabetic patients. The protein is characterized by high digestibility (3.5-4 times more than the protein of cereal crops) and water solubility. Among leguminous crops, the composition of essential amino acids is the richest. The main protein of soya seeds is glycinin, which can coagulate when souring. Soy protein contains the amino acids lysine 2.7% (in wheat protein 0.25%), methionine, and tryptophan, which determine the feed value. Soybeans are cultivated for food, fodder, and technical purposes. It is used for food in the form of oil, margarine, soya cheese, milk, flour, confectionery, canned food, and other products. Soybean seeds serve as raw material for the oil industry. Soybean oil is classified as low-drying and is consumed after refining. It is also used in soap making, the varnish industry, the production of glycerine, linoleum, lubricating oils, gelatine, and lecithin. Soybean oil accounts for 38% of global production, while sunflower oil accounts for 17% [7]. For feed purposes, soya is used in the form of pomace, oilcake, and soya flour. The oilcake contains 40 % protein, 1.4 % fat, and 30 % nitrogen-free extractive substances. The pomace is also an additive in baking, pasta making, and confectionery.

Poppy (*Papaver somniferum*) is a source of valuable edible oil. This oil is rich in unsaturated fatty acids, the main component of which is linoleic acid. The oil of the poppy seed is particularly suitable for dish preparation, and raw consumption and is known to be used as a marinade for meat. Poppy seed oil is not so widespread because of the relatively high price of its production in comparison with other oils with similar properties. Nevertheless, poppy seed oil is a very popular ingredient in contemporary diet. Cultivation of the poppy is complicated, due to the small size of the seed and slow growth in the early stages of culture [9].

Hemp are special varieties of *Cannabis sativa L*. used for industrial or medical use. Hemp can be used in a variety of ways: the seeds are used for oil production or can be consumed fresh, the inflorescences can be used for medicinal purposes, and the fibers can be used to make textiles, rope, paper, or building materials. In the case of oil pressing, the remaining pomace is a valuable component of animal feed.

2.4. Production of the oil crops worldwide and in the Republic of Moldova

Wastes of seed processing into oil are named pomace (produced by the oil press method) and oilseed cake (or oilcake) by the extraction method. It is known for its high protein content and often is used as feed for farm animals. Such wastes contain a large number of essential amino acids. The share of waste accounts for up to 35% of the seed weight. 1 kg of the pomace contains 363 g of digestible protein. 1 kg of cake contains 226 g of digestible protein. The fat content in the waste varies from 1 to 7%, and protein from 33 to 35% [12]. According to other data, the pomace contains 8-10% fat, 36-40% protein, and 20% carbohydrates. The oilcake contains 1-3% of fats [13]. In terms of phosphorus and calcium

content pomace and oilcake are superior to cereal plants. The output of dried husks reaches 56-60% of the seed weight. 1 kg of flour from dried husks contains 38-43 g of protein [9,14].

Most oilseed crops need to be grown in areas with high temperatures for proper fat accumulation in the seeds. The exceptions are winter types of oilseed rape and turnips, which prefer a relatively cool climate with high humidity and precipitation during the growing season. In contrast, poppy, sunflower, and hemp need warmer climates, especially in summer, for good output of the oil. This explains the reason why sunflower is mainly grown in the southern and south-eastern regions of Europe and rapeseed in temperate regions. Nevertheless, important breeding work is underway to expand the growing ranges of these crops, to develop varieties that also thrive in warmer conditions. Soil conditions have little influence on the geographical distribution of oilseeds. Only very shallow soils are unsuitable for oilseed crops unless they are irrigated. In the mild spring climate can be observed the early growth of oilseed crops (such as mustard, rape, or camelina. Flax can adapt to different climatic conditions, from maritime to continental. There are winter and also spring varieties of flax, allowing farmers to choose the type of crop that better suits the local climate. Oilseed pumpkin, although it grows in almost all regions of Europe, does not thrive in very cold or very warm conditions [15].

The biological features of oilseeds allow their cultivation in a wide range of different climatic and soil conditions. In general, they are well adapted to cultivation in different regions with high or insufficient relative air humidity, and have a significant potential for productivity of high-quality oilseeds [14]. The volume of oilseed production within the European Union in recent years is presented in Figure 1 [16].

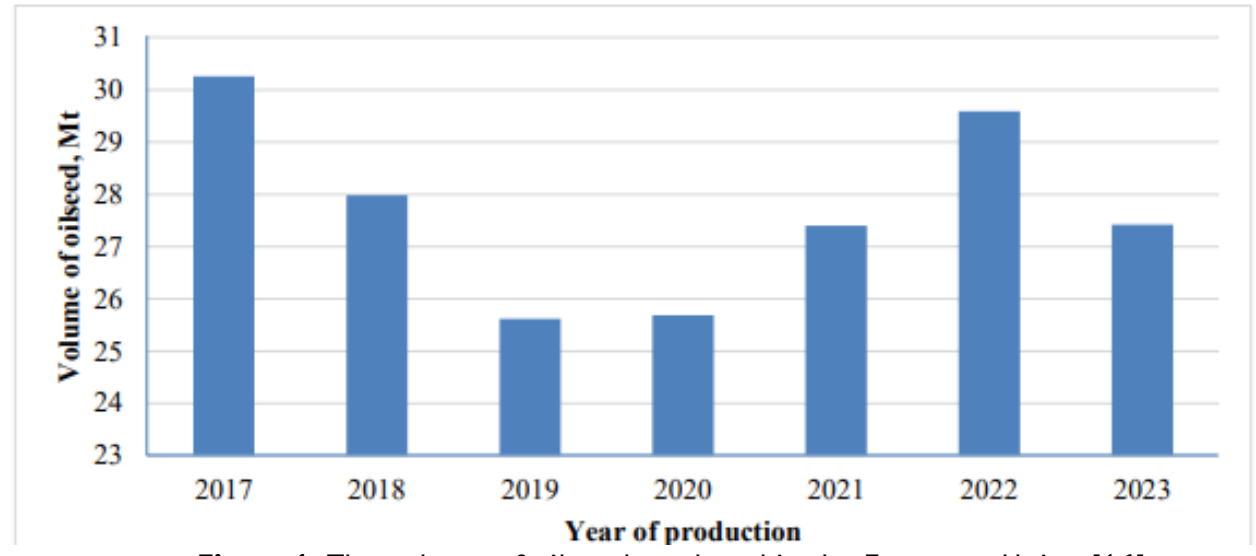


Figure 1. The volume of oilseed produced in the European Union [16].

Oilseed production in the European Union has been unstable in recent years, with growth until 2022 and then a slight decline. The maximum over the past 7 years was in 2017 and amounted to more than 30 million tons.

World oilseed production in 2022/23 was 629.66 Mt (\pm 2.9% to 2021-2022), including soybeans 370.11 Mt (\pm 2.8%), rapeseed 88.56 Mt (\pm 16.8%) and sunflower 52.46 Mt (\pm 7.7%). Harvested area of oilseeds 303.57 Mha (\pm 2.3%), including soya beans 136.54 Mha (\pm 4.1%), rapeseed 41.84 Mha (\pm 8.8%), and sunflower 27.97 Mha (\pm 2.0%). The main producers of oilseeds are China 68.04 Mt (\pm 9.6%), India 42.29 Mt (\pm 2.1%), and the EU 31.88 Mt (\pm 2.6%) [15].

In the Republic of Moldova, oilseed crops are in great demand and their production is increasing (Figure 2) [17].

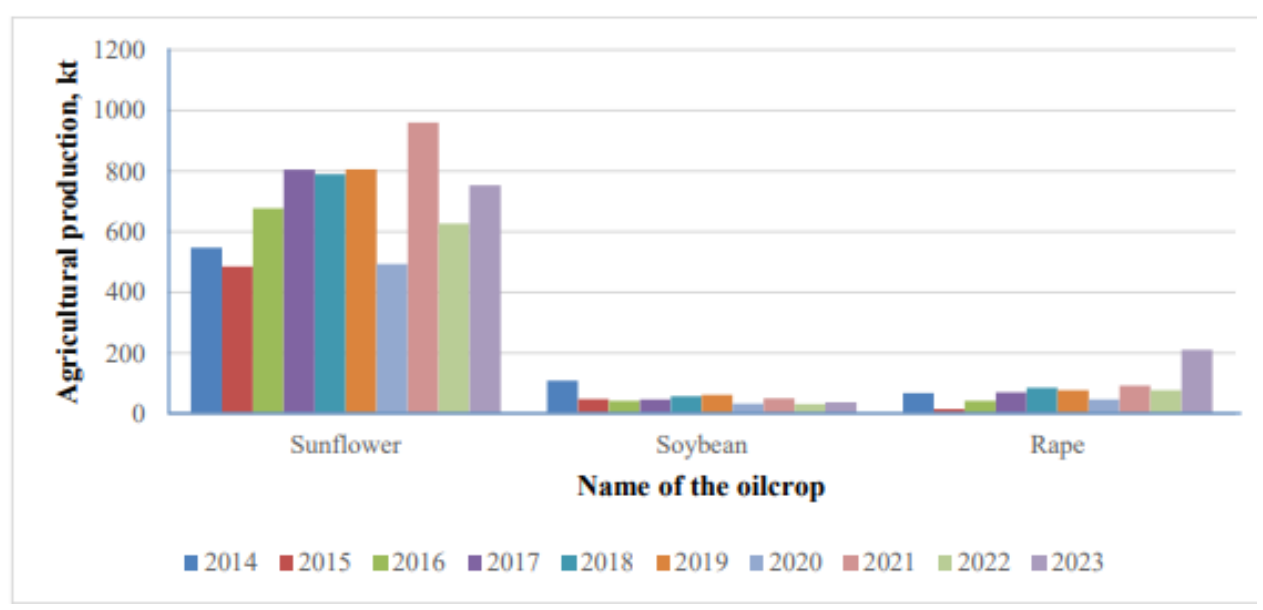


Figure 2. Cultivation of some oilseed crops in the Republic of Moldova [17].

Sunflower is the leading crop due to the widespread consumption of refined sunflower oil. Also widely cultivated are rape and soya.

3. The squeeze obtaining

The pomace used in the research is a direct product of the processing of oilseeds during oil production. Oil can be fabricated in two ways: by pressing and by extraction with various solvents, which influence the quality of the pomace. The oil in seeds consists almost exclusively in their kernels, which are surrounded by a dense hard shell, thanks to which the inner parts of the seed are protected from direct access to air. This ensures the relative stability of the seed during preservation, but at the same time makes it difficult to extract oil during processing. Extraction of oil must be preceded by crushing of both the shells and the kernel of the seed, as the oil is contained within the cells [18]. The extraction of most of the oil contained in the seed by pressing can only be achieved under strong pressure, it is very difficult due to its adhesion to the hard parts of the seed and due to the considerable viscosity of fatty oils at ordinary temperatures. Viscosity decreases with increasing temperature; therefore, when pressing heated seed, oil is more easily extracted from it. Heating the crushed seed before pressing has another meaning: if, when the seed is heated, the temperature is raised so that the protein is curdled, the oil obtained from such seed will contain no protein or much less. Heating the seed before pressing, however, has disadvantages. Some substances contained in the seeds, and, probably, the products of the change of these substances from heating, are more easily dissolved in the heated oil, these are the substances that give the oil a yellow or greenish-yellow coloring and a peculiar flavor. Oils obtained by pressing at ordinary temperature are less colored, cleaner, and have a milder and more pleasant taste than oils obtained by pressing heated seed. The same data show that heating of the seed should not be made more than 60-80°C [19].

Thus, the extraction of oil by pressing can never be complete. For example, in linseed pomace remains between 6.6 and 16.5 % oil. The complete removal of oil from the seeds, as well as from the residue from pressing, from the pomace, is achieved by extraction. In this

method, the pomace is exposed to volatile reagents. In this case, the consequences of the impact of reagents on the pomace are not taken into account, since the goal of this process is to obtain the largest amount of oil [20].

The solvents often used for this process have several main requirements: they must be affordable and available in large quantities in the trade, must dissolve a relatively large amount of oil, and not dissolve other substances contained in the seeds and deteriorate the quality of the oil, must be easily and completely volatile, but at the same time their vapors must easily condense into a liquid. The most often used are the following solvents: carbon sulfide, petroleum volatile oils, and ether. It is believed that petroleum volatile oil has a minimal impact on the quality of the residues from the extraction of oil. Besides, it is the cheapest solvent, doesn't dissolve other substances contained in the seeds and deteriorate the quality of the oil, doesn't change during use, and does not have any harmful effect on the properties of the resulting oil. In all respects ordinary ether is also a convenient solvent: it also mixes with vegetable fatty oils in all proportions, can be easily and completely removed from the oil and the residues, does not undergo any change when used for extraction, has no adverse effect on the oil or the residues, although it dissolves foreign substances. Sulfurous carbon can interact with some of the constituent substances of the seeds and form sulfurous compounds in the residue or the oil. Carbon sulfide is also the most inflammable of the three materials mentioned. The use of common ether would be most convenient for the obtaining of safe oils and residues, but the use of petroleum oils for extraction has become much more widespread because of its cheapness [18,21].

It is obtained safely, and easily clarified by sedimentation and filtration oils and residues in the case of compliance with the following conditions: 1) petroleum oils should be well purified with sulphuric acid and caustic soda so that they contain neither oxygen substances nor hydrocarbons that may be subject to change from the action of air and in general under the conditions of extraction; 2) for extraction should be used only petroleum oils, fully distilled at 100 °C [18].

Both the residue from oil extraction and the oil itself, to completely extract the volatile solvent, should be treated in the end with hot steam, and this steaming should not be carried out for a long time, for the residue to prevent the formation of starch glue, and for the oil to eliminate the decomposition that occurs during the prolonged action of steam on fats [19].

According to the analyses, the residues from extraction contain the following amounts of protein substances: rapeseed residues 28.69% (summer rapeseed), up to 32.7% (winter rapeseed), dried rape residues 35.9-38.65%, linseed residues 31.05-32.0%, hemp residues 33.67-34.45%, poppy residues 31.52-37.0%. The extraction residues contain no more than 2% oil. Thus, comparing extraction residues (oilcake) as feed material with pressed residues (pomace), it is evident that they contain more proteins than pomace, and although they contain almost no fat, they are not inferior to pomace in nutritive value. Extraction residues have the considerable disadvantage that they are friable and therefore more easily adulterated in commerce and less convenient for transport than pomace [21].

4. Squeeze classification

In the oil production process, there is always residual waste - squeeze, which is of high value, primarily for use as animal feed, but can also be used for other purposes. Depending on the type of the initial product - seeds of plant culture, are distinguished sunflower, rapeseed, soybean, peanut, mustard, hemp, corn, and other squeezes.

When processing oil by pressing, pomace is obtained, and when producing oil by extraction, oilcake is obtained. The pomace contains 5-7% of fat, while the oilcake includes less than 2-3%. The study of wheat germ pomace has shown that oilseed pomace retains most of the biologically active substances found in the original seed germ, making it a rich source of proteins, carbohydrates, vitamins, and essential macro- and microelements. This nutrient-dense by-product enhances the nutritional and biological value of food products when utilized as a raw material. Due to its high content of proteins and other essential nutrients, oilseed pomace is an excellent candidate for sustainable food production, contributing to the development of high-quality, plant-based protein supplements and additives in food formulations [19]. Squeezes are also divided into two categories: edible and non-edible. The first category includes soya, rapeseed, linseed, sunflower, and others. It has high nutritional value and is suitable for human and animal food in processed form, as isolate, hydrolysate, protein extract substrate for bioactive compounds, enzymes, pigments, antibiotics, flavors, vitamins, and amino acids. Inedible oilseed cake (castor, mauha, neem, linseed, and karanja) contains toxic compounds. Their composition depends on the way of oil extraction and the composition of the crop [3].

Even though the oilcake as a residue after oil extraction contains many proteins, its purification from the reagents takes a lot of time and resources, and it is not customary to use it for further processing. In contrast, the pomace is a valuable product for further use.

5. Chemical composition of the pomace

While the composition of the different pomace is similar, there are also differences. Sunflowers, soya, and cotton pomace contain more protein. Sunflower and soya pomace contains maximum amounts of lysine and methionine. They are a rich source of vitamins B and E, as well as phosphorus and potassium. Soybean and sunflower pomace are ahead of cereal seeds in terms of sodium and calcium content. Rapeseed pomace is not inferior to sunflower pomace in energy value and is ahead of soya pomace in phosphorus, calcium, copper, and magnesium content. In addition, rapeseed pomace is characterized by a significant content of riboflavin, folic acid, thiamine, natural antioxidants, tocopherol (vitamin E), phenolic compounds, and tannins. Soybean pomace, compared to rapeseed pomace, has more lysine, but less cystine and methionine [20].

In traditional technologies of oil production, based on the heating of raw materials, the effect of temperature leads to a decrease in the number of amino acids in the pomace [21]. If seeds of the oil crops are pressed without separating the seed coat, the pomace gets a darker color and a high fiber content [22]. One of the indicators of soya pomace is a low percentage of fiber, the amount of which in 1 kg of the product is 72 g, while in sunflower pomace this indicator reaches 152 g, and in flax pomace - 145 grams [20].

Raw sunflower seeds contain 16-19% protein per dry matter, but protein products are more often obtained from pomace containing about 35-45% protein [23].

Rapeseed pomace obtained by processing rape seeds contains valuable nutritional substances, including 27-41% of protein, containing essential polyunsaturated fatty acids of the omega-3 family, fiber, vitamins such as choline, niacin, riboflavin, folic acid, thiamine, as well as minerals such as calcium, phosphorus, magnesium, copper, manganese, and others [24,25]. Soybean pomace differs from others in its reduced fiber content, but while remaining a good source of energy and protein, it is highly digestible and highly productive. Its main amino acid is methionine. Rapeseed pomace is richer in sulfur amino acids but is comparable

in amino acid balance with soya. Among carbohydrates in rapeseed pomace, pectins (14.5%) and cellulose stand out. It also contains anti-nutritive substances such as tannins, glucosinates, and phytates. Like sunflower pomace, it is low in lysine and high in sulfurcontaining amino acids. Rapeseed pomace contains a lot of fiber, which causes its low digestibility. Pumpkin, flax, and hemp seed extracts have shown 75.09, 65.23, and 409.51 mg/100 g of dry extract amino acids content. When extracted under a nitrogen atmosphere with pure water, a lower content of total amino acids was found: 20.40 (pumpkin), 18.84 (flax), and 219.50 (hemp) mg/100 g dry extract [26,27].

The protein content of different kinds of pomace is presented in Table 1.

Table 1

Different kinds of pomace protein content [28]

Oilseed pomace	Protein content, %	References
Groundnut	45-60	[29]
Soybean	40-50	[28,30]
Sesame	32-35	[31]
Rapeseed	34-42	[28,32]
Pumpkin seed	35-56	[28,33]
Sunflower seed	20-39	[34,49]
Linseed	25-45	[28,35]

The highest protein content is characteristic of groundnuts, pumpkin seeds, and soybeans. Also, oil crop pomace is rich in various vitamins and minerals (Table 1). The oil content in sunflower and rapeseeds is more than 40%, 15-25% is found in soybean, and up to 56% in peanuts [27]. Some types of pomaces, such as sunflower pomace, are known to contain phenolic compounds that have antioxidant properties [28].

Among the biologically active substances of flaxseed take place essential polyunsaturated fatty acids (oleic, linoleic), dietary fiber, all essential amino acids, as well as vitamins A, B, D, E, minerals Ca, K, Mg, Na, P, Mn, Fe, Zn [29]. The uniqueness of the healing properties of flaxseed is partly due to the significant content of lignans, which exhibit estrogen-like activity in the human body. Thus, the content of the main representative of lignans in flax seeds - the glycoside secoisolariciresinol is 13.6-32.1 mg/g. Scientists in experiments have also established the anticarcinogenic and powerful antioxidant effect of this lignin [30].

Oilseed pomace is a good source of fiber, rich in non-starch polysaccharides. Their chemical composition can differ based on the oil extraction techniques used [31]. Diets high in fiber bring various health benefits, such as the prevention and management of colorectal cancer, coronary heart disease, constipation, diverticular disease, and diabetes [32,33].

The work on the use of rapeseed pomace for food purposes is presented, where is shown that rapeseed pomace is a useful additive in the diet of athletes. It was found that when the pomace is added to red basic sauce in the amount of 5% there is an increase in the content of macro- and micronutrients, which are directly involved in the processes of muscle contraction and excitability of nerve tissues. When consuming sauce with rapeseed pomace for three months, a decrease in cramps and muscle spasms in track and field athletes was noted due to increased calcium absorption [34,35].

6. Protein extraction methods

The development of innovative technologies for pomace processing represents a promising research area. These technologies should focus on producing protein in a way that is waste-free and results in a food-grade product with minimal phenolic content. Existing methods for extracting protein concentrates and production of isolates from sunflower and other crops are well-established. The functional properties of these proteins are influenced by the specific parameters used during the production process [26].

Protein extraction from pomace typically involves using water, alkalis, salt solutions, organic solvents, or acids. Once the protein has transitioned into the liquid phase, it is precipitated at its isoelectric point using hydrochloric acid. The isoelectric point is influenced by the amino acid composition of the proteins by the balance of amine and carboxyl groups. For plant proteins, the isoelectric point generally falls between 4.0 and 4.5 [26].

The other method to obtain protein products from the pomace involves mechanical fractionation, which is commonly used in industrial production. This process includes further technological steps such as grinding and dry fractionation, which help increase the crude protein content while significantly reducing the crude fiber content in specific fractions of protein flour and grits. However, the presence of phenolic compounds causes the protein products to darken, which limits their use in the food industry [26].

For protein isolates and concentrates from oilseed pomace preparation, the most commonly used method is the two-step (extraction-isolation) method patented by Anson and Pader in 1955 [36]. This process begins with the alkaline solubilization of proteins, followed by the removal of insoluble materials, such as starch and fiber, through centrifugation. Afterward, hydrochloric acid is added to the supernatant to precipitate the protein at its isoelectric point (pH 4.0–5.0). The protein is then separated by centrifugation and neutralized [26].

There exist modified methods of protein extraction. Protein extraction can be performed under acidic conditions or in water as outlined by the author Klamczynska [37]. Generally, both acidic and alkaline extraction methods can achieve a high level of purity, often exceeding 90%. Alternatively, instead of using isoelectric point (pHi) precipitation, ultrafiltration can be employed for protein purification. This ultrafiltration method differs from pHi precipitation in that it typically results in proteins with higher solubility and functionality [26].

The author Ali [38] reports the method based on the use of varying concentrations of ascorbic acid and N-acetylcysteine (0, 20, 40, and 60 mg/100 mL) for the protein solubilization and rigorous pH control, followed by centrifugation, filtration, and freezing of the resulting product. To purify the protein from phenolic compounds, various solvents are used for washing. However, if the washing process is insufficient, phenolic compounds may not be entirely removed. Some organic solvents can denature the protein, reducing its biological value, and they can be difficult to fully eliminate from the final product. Another deficiency of these methods is the high-water consumption, which increases the process cost. When alkaline solutions are used for protein extraction, phenolic compounds are oxidized, forming quinones. Upon heating, these quinones bind to the protein, resulting in dark green and brown compounds that diminish the functional properties of the protein. This poses challenges for the use of these protein products in the food industry. That's why, the main task in producing protein products from pomace is to remove phenolic compounds. Sunflower seeds and their derivatives contain a variety of phenolic compounds, including chlorogenic, isoferulic, and caffeic acids, with an average phenolic content of about 2.5%. Chlorogenic

acid is the most abundant phenolic compound in sunflower seeds, accounting for up to 73%, depending on the growing conditions and variety [11]. Thus, it is recommended to extract chlorogenic acid and other phenolic compounds from raw material before the protein extraction. For this, the milled pomace can undergo a series of washes at acidic pH before the protein extraction [38].

The most efficient solvent for extracting chlorogenic acid is an aqueous ethanol solution with a concentration of 50-96%. This process not only removes phenolic compounds but also eliminates other impurities from the pomace. However, a significant disadvantage is that alcohol extraction in high concentrations leads to protein denaturation. The extent of denaturation can be minimized by carefully selecting the extraction temperature and the concentration of the ethanol solution. The optimal temperature range for extracting chlorogenic acid is 20-70 °C. Adjusting the temperature from 50°C to 70 °C does not significantly increase chlorogenic acid yield while lowering the temperature to 20 °C slows the extraction process. Exceeding 70 °C, however, results in substantial protein denaturation. Residual phenolic compounds that remain associated with the proteins give the final products antioxidant properties without changing their water solubility, but they also impart a dark coloration. Nevertheless, there has been growing interest in recent years in retaining these phenolic compounds or even adding them due to their antioxidant activity and potential health benefits, such as disease prevention and anti-aging effects [39].

For protein isolate preparation the method is based on an underwent to isoelectric precipitation of the resulting after the protein extraction supernatants by adjusting the pH to 4.5, followed by mixing, centrifugation, and freeze-drying using a vacuum pump [39].

To obtain powdered concentrate is often used spray drying, which is advantageous because it avoids overheating the product, thereby preserving its quality, and eliminating the need for additional grinding. It also generally results in high solubility. However, successful spray drying requires careful control of temperature parameters and process conditions. The temperature during drying significantly influences both the solubility and functional properties of the resulting protein. When the process parameters are optimized, it is possible to produce a protein with excellent quality [40].

Thus, the author Shaghinova presents the following process for obtaining protein extract from sunflower seeds (Figure 3) [23].

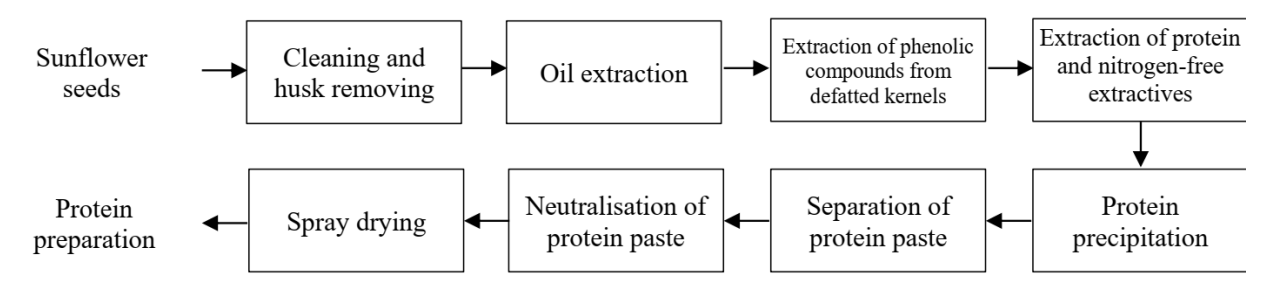


Figure 3. The method of protein preparation production [23].

Peeled and ground sunflower seed kernel should be defatted in a Soxhlet apparatus by exhaustive extraction with diethyl ether and treated with 80% ethanol solution. After extraction, the mixture should be centrifuged to separate the phenolic extract, and the precipitate should be washed with an alcohol solution. Protein and nitrogen-free extractives can be extracted from the precipitate with 0.1% NaOH solution. This method involves reaching the isoelectric point of sunflower protein for its coagulation to form a precipitate,

which can be separated by centrifugation, neutralized, and dried to a powdery state on a laboratory spray dryer. Thus, under laboratory conditions dry powdery protein preparations of light grey color can be obtained from sunflower seeds, which did not darken in the air and contact with water. In this case, the protein preparations had no extraneous odors and had a neutral taste.

There exists a growing need for new green and safe technologies that will reduce the temperature and duration of the extraction process, minimize solvent usage, and improve the quality and yield of extracted proteins [41]. Emerging techniques, such as high-pressure processing, supercritical fluid extraction, microwave-assisted extraction, ultrasound-assisted extraction, cold plasma processing, pulsed electric fields, and radio frequency treatment, are enhancing extraction efficiency and minimizing protein degradation. These methods generally have a lower impact on the environment and are considered safe for human and also animal consumption due to the minimal use of harmful reagents [42]. Furthermore, these methods can improve the nutritional value of proteins, and their functional properties and may even produce bioactive peptides. However, the high energy inputs can cause structural changes in proteins, which may negatively impact their technical functionalities, such as emulsification, solubility, water-holding capacity, gelling, and foaming abilities. Despite these challenges, these technologies can modify the structural properties of allergenic plant proteins, which often have fewer technological applications compared to animal proteins. For example, power ultrasound can be used to adjust the functional, physical, and structural characteristics of protein-based components during extraction and modification [43].

Traditional protein solubilization procedures often incorporate ultrasonication, as it effectively disrupts the cell matrix and enhances extractability. The ultrasonic energy applied to the protein influences changes in its functional properties, including emulsification, solubility, foaming capacity, and hydrophobicity. Emerging technologies have shown significant improvement in the efficiency of protein extraction [44].

During the microwave-assisted extraction the microwave energy creates intense stress on the plant cell walls, leading to more uniform heating, eventual cell wall rupture, and the release of desired components. This method can significantly affect the structural properties and proteins and peptides activity due to the increased dielectric constant of microwaves. Microwave-assisted extraction offers several advantages, including an increased extraction rate, higher reproducibility, uniform heating, reduced solvent and energy consumption, and enhanced functional properties [45].

Another innovative approach is the use of moderate electric field extraction, a potentially reversible permeabilization technique that employs electric fields ranging from 1 to 100 V/cm. Moderate electric field extraction works by inducing internal heating and electroporation, which not only saves time and energy but also improves the properties and yield of the proteins [5].

7. Fiber extraction methods

Dietary fiber refers to a group of carbohydrate polymers, that cannot be digested by enzymes in the human digestive system. This group includes insoluble components such as cellulose, and lignin hemicelluloses, as well as soluble components like pectin, gums, inulin, mucilages, and resistant starch [46].

There exist various methods for dietary fiber extraction, including traditional techniques such as dry and wet processing, chemical, microbial, and enzymatic gravimetric

methods, and innovative extraction techniques using water, ethanol, steam, hydrostatic pressure, ultrasonic treatment, and pulsed electric fields. The extraction method can affect the composition and characteristics of dietary fiber. Among traditional methods, wet processing is considered the most cost-effective and efficient, yielding a purity of 50-90% in the final product. However, using alkali or acid may damage the fiber structure, and enzymatic methods can result in incomplete extraction. Innovative methods offer benefits like a higher recovery rate and lower environmental impact [3].

The extraction of dietary fiber typically involves three stages. The first stage is pretreatment, which focuses on removing microbes without affecting the biological activity of the material. Techniques used at this stage include microfiltration, foam mat, de-watering, and electro-osmotic treatment. The second stage is the extraction process, which can be performed using either classical methods (such as solvent extraction, steam distillation, or maceration) or advanced green methods. These modern methods include extraction with water or ethanol, supercritical fluid extraction, pulsed electric field, mixtures of water/organic solvents with carbon dioxide, enhanced solvent extraction, microwave or ultrasound-assisted extraction, accelerated solvent extraction, enzyme-assisted extraction and high-voltage electric discharge [47].

These innovative methods offer several advantages, such as high-quality extraction, minimal solvent use, selective recovery, shorter extraction times, reduced waste, and lower environmental impact. Additionally, they align with sustainable practices, allowing the use of waste and by-products in line with the circular economy model [47].

However, there are some drawbacks to these methods. For instance, microwave-assisted extraction can have high energy consumption, ultrasonic extraction may present separation challenges, and pulsed electric field technology can be less user-friendly. Traditional methods, while effective, generally require longer extraction times and larger volumes of expensive and toxic, solvents. However, compared to traditional techniques, modern methods offer better efficiency, reproducibility, and control over the extraction process [48].

The final stage of extraction involves purification, which can be achieved through alcohol precipitation, ultrafiltration, or chromatographic techniques [48].

The author Zheng [49] studied how particle size and solvent treatment affect the characteristics of the dietary fiber from the oil pomace. Reduction of particle size influence led to an increase in entrapment, swelling, and water-holding capacities. Cellulase hydrolysis negatively affected the color and oil-holding capacity, but it enhanced porosity, carbohydrate content, swelling, and water-holding capacities. In contrast, acid treatment produced opposite effects [3].

Fiber extraction is known enzymatic gravimetric method, described by the author Sunil [50]. In this procedure, a defatted sample is subjected to digestion of the starches using the phosphate buffer and thermo amylase and digestion of the proteins using pepsin and pancreatin, followed by cooling and filtration. To obtain insoluble dietary fiber the author proposes washing of the retained residue with ethanol and acetone solution, drying, and incineration. For soluble dietary fiber obtaining, the filtrate can be subjected to sedimentation by ethanol, followed by filtration, drying, and incineration.

8. Chemical composition of the oil crop pomace protein and fiber

In other scientific works, physicochemical parameters of protein concentrate from different types of crops were studied [39]. Sunflower pomace is the most accessible for research. The chemical composition of the sunflower pomace and protein concentrates, obtained by different methods is presented in Table 2.

Table 2 **Chemical composition of the sunflower pomace and protein concentrates** [38,39,51]

Samula	Protein	Phenolic	Ash content,	Moisture
Sample	content, %	compounds, %	%	content, %
Sunflower pomace	31.5-31.8	2.6-2.8	7.6-8.4	10.1-11.9
Protein preparation	46.1-47.0	5.8-6.2	8.7-9.6	6.7-6.9
Proteins with phenolic compounds				
extraction in water	74.7-76.3	1.8-2.2	4.6-5.4	8.0-8.2
Proteins with phenolic compounds				
extraction in Na ₂ SO ₃ solution	70.8-72.0	1.3-1.5	6.2-6.6	5.1-5.7
Proteins with phenolic compounds				
extraction in ethanol	63.1-63.3	1.3-1.5	9.1-10.9	8.7-10.1
Proteins with phenolic compounds				
extraction in methanol	59.7-60.0	1.4-1.6	12.0-13.0	10.1-11.7
Protein concentrate extracted at pH	58.0-58.3	1.2-1.4	4.9-5.5	4.1-5.8
9	20.0-20.3	1.2-1.4	4.5-3.3	4.1-3.0
Protein extracted with ascorbic acid	56.1-58.1	1.2-1.3	5.4-5.8	4.8-6.8
Protein extracted with N-	57.9-59.1	1.0-1.2	6.1-6.5	5.9-6.9
acetylcysteine	37.7-39.1	1.0-1.2	0.1-0.5	J.J-0.9

The use of aqueous alcoholic solutions achieved a greater reduction in phenolic compounds compared to sodium sulfite; however, alcohol-based extraction was less effective for extracting components that dissolve more readily in water. Additional steps for removing phenolic compounds using aqueous extraction procedures resulted in protein isolates with higher protein content (76-78% dry basis) and lower phenolic levels, without notable differences in moisture content.

The data from other studies are also known protein 41.4%, ash 11.4%, and moisture contents 6.3%, all based on dry weight [51]. The values of these studies differ due to the use of different batches of sunflower, different degrees of purification, and research errors.

Extraction of phenolic compounds results in higher protein content. The type of reagent and pH affect the physicochemical parameters. For example, when N-acetylcysteine is used, the amount of ash is higher than when ascorbic acid is used. At the same time, as the concentration of the additives increases, the values of the indices also increase. The elimination of phenolic compounds results in an increase in the protein content of the concentrates [38].

According to various sources, protein concentrates contain 30-80% of protein, and protein isolates >90% of protein [47].

Dietary fiber from the pomace consists of both soluble and insoluble components. Both types of fiber contribute to increasing food volume and weight without significantly raising calorie intake, which promotes satiety and reduces appetite. They also help balance the pH in the small intestine, inhibiting harmful bacteria and protecting the digestive system. Insoluble dietary fiber, in particular, has a stronger anti-obesity effect than soluble by

promoting lipid absorption and excretion, and it also reduces the risk of type 2 diabetes. These benefits are linked to the swelling and adsorption properties of dietary fiber, which are influenced by its microstructure [52].

9. Application area

Protein extracted from oil crop pomace has bioactive properties that can be enhanced by chemical or enzymatic hydrolysis with the aim of protein hydrolysate production. For example, author Girgih [53] reported higher angiotensin-converting enzyme inhibitory activity and antioxidant activity of pomace hydrolysates.

Protein isolates are known for emulsifier properties as they have high emulsifying activity and moisture retention capacity. Protein hydrolysates increase the output of culinary products due to moisture retention capacity and also improve the organoleptic characteristics of meat products. Enzymatic hydrolysates can be applied in the production of meat flavorings. For example, the addition of canola protein concentrate to sausages improves their aroma, flavor, and texture, which was confirmed by tasting [54].

Oilseed pomace is a functional product and is actively used in the production of valuable food additives. Protein extracts from the pomace can be used in many applications as additives. Carbohydrate-rich pomace, such as pumpkin pomace, is used as an additive for meat and dairy products. Pomace rich in proteins and fibre can be added to confectionery and bakery products [55].

There is a known study in which the author uses pomace of sunflower, coconut, pumpkin, and flax to create a food additive in the form of tablets to which flavorings can be added for better taste [56].

Bioactive peptides, specific fragments of proteins, exhibit biological activity and have a positive impact on health. Among this is demonstrated hypocholesterolemic, antioxidant, immuno-modulatory, and antithrombotic activity. The controlled cleavage of soybean protein hydrolysate, followed by hydrolysis with microbial protease, produces peptides with enhanced functionality, such as improved iron-chelating activity and better surface-active properties [57].

Protein isolates are used as a functional ingredient in many food products such as protein bars and shakes, meat substitutes, frozen desserts, cheese substitutes, and protein-enriched pasta. Protein isolates have gelling properties, solubility, and surface-active properties and are also used as food additives. Other beneficial properties and uses of proteins are presented in Table 3.

Benefits of protein from oilseed pomace [26]

Other beneficial The name of **Negative effect Solution Applications** References the pomace nutrients Interferes with Cholesterol-Sunflower Enzymatic Neutralabsorption of [32] lowering seed pomace treatment ceuticals minerals phytosterols **Antioxidants** Sesame oil (resulting in Bakery [29] pomace better keeping quality) Ferulic acid Flax-seed Heat Bakery and [27] (antioxidant) confectionery pomace treatment

Table 3

				Continuati	on Table 3
Pumpkin seed pomace	Anti-oxidative peptides		Fermentation, thermal, biological or solvent extraction	Fermented beverages, and tablets coated with starch/honey/ chocolate/cara mel	[31]
Rapeseed pomace	N, P, and K	Reduce feed intake, impaired thyroid function, liver enlargement	Immersion in water, microwave or acid/alkali treatment	Protein concentrates, infant products etc.	[30]
Soybean	Ca, P, Na	Hemolysis, interference in lipid-soluble vitamins, cholesterol and dietary lipids	Thermal, biological or solvent extraction	Nuggets, desserts, fermented beverages etc.	[30]

The author Petraru [3] reports on the antioxidant properties of rapeseed bioactive peptides, blood pressure regulation capacity, and bile acid-binding capacity. At a concentration of 30-50 mg/L it inhibits thrombosis activity up to 90%. However, the production of food additives from some types of pomaces (for example, rapeseed pomace) requires considerable expenses associated with the use of enzyme preparations and other reagents, creation of optimal conditions for biochemical processes, drying, grinding of the obtained products, in addition, creation of conditions for the development of microbiological processes in wet media, which is an additional risk factor about the safety of end products. The wide application of the methods of protein preparations obtained in practice is restrained by the complexity of the management of these processes and the insufficient output of proteins due to their strong connection with other components and denaturation in the process of oil extraction.

The addition of 10% sesame protein concentrate to snacks improves their sensory properties, increases protein content, and reduces carbohydrate content [58]. Antithrombotic activity has been identified in peanut peptides, which will improve the health benefits of the products to which it is added [59].

Dietary fiber extracted from the wastes can serve as a functional ingredient, and supplement in both food and pharmaceutical industries. The functionality and effects of dietary fiber vary based on its physicochemical properties. For instance, dietary fiber with high water-holding capacity can promote satiety, while fibers with strong binding activities can protect against damage to the epithelial cells. Dietary fiber offers numerous health benefits, such as lowering the risk of cancer, coronary heart disease, diabetes, and obesity [60].

In the food industry, dietary fiber is valued for improving organoleptic, nutritional, and textural qualities. It enhances water and oil-holding capacity, emulsification, and reduces syneresis. Additionally, it helps extend shelf life and boosts oxidative stability [60]. Utilizing

fiber from by-products is essential for sustainable production, as it provides health benefits, is environmentally friendly, low-cost, and supports a zero-waste circular economy [3].

10. Conclusions

Oilseed pomace, which is a waste product of the oil mill industry, is rich in various substances. Therefore, this product is valuable for the food industry. The processing of the pomace will provide valuable products that can be used as food additives as sources of protein of vegetable origin and fiber.

There are 2 general methods of oil production: pressing and extraction. A comparison of all available data concerning the press and extraction methods in large-scale production leads to the following conclusions: 1) the extraction method makes it possible to obtain a larger quantity of oil of much better quality; 2) the cost of the device and the cost of oil production in the extraction method is less than in the press method; 3) the press factories do not present any special danger in fire terms, the oil-extraction ones are very dangerous. Despite this, the method of oil production directly affects the quality and properties of the pomace. Therefore, the most favorable methods are those that do not involve the use of chemical reagents. Pressing is one such method of oil production. The pomace obtained after the mechanical way of oil production contains exceptional levels of protein and some amounts of fiber.

The article mainly focused on sunflower, pumpkin, flax, rape, and soya pomace. The most protein-rich pomace was pumpkin (55-56%), soya (50-50%), and sunflower (37%) pomace.

Protein extraction from the pomace is widespread and there are known several methods for obtaining protein concentrate and isolate. These technologies should prioritize producing protein in a waste-free manner, ensuring the final product is food-grade and contains minimal phenolic compounds. The presented extraction methods show good results in terms of protein yields and are up to 90%.

Green technologies that have a minimal impact on the environment are becoming increasingly popular. These include high-pressure processing, supercritical fluid extraction, microwave-assisted extraction, ultrasound-assisted extraction, cold plasma processing, pulsed electric fields, and radio frequency treatment. The use of aqueous alcoholic solutions gives better results in protein output and extraction of phenolic compounds results in higher protein content.

Extraction of fiber from pomace is less common due to its lower content, but it is also known to be used. The most common method is solvent extraction. The resulting products are widely used in the food industry as additives with beneficial properties for the organism.

Acknowledgments: The would like to thank the Institutional Project, subprogram 020405 "Optimizing food processing technologies in the context of the circular bioeconomy and climate change", Bio-OpTehPAS, being implemented at the Technical University of Moldova.

Conflicts of Interest: The authors declare no conflict of interest.

References

- 1. Sá, A.G.A.; Moreno, V.M.F.; Carciofi, B.A.M. Plant proteins are a high-quality nutritional source for the human diet. *Trends Food Sci. Technol.* 2020, 97, 170-184.
- 2. Langyan, S.; Yadava, P.; Khan, F.N.; Dar, Z.A.; Singh, R.; Kumar, A. Sustaining protein nutrition through plant-based foods. *Front. Nutr.* 2022, 8, 772573.

- 3. Petraru, A.; Amariei, S. Oil press-cakes and meals valorization through circular economy approaches a review. *Appl. Sci.* 2020, 10(21), 7432.
- 4. Fărcaş, A.C.; Socaci, S.A.; Diaconeasa, Z.M. *Food Preservation and Waste Exploitation*. IntechOpen, London, UK, 2019, pp. 1–11.
- 5. Mathews, A.; Tangiralaa, A.D.; Thirunavookarasu, N.; Kumar, S.; Anandharaj, A.; Rawsona, A. Extraction and modification of protein from sesame oil cake by the application of emerging technologies. *Food Chemistry Advances* 2023, 2, 100326.
- 6. Hessle, A.; Eriksson, M.; Nadeau, E.; Turner, T.; Johansson, B. Cold-pressed hemp seedcake as a protein feed for growing cattle. *Acta Agric. Scand. Sect. A Anim. Sci.* 2008, 58, pp. 136–145.
- 7. Prahova, T.Yu.; Prahov, V.A.; Brazhnikov, V.N.; Brazhnikova, O.F. Maslichnye kul'tury bioraznoobrazie, znachenie i produktivnost'. *Niva Povolzh'ya* 2019, 3(52), pp. 30-37.
- 8. Organic cultivation of oilseeds. Available online: https://www.fibl.org/fileadmin/documents/shop/1243-maslichnyye.pdf (accessed on 17 July 2024).
- 9. Agriculture, agronomy, farming. Available online: https://universityagro.ru/%D1%80%D0%B0%D1%81%D1%82%D0%B5%D0%BD%D0%B8%D0%B5%D0%B2 %D0%BE%D0%B4%D1%81%D1%82%D0%BE/%D0%BC%D0%B0%D1%81%D0%BB%D0%B8%D1% 87%D0%BD%D1%8B%D0%B5-%D0%BA%D1%83%D0%BB%D1%8C%D1%82%D1%83%D1%80%D1%8B/ (accessed on 16 July 2024).
- 10. Kalenska, S.M.; Stoliarchuk, T.A. Varietal features of oil linseed yield formation depending on sowing rate and inter-row spacing in the conditions of right-bank forest-steppe zone of Ukraine. *Plant Varieties Studying and Protection* 2018, 3, 302-309.
- 11. Lisicin, A.N.; Bykova, S.F.; Davidenko, E.K.; Minasyan, N.M. Biologicheskie osobennosti sortov rapsa i fiziologicheskie cennosti zhmykhov i shrotov. *Maslozhirovaya promyshlennost'* 2007, 6, pp. 18-20.
- 12. Kolomejchenko, V.V. Rastenievodstvo. Agrobiznescentr, Moskva, Rossiya, 2007, 600 p.
- 13. Niklyaev, V.S. *Osnovy tekhnologii sel'skokhozyajstvennogo proizvodstva*. Zemledelie i rastenievodstvo, Bylina, Moskva, Rossiya, 2000, 555 p.
- 14. Proskurnya, M.A.; Burlakova, L.V.; Loshkomojnshov, I.A. Biologicheskie svojstva pishchevykh volokon, poluchennykh iz zhmykhov maslichnykh kul'tur sibirskoj kollekcii. *Agrarnyj vestnik Urala* 2008, 4, pp. 48-50.
- 15. Pahomova, O. N. Perspektivnost' ispol'zovaniya zhmykhov i shrotov maslichnykh kul'tur dlya povysheniya pishchevoj i biologicheskoj cennosti produktov pitaniya. *Nauchnye zapiski Orelgieht* 2011, 2(4), pp. 378-379.
- 16. Statista. Trending statistics. Available online: https://www.statista.com/statistics/614430/oilseed-production-volume-european-union-28/ (accessed on 18 September 2024).
- 17. National Bureau of Statistics of the Republic of Moldova. Available online: https://statistica.gov.md/ro (accessed on 23 July 2024).
- 18. Academic. Available online: https://dic.academic.ru/dic.nsf/brokgauz_efron/65378/%D0%9C%D0%B0%D1%81%D0%BB%D0%BE%D0%B 1%D0%BE%D0%BD%D0%BE%D0%B5 (accessed on 25 July 2024).
- 19. Alekseeva, T.V.; Zagorul'ko, E.A.; Rodionova, N.S.; Korystin, M.I.; Ivannikov, A.V.; Zyablov, M.M. Issledovanie processa nabukhaniya zhmykha zarodyshej pshenicy. *Fundamental research* 2013, 6, pp. 1324-1328.
- 20. Shcherbina, D.S.; Mezenova, N.YU. Issledovanie biopotenciala zhmykha l'nyanogo semeni v kachestve funkcional'noj dobavki k pishche. *Vestnik molodezhnoj nauki* 2020, 3(25), 10.
- 21. Barsukova, M.S.; Orlov, V.V.; Tarasova, R.N.; Ozhimkova, E.V. Ehkstrakciya, analiz i perspektivy ispol'zovaniya belkovykh kompleksov iz shrota *Linum Usitatissimum. Perspektivy nauki* 2015, pp. 106-108.
- 22. Egorova, E.Yu.; Bochkarev, M.S.; Reznichenko, I. YU. Opredelenie tekhnicheskikh trebovanij k zhmykham netradicionnykh maslichnykh kul'tur pishchevogo naznacheniya. *Tekhnika i tekhnologiya pishchevykh proizvodstv* 2014, 1, pp. 131-137.
- 23. Shaginova, L.O.; Krylova, I.V.; Dem'yanenko, T.F.; Domoroshchenkova, M.L. Issledovanie processa polucheniya belkovogo preparata iz semyan podsolnechnika dlya ispol'zovaniya v pishchevoj promyshlennosti. *Novye tekhnologii* 2021, 17(3), pp. 41-50.
- 24. Mustafaev, S.K.; Mkhitar'yanc, L.A.; Kornena. E.P. *Tekhnologiya otrasli (priemka, obrabotka i khranenie maslichnykh semyan)*. GIORD, Sankt-Peterburg, Rossiya, 2012, pp. 33-36.
- 25. Renzyaeva, T.V.; Renzyaev, O.P.; Renzyaev, A.O. Razrabotka sposoba povysheniya kachestva produktov pererabotki rapsa i ryzhika. *Maslozhirovaya promyshlennost'* 2009, 3, pp. 32-34.
- 26. Singh, R.; Langyan, S.; Sangwan, S.; Rohtagi, B.; Khandelwal, A.; Shrivastava, M. Protein for Human Consumption From Oilseed Cakes: A Review. *Front. Sustain. Food Syst.* 2022, 6, 856401.

- 27. Srivastava, D.; Mathur, A.N. Use of de-oiled groundnut cake flour as an alternate source of nutrition. *Int. J. Agric. Eng.* 2018, 11, pp. 150–152.
- 28. Chen, C.C.; Shih, Y.C.; Chiou, P.W.S.B. Evaluating nutritional quality of single stage- and two stage-fermented soybean meal. *Asian-Aust. J. Anim. Sci.* 2010, 23, pp. 598–606.
- 29. Yasothai, R. Chemical composition of sesame oil cake—review. *Int. J. Sci. Environ. Technol.* 2014, 3, pp. 827–835.
- 30. Sarwar, M.F.; Sarwar, M.H.; Sarwar, M.; Qadri, N.A.; Moghal, S. The role of oilseeds nutrition in human health: A critical review. *J. Cereals Oilseeds* 2013, 4, pp. 97–100.
- 31. Nourmohammadi, E.; Mahoonak, A.S.; Alami, M.; Ghorbani, M. Amino acid composition and antioxidative properties of hydrolyzed pumpkin (*Cucurbita pepo L.*) oil cake protein. *Int. J. Food Prop. 2017*, 20, pp. 3244–3255.
- 32. Vasudha, C.; Sarla, L. Nutritional quality analysis of sunflower seed cake (SSC). *Pharma Innov. J.* 2021, 10, pp. 720–728.
- 33. Hicks, T.M.; Verbeek, C.J.R. *Protein-rich by-products: production statistics, legislative restrictions, and management options.* Protein Byproducts, Amsterdam, Netherlands, 2016, pp. 1-18.
- 34. Toshev, A. Dzh.; Zhuravleva, N.D. Razrabotka tekhnologii sousov s dobavkoj rastitel'nogo proiskhozhdeniya s povyshennoj pishchevoj cennost'yu. *Vestnik Yuzhno-Ural'skogo gosudarstvennogo universiteta* 2016, 4(2), 94-101.
- 35. Bharathidasan, A.; Chandrasekaran, D.; Natarajan. A.; Ravi, R.; Viswanathan, K.; Ezhilvalavan, S. Non-starch polysaccharides and phytate phosphorus content of commonly available poultry feed ingredients. *Tamilnadu J Vet Anim Sci* 2008, 5, pp. 20–24.
- 36. Anson, M. L.; Pader, M. An Extraction of Soy Protein. US Patents US2785155A. Available online: https://patents.google.com/patent/US2785155A/en (accessed on 3 September 2024).
- 37. Klamczynska, B.; Czuchajowska, Z.; Baik, B.K. Composition, soaking, cooking properties, and thermal characteristics of starch of chickpeas, wrinkled peas, and smooth peas. *Int. J. Food Sci. Technol.* 2001, 36, pp. 563–572.
- 38. Ali, M.; Schmidt, C.; Walczak, M.; Förster, A.; Sayed, A.; Khalil, M.; Rizk, A.; Aly, S.; Hellwig, M. Improvement of protein extraction from sunflower oil cake using ascorbic acid and N-acetylcysteine: Effects on chemical, structural, and functional properties. *Journal of Food Measurement and Characterization* 2024, 18(8), pp. 1-15.
- 39. Salgado, P.R.; Molina Ortiz, S.E.; Petruccelli, S.; Mauri, A.N. Sunflower protein concentrates and isolates prepared from oil cakes have high water solubility and antioxidant capacity. *Journal of the American Oil Chemists' Society* 2011, 88(3), pp. 351-360.
- 40. Targino-Hoskin, R.; Plundrichb, N.; Vargochik, A.; Lilaa, M.A. Continuous flow microwave-assisted aqueous extraction of pomace phytoactives for production of protein-polyphenol particles and a protein-enriched ready-to-drink beverage. *Future Foods* 2022, 5, 100137.
- 41. Naik, M.; Natarajan, V.; Rawson, A.; Rangarajan, J.; Manickam, L. Extraction kinetics and quality evaluation of oil extracted from bitter gourd (*Momardica charantia L.*) seeds using emergent technologies. *LWT* 2021, 140, 110714.
- 42. Kumar, M.; Tomar, M.; Potkule, J.; Verma, R.; Punia, S.; Mahapatra, A. Advances in the plant protein extraction: Mechanism and recommendations. *Food Hydrocolloids* 2020, 115, 106595.
- 43. Roselló-Soto, E.; Galanakis, C.M.; Brnčić, M.; Orlien, V.; Trujillo, F.J.; Mawson, R. Clean recovery of antioxidant compounds from plant foods, byproducts and algae assisted by ultrasounds processing. Modeling approaches to optimize processing conditions. *Trends in Food Science and Technology* 2015, 42(2), 134–149.
- 44. Sá, A.G.A.; Laurindo, J.B.; Moreno, Y.M.F.; Carciofi, B.A.M. Influence of emerging technologies on the utilization of plant proteins. *Frontiers in Nutrition* 2022, 9, pp. 1–19.
- 45. Vanga, S.K.; Wang, J.; Raghavan, V. Effect of ultrasound and microwave processing on the structure, in-vitro digestibility and trypsin inhibitor activity of soymilk proteins. *LWT* 2020, 131, 109708.
- 46. Gislaine, N.S.; Tonon, V.; Mellinger, S.; Galdeano, M.C.; Iacomini, M.; Santiago, M.; Almeida, E.L.; Freitas, S.P. Grape seed pomace as a valuable source of antioxidant fibers. *J Sci Food Agric*. 2019, 99(10), pp. 4593-4601.
- 47. Petraru, A.; Amariei, S. Recovery of bioactive compounds from oilcakes-a review. *Journal of Faculty of Food Engineering* 2022, 21(4), pp. 364-381.
- 48. Šuput, D.; Lazić, V.; Popović, S.; Hromiš, N.; Bulut, S.; Pezo, L.; Banićević, J. Effect of process parameters on biopolymer films based on sunflower oil cake. *Journal on Processing and Energy in Agriculture* 2018, 22, pp. 125–128.

- 49. Zheng, Y.; Li, Y. Physicochemical and functional properties of coconut (*Cocos nucifera L.*) cake dietary fibers: Effects of cellulase hydrolysis, acid treatment, and particle size distribution. *Food Chemistry* 2018, 257, pp. 135–142.
- 50. Sunil, L.; Appaiah, P.; Kumar, P.K.; Gopala Krishna, A.G. Preparation of food supplements from oilseed cakes. *J Food Sci Technol.* 2015, 52(5), pp. 2998-3005.
- 51. Salgado, P.R.; Drago, S.R.; Ortiz, S.E.M.; Petruccelli, S.; Andrich, O.; González, R.J. Production and characterization of sunflower (*Helianthus annuus L.*) protein-enriched products obtained at pilot plant scale. *LWT-Food Sci. Technol.* 2012, 45(1), pp. 65–72.
- 52. Robertson, M.D.; Wright, J.W.; Loizon, E.; Debard, C.; Vidal, H.; Shojaee-Moradie, F.; Russell-Jones, D.; Umpleby, A.M. Insulin-sensitizing effects on muscle and adipose tissue after dietary fiber intake in men and women with metabolic syndrome. *J Clin Endocrinol Metab* 2012, 97(9), pp. 3326–3332.
- 53. Girgih, A.; Udenigwe, C.; Aluko, R. Reverse-phase HPLC separation of hemp seed (*Cannabis sativa L.*) protein hydrolysate produced peptide fractions with enhanced antioxidant capacity. *Plant Foods Hum. Nutr.* 2013, 68, pp. 39–46.
- 54. Aider, M.; Barbara, C. Canola proteins: Composition, extraction, functional properties, bioactivity, applications as a food ingredient and allergenicity—A practical and critical review. *Trends Food Sci. Technol.* 2011, 22, pp. 21–39.
- 55. Prakash, K.; Naik, S.; Vadivel, D.; Hariprasad, P.; Gandhi, D.; SaravanaDevi, S. Utilization of defatted sesame cake in enhancing the nutritional and functional characteristics of biscuits. *J. Food Process. Preserv.* 2018, 42, e13751.
- 56. Paweł, S.; Kazimierz, Z.; Starek, A.; Zukiewicz-Sobczak, W.; Sagan, A.; Zdybel, B.; Andrejko, D. Compaction Process as a Concept of Press-Cake Production from Organic Waste. *Sustainability* 2020, 12, 1567.
- 57. Langyan, S.; Khan, F.N.; Yadava, P.; Alhazmi, A.; Mahmoud, S.F.; Saleh, D.I. In silico proteolysis and analysis of bioactive peptides from sequences of fatty acid desaturase 3 (FAD3) of flaxseed protein. *Saudi J. Biol. Sci.* 2021, 28, pp. 5480–5489.
- 58. Sisay, M.T.; Emire, S.A.; Ramaswamy, H.S.; Workneh, T.S. Effect of feed components on quality parameters of wheat–tef–sesame–tomato based extruded products. *J. Food Sci. Technol.* 2018, 55, pp. 2649–2660.
- 59. Zhang, S.B. *In vitro* antithrombotic activities of peanut protein hydrolysates. *Food Chem.* 2016, 202, pp. 1–8.
- 60. Zheng, Y.; Li, Y. Physicochemical and functional properties of coconut (*Cocos nucifera L*) cake dietary fibers: Effects of cellulase hydrolysis, acid treatment and particle size distribution. *Food Chem.* 2018, 257, pp. 135–142.

Citation: Sergheeva, E.; Netreba, N. Oil crop pomace as a potential source of protein and dietary fiber. *Journal of Engineering Science* 2024, XXXI (3), pp. 196-215. https://doi.org/10.52326/jes.utm.2024.31(3).14.

Publisher's Note: JES stays neutral with regard to jurisdictional claims in published maps and institutional affiliations.



Copyright:© 2024 by the authors. Submitted for possible open access publication under the terms and conditions of the Creative Commons Attribution (CC BY) license (https://creativecommons.org/licenses/by/4.0/).

Submission of manuscripts:

jes@meridian.utm.md